Investigation of novel CD1a-lipid antigen presentation pathways in the skin

By

Ciara Alice Maguire

DPhil candidate in

Biomedical and Clinical Sciences

Kellogg College

Supervisor: Professor Graham Ogg

Weatherall Institute of Molecular Medicine

University of Oxford

Abstract

Investigation of novel CD1a-lipid antigen presentation pathways in the skin

Ciara Maguire Kellogg College

Thesis submitted for the degree of Doctor of Philosophy Hilary Term 2024

CD1a presents lipid antigens to T cells in the skin. Activating and inhibitory ligands have been identified but the role of CD1a in inflammatory disease has yet to be fully elucidated. This pathway represents a potentially accessible therapeutic target given the epidermal location of Langerhans cells. The aim of this project was to identify lipid ligands for CD1a, using psoriasis as a disease example. Candidate pathways were identified using RNA-Seq data from biopsies of patients with psoriasis (including those under treatment with ultraviolet phototherapy or the anti-IL-17A biologic therapy secukinumab), atopic dermatitis and healthy controls. The findings were integrated with public datasets and were validated using imaging mass cytometry at the protein level. These data, alongside clinical and scientific knowledge of the disease, allowed selection of candidate lipids for assessment. Candidates were investigated using iso-electric focussing gels, CD1a multimer binding and T cell cytokine assays.

RNA-Seq analysis identified differential expression of genes encoding proteins of lipid enzyme pathways, including retinoid metabolism, in psoriatic skin. Ligand discovery identified retinyl esters and nitro-fatty acids as binding to the CD1a cleft with possible effects on T cell IFN-γ secretion. In summary, this exploratory work identified lipid antigens for CD1a, to be characterised in further studies, as well as examining differential gene expression across psoriasis therapeutic subgroups. In addition to providing insights to disease biology, the data point to new therapeutic approaches.

Acknowledgements

Many thanks to my supervisor Professor Graham Ogg, second supervisor Professor Enzo Cerundolo (R.I.P.), post-docs Dr Rachel Etherington and Dr Koshika Yadava and members of the Ogg lab, past and present, particularly those highlighted in this thesis as collaborators on this project. I am very grateful to Professor Helen McShane and Louise Samson of the Medical Science Division for their help and support during my time at Oxford. I would also like to thank the HIU laboratory management and administrative teams, the staff of the Weatherall Institute of Molecular Medicine Flow Cytometry Facility and other institute staff who assisted me in many ways during the course of this PhD. I am grateful to our collaborators, Professor Moody (Harvard University), Professor Rossjohn (Monash University) and Professor Besra (University of Birmingham) who supported this project. Finally, my gratitude to my family and friends for their encouragement along the way.

Covid-19 statement

The COVID-19 pandemic negatively impacted the work in this thesis. The Weatherall Institute of Molecular Medicine was closed from March-July 2020 and until 2022, a rota system operated restricting access to the lab. This affected bench and tissue culture experiments investigating candidate CD1a antigens and CD1a-lipid reactive T cells. Patient samples were limited during the lockdown periods. There were also delays obtaining consumables from overseas. These factors limited experimental work. A six-month research extension was obtained but restrictions remained in place during this period.

Abbreviations

AD	Atopic Dermatitis
APC	Antigen Presenting Cell(s)
APOE	Apolipoprotein E
atRA	All-trans-retinoic acid
BH	Benjamini-Hochberg
BMI	Body Mass Index
CD1	Cluster of Differentiation 1
CE	Cholesteryl esters
CEH	Cholesteryl Ester Hydrolase
CHS	Contact hypersensitivity
CML	Chronic Myelogenous Leukaemia
CMM	Chloroform/Methanol/MilliQ water solution
CRABP2	Cellular Retinoic Acid Binding Protein 2
CRP	C-Reactive Protein
CyTOF	Cytometry Time-of-Flight
DAG	Diacylglycerol(s)/diglyceride(s)
DC	Dendritic Cell(s)
DCT	Distilled Coal Tar
DEG	Differentially Expressed Genes
DW	Distilled Water
DMSO	Dimethyl Sulfoxide
EFA	Essential Fatty Acid
EV	Empty Vector
IEF	Iso-Electric Focussing

IFN-γ	Interferon gamma
IF IHC	Immunofluorescence Immunohistochemistry
ILC	Innate Lymphoid Cell(s)
FA	Fatty Acids
FABAC	Fatty Acid Bile Acid Conjugate
FABP5	Fatty Acid Binding Protein 5
FACS	Fluorescence Activated Cell Sorting
FBS	Foetal Bovine Serum
FC	Fold Change
FSC	Forward scatter (flow cytometry)
GD3	GD3 Ganglioside- Milk, Bovine -ammonium salt
GO	Gene Ontology
GSEA	Gene Set Enrichment Analysis
hBD-2	Human β-Defensin-2
HPLC	High Performance Liquid Chromatography
HSP	Heat Shock Protein
HTA	Human Tissue Authority
IEF	Iso-electric focussing
ILC	Innate lymphoid cells
IMQ	Imiquimod
KC	Keratinocyte
Keap1	Kelch-like ECH-associating protein 1
LAL	Lysosomal Acid Lipase
LC	Langerhans Cell(s)
LCFA	Long Chain Fatty Acids
LCN2	Lipocalin 2

LDL	Low Density Lipoprotein
LRP	LDL Receptor Related Protein
LPC	Lysophosphatidylcholine
LPS	Lipopolysaccharide(s)
MACS	Magnetic-Activated Cell Sorting
MHC	Major Histocompatibility Complex
MoDC	Monocyte Derived Dendritic Cell(s)
MUFA	Monounsaturated Fatty Acids
NB-UVB	Narrow band UVB (311/312nm)
NFA	Nitro-Fatty Acids
NHEK	Normal Human Epidermal Keratinocytes
NICE	National Institute for Health and Care Excellence
NOS	Nitric Oxide Synthase
9-NO	9-nitrooleate
10-NO	10-nitrooleate
NO2-CLA	Nitro-conjugated linoleic acid
Nrf2	Nuclear factor erythroid 2-related factor 2
PBMC	Peripheral Blood Mononuclear Cell(s)
PBS	Phosphate Buffered Saline
PCA	Principal Component Analysis
pDC	Plasmacytoid Dendritic Cell
pI	Iso-electric point
PPAR	Peroxisome Proliferator Activated Receptor
PS	Psoriasis
PS L	Psoriasis (lesional – clinically involved by disease process)
PS NL	Psoriasis (non-lesional- clinically uninvolved by disease process)

PS R	Psoriasis (resolved – clinically resolved with treatment)
Psoriderm™	Psoriderm™ emulsion 40% w/v bath additive
PUFA	Polyunsaturated Fatty Acids
RA	Retinoic acid
RAGE	Receptor for Advanced Glycation End Products
RAR	Retinoic Acid Receptor
RARE	Retinoic Acid Response Element
RBP	Retinol Binding Protein
RCT	Randomised Controlled Trial(s)
RE	Retinyl Esters
RO	Retinyl Oleate
RS	Retinyl Stearate
RP	Retinyl Palmitate
RT	Room Temperature
RXR	Retinoid X Receptor
SC	Stratum Corneum
SG	Stratum Granulosum
SREBP/SREBPF	Sterol Regulatory Element Binding Protein/Sterol Regulatory Element Binding Transcription Factor
SSC	Side scatter (flow cytometry)
TAG	Triacylglycerol(s)/trigycleride(s)
TCR	T Cell Receptor
TEWL	Trans-epidermal water loss
TLR	Toll-like Receptor
TTR	Transthyretin
UMAP	Unsupervised Uniform Manifold Approximation and Projection

VDR	Vitamin D Receptor
VEGF	Vascular Endothelial Growth Factor
VLCFA	Very Long Chain Fatty Acids
VLDLR	Very Low-Density Lipoprotein Receptor
VST	Variance Stabilisation Transition
WGCNA	Weighted Gene Co-expression Network Analysis
WHO	World Health Organisation

Abstract **1**

Acknowledgements **2**

Abbreviations **4**

1 Chapter 1 Introduction **17**

1.1 The skin in health and disease 17

1.1.1 Healthy skin 17

1.1.2 Psoriasis 18

1.2 Lipids in the skin 20

1.2.1 Lipids in healthy skin 20

1.2.2 Lipids in psoriatic skin 21

1.3 The cutaneous immune system 22

1.3.1 T cells in healthy and diseased skin 22

1.3.2 Key cytokines in psoriasis 26

1.3.3 Antigen presenting cells in healthy and diseased skin 29

1.4 The Role of CD1a in healthy and diseased skin 31

1.4.1 APC and CD1a 31

1.4.2 CD1a structure and ligands 32

1.4.3 CD1a-autoreactive T cells 35

1.5 Thesis aims 36

2 Chapter 2 Materials and Methods **37**

2.1 Media and buffers 37

2.1.1 Media 37

2.1.2 Buffers 40
2.2 Cell culture 40
2.2.1 Cell culture notes 40
2.2.2 Freezing and Thawing Cells 42
2.2.3 K562 cell culture 42
2.2.4 PBMC isolation 42
2.2.5 MACS (Magnetic-Activated Cell Sorting) separation 43
2.2.6 T cell culture 44
2.2.7 Differentiation of dendritic cells from monocytes 44
2.3 Flow cytometry staining 45
2.4 Lipids 48
2.4.1 Lipid solutions 48
2.4.2 Iso-Electric Focussing (IEF) Gels 59
2.4.3 Toxicity Testing 63
2.4.4 Autofluorescence Testing 63
2.5 Tetramer and dextramer staining 63
2.5.1 Tetramer staining (using T cells) 64
2.5.2 Dextramer staining (using PBMC) 66
2.6 T cell assays 68
2.6.1 Interferon-γ ELISpot 68
2.6.2 ELISA using CD1a-autoreactive T cell clones 69
2.6.3 BK6 Functional Assay 70

2.7 Assessing CD1a expression on moDC 72
2.8 Collaborative work 73
2.8.1 RNA-Seq 73
2.8.2 Hyperion™ staining and analysis 73
3 Chapter 3 RNA-Seq analysis 74
3.1 Background 74
3.1.1 Introduction 74
3.1.2 Assessment of differential gene expression in PS L and PS NL skin compared to HC skin 79
3.1.3 Assessment of differential gene expression in PS compared to AD skin 81
3.1.4 Patient Cohort 82
3.2 RNA-Seq data analysis approach 89
3.2.1 RNA extraction and validation (Work of Dr Randeep Singh, Ogg Lab) 89
3.2.2 RNA sequencing (Work of Dr Jeongmin Woo, Ogg Lab) 89
3.3 Results 91
3.3.1 Unsupervised analysis by Principal Component Analysis 91
3.3.2 Assessment of DEG by psoriasis treatment modality: Volcano plots and scatter plots 92
3.3.3 NB-UVB-treated group 94
3.3.4 Secukinumab-treated group 95
3.3.5 Assessment of DEG in healthy and diseased skin: Venn Diagrams 97
3.3.6 RNA-Seq of cytokine mRNA in healthy and diseased skin 108
3.3.7 Module-trait relationships and Gene Ontology 112

3.3.8 Co-expression networks 118
3.3.9 RNA-Seq results summary 125
3.4 Discussion 125
3.5 Chapter Summary 131
4 Chapter 4 Retinyl Esters 132
4.1 Introduction 132
4.1.1 Retinyl Ester metabolism 132
4.1.2 Retinyl Esters in healthy skin 134
4.1.3 Retinyl Esters and psoriasis 135
4.2 Results: Retinyl Esters 137
4.2.1 Interrogation of RNA-Seq data for retinoid-relevant genes 137
4.2.2 Optimisation of Retinyl Ester solubility 143
4.2.3 Investigation of Retinyl Ester binding to CD1a 143
4.2.4 Assessment of toxicity of K562 cells by Retinyl Esters 145
4.2.5 Tetramer and dextramer staining with Retinyl Esters 148
4.2.6 The effect of Retinyl Esters on CD1a expression on moDC and K562 cells 151
4.2.7 Assessment of cytokine production by CD1a-reactive T cells 153
4.2.8 Clonal assay using the CD1a-autoreactive BK6 TCR 158
4.2.9 Retinyl Esters results summary 159
4.3 Discussion 159
4.4 Chapter Summary 163
5 Chapter 5 Nitro-Fatty Acids 164

5.1 Introduction 164
5.1.1 Nitro-fatty acid pathways 164
5.1.2 Nitro-fatty acids *in vivo* 165
5.1.3 Nitro-Fatty Acids and inflammation 166
5.1.4 Nitro-Fatty Acids and psoriasis 167
5.2 Results: Nitro-Fatty Acids 169
5.2.1 Interrogation of RNA-Seq data for Nitro-Fatty Acid-relevant genes 169
5.2.2 Investigation of Nitro-Fatty Acid binding to CD1a 175
5.2.3 Assessment of toxicity on K562 cells by Nitro-Fatty Acids 179
5.2.4 Tetramer and Dextramer staining with Nitro-Fatty Acids 181
5.2.5 The effect of Nitro-Fatty Acids on CD1a expression on moDC and K562 cells 187
5.2.6 Assessment of cytokine production by CD1a-reactive T cells 189
5.2.7 Clonal assay using the CD1a-autoreactive BK6 TCR 191
5.2.8 Nitro-Fatty Acids results summary 191
5.3 Discussion 191
5.4 Chapter summary 195
6 Chapter 6 Sterols and other CD1a candidate lipid ligands 196
6.1 Sterols: Molecules of the cholesterol pathway 196
6.1.1 Sterol pathways and psoriasis pathogenesis 196
6.2 Lipid pathways and psoriasis treatment – coal tar derivatives and acitretin 201
6.2.1 Coal tar derivatives 201
6.2.2 Acitretin 202

6.3 Other lipids of interest 203
6.4 Results I: Sterols and related molecules 204
6.4.1 Interrogation of RNA-Seq data for sterol-relevant genes 204
6.4.2 Optimisation of sterol solubility 208
6.4.3 Investigation of cholesterol and cholesteryl ester binding to CD1a 209
6.4.4 Assessment of toxicity and effects on CD1a expression on K562 cells by cholesterol and cholesteryl esters 213
6.4.5 Tetramer and Dextramer staining with cholesterol 215
6.4.6 The effect of cholesterol and cholesteryl esters on CD1a expression on K562 cells 217
6.4.7 Assessment of cytokine production by CD1a-reactive T cells 217
6.4.8 Cholesterol and cholesteryl esters: Results Summary 219
6.5 Results II: Coal Tar Derivatives and Acitretin 219
6.5.1 Optimisation of solubility for coal tar derivatives and acitretin 219
6.5.2 Investigation of coal tar derivatives and acitretin binding to CD1a 220
6.5.3 Assessment of toxicity on K562 cells by coal tar derivatives and acitretin 223
6.5.4 The effect of coal tar derivatives and acitretin on CD1a expression by moDC 225
6.5.5 Investigation of effect of coal tar derivatives and acitretin on CD1a-reactive T cell responses 227
6.5.6 Coal tar derivatives and acitretin: Results summary 231
6.6 Other lipids 231
6.7 Discussion 233
6.7.1 Sterols 233

6.7.2 Coal Tar Derivatives and Acitretin 235

6.8 Chapter summary 236

7 Chapter 7 Confirmatory analysis of expression of relevant lipid pathway genes and proteins in inflammatory skin disease 237

7.1 Background 237

7.2 Specific materials and methods 237

7.2.1 GEO Profiles 237

7.2.2 Single Cell Database 239

7.2.3 Immunofluorescence Immunohistochemistry 240

7.2.4 Hyperion™ 242

7.3 Results I: Selection of candidate genes for validation 245

7.3.1 Candidate genes of interest 245

7.3.2 *CRABP2*: Cellular Retinoic Acid Binding Protein 2 254

7.3.3 *FABP5*: Fatty Acid Binding Protein 5/Epidermal Fatty Acid Binding Protein 257

7.3.4 *LCN2*: Lipocalin 2/Neutrophil gelatinase-associated lipocalin (NGAL)/24p3 261

7.3.5 *APOE*: Apolipoprotein E 266

7.4 Results II: Validation of candidate genes of interest 269

7.4.1 Immunofluorescence Immunohistochemistry 270

7.4.2 Hyperion™ 275

7.4.3 Validation of candidate genes results summary 285

7.5 Discussion 285

7.6 Chapter Summary 290

8 Chapter 8 Final overall discussion and future directions 291

8.1 Summary of results 291

8.2 Limitations of methods used 293

8.3 Future Directions 295

8.4 Final thoughts 296

References 298

List of Figures 353

List of Tables 358

1 Chapter 1 Introduction

1.1 The skin in health and disease

1.1.1 Healthy skin

Human skin is composed of three main layers: the epidermis, the dermis and the subcutaneous tissue. Each layer differs in its composition and role. The epidermis, which is exposed to the outside environment, is composed of four strata of keratinocytes from the inside out: the basal layer (stratum basalis), the spinous layer (stratum spinosum), the granular layer (stratum granulosum) and the horny layer (stratum corneum). On the palms of the hands and the soles of the feet, there is an additional layer, the clear layer (stratum lucidum), between the stratum granulosum and the stratum corneum.

Keratinocytes are generated in the basal layer and evolve morphologically as they travel upwards to the horny layer, whence they are shed. Interspersed with keratinocytes in the basal layer are melanocytes, which distribute melanin pigment to keratinocytes. Langerhans cells (LC), which are the main antigen presenting cells (APC) of the epidermis, are located in the spinous layer and densely express CD1a on their surface. Merkel cells, which act as receptors for touch, are also found in the epidermis.

The dermis consists of a fibrous stroma with collagen and elastin in a hyaluronic acid matrix. Skin appendages such as hair follicles in the pilosebaceous unit and eccrine/apocrine glands are located here. Unlike the epidermis, it contains vascular and lymphatic networks and so is easily accessible to immune cells.

The subcutaneous layer consists of adipose tissue and a comparatively larger lymphovascular system.

1.1.2 Psoriasis

Psoriasis is a common inflammatory disease worldwide and affects 1.5% of the population in Western Europe (Griffiths et al., 2021). The most common presentation is plaque psoriasis (psoriasis vulgaris), characterised by scaly, red areas of skin over extensor surfaces (elbows, knees), with an additional predilection for the scalp, navel and skin folds. The plaques may be pruritic/painful or relatively asymptomatic.

The skin structure is altered with characteristic features of regular acanthosis (thickening) of the epidermis due to abnormal keratinocyte differentiation, often with retained nuclei (parakeratosis) and a reduced or absent granular layer. Neutrophilic micro-abscesses may be seen in the epidermis. Dilated blood vessels are noted in the papillary dermis with a predominantly lymphocytic inflammatory infiltrate.

Other forms of psoriasis include guttate psoriasis, pustular psoriasis, intertriginous/inverse psoriasis and erythrodermic psoriasis. Psoriasis may also involve the nails, the joints (psoriatic arthritis) and the eyes. Associations exist between psoriasis, metabolic syndrome and psychiatric illness.

RNA sequencing (RNA-Seq) data and protein validation discussed in this thesis (**Chapter 3**, **Chapter 7**) are from biopsies of patients with plaque psoriasis and discussions related to treatment below will focus on this subtype.

The clinical treatment pathway for patients with psoriasis (**Figure 1.1**) usually involves an initial period of treatment with topical therapy (topical steroids, topical vitamin D analogues and coal tar preparations) under primary care with concomitant referral to a dermatologist for severe, extensive (>10% Body Surface Area), acute or high impact disease. Tools including the Dermatology Life Quality Index (DLQI) questionnaire(Finlay & Khan, 1994) (score range 0-30) to ascertain the impact of disease on quality of life and the Psoriasis Assessment of Severity Index (PASI) score(Fredriksson & Pettersson, 1978) (score range 0-72) are calculated on the basis of clinical severity. Results, in

addition to patient preference and co-morbidities such as psoriatic arthritis, inform treatment choice. For patients without joint disease, phototherapy with UV light (narrow band UVB (NB-UVB), with psoralen UVA (PUVA) second line) is an initial option. If this treatment fails or is contraindicated, immunosuppressive therapy may be considered. In some cases, such as a contraindication to immunosuppression, acitretin (**Chapter 6**) may be used. For patients with severe disease (PASI score ≥10 and a DLQI >10) who have failed or have contraindications to the above treatments, biologic therapies (**Table 1.1**) may be offered.

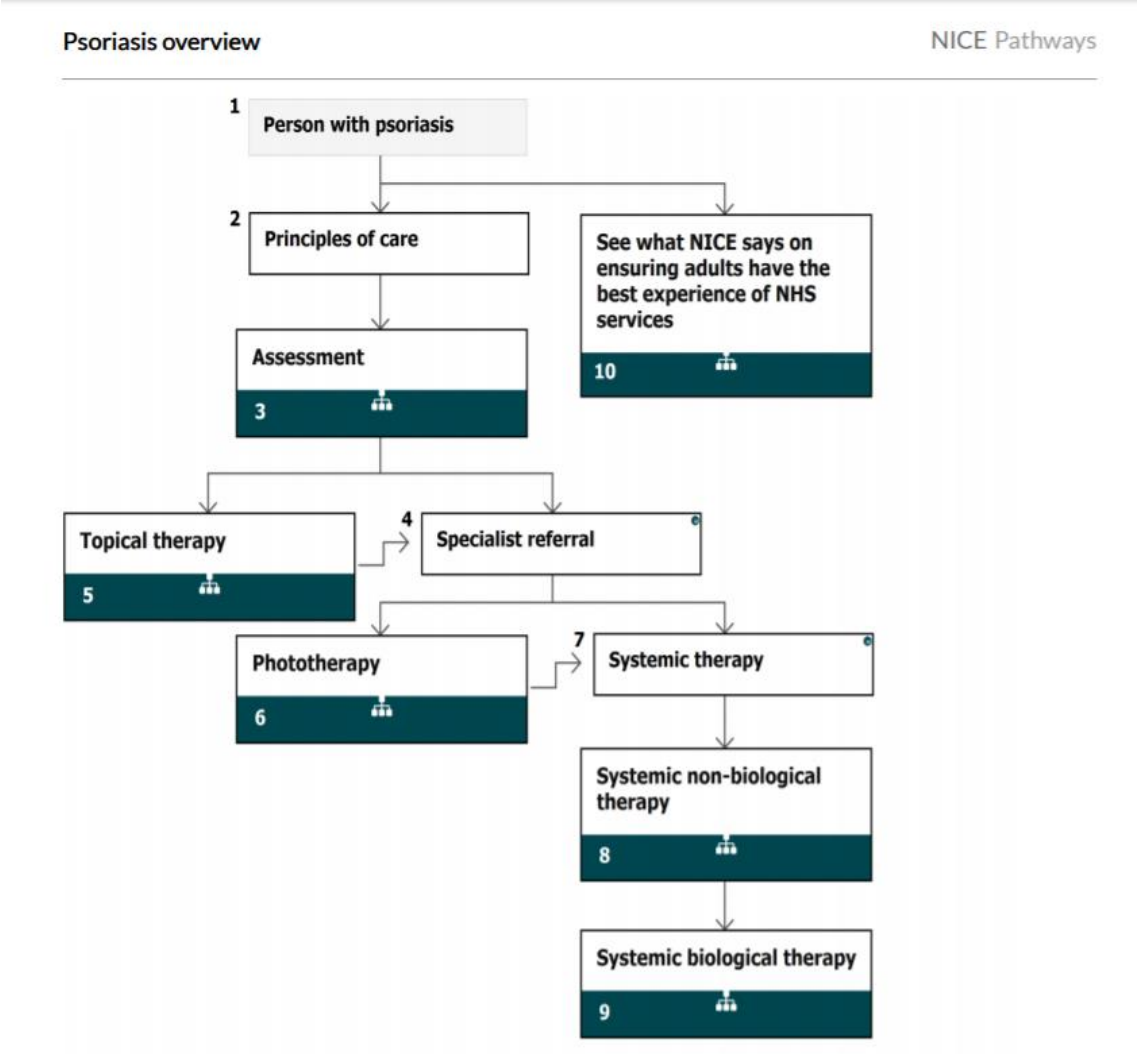


Figure 1.1 Algorithm for psoriasis treatment according to NICE (National Institute for Health and Care Excellence) guidelines, www.nice.org.uk.

Table 1.1 Biologic therapies currently approved for use in psoriasis (NICE UK).

Target	Drug
TNF-α	Infliximab, adalimumab, etanercept, certolizumab
IL-12/23 p40 subunit	Ustekinumab
IL-23 p19 subunit	Risankizumab, tildrakizumab, guselkumab
IL-17A	Secukinumab, ixekizumab
IL-17A/F	Bimekizumab
IL-17A receptor (IL-17RA)	Brodalumab

1.2 Lipids in the skin

1.2.1 Lipids in healthy skin

Epidermal lipids include glycolipids and phospholipids, sterols, sterol esters and mono-, di- and triacyl glycerols (Nicolaides, 1974). Phospholipids are the main component of the cell membrane fatty bilayer. Sphingolipids (a subtype of phospholipids) found in the epidermis comprise ceramides and glucosylceramides (Motta et al., 1994). Cutaneous lipids support the integrity of the skin barrier and epidermal damage in mice results in increased biosynthesis of sterols and fatty acids (FA) (Grubauer et al., 1987). The omega-3 (ω-3) and omega-6 (ω-6) polyunsaturated fatty acids (PUFA) α-linolenic acid and linoleic acid are essential to skin health and their derivatives EPA (eicosapentaenoic acid) and DHA (docosahexaenoic acid) have roles in barrier function and modulation of inflammatory skin disease and cancer via Peroxisome Proliferator Activated Receptor (PPAR) and Toll-like receptor (TLR) signalling, as summarised by McCusker et al (McCusker & Grant-Kels, 2010). Mice with dietary deficiency of essential FA demonstrated increased sterol and FA biosynthesis in both the epidermis and dermis, which was not fully reversed by occlusion (Grubauer et al., 1987).

Sebum acts as a lubricator for the skin and is composed of free FA, cholesteryl esters (CE) and triglycerides, wax esters, diglycerides, squalene and cholesterol (Ro & Dawson, 2005). Most free FA in sebum have 18 carbon (stearic, oleic, linoleic) or 16 carbon (palmitic, sapienic, palmitoleic) chains (Ro & Dawson, 2005).

1.2.2 Lipids in psoriatic skin

The field of lipidomics is advancing rapidly and has been applied across a range of inflammatory skin diseases, as summarised by Gruber et al (Gruber et al., 2019). Genes involved in lipid biosynthesis, metabolism and catabolism are altered in psoriatic skin, as discussed in more detail in **Chapter 3**.

Ceramides make up approximately three quarters of the polar lipids found in both normal stratum corneum and psoriatic scale but relative subtypes differed between healthy and diseased groups (Motta et al., 1994). A comparison of covalently bound lipids in stratum corneum of psoriasis compared to healthy and sunburnt skin found an increase in unsaturated fatty acids (particularly 16:0, 18:0, 18:1, 18:2 and 20:0 species) and reduction in Cer-B in psoriatic scale (Wertz et al., 1989). Omega-6 PUFA derivatives are increased in biopsies of psoriatic compared to healthy control skin (Sorokin et al., 2018). Trans-epidermal water loss (TEWL) is increased in lesional psoriasis compared to non-lesional and control skin (Motta et al., 1994). A reduction in sebaceous gland size and density has been reported in psoriatic versus healthy skin on the body and scalp (Headington et al., 1989; Rittié et al., 2016; Werner et al., 2008). It would follow that sebum, a source of lipids as detailed above, would therefore also be reduced.

Phospholipases cleave phospholipids to release fatty acyl chains. Cytosolic phospholipase A2 δ (PLA2G4D) has been demonstrated in lesional psoriatic, but not normal, skin (Chiba et al., 2004). Mast cell PLA2G4D has been theorised to generate neo-lipid antigens for presentation by CD1a in psoriasis (Cheung et al., 2016). Keratinocyte PLA2G2F, a secretory PLA2, shows increased expression in psoriasis; IL-22 also increased expression of PLA2G2F in primary keratinocytes (Yamamoto et al., 2015). A delayed initial repair response to barrier compromise and increased pH of the stratum corneum was seen in sPLA2IIF knockout mice (Ilic et al., 2014).

1.3 The cutaneous immune system

1.3.1 T cells in healthy and diseased skin

The main antigen presenting cell of the epidermis is the Langerhans cell (LC), characterised by its dense expression of CD1a. Aside from LC, $CD8^+$ tissue-resident memory T cells are the most prevalent epidermal immune cell (Ho & Kupper, 2019). In the dermis, T cells, dermal and plasmacytoid dendritic cells (DC), macrophages, natural killer (NK) cells, innate lymphoid cells (ILC), B cells, mast cells and fibroblasts are found (Debes & McGettigan, 2019; Nestle et al., 2009; Villanova et al., 2014).

Each square centimetre of healthy human skin is estimated to contain around one million T cells, almost double the number of T cells in the peripheral circulation (Clark et al., 2006). $CD4^+$ and $CD8^+$ cells exist in approximately equal amounts, most express activation markers (HLA-DR and IL-2R) and >90% are located around the venules of superficial vascular plexuses and appendages in the dermis (Bos et al., 1987). A minority (<2%) are epidermal and, as for T cells directly sub-epidermally and in the reticular dermis, these principally consist of $CD8^+$ T cells (Bos et al., 1987). Epidermal T cells are mostly of the αβ subtype and are mainly located in the basal layer (Foster et al., 1990).

Skin-resident T cells

Skin-resident T cells exhibit a wide T cell receptor (TCR) repertoire and mostly express homing markers including cutaneous lymphocyte-associated antigen (CLA), CCR4 and CCR6 and approximately half express CCR8 and CXCR6 (Clark et al., 2006). In the skin, CLA^{pos} memory T cells (including $CD4^+$, $CD8^+$ and T_{reg}) make up 80-90% of $CD3^+$ cells, while in the blood, the frequency is approximately 15% (Clark et al., 2006; Li et al., 2016). T cell populations in normal skin are made up of different types of memory T cells:

resident memory (T_{RM}) and recirculating memory (T_{RCM}) T cells, with recirculating memory T cells further subdivided into central memory (T_{CM}) and effector memory (T_{EM}) subgroups. The majority of T cells have an αβ TCR and a minority have a γδ TCR, which is also the case in psoriasis.

T cell subsets in the skin

T cells, particularly in the epidermis, are required for the development of the clinical features of psoriasis (Gottlieb et al., 1995). The density of T cells in psoriatic lesional skin, both before and after treatment (with UVB phototherapy or the anti-TNF therapy etanercept) is greater than that in non-lesional psoriatic or normal skin (Matos et al., 2017). There is extensive epidermal (approx. 100-fold increase) and dermal (approx. 10-fold increase) T cell infiltration in active psoriatic lesions compared to healthy control skin, with $CD8^+$ T cells predominating in the epidermis and $CD4^+$ T cells making up the majority of dermal T cells (Cheuk et al., 2014). Although there are more $CD4^+$ than $CD8^+$ T cells in psoriatic skin, in the epidermis, $CD8^+$ predominate (Gottlieb et al., 1995).

T cell infiltrates in psoriasis are polyclonal without a dominant T cell clone (Harden, Hamm, et al., 2015). Although >93% of these clones disappear in psoriatic skin that has clinically resolved with etanercept, oligoclonal αβ T cells capable of producing IL-17 may persist in clinically resolved skin and were also identified to a lesser degree in non-lesional skin from the same patients (Matos et al., 2017). TCR from some of these clones were shared among multiple patients with psoriasis but not found in skin samples from healthy controls (Matos et al., 2017). These findings corroborate murine studies that have shown that skin resident T cells in the non-lesional skin of patients with psoriasis may incite the development of psoriatic lesions in the presence of a suitable trigger, without the need for recruitment of T cells from the peripheral blood (Boyman et al., 2004). This was attributed to local T cell proliferation regulated by TNF-α and TNF-α

blockade impaired disease development (Boyman et al., 2004). These findings suggest that recruitment of T cells from the circulation may not be required to elicit psoriasis in non-lesional skin and may also explain why disease recurrence may localise to previously affected sites.

$CD4^+$ T cells in psoriasis

Healthy skin $CD4^+$ subsets including T_H1, T_H2, T_H17, T_H22, T_R1, T_H9, regulatory T cells (T_{reg}) and follicular B helper T cells (T_{FH}). For clarity, the focus below is on cell types found in both healthy and psoriatic skin.

T_H1 cells

T_H1 cells help provide defence against intracellular pathogens while also contributing to delayed type hypersensitivity reactions. T_H1 lineage development is determined by T-bet, a potent transactivator of the *IFNG* gene which is expressed on T_H1 cells in response to TCR signalling (Szabo et al., 2000). The main cytokine responsible for induction of T_H1 development is IL-12 (Jacobson et al., 1995; Thierfelder et al., 1996; Trinchieri et al., 1992).

A T1 [both $CD4^+$ T_H1 (helper T cells) and $CD8^+$ T_c1 (cytotoxic T cells)] differentiation bias has been identified in the lesional epidermis and blood of psoriasis patients when compared to the blood of healthy controls (Austin et al., 1999). Most studies that informed the concept of psoriasis as a T_H1-mediated disease were based on p40 blocking antibodies. This subunit is now recognised to be shared by IL-23 (IL-12/23p40), a T_H17 driver (Oppmann et al., 2000). *IL23p19* and *IL12p40* mRNA were increased in human psoriatic lesional skin compared with non-lesional skin and healthy controls, however, IL-12p35 was not (Chan et al., 2006). T_H1 cells secrete a number of cytokines, including IFN-γ and TNF-α.

T_H17 cells

This subset was distinguished as separate from T_H1 and T_H2 lineages in 2005 (Harrington et al., 2005; H. Park et al., 2005). In health, T_H17 cells are involved in antimicrobial defence including against fungal pathogens (Acosta-Rodriguez et al., 2007); they are now considered key to psoriasis pathogenesis. The differentiation of this $CD4^+$ subset is regulated by the transcription factor RORγt (*in vitro*/murine studies); the transcription of its gene, the *Rorc* locus, is in turn directed by IL-6 and TGF-β (Ivanov et al., 2006). T_H17 produce IL-17A, IL-17F, TNF-α, IL-21 and IL-22. They are regulated by IL-23 (Harrington et al., 2005; Langrish et al., 2005). However, some argue that psoriasis is an IL-17A driven disease rather than a T_H17 disease (Brembilla et al., 2018).

T_H22

T_H22 cells were first identified in 2009 as a subset of $CD4^+$ memory T cells expressing skin homing markers CLA, CCR4, CCR6 and CCR10 and exclusively producing IL-22 (not IL-17A or IFN-γ) in response to TNF-α and IL-6 from plasmacytoid DC (Duhen et al., 2009). Some subsets of T_H22 cells can also produce IL-13 (Trifari et al., 2009). Aryl hydrocarbon receptor agonists promote the production of IL-22 while downregulating IL-17 production (Trifari et al., 2009). IL-22 induces epidermal inflammation and hyperplasia and migration of keratinocytes (Boniface et al., 2005). It is increased in the blood of patients with moderate and severe psoriasis compared to healthy controls (Wolk et al., 2006). CD1a autoreactive T cells have been identified within the family of T_H22 cells, supporting the role of CD1a in psoriasis (De Jong et al., 2010).

T_{reg}

Regulatory T cells, or T_{reg}, were originally identified in murine studies as moderators of the immune response (Sakaguchi et al., 1995). The transcription factor Foxp3 is important for T_{reg} development (Hori et al., 2003). $Foxp3^+$ T cells make up approximately 10% of T cells in normal human skin in homeostasis (Clark et al., 2008; Clark & Kupper, 2007). The majority of $CD4^+CD25^{high}Foxp3^+$ T_{reg} in peripheral blood are $CD45RO^+$ and express the skin homing markers CLA, CCR4 and CCR6, suggesting a role in the regulation of skin immune responses (Hirahara et al., 2006).

In psoriasis, there is evidence for T_{reg} dysfunction and the balance between pro-inflammatory T cells and regulatory T cells is altered (Bovenschen et al., 2011; Sugiyama et al., 2005).

$CD8^+$ T cells in psoriasis

Of note, the constellation of cytokines produced in active psoriasis (IL-17, IL-22, IFN-γ) can be produced by $CD8^+$ T cells as well as the expected $CD4^+$ T cell subsets (T_H17, T_H22, T_H1) (Hijnen et al., 2013; Res et al., 2010). In lesional psoriasis, epidermal $CD4^+$ and $CD8^+$ T cells show increased *IL17A*, *IL22* and *IFNG* expression compared to their dermal counterparts (Cheuk et al., 2014). $CD8^+CLA^{pos}$ epidermal T cells co-expressing CD103, CCR6 and IL-23R were also enriched in the epidermis of resolved psoriasis following treatment with anti-TNF or anti-IL-12/23 biologic therapies (Cheuk et al., 2014). These cells predominantly produced IL-17A on *ex vivo* stimulation, whereas their $CD4^+$ counterparts mainly secreted IL-22 (Cheuk et al., 2014).

1.3.2 Key cytokines in psoriasis

In this thesis, differential expression of multiple genes encoding psoriatic cytokines will be discussed, including following treatment with the anti-IL17A biologic therapy

secukinumab (**Chapter 3**). Cytokine pathways in psoriasis are a vast area of research and only key points regarding each one are summarised here. Regulatory cytokines (IL-10, TGF-β) also play a role in psoriasis but are not discussed here.

T_H1 cytokines

IFN-γ

IFN-γ is the main effector cytokine of T_H1 cells and IFN-γ^+ T cells are increased in lesional psoriasis compared to healthy skin (Kryczek et al., 2008). IFN-γ promotes expression of MHC Class II molecules on keratinocytes (Griffiths et al., 1989). IFN-γ activates APC to produce IL-1 and IL-23, promotes migration of IL-17^+ T cells and acts synergistically with IL-17 to induce the antimicrobial peptide human β-defensin-2 (hBD-2) in keratinocytes (Kryczek et al., 2008). IFN-γ also increases expression of the IL-22 receptor subunits (IL22R1 and IL-10R2) on keratinocytes *in vitro* (Wolk et al., 2004). $CD8^+$ T cells are the main epidermal T cell source of IFN-γ (Austin et al., 1999). *IFNG* is upregulated in PS lesional skin (Gudjonsson, Ding, et al., 2010; Yao et al., 2008). Anti-TNF-α therapy with infliximab suppresses *IFNG* mRNA and this may partially account for its mode of action in psoriasis (Haider, Cohen, et al., 2008).

IFN-γ serum levels are significantly increased in patients with moderate/severe psoriasis compared with healthy controls (Arican et al., 2005; Chodorowska, 1998; Mehta et al., 2017). However, humanized anti-IFN-γ antibody therapies have as yet demonstrated a lack of clinical efficacy (Harden, Johnson-Huang, et al., 2015).

T cells from the blood of psoriasis patients with moderate/severe psoriasis demonstrated a T1 phenotype and a larger population of IFN-γ producing cells (mainly $CD8^+$) compared to controls, as did lesional intra-epidermal T cells (Austin et al., 1999). IFN-γ secretion by polyclonal and clonal T cells from healthy controls and patients with psoriasis will be examined in this thesis (**Chapter 4**, **Chapter 5**, **Chapter 6**).

TNF-α

TNF-α has a number of effects on antigen presentation by dendritic cells, keratinocyte proliferation and production of antimicrobial peptides. It is important for optimisation of IFN-γ production. *TNF* mRNA is increased in lesional psoriatic skin compared to healthy control (Chan et al., 2006; Gudjonsson, Ding, et al., 2010; Yao et al., 2008). It is also increased in non-lesional psoriatic skin compared to healthy control (Chan et al., 2006; Yao et al., 2008). TNF blockade downregulates *IL17* and *IL22* mRNA in the lesional skin of psoriasis patients (Zaba et al., 2007). Anti-TNF-α therapies such as infliximab, adalimumab and etanercept (**Table 1.1**) are clinically successful treatments for moderate-severe psoriasis.

T_H17 cytokines

IL-17

IL-17 can be produced by multiple cell types. IL-17$^+$ mast cells and neutrophils are found in psoriatic skin (Lin et al., 2011; Res et al., 2010), while T_H17 cells are characterised by the production of this cytokine. There are six types of IL-17: IL-17A, IL-17B, IL-17C, IL-17D, IL-17E (=IL-25) and IL-17F. IL-17A and IL-17F are disulphide-linked heterodimers, while the others are disulphide-linked homodimers. There are five types of IL-17 receptor, IL-17RA- IL-17RE, based on different combinations of subunits. IL-17A acts via the IL-17RA/IL-17RC receptor.

The power of IL-17 to modify inflammatory processes mainly derives from its collaborative action with other cytokines, its activation of inflammatory MAP kinase pathways and its regulation of multiple genes and stabilisation of mRNA transcripts, as reviewed by Amatya et al (Amatya et al., 2017). IL-17A increases expression of *HBD2*, *S100A7*, *S100A8* and *S100A9* transcripts in primary keratinocytes (Liang et al., 2006).

IL17A mRNA expression is increased in human psoriatic lesional skin compared to non-lesional and healthy control skin (Chan et al., 2006).

IL-22

IL-22 is a member of the IL-10 cytokine family. It is produced by T_H17 and T_H22 cells. IL-22 can also be produced by macrophages and some dendritic cells in lesional psoriatic skin (Res et al., 2010). The IL-22 receptor is made up of two subunits. The IL-22R1 receptor subunit is expressed in skin, pancreatic, intestinal and hepatic, renal and lung tissue, whereas the IL-10R2 subunit is much more widespread (Wolk et al., 2004).

STAT3 is activated in keratinocytes upon binding of IL-22 (Boniface et al., 2005; Wolk et al., 2004). IL-22 upregulates the transcription of genes coding for keratin 6, several proteins of the S100 family, Platelet Derived Growth Factor A and the chemokine CXCL5 (Boniface et al., 2005). IL-22 downregulates several genes associated with keratinocyte differentiation (Boniface et al., 2005; Wolk et al., 2006). IL-22 acts synergistically with IL-17 cytokines (A and F) to promote production of anti-microbial peptides (hBD-2, S100A7, S100A8, S100A9) (Liang et al., 2006).

IL22 mRNA is upregulated in psoriatic lesional compared with healthy control skin and IL-22 was found in the circulation of two thirds of patients with psoriasis, compared to 5% of healthy controls (Boniface et al., 2007). The results of Phase II clinical trials of an anti-IL-22 monoclonal antibody, fezakinumab, in atopic dermatitis have been published, however, it has not been similarly assessed in psoriasis (Guttman-Yassky et al., 2018).

1.3.3 Antigen presenting cells in healthy and diseased skin

Professional APC expressing MHC Class II include DC, macrophages and B cells. The main APC of the skin are mononuclear phagocytes, which include LC and dermal DC,

with the latter further subdivided into myeloid DC (also known as conventional DC) and plasmacytoid DC (pDC). Single cell studies now show marked heterogeneity of these subsets with alterations in disease (Reynolds et al., 2021).

Langerhans cells

Langerhans cells (LC) are the main APC of the epidermis and are distributed among the keratinocytes in the supra-basal layers. LC are characterised by their expression of CD1a, Langerin (CD207) and Birbeck granules. LC may initiate tolerogenic or inflammatory responses in human skin depending on environmental triggers. There are conflicting results from studies evaluating the density of LC in psoriatic epidermis and peri-lesional skin, as reviewed by Eidsmo et al (Eidsmo & Martini, 2018).

Dendritic Cells

There are tenfold more dendritic cells (DC) in adult human skin compared to peripheral blood (Kashem et al., 2017). Human dermal DC in healthy skin consist of $XCR1^+$ DC (cDC1, which are present in small amounts), $CD11b^+$ DC (cDC2 which are also $CD1c^+$, which predominate) and double negative DC, while inflammatory DC (MHC Class II^+ and $CD11c^+$) transiently exist in the skin during inflammation but not in healthy skin and include TipDC, IDEC and slanDC, as summarised by Kashem et al (Kashem et al., 2017).

Plasmacytoid DC and psoriasis

Plasmacytoid DC (pDC) produce type I interferons in response to viral infection. Plasmacytoid pre-DC are key to the upstream pathway of psoriasis pathogenesis *in vivo*, through their production of IFN-α, and are significantly increased in lesional and non-lesional psoriasis compared to healthy control (Nestle et al., 2005). The expression of

type I interferons and type I IFN-inducible genes is significantly increased in psoriatic lesional skin compared to healthy control skin (Yao et al., 2008). Xenotransplantation of clinically uninvolved psoriatic skin onto mice demonstrated increased human *IFNA* mRNA expression prior to the development of clinical psoriasis, while administration of neutralizing anti-IFNα/β receptor antibody prevented T cell activation and expansion, and in turn the development of clinical disease (Nestle et al., 2005). Unfortunately, use of a monoclonal antibody to IFN-α was deemed clinically ineffective in humans (Bissonnette et al., 2010), suggesting that it may be key to the precipitation, rather than maintenance, of plaque psoriasis.

Keratinocytes as APC

As well as MHC Class I, keratinocytes express MHC Class II molecules under certain conditions. IFN-γ can induce HLA-DR, HLA-DQ and ICAM-1 expression on human keratinocytes isolated and cultured from normal skin (Griffiths et al., 1989). MHC Class II molecules (HLA-DR) have been identified on keratinocytes in psoriasis biopsies (Auboeck et al., 1986). Primary keratinocytes expressing MHC Class II and ICAM-1 are able to prompt both T_H1 and T_H2 responses on presenting peptide antigens to $CD4^+$ T cell clones (Black et al., 2007).

1.4 The Role of CD1a in healthy and diseased skin

1.4.1 APC and CD1a

Groups 1 CD1 molecules are expressed on APC including LC, myeloid DC and macrophages, as well as on thymocytes. CD1 molecules are generally considered monomorphic, although across species they are polymorphic. The differences in CD1a

composition may represent evolutionary adaptation to allow the most relevant antigens for each species to be presented (Le Nours et al., 2018).

CD1a is particularly densely expressed on LC, in higher amounts than even MHC Class II (Meunier et al., 1996). CD1a-autoreactive T cells promote dendritic cell maturation, linking the innate and adaptive immune systems (Vincent et al., 2002). Co-culture of allogeneic T cells with Dex-TNF-α stimulated activated monocyte-derived Langerhans cells, with secretion of IL-6 and TNF-α and production of IL-22 in the presence of squalene (Otsuka et al., 2018).

1.4.2 CD1a structure and ligands

The CD1a binding cleft consists of an A' and an F' pocket and is the smallest of the CD1 members at ~1300Å in volume, accommodating the alkyl tails of the binding ligand in the A' pocket and most of the fatty acid chain and hydrophobic head group in the F' pocket (Zajonc et al., 2003). CD1a also has an accessory portal above the F' pocket (Birkinshaw et al., 2015). The A' pocket acts as a "molecular ruler" for the hydrophobic acyl chains of CD1a ligands, accommodating those C_{18}-C_{23} long, while the entire CD1a binding cleft can bind those C_{32}-C_{42} in total (Zajonc et al., 2003). De Jong et al subsequently identified permissive antigens with variable carbon chains of C_{16} to C_{51} (De Jong et al., 2014), while most recent evidence reports a CD1a ligand chain length of C_{15}-C_{42} (Huang et al., 2023). In general, CD1 ligands have an amphipathic structure, consisting of hydrophilic head groups made up of peptide, carbohydrate or inorganic esters attached to hydrophobic "flexible aliphatic hydrocarbon chains" which nest within the CD1 binding groove (Van Rhijn et al., 2015). Several models for CD1 binding have been suggested, including headgroup discrimination, interference/absence of interference and CD1 remodelling (Moody & Cotton, 2017). Ligands may be permissive or non-permissive. Non-permissive ligands may have large polar head groups that block TCR binding to CD1a. While glycolipids or

phospholipids, including sphingomyelin and phosphatidylcholine, acted as non-permissive ligands to inhibit the autoreactivity of T cells of the BC2 T cell line, apolar lipids, such as those found in sebum, may displace them from the binding cleft and produce a T cell response (De Jong et al., 2014).

A range of CD1a lipid antigens have been described to date (**Table 1.2**) and for some the CD1a-ligand crystal structure has been defined (Cotton et al., 2021; J. H. Kim et al., 2016; Nicolai et al., 2020; Zajonc et al., 2003, 2005). Recently, comparative lipidomic analysis across CD1 isoforms has defined a wider range of CD1a ligands than previously considered (Huang et al., 2023).

*Table 1.2 Known CD1a antigens. *Farnesol, as an intermediate in the cholesterol biosynthetic pathway, may also be endogenous but has been assessed in the context of external exposure in allergic contact dermatitis.*

Endogenous ligands	Exogenous ligands
Sulfatide (Shamshiev et al., 2002)	Didehydroxymycobactins (DDM) (Moody et al., 2004; Zajonc et al., 2005) Lysylphosphatidylglycerol (Monnot et al., 2023)
Membrane glycolipids and phospholipids including phosphatidylcholine, lysophophatidylcholine, phosphatidylinositol, sphingomyelin (Birkinshaw et al., 2015; De Jong et al., 2014; Monnot et al., 2023)	Urushiol (J. H. Kim et al., 2016)

Small “headless” antigens: squalene, triacylglyceride, free fatty acids, wax esters (De Jong et al., 2014)	*Farnesol and related (Nicolai et al., 2020)

Many CD1a ligands such as apolar lipids are found extracellularly in the stratum corneum and sebum(Kellum, 1967; Lampe et al., 1983; Nicolaides, 1974) and therefore are hypothesised to only be encountered by CD1a upon breach of these compartments during trauma or inflammation. On release, these small lipids are suggested to overwhelm and displace the ubiquitous inhibitory polar lipids thought to be present in the CD1a cleft at homeostasis, activating a CD1a-mediated immune response (De Jong, 2015).

Aside from exposing compartmentalised lipids, inflammation can also stimulate phospholipase activity with increased generation of small, permissive CD1 ligands from ubiquitous phospholipids and resultant CD1-autoreactive T cell stimulation. This has been shown for CD1a in the context of inflammatory skin disease, for both endogenous (from mast cells in psoriasis) (Cheung et al., 2016) and exogenous (from house dust mite in atopic dermatitis) (Jarrett et al., 2016) phospholipases. It has also been described for the venom of wasps and bees (Bourgeois et al., 2015). Bacterial and fungal phospholipases may also conceivably be a potential source of CD1a ligands, suggesting a role for the cutaneous microbiome in health and disease. Triglycerides and esters are broken down by commensal bacteria and yeasts such as *Proteobacteria* and *Malassezia* to produce free FA. Phospholipases are also part of the armament of many common cutaneous pathogens including *Staphylococcus aureus* (Caporarello et al., 2015; C. Hardman et al., 2017), *Propionibacterium acnes* (Scholz & Kilian, 2016) and *Malassezia spp* (Dawson, 2007; Tee et al., 2019). *Malassezia spp* alter sebum composition through the degradation of triglycerides, resulting in saturated free FA, which they consume, and

unsaturated free FA which persist (Ro & Dawson, 2005). The results of studies attempting to evaluate the cutaneous microbiome in psoriasis are conflicting and no consensus has been reached as to whether the microbiome in psoriasis is more or less diverse than in healthy skin (Alekseyenko et al., 2013; Chang et al., 2018; Fahlén et al., 2012; Gao et al., 2008). It is known that microbiome in lesional and non-lesional psoriasis may be altered by NB-UVB phototherapy and immunosuppressant/biologic therapy (Alekseyenko et al., 2013; Assarsson et al., 2018).

1.4.3 CD1a-autoreactive T cells

CD1 autoreactivity is T cell recognition of CD1 bound to an endogenous lipid antigen (De Jong et al., 2010). CD1-autoreactive T cells can promote DC maturation, through recognition of Group 1 CD1 molecules on the surface of immature dendritic cells (Vincent et al., 2002). Porcelli et al demonstrated binding of a $CD4^-/CD8^-$ αβ TCR on a cytolytic T cell line to CD1a back in 1989 (Porcelli et al., 1989). The response of *ex vivo* polyclonal T cells to endogenous CD1a is greater than to other Group 1 or Group 2 CD1s (De Jong et al., 2010). This is also seen in clonal experiments (De Lalla et al., 2011). CD1a-autoreactive T cells are a normal part of the αβ T cell repertoire; consisting of an estimated 0.02%-0.4% of peripheral blood memory T cells (De Jong et al., 2010). They produce IFN-γ and IL-22 and express skin homing molecules including CC4, CCR6 and CCR10 (De Jong et al., 2010). More recently, it has been suggested that up to 26% of T cells in healthy skin are CD1a-autoreactive (Bryan et al., 2024).

The crystal structure of αβ TCR-CD1a-ligand binding was elucidated using the BK6 cell line by Birkenshaw and Pellici (Birkinshaw et al., 2015). BK6 TCR binding to CD1a did not involve direct interaction with the bound lipid ligand across a range of permissive and non-permissive CD1a ligands. Those ligands with large head groups were able to block TCR binding by interfering with A' roof residues (Birkinshaw et al., 2015). More recently,

a γδ TCR ternary structure has also been solved, revealing an unusual TCR orientation to the side of CD1a (Wegrecki et al., 2022).

1.5 Thesis aims

The overall aim of this thesis was to investigate novel CD1a-lipid antigen presentation pathways in the skin, particularly in the context of cutaneous inflammation, using psoriasis as a disease example. This aim was addressed through the following specific objectives:

1) Define alterations in candidate lipid enzyme pathways in psoriatic skin based on gene expression and protein expression.
2) Use these and publicly available research resources to identify CD1a antigens with relevance to disease and treatment.

2 Chapter 2 Materials and Methods

2.1 Media and buffers

2.1.1 Media

Media used are described in **Table 2.1**.

Table 2.1 Media. DMSO; dimethyl sulfoxide.

Medium	Composition
R-HEPES	RPMI 1640 (Sigma-Aldrich, R8758 or Gibco, 21875-034), 1% HEPES (Thermo Fisher, 15630056)
K562 Media	RPMI 1640 (Sigma-Aldrich, R8758 or Gibco, 21875-034), 10% filtered Foetal Bovine Serum (Sigma-Aldrich, F9665) Lot ending #1010 or #3716, 10mM HEPES (Thermo Fisher, 15630056), 2mM L-Glutamine solution (Sigma-Aldrich, G7513), 100 IU/mL pencillin/100µg/mL Pencillin-Streptomycin (Sigma-Aldrich, P0781), 1x MEM NEAA (Thermo Fisher, 11140050), 1mM sodium pyruvate (Thermo Fisher, 11360070), 50µM 2-mercaptoethanol (Thermo Fisher, 31350010), 200µg/mL Geneticin G-418 sulphate (Gibco, 108321-42-2)
Complete Media (R10)	RPMI 1640 (Sigma-Aldrich, R8758 or Gibco 21875-034), 10% filtered Foetal Bovine Serum (Sigma-Aldrich, F9665) Lot ending #1010 or #3716, 10mM HEPES (Thermo Fisher, 15630056), 2mM L-Glutamine solution (Sigma-Aldrich, G7513), 100 IU/mL pencillin/100µg/mL Pencillin-Streptomycin (Sigma-Aldrich, P0781), 1x MEM NEAA (Thermo Fisher, 11140050), 1mM sodium pyruvate (Thermo Fisher, 11360070), 50µM 2-mercaptoethanol (Thermo Fisher, 31350010)
Complete Media CD1a (CMCD1a)	RPMI 1640 (Sigma-Aldrich, R8758 or Gibco 21875-034), 10% filtered Foetal Bovine Serum (Sigma-Aldrich, F9665) Lot ending #1626V or #200102, 10mM HEPES (Thermo Fisher, 15630056), 2mM L-Glutamine solution (Sigma-Aldrich, G7513), 100 IU/mL pencillin/100µg/mL Pencillin-Streptomycin (Sigma-Aldrich,

	P0781), 1x MEM NEAA (Thermo Fisher, 11140050), 1mM sodium pyruvate (Thermo Fisher, 11360070), 50µM 2-mercaptoethanol (Thermo Fisher, 31350010)
T cell media	RPMI 1640 (Sigma-Aldrich, R8758 or Gibco 21875-034), 10% filtered human serum (Sigma-Aldrich, H4522) Lot ending #8068 or #9067, 10mM HEPES (Thermo Fisher, 15630056), 2mM L-Glutamine solution (Sigma-Aldrich, G7513), 100 IU/mL pencillin/100µg/mL Pencillin-Streptomycin (Sigma-Aldrich, P0781), 1x MEM NEAA (Thermo Fisher, 11140050), 1mM sodium pyruvate (Thermo Fisher, 11360070), 50µM 2-mercaptoethanol (Thermo Fisher, 31350010), 200IU/mL IL-2 (Biolegend, 589108)
Monocyte-derived dendritic cell (moDC) media	CMCD1a plus recombinant human GM-CSF (Biolegend, 572905) at a final concentration of 100ng/mL and recombinant human IL-4 (Biolegend, 574008) at a final concentration of 50ng/mL
Freezing mix	90% filtered Foetal Bovine Serum #1010, 10% DMSO (Sigma-Aldrich, 276855)

2.1.2 Buffers

Buffers used are described in **Table 2.2**.

Table 2.2 Buffers. MACS; Magnetic Activated Cell Sorting, FACS; Fluorescence Activated Cell Sorting, PBS; phosphate-buffered saline.

Buffer	Composition
MACS buffer	0.5% Bovine Serum Albumin (Sigma-Aldrich, A7906) or FBS (Sigma-Aldrich, F9665) Lot ending #1010 or #3716, 2mM EDTA (0.5M EDTA, Invitrogen, AM9260G) in 500mL sterile PBS
FACS buffer	2% filtered Foetal Bovine Serum (Sigma-Aldrich, F9665) Lot ending #1010 or #3716, 1mM EDTA (0.5M EDTA, Invitrogen, AM9260G) in 500mL sterile PBS

2.2 Cell culture

2.2.1 Cell culture notes

Foetal bovine serum (FBS): The FBS used for making R10 and K562 media was general laboratory stock (#1010). For monocyte-derived DC (moDC) and co-culture experiments using K562 and T cells from 2020 onwards, lots #1626V and #200102, which on screening were found to most effectively promote CD1a expression, were used to make CMCD1a media.

All counting was performed using the Countess cell counter (Life Technologies) following dilution of cells 1:1 with trypan blue 0.4% (Gibco, 15250-061) to assess viability. Final cell numbers per well for co-culture experiments are detailed in **Table 2.3**.

All cells were incubated at 37°C and 5% CO2 for antigen pulsing, co-culture and toxicity experiments. Unless otherwise specified, all centrifugation was at 400xg for 5 minutes. Washing implies addition of R-HEPES followed by centrifugation at 400xg for 5 minutes.

For antigen pulsing of K562 cells/moDC and co-culture in 96-well plates, peripheral wells

were filled with 1mL or 200µL of phosphate-buffered saline (PBS) respectively. Overnight refers to an incubation of minimum 16 hours.

Table 2.3 Final concentrations of cells for co-culture step of experiments.

Experiment	**Cells**	**Step**	**Final cell number/well**
ELISpot	K562	Antigen pulsing	0.5 x 10^6 cells/well (2018/19) 1 x 10^6 cells/well (2020/1)
		Co-culture	0.025 x 10^6 cells/well
ELISA	K562	Antigen pulsing	1 x 10^6/well
		Co-culture	0.15 x 10^6 cells/well
BK6 Functional Assay	K562	Antigen pulsing	0.5 x 10^6/well
		Co-culture	0.025 x 10^6 cells/well
ELISpot	T cells (polyclonal)	Co-culture	0.075 x 10^6 cells/well
ELISA	T cells (clones)	Co-culture	0.1 x 10^6 cells/well
BK6 Functional Assay	T cells (Jurkats)	Co-culture	0.075 x 10^6 cells/well

2.2.2 Freezing and Thawing Cells

Cells were frozen suspended in 1mL of freezing mix in cryovials that were stored for a minimum of 24 hours in Mr Frosty (containing 250mL isopropyl alcohol) at -80°C, then transferred to boxes within the -80°C. Samples were stored in accordance with Human Tissue Authority (HTA) guidelines.

Cryovials were thawed by warming in the water bath at 37°C for 1-2 minutes until the ice was just melted, then the contents transferred into Falcon tubes containing warmed media using a P1000 pipette. Further warmed media was then added dropwise. Cells were centrifuged, washed twice then transferred to flasks or plates as appropriate.

2.2.3 K562 cell culture

K562 cells are an immortal human chronic myelogenous leukaemia (CML) cell line transduced using a lentiviral vector to express either CD1a or empty vector (EV) (kind gift of Professor Branch Moody, Harvard). This model has been validated for use in CD1a work (De Jong et al., 2010). Cells were intermittently screened for mycoplasma contamination and stained to assess expression of CD1a and CD45. In this thesis, "K562 cells" refer to K562-EV and K562-CD1a collectively.

2.2.4 PBMC isolation

Blood samples from healthy adults at the Weatherall Institute of Molecular Medicine and patients from the dermatology clinic at Churchill Hospital (COREC reference number 14/NW/1153 Cellular immune responses in inflamed skin) were collected in 9mL Lithium Heparin vacuum tubes following informed consent. 13mL of Lymphoprep™ (STEMCELL™ Technologies, 07851/07861) was layered under 25mL of blood diluted 1:1 with R-HEPES in 50mL Falcon tubes, which were then centrifuged at 800xg for 20

minutes at acceleration 9, deceleration 0. Mononuclear cells at the interface between serum (above) and Lymphoprep™ (below) were transferred to a new Falcon tube, topped up to 50mL with R-HEPES, then centrifuged at 600-800xg for 10 minutes at acceleration 9, deceleration 9. The pellet was washed twice more with 50mL R-HEPES, spinning at 400xg for 5 minutes. From 2020 on, the SepMate Protocol and SepMate tubes (SepMate #85450) were used, with 15mL of Lymphoprep™ applied to the tube prior to the addition of blood diluted in R10. Tubes were centrifuged at 1200xg for 10 minutes with acceleration 9, deceleration 9, then transfer of supernatant to a fresh 50mL Falcon tube was followed by washes with R10 at 800xg for 8 minutes and 300xg for 5 minutes. The cells were then counted and either frozen or further processed for use in experiments.

2.2.5 MACS (Magnetic-Activated Cell Sorting) separation

CD3 (T cells) or CD14 (moDC) MicroBeads were used (Miltenyi Biotec, 030-050-101 (CD3), 130-050-201 (CD14)). Peripheral blood mononuclear cells (PBMC) were centrifuged, the pellet re-suspended in 80µL of MACS buffer per 10^7 cells and the appropriate microbeads at 20µL per 10^7 cells added with sample incubation at 4°C for 15 minutes. Cells were washed with 1-2mL of MACS buffer per 10^7 cells. LS columns (Miltenyi Biotec, 130-042-401) with 30µm pre-separation filters (Miltenyi Biotec, 030-041-407) were placed into the QuadroMACS™ magnetic separator (Miltenyi Biotec, 130-090-976). Columns were prepped with 3mL of MACS buffer. The cell pellet was re-suspended in 500µL of MACS buffer per 10^8 cells then added to the column, followed by three further washes of MACS buffer, each passing fully through the column prior to the next addition. The filter was discarded and the column removed from the magnetic separator and placed atop a fresh 15mL Falcon tube. After addition of 5mL of appropriate media to the column, the positive fraction was discharged into the Falcon tube for counting. Cells were

plated in appropriate media and incubated for a minimum of 2-3 days prior to experimental use to allow for discharging of MACS beads and cell recovery.

2.2.6 T cell culture

Following MACS of PBMC, $CD3^+$ cells were cultured in T cell media with IL-2 (Biolegend, 589108) at 200IU/mL. Cells were cultured in 48-well plates at 2 x 10^6 cells/mL for 2-3 days prior to use in assays.

2.2.7 Differentiation of dendritic cells from monocytes

Day 0: The $CD14^+$ fraction post-MACS was re-suspended at 0.6 x 10^6/mL in moDC media and plated as 1mL/well to a 48-well non-tissue coated plate. A separate well of cells at the same concentration was plated in CMCD1a as a $CD14^+$ only control.

Day 3: Cellular differentiation was assessed microscopically +/- photographed, then 500µL of media was carefully removed from the side of each well without disturbing the cells. Cells were either pulsed with 500µL of 2x antigen solution in moDC media or fed with 1x of freshly made moDC media, gently discharged against the side of the well, avoiding re-suspension. The $CD14^+$ only well was fed with CMCD1a.

Day 5: As for Day 3, but no media removed/replaced for wells that were not for Day 5 pulsing.

Note: Previous experiments (2019) used either non-tissue coated 24-well plates (1mL of cells at 1 x 10^6/mL with an additional 1mL of moDC media at feeding) if <10^6 cells in total. If more, a non-tissue culture coated single round plate was used with the same concentration. Antigen pulsing was performed on Day 5 only (except for one donor) and cells counted and re-suspended at 2 x 10^6/mL and plated to a 96-well plate as 50µL per well with 50µL of 2x antigen solution.

2.3 Flow cytometry staining

Flow cytometry staining was performed to assess cell viability, expression of surface markers and functional responses across a range of experiments. Each plate contained samples for assessment, single-stain and FMO (fluorescence minus one) controls. Cells were washed in PBS, antibodies (**Table 2.4**) applied and the plate incubated at 4°C for 20 minutes. It was then washed 1.5 times and fixed using 4% formaldehyde at room temperature (RT) for 15 minutes, then washed 1.5 times and re-suspended in FACS buffer for analysis. All flow cytometry was performed on the Attune NxT and analysed using FlowJo™ version 10 software.

Table 2.4 Flow Cytometry antibodies.

Specificity	Fluorophore	Supplier	Clone	Cat No	Dilution	Diluent
CD1a	APC	Biolegend	HI149	300110	1:100	FACS buffer
CD1a	BV421	Biolegend	HI149	300127	1:100	FACS buffer
CD1a	PE	Biolegend	HI149	300105	1:100	FACS buffer
CD45	FITC	Biolegend	2D1	368507	1:100	FACS buffer
CD45	PE	Biolegend	2D1	368510	1:100	FACS buffer
HLA-DR	FITC	Biolegend	L243	307604	1:100	FACS buffer
HLA-DR	PerCP	Biolegend	L243	307628	1:100	FACS buffer
HLA-DR	Pacific Blue	Biolegend	L243	307633	1:100	FACS buffer
CD11c	PerCP	Biolegend	Bu15	337234	1:100	FACS buffer
CD11c	PE	Biolegend	Bu15	337205	1:100	FACS buffer
CD11c	PE/Cy7	Biolegend	VS143	337215	1:100	FACS buffer
CD14	APC	Biolegend	HCD14	325608	1:100	FACS buffer
Live/Dead	Aqua	Invitrogen	-	L34965	1:500	PBS (FACS buffer if used in combination with other antibodies)
Live/Dead	DRAQ7	Biolegend	-	424001	1:100	PBS
Annexin V	BV510	Biolegend	-	640937	1:100	Annexin V binding buffer (Biolegend 422201)
CD3	BV711	Biolegend	UCHT1	300464	1:100	FACS buffer
CD69	APC	Biolegend	FN50	310910	1:100	FACS buffer
CD4	PE/Cy7	Biolegend	SK3	344611	1:100	FACS buffer
CD8a	APC	Biolegend	Hit8a	300912	1:100	FACS buffer
CD8a	PerCP	Biolegend	RPA-T8	301030	1:100	FACS buffer
CD25	PE	Biolegend	M-A251	356104	1:100	FACS buffer
Tetramer/ Dextramer	Streptavidin PE	Biolegend	-	405245	-	-
Tetramer	Streptavidin APC	Biolegend	-	405243	-	-
Tetramer	Streptavidin BV421	Biolegend	-	405225	-	-

When using Fixable Aqua as Live/Dead stain:

Fixable aqua at 1:500 in FACS buffer was combined with other antibodies for comprehensive staining (50µL/well). In some early experiments, cells were stained first with fixable aqua at 1:1000 in PBS (40µL/well) at 4°C for 20 minutes, then washed in FACS buffer before staining with other antibodies.

When using DRAQ7 as Live/Dead stain:

The single-stain and FMO controls and mastermixes were applied first at 50µL/well, then after washing 1.5 times, DRAQ7 at 200µL per well was added. Samples were ideally run within 2 hours of staining, with no washing or fixation steps required.

When using Annexin V to stain for apoptosis:

Annexin V was applied between the single-stain controls/mastermixes and DRAQ7 step, with only one wash between Annexin V and DRAQ7 application.

Making beads for single-stain controls:

Compensation beads used are described in **Table 2.5**.

Table 2.5 Compensation beads for flow cytometry.

Beads	Stain
ArC™ Reactive beads (pre-incubation)/ArC™ Reactive negative beads (post-incubation) (Thermo Fisher, A10346)	Live/Dead Aqua
UltraComp eBeads™ (Invitrogen, 01-2222-42)	All other antibodies

1µL of antibody was added to 1 drop of the relevant vortexed beads in an Eppendorf tube and incubated for 20 minutes at 4°C. For Live/Dead, one drop of ArC™ Reactive negative beads was added and the beads re-suspended in FACS buffer. For all other antibodies, the tube was then centrifuged, supernatant removed and beads re-suspended in FACS buffer.

In some cases, beads were mixed with single-stain controls cell samples before running compensation controls on the Attune NxT.

2.4 Lipids

2.4.1 Lipid solutions

Lipids were dissolved in solvents as per **Table 2.6**. Original stocks were stored at -20°C, except retinyl oleate (-80°C). Once made up in solvent, they were stored in brown glass vials under nitrogen. Aliquots were brought to RT prior to experimental use and sonicated at 65˚C for 20 minutes (2019: 50˚C for 5 minutes for Retinyl Esters, DCT/Psoriderm™/Acitretin ELISpot). They were further dissolved in media in brown glass vials and sonicated at 37˚C for 20 minutes (2019: 50˚C for 5 minutes in Eppendorf/Falcon tubes).

Table 2.6 Candidate CD1a lipid antigens. Fx Ax: Functional Assay.

Lipid	**Original form**	**Provenance**	**Preparation**	**Vehicle**	**Storage once made up in solvent**	**Stock/ used for IEF Gel**	**Final concentration for pulsing**
All-trans-retinyl oleate (RO)	Yellow oil	Toronto Research Chemicals, R275410	Dissolved in chloroform, aliquoted, then dried down	DMSO	4°C	40mM	K562 ELISpot: 2μM, 0.2μM (2019) 50μM (2020/1) ELISA: 50μM BK6 Fx Ax: 50μM, 25μM

							moDC 25μM
All-trans-retinyl stearate (RS)	Pale yellow solid	Toronto Research Chemicals, R275610	Dissolved in chloroform, aliquoted, then dried down	DMSO	4°C	40mM	K562 ELISpot: 2μM, 0.2μM (2019) 50μM (2020/1) ELISA: 50μM BK6 Fx Ax: 50μM, 25μM moDC

							25µM
All-trans-retinyl palmitate (RP)	Yellow solid	Toronto Research Chemicals Toronto Research Chemicals 79-81-2/R275450	Dissolved directly in DMSO	DMSO	4°C	40mM	K562 ELISpot: 2µM, 0.2µM (2019) 50µM (2020/1) ELISA: 50µM BK6 Fx Ax: 50µM, 25µM moDC 25µM

9-nitrooleate (9-NO)	In a solution in ethanol	Santa Cruz Biotechnology 875685-44-2 or Chem Cruz SC-204632	Dried down then dissolved in DMSO	DMSO	-20°C	20mM	K562 ELISpot: 5µM ELISA: 5µM BK6 Fx Ax: 5µM moDC 5µM
10-nitrooleate (10-NO)	In a solution in ethanol	Cayman Chemical Company, 10008043	Dried down then dissolved in DMSO	DMSO	-20°C	20mM	K562 ELISpot: 5µM

							ELISA: 5μM BK6 Fx Ax: N/A <u>moDC</u> 5μM
NO2-CLA	In a solution in ethanol	Cayman Chemical Company 30160	Dried down then dissolved in DMSO	DMSO	-20°C	20mM	<u>K562</u> ELISpot: 10μM ELISA: 10μM

							BK6 Fx Ax: 10μM <u>moDC</u> 10μM
Cholesterol	Powder	Sigma-Aldrich C8667 or C045	Nil	See chapter 6	Made up fresh each time	40mM	<u>K562</u> ELISpot: 200μM ELISA: 200μM or 200μg/mL <u>moDC</u> 200μM

Cholesteryl Oleate	Powder	Sigma-Aldrich C9253	Nil	See chapter 6	Made up fresh each time	40mM	K562 N/A moDC 200μM
Cholesteryl Palmitate	Flakes	Sigma-Aldrich C6072	Nil	See chapter 6	Made up fresh each time	40mM	K562 N/A moDC 200μM
Aramchol	Crystalline solid	Cayman Chemical Company 22478	Nil	DMSO or 0.25%	4°C	40mM, 20mM	N/A

				tyloxapol/2% DMSO			
Hydroxy cholesterols	Powder	Avanti Polar Lipids 700019P (25-OHC) Sigma-Aldrich SML2042 (27-OHC)	Nil	DMSO or 0.25% tyloxapol/2% DMSO	4°C	20mM, 10mM	N/A
Acitretin	Yellow powder	European Pharmacopoeia, A0225000	Dissolved in chloroform, aliquoted, then dried down	DMSO	4°C	40mM	<u>K562</u> 50μM, 25μM <u>moDC</u> 50μM, 25μM

Distilled coal tar solution	Brown liquid	Alfa Aesar, 43671	Aliquoted, then dried down with nitrogen stream	Ethanol or DMSO	-20°C	25mg/mL	K562 50µg/mL, 25µ/mL moDC N/A
Psoriderm™ 40% w/v bath additive	Brown liquid	Dermal™, over-the-counter purchase, Lot N3470	Aliquoted, then dried down with nitrogen stream	Ethanol or DMSO	-20°C	25mg/mL	K562 50µg/mL, 25µg/mL moDC N/A

Bakuchiol	Yellow oil	Cayman Chemical Company, 11684	Nil	DMSO	Made up fresh	40mM	N/A
Thymoquinone	Yellow crystalline solid	Cayman Chemical Company, 15039	Dissolved in chloroform:methanol 2:1, aliquoted, then dried down with nitrogen stream	DMSO	Made up fresh	40mM	N/A
Curcumin	Orange-yellow crystalline powder	Enzo Life Sciences, ALX-350-028-M010	Nil	DMSO	Made up fresh	40mM	N/A

2.4.2 Iso-Electric Focussing (IEF) Gels

IEF gels separate proteins based on their iso-electric point [pH(I) or pI], the pH at which their net charge is equal to zero. Loading of the CD1a cleft with different lipids may alter its pH and therefore pI, making IEF an appropriate assay to ascertain lipid loading to CD1a. Results are also affected by endogenous lipids contained in the CD1a cleft so a control, "endo", with PBS only added to CD1a is used. Two different types of CD1a were used for the experiments documented in this thesis (**Table 2.7**).

*Table 2.7 CD1a used for IEF gels. *Work of Dr Yi-Ling Chen and Jessica Ng, used for all IEF gels unless otherwise stipulated. **From NIH Tetramer Core Facility at Emory University, Atlanta, GA, USA.*

CD1a	Purification	Stock concentration	Atomic mass	FC	Biotinylated	Storage
In-house*	Using a non-acidic process from 293T cells	2mg/mL (approx. 40μM)	49kDa	Without	No	-80°C then 4°C for up to 2 weeks
NIH**	293T cells	2mg/mL (approx. 40μM)	50kDa	Without	Yes	-80°C

All incubations were overnight at RT, protected from light.

Gel experiments were performed over two days (Day 1: loading with candidate lipid/Day 2: run) or three days (Day 1: pre-loading with known CD1a ligand/Day 2: loading with candidate lipid/Day 3: run). For 2-day gels, candidate lipids were loaded at a calculated

molar excess (50-200) vs CD1a. Known CD1a ligands used for 3-day gels were bovine ganglioside 3 (GD3) (Avanti Polar Lipids, 860060P), lysophosphatidylcholine 18:1 (1-oleoyl-2-hydroxy-sn-glycero-3-phosphocholine, LPC) (Avanti Polar Lipids, 845875P) or sphingomyelin 24:1 (N-nervonoyl-D-erythro-sphingosylphosphorylcholine, SM) (Avanti Polar Lipids, 860593P), which were made up as 40mM in 0.25% tyloxapol/2% DMSO (GD3) or 0.5% CHAPS (LPC, SM) then loaded as 1µL of a 33x (13.3mM) solution, while the candidate lipid was loaded as 1µL at 100x (retinyl esters 40mM) or 50x (NFA 20mM).

General method 2-day gel:

Day 1: 8µL or 9µL of RT CD1a was loaded with 2µL or 1µL respectively of PBS ("endo"), solvent control (mock) or candidate lipid, to a final volume of 10µL, in a PCR tube. Tubes were tapped to mix, gently centrifuged (repeat x 1) and incubated in a drawer overnight at RT (minimum 16 hours).

Day 2: Anode buffer was prepared by adding 12mL of 50x IEF Anode Buffer (Novex, LC5300) to 588mL of MilliQ water. Cathode buffer was prepared by adding 20mL of 10x IEF Cathode Buffer (Novex, LC5370) to 180mL of MilliQ water. The wells of an IEF precast gel of pH 3-7 (1mm thick, 5% acrylamide) (Novex, EC6645BOX) were rinsed with cathode buffer, the gel held in place using an XCell SureLock™ Mini-Cell system and the upper chamber filled with cathode buffer. The first well was loaded with 5µL of IEF marker (Invitrogen, 3921201). Samples were mixed 1:1 with 10µL of IEF sample buffer (Novex, LC5371) to make a final volume of 20µL, loading 18µL/well. The lower buffer chamber was filled with anode buffer. The gels were run on ice inside a polystyrene box to prevent overheating, at 100V constant for one hour, 200V constant for 1 hour then 500V constant for 30 minutes. Once complete, the gel was trimmed and removed from its cassette and fixed at RT in 12% trichloroacetic acid (TCA) (Sigma-Aldrich, T8657) in MilliQ water for 45 minutes to 1 hour. It was then rinsed well with distilled water (DW)

including gentle shaking, the DW refreshed and microwaved for one minute. It was drained, then microwaved for a further one minute in Simply Blue Safe Stain (Thermo Fisher, LC6060). It was washed with DW, left on the shaker overnight and subsequently photographed on the Invitrogen iBrightFL1000machine (Thermo Fisher).

3-day gels were similar but used 1µL of known CD1a ligand on Day 1 and 1µL of the candidate lipid ligand on Day 2. An example using LPC (Day 1) and retinyl oleate (Day 2) is shown in **Table 2.8**.

Table 2.8 IEF gel (3-day) for retinyl oleate, using LPC as the known CD1a ligand. LPC; Lysophosphatidylcholine, RO; Retinyl Oleate.

Tube	**Endo**	**RO mock^{LPC+} (DMSO) 100x**	**RO^{LPC+} (DMSO) 100x**	**RO mock^{LPCneg} (DMSO) 100x**	**RO^{LPCneg} (DMSO) 100x**	**LPC mock (- ctrl)**	**LPC (+ ctrl)**	**RO end well**
Volume of CD1a (µL)	8	8	8	8	8	8	8	8
Volume of lipid (RE) (µL)			1		1			1
Volume of lipid mock (DMSO) (µL)		1		1				
Volume of LPC (µL)		1	1				1	
Volume of LPC mock (0.5% CHAPS) (µL)				1	1	1		
Volume of PBS (µL)	2					1	1	1

2.4.3 Toxicity Testing

Toxicity testing of lipids and solvents was performed by making serial dilutions with a volume of 100µL/well in a 96-well plate and adding K562 cells (EV and CD1a) 1 x 10^6/mL at 100µL/well. The plate was incubated for a minimum of 24 hours and then viability and CD1a expression assessed by FACS staining for Live-Dead and CD1a. In cases where autofluorescence was an issue, such as with DCT, viability was assessed using trypan blue. Due to the limited availability of fresh blood samples, toxicity testing was not performed on monocyte-derived dendritic cells. Instead, suitable concentrations were extrapolated from K562 toxicity test results.

2.4.4 Autofluorescence Testing

Samples of lipids (coal tar derivatives, acitretin) were plated with and without K562 cells. All laser channels on the flow cytometer were selected and K562 EV and CD1a cells run to set forward and side scatter. Lipids with and without cells, cells alone and FACS buffer alone were then run to assess for autofluorescence of the lipids that could be interfering with flow cytometry results for other experiments.

2.5 Tetramer and dextramer staining

The generation of CD1a-based multimers (tetramers and dextramers) is a relatively new technique that has been developed to measure the frequency of CD1a-reactive T cells (Kasmar et al., 2013). Comparison may be made between staining of T cells binding to endogenous lipids of the CD1a cleft and lipids that have been exogenously loaded.

2.5.1 Tetramer staining (using T cells)

Tetramer staining was performed to assess candidate lipid binding to CD1a. T cells were obtained from fresh PBMC samples and rested for 2 days. All incubations involving tetramers were performed protected from light.

Day 1: In-house biotinylated CD1a 2mg/mL monomer was loaded with lipid or PBS as per **Table 2.9** and incubated overnight at RT.

Table 2.9 Loading of biotinylated CD1a monomers.

	Endo (BV421)	**Lipid 1 (PE)**	**Lipid 2 (APC)**
CD1a (µL)	5	5	5
Lipid (µL)	0	1	1
PBS (µL)	5	4	4

Day 2: Tetramers were assembled using streptavidin as per **Table 2.10**. In between each addition, tubes were gently tapped to mix, then incubated at RT for 10 minutes.

Table 2.10 Tetramer assembly. TBS; tris-buffered saline.

SAV (Concentration)	**1:10 dilution (0.1mg/mL) x2**	**Neat (1mg/mL) x8**	**Amount of TBS to top up (µL)**
BV421 (0.5mg/mL)	3µL (~0.3µM)	3µL (~3µM)	0
PE	1.5µL (~0.3µM)	1.5µL (~3µM)	15

(High concentration 1mg/mL)			
APC (High concentration 1mg/mL)	1.5µL (~0.3µM)	1.5µL (~3µM)	15

Once made up, 15µL of TBS was added to the tubes containing lipids so all had equivalent volumes (40µL of 0.25µg/µL). Tetramers were stored at 4°C, protected from light, for use within 10-14 days.

Day 3: T cell concentration was adjusted to 2 x 10^6/mL and plated at 200µL/well to a 96-well round-bottomed plate. Cells were centrifuged and washed once with 200µL FACS buffer. Tetramer staining was performed as per **Table 2.11**.

Table 2.11 Tetramer staining. FACS-B; FACS buffer, SSC; Single-Stain Control, FMO; Fluorescence Minus One control, L/D; Live/Dead, MMA; Mastermix A, MMB; Mastermix B. (GFP); GFP used in BK6 tetramer staining experiments only. Step 1 in bold type, step 2 in italics.

	1	**2**	**3**	**4**	**5**	**6**	**7**
Samples		Donor 1 **MMA** *MMB*	Donor 2 **MMA** *MMB*				
Donor 1 FMO	**FCS-B** *FACS-B*	**MMA** *FMO L/D*	**MMA** *FMO CD3*	**FMO BV421** *MMB*	**FMO PE** *MMB*	**FMO APC** *MMB*	Donor 1
Donor 2 FMO	**FACS-B** *FACS-B*	**MMA**	**MMA**	**FMO BV421**	**FMO PE**	**FMO APC**	Donor 2

		FMO L/D	*FMO CD3*	*MMB*	*MMB*	*MMB*	
SSC (Donor 1 + Donor 2)	**FACS-B** *FACS-B (Unstained)*	**FACS-B** *SSC L/D*	**FACS-B** *SSC CD3*	**FACS-B** *SSC BV421*	**FACS-B** *SSC PE*	**FACS-B** *SSC APC*	**FACS-B** *FACS-B (GFP)*

Step 1 staining (tetramers):

Mastermix A (MMA) contained all tetramers beings used (BV421, PE, APC) 1:50 in FACS buffer. 50µL of tetramer/mastermix or FACS buffer was added to the relevant wells. The plate was incubated at RT for 30 minutes, then 1µL of the activating clone OKT3 (cat 317302) at 0.1µg/µl in FACS buffer was plated to each well to promote T cell receptor clustering. The plate was incubated at RT for 10 minutes.

Step 2 staining (surface):

Mastermix B (MMB) contained Live-Dead and CD3 (a different clone to OKT3) at 1:50. 50µL of 2x single-stain controls were produced for Live-Dead, CD3, BV421, PE and APC and added to the relevant wells, with 50µL of FACS buffer to unstained wells. The plate was incubated on ice for 15 minutes, then washed, fixed and washed as for standard flow cytometry staining (**Section 2.3**).

2.5.2 Dextramer staining (using PBMC)

CD1a-based dextramers were generated by Dr Yi-Ling Chen and research assistant Jessica Ng using in-house CD1a and stored at -80C. All incubations involving dextramers were performed protected from light.

Day 1: In-house biotinylated CD1a was loaded with candidate lipids as per **Table 2.12** and incubated at 37˚C overnight.

Table 2.12 Loading of biotinylated CD1a dextramers. TBS; tris-buffered saline.

CD1a	**14% DMSO/4% CHAPS in TBS**	**Candidate lipid**
5µL	4µL	1µL

Day 2: Dextramers were assembled by adding 7.5µL of loaded CD1a to 9µL of PE streptavidin, mixed well and incubated for 10 minutes at RT. For the dextran negative control, 7.5µL of 7%DMSO/2% CHAPS in TBS (above vehicle diluted 1:1 in TBS) was added to 9µL PE streptavidin instead. 0.625µL of 1mg/mL biotin-labelled Dextran (-20C frozen aliquot of 5mg/mL in DW further diluted in PBS) was mixed well with all samples and incubated for 30 minutes at RT. Finally, 3µL of 0.8mM D-Biotin in PBS (D-Biotin 50mM, Invitrogen, B20656) as blocking solution was added to stop the reaction and assembled dextramers were incubated at 4˚C overnight.

Day 3: Frozen PBMC were thawed and re-suspended in CMCD1a at 1 x 10^6/mL, rested in the incubator for one hour, then plated at 0.1 x 10^6 cells/well and centrifuged at 400xg for 5 minutes. Cells were re-suspended in 19µL of FACS buffer (Invitrogen,00-4222-26) and 1µL of Human TruStain FcX™ Fc receptor blocking solution and incubated at RT for 5 minutes. 5µL of the relevant assembled dextramer was added to each sample well, mixed well and incubated at RT for 30 minutes. 1µL of 0.1µg/µL OKT3 was added to each sample well and incubated at RT for 10 minutes. SSC and FMO wells contained FACS buffer only. Surface staining and fixing of samples and SSC/FMO controls were

performed as per **Section 2.3** using 2x concentration of Live-Dead Aqua and surface antibodies, with UCHT1 used as the CD3 clone to avoid interference with OKT3.

2.6 T cell assays

2.6.1 Interferon-γ ELISpot

Note: ELISpot experiments were done in complete media in 2018/19 but CMCD1a in 2020/21.

Day 1: Donor T cells were washed twice in R-HEPES then counted in 1mL CMCD1a and the concentration adjusted to 2 x 10^6 cells/mL. They were plated to a 48-well plate and incubated overnight. K562 cells were centrifuged, washed twice, counted in CMCD1a and the concentration adjusted to 2 x 10^6 cells/mL. They were plated to a 48-well plate in a 1:1 ratio with 2x antigen solution (**Table 2.3**). Sonicated CMCD1a only was added to the unpulsed wells. The plate was incubated for a minimum of 21 hours. Wells of a labelled ELISpot plate (Merck Multiscreen® Filter plates, MSIPS4510) were coated with 50µL of 35% ethanol in DW for a maximum of one minute, then washed five times with 200µL of sterile DW. Antibody (anti-human IFNγ mAB 1-D1K, purified, 1mg/mL, Mabtech, 3420-3-1000) was prepared as 15µL/mL of PBS and 70µL applied to each well after the plate was blotted dry. The plate was sealed and incubated overnight at 4°C.

Day 2: Pulsed K562 cells were re-suspended and washed twice before being counted in 1mL CMCD1a and the concentration adjusted to 0.25 x 10^6 cells/mL. The ELISpot plate was washed 5 times with plain RPMI (200µL/well), then blotted well and incubated with 100-200µL/well of CMCD1a for a minimum of 30-60 minutes. T cells were re-suspended, wells washed with CMCD1a, cells counted and concentration adjusted to 0.75 x 10^6

cells/mL. A PMA/ionomycin positive control was prepared to a final concentration of PMA 30ng/mL and ionomycin 15ng/mL. 100µL of K562 and 100µL of T cells were plated to the ELISpot plate (each sample in duplicate) which was then incubated for 16-24 hours.

Day 3: The ELISpot plate was washed five times with PBS, then 50µL/well of Human IFNγ Assay mAB 7-B6 1-Biotin 1mg/mL (Mabtech, 3420-2A) at 1:1000 in PBS +/- 0.5% FBS #1010 plated and incubated at RT in the dark for 2-3 hours. This step was repeated but using γ Streptavidin-ALP (Mabtech, 3420-2A) and incubating for 1-2 hours. The developing buffer solution was made up using AP (alkaline phosphatase) Conjugate substrate kit (Bio-Rad, 1706432). The ELISpot plate was washed thrice with PBS, then thrice with DW, then 100µL/well of developing buffer solution plated. Once spots appeared in the wells and a good response to the positive control was noted, the plate was washed well with DW, its plastic backing removed, and transferred to a drawer (dark, at RT) to dry out. Once completely dry, it was read using ELISpot 7.0 software on the ELISpot reader (AID Fluorescent Lamp, Advanced Imaging Devices Gmbh).

2.6.2 ELISA using CD1a-autoreactive T cell clones

Day 1: K562 cells were centrifuged, washed twice, then counted in 10mL CMCD1a and the concentration adjusted to 2 x 10^6 cells/mL. They were then plated to a 48-well plate in a 1:1 ratio with 2x antigen solution. Sonicated CMCD1a only was added to the unpulsed wells. The plate was incubated for 21- 22 hours.

Day 2: Pulsed K562 cells were washed, counted and concentration adjusted to 1.5 x 10^6 cells/mL in CMCD1a. CD1a-autoreactive T cell clones cultured by Dr Yi-Ling Chen were

washed once and the concentration adjusted to 1 x 10^6 cells/mL in CMCD1a cytokine cocktail according to the clone type.

100µl of K562 cells were co-cultured with 100µl T cell clones in a 96-well flat-bottomed plate and incubated overnight (24-25 hours).

Day 3: Cells were re-suspended and transferred into a 96-well round-bottomed plate, then centrifuged at 400xg for 5 minutes. 130µL of supernatant was carefully collected from each well taking care not to disturb the pellets and divided between two new 96-well round-bottomed plates. The plates were then labelled, sealed and frozen at -80°C until ready for ELISA.

ELISA was performed using the Biolegend ELISA Max™ Deluxe Set for interferon-γ (Biolegend, cat 430115) as per the manufacturer's protocol except:

- Half-well (Corning Costar® Assay Plate 96-well, cat 3690) rather than full well plates were used
- Plates were washed with PBS + 0.05% TWEEN (Sigma-Aldrich, P9416) using the ELISA plate washer (Thermo Scientific™ Wellwash™ Versa) 250µL/well x 3 without pauses, except for the wash after Avidin-HRP incubation which was 250µL/well x 5 with one-minute pauses

Once processing was complete, plates were read on the CLARIOstar® (BMG Labtech).

2.6.3 BK6 Functional Assay

This assay used flow cytometry to evaluate changes in cell surface markers (CD1a, CD3, CD69) on the Jurkat BK6 T cell line (kind gift of Professor Jamie Rossjohn, Monash) following 24-hour co-culture with lipid-pulsed K562 cells. BK6 cells are J76 cells(Porcelli et al., 1989) transduced to express the TCR sequence of the CD1a-reactive BK6 T cell

clone. They also express Green Fluorescent Protein (GFP), β2M and some CD1a at baseline while lacking endogenous α and β TCR chains. J76 $\beta2M^{neg}$ cells lack endogenous TCR α and β chains and a GFP tag. β2M has also been removed and they therefore lack surface expression of CD1a. Normal Jurkats have endogenous TCR α and β chains and maintain β2M but have no GFP tag.

Day 1: All three Jurkat T cell lines (BK6, $\beta2M^{neg}$ and normal Jurkats) were re-suspended, washed twice, counted in 1mL CMCD1a and the concentration adjusted to 1 x 10^6 cells/mL, then incubated overnight in a 48-well plate. K562 cells were centrifuged, washed twice, then counted in 10mL CMCD1a and the concentration adjusted to 2 x 10^6 cells/mL. They were then plated to a 48-well plate in a 1:1 ratio with 2x antigen solution (**Table 2.3**) and incubated for a minimum of 21 hours.

Day 2: Adjustment of cell concentrations was as for Day 2 ELISpot. 100µL of K562 cells were plated to a 96-well round-bottomed plate in duplicate for each condition (retinyl esters) or singly to a flat-bottomed plate (nitro-fatty acids). 100µL of BK6 cells were then added to all the sample wells. Control wells were plated as per **Table 2.13**. The plate was incubated for a minimum of 24 hours, then stained for flow cytometric analysis as per **Section 2.3**.

Table 2.13 BK6 Functional Assay: Cell plating for control wells.

Control	Cells
Unstained	50µL K562-EV 50µL K562-CD1a 100µL $\beta2M^{neg}$

Single-stain controls (Live/Dead, CD1a, CD3, CD69)	100µL β2M^{neg} 100µL normal Jurkats
GFP	100µL β2M^{neg} 100µL BK6
FMO (Live/Dead, CD1a, CD3, CD69)	50µL K562-EV 50µL K562-CD1a 100µL BK6
FMO GFP	50µL K562-EV 50µL K562-CD1a 100µL β2M^{neg}
Negative controls (EV only, CD1a only, BK6 only)	100µL cells 100µL CMCD1a
Positive control	100µL BK6 100µL 0.025% solution of CD3/CD28 (STEMCELL™ technologies Immunocult™ Human CD3/CD8 T cell activator, 10971) in CMCD1a

2.7 Assessing CD1a expression on moDC

MoDC were cultured as outlined in **Section 2.2.7** and pulsed on Day 3 +/- Day 5 using 1:1 pulsing with 2x antigen concentrations. On Day 6, minimum 24 hours after Day 5 pulsing, cells were transferred to 96-well round-bottomed plates and stained for flow cytometry as per **Section 2.3** using CD1a, HLA-DR, CD11c and CD14.

2.8 Collaborative work

2.8.1 RNA-Seq

RNA extraction and validation and bioinformatic analysis were performed as a collaborative effort with other members of the Ogg lab (Dr Randeep Singh, Dr Jeongmin Woo). Specific contributions and methods are outlined in **Chapter 3**.

2.8.2 Hyperion™ staining and analysis

Hyperion™ staining and analysis was performed by Dr Rachel Etherington of the MRC Weatherall Institute of Molecular Medicine Cytof facility. Further details on specific methodology are described in **Chapter 8**.

3 Chapter 3 RNA-Seq analysis

3.1 Background

3.1.1 Introduction

Assessment of differential gene expression permits comparison of the gene signature across different tissues in health and disease. In the skin, where baseline pathology and response to treatment are evaluated clinically, differentially expressed genes (DEG) may provide insight into disease pathogenesis, potentially informing the identification of suitable therapeutic targets, as well as treatment response, including pathways resistant to therapy and rationale for relapse.

There are many mRNA microarray and RNA-Seq studies available that have examined differential gene expression in psoriatic lesional (PS L) skin compared either to non-lesional (PS NL) skin or healthy control (HC) skin. A selection of these studies is described in **Table 3.1**.

*Table 3.1 Published mRNA expression studies. L; Lesional (skin macroscopically involved by disease process), NL; Non-Lesional (skin not macroscopically involved by disease process), HC; healthy control, PS; psoriasis, AD; atopic dermatitis, DEG; differentially expressed genes, FC; Fold Change, FDR; False Discovery Rate. Studies designating samples as uninvolved skin have been labelled as NL here. *Included in Gene Set Enrichment Analysis by Suárez-Fariñas et al.* (Suárez-Fariñas et al., 2010). *† Included in meta-analysis derived (MAD) transcriptome 3 by Tian et al.* (Tian et al., 2012). *‡ Included in meta-analysis derived (MAD) transcriptome 5 by Tian et al* (Tian et al., 2012). *In some cases, there were differences in data within the manuscripts, online portals, subsequent reviews or meta-analyses; data in this table are based on the published articles as referenced.*

Source	Samples	DEG	Study type
Oestereicher et al(Oestreicher et al., 2001)	PS: 8 L and NL (paired) HC: 3	159 (PS L vs PS NL)	Affymetrix oligonucleotide array (>7,000 genes) HuGeneFL GENECHIP® software
Bowcock et al(Bowcock et al., 2001)	PS: 15 (12 paired L/NL, 2 x L only, 1 x NL only) HC: 6	177 (PS L vs HC) (10 of these were DEG for PS NL vs HC)	Affymetrix oligonucleotide arrays (12,000 known genes)- U95A GeneChip® probe arrays, K-means clustering
*Zhou et al(Zhou et al., 2003)	PS: 16 L and NL (paired) HC: 8 (Note crossover of samples with those from Bowcock et al)(Bowcock et al., 2001)	1,338 (PS L/NL/HC) 600 (PS L vs NL/HC) Method 1(FC >2, t-tests p<0.05): 612 (PS L vs PS NL): 498 upregulated 362 downregulated 710 (PS L vs HC):	Affymetrix array U95A-E

		714 upregulated 208 downregulated 205 (PS NL vs HC): 197 upregulated 8 downregulated Method 2 (K-means clustering): 438 (PS L vs NL/HC)	
Kulski et al(Kulski et al., 2005)	PS: 4 PS L and NL (paired) HC: 3	173 (PS L vs PS NL): 164 upregulated 9 downregulated 321 (PS L vs HC): 263 upregulated 58 downregulated 125 (PS NL vs HC): 102 upregulated 23 downregulated	Affymetrix HUG95AV2
*†‡Gudjonsson et al(Gudjonsson et al., 2009)	PS 58 L and NL (paired) HC: 64	179 (PS NL vs HC): 58 upregulated 121 downregulated	Affymetrix HU133 Plus 2
Gudjonsson et al(Gudjonsson, Ding, et al., 2010)	PS: 58 L and NL (paired) HC: 64	1,326 DEtranscripts 918 DEG (PS L vs HC): 549 upregulated 369 downregulated	Affymetrix HU133 Plus 2
Jabbari et al(Jabbari et al., 2012)	PS: 3 PS L and NL (paired)	2,629 (RNA-Seq FC>1.5, FDR <0.1) (PS L vs PS NL)	RNA-Seq using Illumina GA-IIx and Affymetrix Human Genome U133A 2 arrays in parallel as comparator

	HC: None	569 (microarray, 46% of which were identified by RNA-Seq) (PS L vs PS NL)	
*†‡Yao et al(Yao et al., 2008)	PS: 26 PS L and NL (paired) plus additional 5 PS L (3 NL excluded from data analysis) HC: 21	2,873 (PS L vs NL): 1,408 upregulated 1,465 downregulated 4,278 (PS L vs HC): 2,016 upregulated 2,262 downregulated 949 (PS NL vs HC): 460 upregulated 489 downregulated	Affymetrix Human Genome U133 plus v2 array
*‡Suárez-Fariñas et al(Suárez-Fariñas et al., 2010)	PS: 15 L and NL (paired) HC: None	1,282 (PS L vs PS NL): 579 upregulated 703 downregulated	Affymetrix Human Genome U133a2
†‡Suárez-Fariñas et al(Suárez-Fariñas et al., 2012)	PS: 85 L and NL (81 paired L/NL, 4 x L only, 4 x NL only) HC: None	4,175 (PS L vs PS NL): 2,129 upregulated 2,046 downregulated	Affymetrix HG U133 Plus 2.0
‡Reischl et al(Reischl et al., 2007)	PS: 13 L and NL (paired) HC: None	179 (PS L vs PS NL)	Affymetrix HG-U133A
Yu et al(Z. Yu et al., 2020)	PS: 5 L and NL (paired)	4,946 (PS L vs PS NL): 2,431 upregulated 2,515 downregulated	Illumina HiSeq 4000 (cDNA library and miRNA-Seq)

	HC: 5	9,513 (PS L vs HC): 4,555 upregulated 4,958 downregulated 5,383 (PS NL vs HC): 2,546 upregulated 2,837 downregulated	
Deng et al(Deng et al., 2022)	PS: 13 L and NL (paired) HC: None (12 ankylosing spondylitis skin samples as control)	7,916 (PS L vs PS NL): 3,836 upregulated 4,080 downregulated	RNA-Seq (polyA enriched) using Illumina NovaSeq 6000 Sequencing platform (pair-end, 150bp)
Kim Lee et al(J. E. Kim et al., 2024)	PS: PS L (9), PS NL (7) AD: AD L 10, AD NL 10 HC: 6 (from previous study)(J. Kim et al., 2016)	11,386 (PS L vs HC): 5,122 upregulated 6,264 downregulated	Affymetrix Human Genome U133 Plus 2 Array

3.1.2 Assessment of differential gene expression in PS L and PS NL skin compared to HC skin

As noted in **Table 3.1**, there is variability in the number of DEG identified depending on the sample size, technique used and analysis criteria. Microarray with adjunct RT-PCR has now largely been supplanted by RNA-Seq, which can detect a larger number of differentially expressed genes and higher fold change detection at lower mRNA expression levels (Jabbari et al., 2012; Suárez-Fariñas et al., 2010). In addition, patient characteristics and sampling sites may affect study results. It is also notable that there may be a sizeable difference in the number of DEG between PS L and PS NL skin between individual patients; Oestereicher et al demonstrated between 340 and 1321 DEG across 8 PS patients (Oestreicher et al., 2001). Kim et al found that DEG between psoriatic and healthy control samples differed between mild (PASI <12) and moderate-severe psoriasis (PASI ≥12), even though histological features were comparable (J. Kim et al., 2016).

Genome-wide expression profiling from 62 patients demonstrated significantly increased expression of transcripts associated with keratinocytes in PS L vs PS NL skin in more than 90% of subjects (Swindell et al., 2012). Genes involved in terminal differentiation of keratinocytes are highly upregulated in PS L vs HC skin (Gudjonsson, Ding, et al., 2010). Significant overexpression of mRNA of type I interferons has been identified in PS L vs PS NL and HC skin, while *IFNG, IFNGR1, IFNGR2* and *TNFA* mRNA was significantly overexpressed in PS L vs PS NL and HC skin, as well as in PS NL vs HC skin (Yao et al., 2008). *S100* genes of the innate immune response are among those most highly upregulated in PS L vs HC skin (Gudjonsson, Ding, et al., 2010). DEG between psoriatic lesional (PS L) and uninvolved (PS NL) skin are shared with DEG in delayed type hypersensitivity reactions and a tape stripping wound healing model, including *KRT16*,

S100A2, *S100A7*, *S100A9*, *PI3* and *DEFB2* (=*DEFB4A*) transcripts (Oestreicher et al., 2001). The most enriched KEGG terms of differentially expressed mRNAs in PS L and PS NL vs HC skin included those for PPAR signalling, biosynthesis of unsaturated FA and FA elongation (Z. Yu et al., 2020).

A meta-analysis on three gene array studies (Gudjonsson et al., 2009; Suárez-Fariñas et al., 2012; Yao et al., 2008) examined DEG between PS NL and HC skin: There were 252 DEG (Fold Change (FC)≥1.4, False Discovery Rate (FDR)≤0.05) between 41 patients with moderate-severe psoriasis (PASI >12, BSA >10, not on active psoriasis treatment) vs normal skin from 12 healthy controls. Upregulation of genes pertinent to IL17, IL-22 and IFN-γ signalling pathways, including those encoding these key cytokines themselves (*IL17A*, *IL17F*, *IL22*, *IFNG*), as well as *DEFB4*, *S100A7*, *S100A7A*, *S100A8* and *S100A9*, was found in PS NL skin (Chiricozzi et al., 2016). Significantly increased $CD3^+$ cells and DC-$LAMP^+$ cells were also found in PS NL compared to HC skin (Chiricozzi et al., 2016).

Microarray comparisons have been attempted by standardising FC and p-value criteria (FC>2, p<0.05) across several studies (Gudjonsson, Ding, et al., 2010; Suárez-Fariñas et al., 2012). However, overlap in the genes detected was variable, illustrating the difficulties in comparing studies of different design, sample size and microarray platform, before considering other factors such as batch effect. Gene Set Enrichment Analysis (GSEA), where comparison of DEG lists from different studies with a raw data set from the main study is used, has been trialled to overcome these problems (Suárez-Fariñas et al., 2010). The result was 164 shared DEG (126 upregulated, 38 downregulated) between PS L and PS NL skin across four different studies, including genes regulated by IFN-γ coding for antimicrobial peptides (e.g. *DEFB4*, *LCN2*), several S100 proteins and pro-inflammatory proteins (e.g. IL-8), but excluding genes known to be relevant to

psoriasis pathogenesis e.g. *IFNG*, *IL17A*, *NOS2* (ascribed to low detection by microarray) (Suárez-Fariñas et al., 2010). A meta-analysis of five of the studies in **Table 3.1** was performed to produce a "meta-analysis derived" (MAD) transcriptome, MAD-5, consisting of 193 PS L and PS NL pairs with 677 upregulated and 443 downregulated genes. This increased to 1084 upregulated and 748 downregulated genes when only the three studies using larger probe-sets were considered (MAD-3) (Tian et al., 2012). The intersection of results of the five studies demonstrated 78 upregulated and 22 downregulated genes only (Tian et al., 2012). However, the authors noted that the microarray approach is limited in its detection of low-abundance transcripts such as those for key cytokines in psoriasis (Tian et al., 2012). Fatty acid metabolism was one of the top twelve significantly altered pathways in the MAD-3 transcriptome and the top 25 upregulated genes included those coding for antimicrobial peptides (*S100A7A*, *S100A9* and *S100A12*, *DEFB4* and *LCN2*) (Tian et al., 2012). Production of Nitric Oxide and Reactive Oxygen Species in Macrophages was a significant top 20 MAD-3 pathway identified by Ingenuity Pathway Analysis, which may be relevant to the generation of NFA (**Chapter 5**) (Tian et al., 2012).

3.1.3 Assessment of differential gene expression in PS compared to AD skin

A 12,000 gene microarray/RT-PCR study of PS L and AD L skin in patients with no prior systemic treatment demonstrated a statistically significant, >2-fold increase in expression of 62 genes in PS L vs AD L skin. Genes of interest significantly upregulated in PS L vs AD L included *iNOS*, *HBD2* (*DEFB4A*), *S100A12* as well as various chemokines (*CXCL-8, CCL-4, CXCL-2*, *CCL-20, CXCR4, CXCR-2*) and *PPARγ* (Nomura et al., 2003). Eighteen genes demonstrated a statistically significant, >2-fold increase in AD L skin vs PS L skin, including a ratio of 2.62 for *CD1a* (p=0.032) (Nomura et al.,

2003). Another group reported 183 DEG when comparing epidermis of PS L and AD L skin (De Jongh et al., 2005). mRNA levels of genes encoding antimicrobial peptides such as calgranulin B, psoriasin and particularly hBD-2 are all significantly upregulated in PS L compared to AD L skin (De Jongh et al., 2005).

Overall, there is a plethora of differential gene expression data on PS L skin, with key groups of genes and pathways pertaining to skin function and the immune response identified. Most studies focus on skin that has not been treated systemically, although there are a minority that examine changes in gene expression following therapeutic intervention. However, understanding of differences between treatment-resistant, persistently inflamed lesional skin and adjacent resolved skin is limited due to a paucity of studies. Such analyses offer the opportunity to identify key driver nodes of inflammation. Our study seeks to identify differential gene expression in this context.

3.1.4 Patient Cohort

A total of 45 skin biopsies were obtained from 25 patients, five in each of the following groups (**Table 3.2**):

- Patients with psoriasis under topical treatment only
- Patients with psoriasis under treatment with NB-UVB phototherapy
- Patients with psoriasis under treatment with the anti-IL17A monoclonal antibody secukinumab
- Patients with atopic dermatitis under topical treatment only
- Healthy controls

Fourteen women and eleven men were involved in the study. Although exact age and sex matching was not possible, where feasible, consistency in the site of biopsy (lower back) was maintained (18 out of 25 samples).

Table 3.2 Patient cohort. EASI; Eczema Area and Severity Index, PASI; Psoriasis Area and Severity Index. M; male, F; female, L; left, R; right.

Old ID	New ID		Age	Gender	PASI	EASI	Other disease	Treatment	Site
PS2779		Psoriasis	57	F	15		Nail involvement	Topical therapy	Lower back
PS2780		Psoriasis	65	F	5		Nail involvement, arthritis	Topical therapy	Lower back
PS2781		Psoriasis	37	F	9		Nail involvement	Topical therapy	Lower back
PS2784		Psoriasis	75	M	5			Topical therapy	Lower back
PS2585B		Psoriasis	50	F	5		Nail involvement	Topical therapy	Upper arm
PS2507	PS2574	Psoriasis	64	M	13		Nil	NB-UVB 5 weeks	R lower back
PS2500	PS2567	Psoriasis	39	F	5		Arthritis	NB-UVB 5 weeks	R lower back
PS2501	PS2568	Psoriasis	38	M	26		Nail involvement, arthritis	NB-UVB 5 weeks	R lower back
PS2493	PS2560	Psoriasis	67	F	12		Nil	NB-UVB 5 weeks	R lower back
PS2484	PS2551	Psoriasis	49	F	5		Nil	NB-UVB 5 weeks	R leg
PS2652		Psoriasis	70	F	12		Nail involvement, arthritis	Secukinumab	R lower leg
PS2627		Psoriasis	64	M	7		Nil	Secukinumab	L chest
PS2623		Psoriasis	51	F	5		Nail involvement, arthritis	Secukinumab	R lower back
PS2585		Psoriasis	51	M	15		Arthritis	Secukinumab	R lower back

PS2510	PS2577	Psoriasis	49	M	18		Arthritis	Secukinumab	R lower back
AD2639		AD	23	F		30	Hay fever, no asthma	Topical therapy	R lower back
AD2640		AD	24	M		20	Hay fever, no asthma	Topical therapy	R lower back
AD2638		AD	42	F		15	Hay fever, no asthma	Topical therapy	R lower back
AD2634		AD	35	M		22	Hay fever, asthma	Topical therapy	R lower back
AD2628		AD	60	M		5	Hay fever, no asthma	Topical therapy	R leg
C100		Control	35	M					Mid back
C101		Control	62	F					Lower back
C103		Control	50	M					Lower back
C104		Control	39	F					Lower back
C105		Control	60	F					Mid back

Ellipse biopsies were taken across the lesion margin (**Figure 3.1**), in order to incorporate clinically active disease (referred to hereafter as lesional skin; PS L) and adjacent skin that had either never been affected (untreated group, referred to hereafter as non-lesional skin; PS NL) or had previously been affected, but had resolved with the choice of administered treatment (NB-UVB/secukinumab, referred to hereafter as resolved skin; PS R).

Biopsies were divided and flash frozen and segments of each sent for:

1 Lipidomic analysis by our collaborators at Harvard University

2 RNA-Sequencing analysis

3 Formalin-fixed sectioning for immunohistochemistry (protein validation of RNA-Seq)

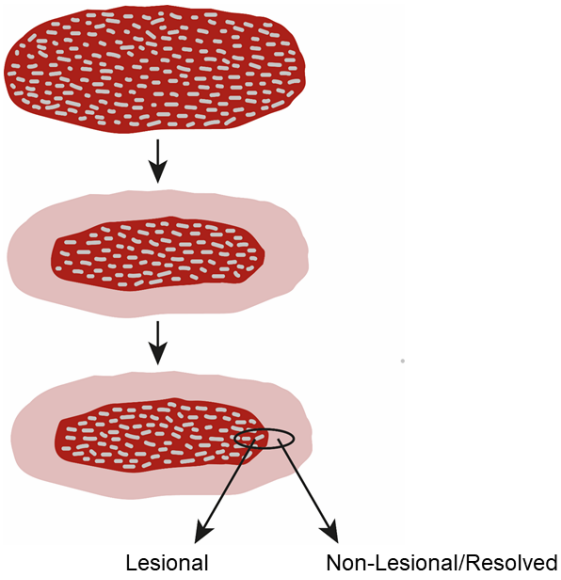


Figure 3.1 Schematic of elliptical skin biopsy.

The recommended management of isolated cutaneous psoriasis is in a stepwise fashion according to disease severity and biopsychosocial impact. To define unique and shared

pathways, our psoriasis cohort was selected from different points in the treatment algorithm (see **Chapter 1**, **Figure 1.1**).

We classified patients as untreated if they were under topical therapy only. Creams or ointments were not applied for at least four weeks prior to biopsy.

The NB-UVB group were patients receiving their first course of full body phototherapy with narrow-band UVB light and were all biopsied in their fifth week of treatment. Patients generally undergo treatment with NB-UVB (311-312nm) 2-3 times per week for approximately three months. Postulated immunosuppressive effects of NB-UVB include cis-isomerization of urocanic acid (UCA) in the stratum corneum, DNA damage, induction of cytokines and effects on immune cells including T cells, NK cells and LC (Duthie et al., 1999). Specific suggested mechanisms of NB-UVB in improving psoriasis include downregulation of IL-17, IL-6, Toll-like receptor and p38 MAPK signalling pathways (Vacharanukrauh et al., 2021). Epidermal RNA analysis identified downregulation of genes involved in type I and type II interferon signalling and the anti-viral response (vs the pre-existing psoriatic lesion) following a course of treatment with NB-UVB (Rácz et al., 2011). However, upregulation of IFN I signalling and modulation of genes related to apoptosis pathways has been identified within hours of exposure to NB-UVB (Addison et al., 2021). *IL-17* and *IL-22* mRNA correlated with normalisation of epidermal thickness and K16 expression and staining at week 6 of NB-UVB therapy (Johnson-Huang et al., 2010). Alterations in genes involved in epidermal differentiation is also noted following NB-UVB therapy (Rácz et al., 2011).

A meta-analysis of nine randomised controlled trials (RCT) using NB-UVB as monotherapy demonstrated at least PASI 75 (≥75% improvement in Psoriasis Area and Severity Index score compared to baseline) in 62% of patients (95% CI 45-79) (Almutawa et al., 2013).

Biologic therapy with monoclonal antibodies is recommended for patients who have failed phototherapy and immunosuppressive treatment, or where such treatment is contra-indicated. Secukinumab (Cosentyx™) is a recombinant human anti-IL-17A antagonist administered by subcutaneous injection at a dose of 300mg weekly for five weeks, then monthly, with evaluation of PASI and DLQI scores at 16 weeks. It is also licensed for the treatment of psoriatic arthritis and ankylosing spondylitis. Four main Phase III RCT, FEATURE (Blauvelt et al., 2015), JUNCTURE (Paul et al., 2015), ERASURE (Langley et al., 2014) and FIXTURE (Langley et al., 2014), have assessed the safety and efficacy of secukinumab, with PASI 75 at 12 weeks ranging from 75.9% to 86.7% versus 0% to 4.9% for placebo ($p<0.001$-$p<0.0001$). To put this in context, comparison trials with other biologic therapies at 12 weeks demonstrate PASI 75 of 77.1% with secukinumab versus 44% with etanercept ($p<0.001$)(Langley et al., 2014) and 91% with secukinumab versus 79.1% with ustekinumab standard dosing ($p<0.0001$) (Thaçi et al., 2015). The effect of secukinumab was also found to be remarkably persistent in a prospective observational study: PASI 75 was achieved in 83.5% of patients at week 12 and 78.5% of patients at week 52 (Ortiz-Salvador et al., 2019). Biopsies for this group in our cohort were taken from clinical responders at least three months after treatment initiation.

Atopic dermatitis patients were chosen as an inflammatory comparator group. These patients were treated with topical steroids only. There were also five healthy controls who had a single biopsy taken. All samples were from White British patients.

3.2 RNA-Seq data analysis approach

RNA extraction and validation and bioinformatic analysis were performed as a collaborative effort with other members of the Ogg lab.

3.2.1 RNA extraction and validation (Work of Dr Randeep Singh, Ogg Lab)

RNA extraction and validation on lesional, non-lesional/resolved skin biopsies were performed by Dr Randeep Singh using the RNeasy (registered) Fibrous Tissue Mini Kit (Qiagen, 74704, March 2016) and Agilent RNA 6000 Pico Kit Quick Start Guide (Agilent, 5067-1513). The only modification to the kit protocol was that 700µL of Buffer RLT was used when homogenising the tissue rather than 300µL. RNA integrity was determined using an Agilent 2100 Bioanalyzer (Agilent Technologies UK Ltd, Stockport, UK), with an average RIN value across all psoriasis (including NB-UVB and secukinumab-treated) and AD samples of 8.3.

3.2.2 RNA sequencing (Work of Dr Jeongmin Woo, Ogg Lab)

RNA-Seq paired end libraries were prepared using an Illumina® TruSeq™ stranded mRNA Sample Preparation Kit (Illumina Inc.). Paired End (2 x 75bp) RNA sequencing was performed by Oxford Genomics Centre using the Illumina HiSeq 4000 platform with 30 million reads per sample. The quality of the read sequences was assessed using the FastQC package (www.bioinformatics.babraham.ac.uk/projects/fastqc) and adaptor sequences were removed using Cutadapt. Read sequences were aligned against human genome assembly (National Center for Biotechnology Information), build38 (hg38) using STAR (version 2.5.3). Mappings were converted to gene specific read count values using the featureCounts function from the Subread package with default parameters. Sample quality metric and raw read counts were imported in R for further processing. The DESeq2 (version 1.24.0) Bioconductor package was used to estimate library size factors,

normalise count and perform differential expression analysis. The Wald test was used to perform differential expression analysis in a pairwise manner whereas the Likelihood Ratio Test (LRT) was used to analyse differentially expressed genes across three disease statuses by comparing the "full" model with the disease status as a factor, to the "reduced" model which was the intercept. Benjamini-Hochberg (BH) multiple testing correction was used to compute FDR.

The 10,000 most variable genes were used to perform principal component analysis (PCA), where variance-stabilised transformation expression was used as input. Functional gene set enrichment analysis based on Gene Ontology (GO) terms was performed using the clusterProfiler R package (G. Yu et al., 2012). GO gene sets were tested for overrepresentation in each set of DEG by computation of enrichment p-values using the default parameter of "enricher" function, which implements a hypergeometric test. Hypergeometric p-values were adjusted for multiple testing using the Benjamini-Hochberg correction.

The pcaExplorer package (Federico Marini, Harald Binder pcaExplorer: an R/Bioconductor package for interacting with RNA-seq principal components BMC Bioinformatics, 2019 - https://doi.org/10.1186/s12859-019-2879-1) on R Studio (R Core Team (2020). R: A language and environment for statistical computing. R Foundation for Statistical Computing, Vienna, Austria. URL https://www.R-project.org/.) and Venny 2.1 (*Oliveros, J.C. (2007-2015) Venny. An interactive tool for comparing lists with Venn's diagrams.* https://bioinfogp.cnb.csic.es/tools/venny/index.html) were used to make box plots and Venn diagrams of the data respectively.

3.3 Results

3.3.1 Unsupervised analysis by Principal Component Analysis

Principal Component Analysis (PCA) demonstrates clustering of samples based on similarity with regards to a particular parameter. Here, it was used to assess for clustering by disease type and treatment among the 10,000 most variable genes across all the biopsy samples.

Plots (**Figure 3.2**) showed clustering of samples by disease group, suggesting marked differences in gene expression between diseases (PS, AD) and between diseases and healthy controls. There was a gradient between lesional and non-lesional samples within disease types (diamond vs square), suggesting subtle differences in tissue type. There was no obvious difference between psoriasis samples under different therapeutic modalities.

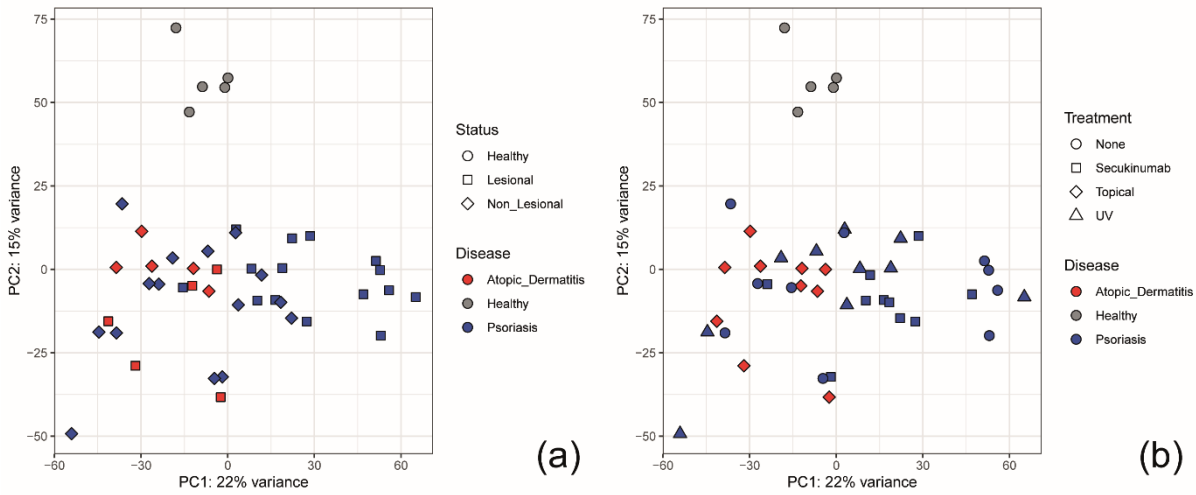


Figure 3.2 Principal Component Analysis (PCA) plots comparing (a) PS, AD and HC (b) PS by treatment group. UV; NB-UVB.

3.3.2 Assessment of DEG by psoriasis treatment modality: Volcano plots and scatter plots

Volcano plots permit a more detailed look at the differences in upregulated and downregulated genes for each treatment group, while fold change (FC) scatter plots facilitate visual comparison of differential gene expression between groups. GO term analysis was also performed for each treatment group using the FC scatter plot data.

Based on FC scatter plots (see later **Figures 3.4, 3.6, 3.8)** comparing HC vs both PS L and PS NL/PS R skin, some master regulator genes, such as the homeobox (*HOX*) genes, were upregulated, while genes involved in lipid synthesis, such as *MOGAT1* and *AWAT1,* were downregulated in both L and NL/R tissue. Untreated PS L and PS NL skin showed downregulation of several keratin associated protein (*KRTAP*) genes.

Untreated Group

Pairwise analysis of DEG between PS L, PS NL and HC:

In the untreated group, there were 1090 DEG for PS L vs HC and 739 DEG for PS NL vs HC. The number of downregulated genes was more than double the number of upregulated genes for both groups. Downregulation of genes involved in lipid synthesis is prominent in PS L skin (**Figure 3.3 (a)**), while downregulation of some specific keratin genes is marked in both PS L and PS NL skin (**Figure 3.3, Figure 3.4**).

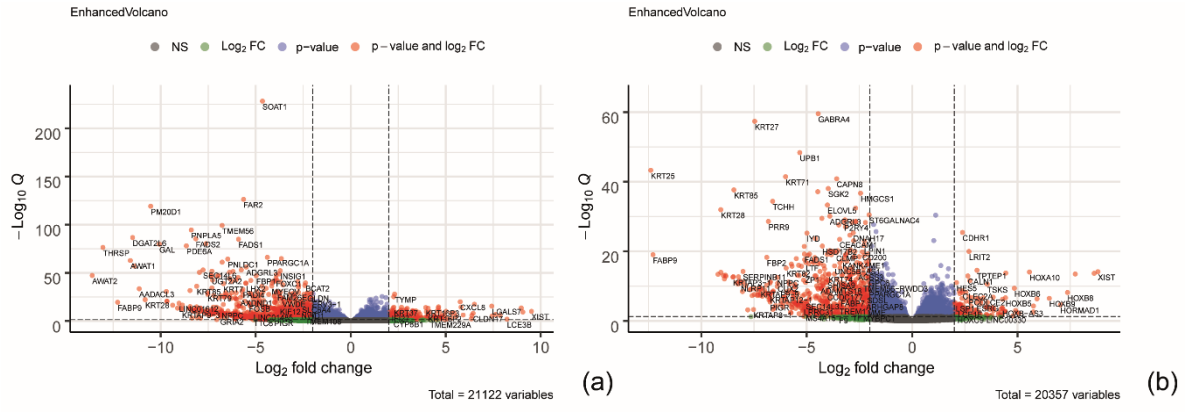


Figure 3.3 Differential gene expression untreated psoriasis (a) PS L vs HC (b) PS NL vs HC (Log2Fold Change>2, BH adjusted p-value <0.01). PS L; lesional psoriasis, PS NL; non-lesional psoriasis, HC; healthy control.

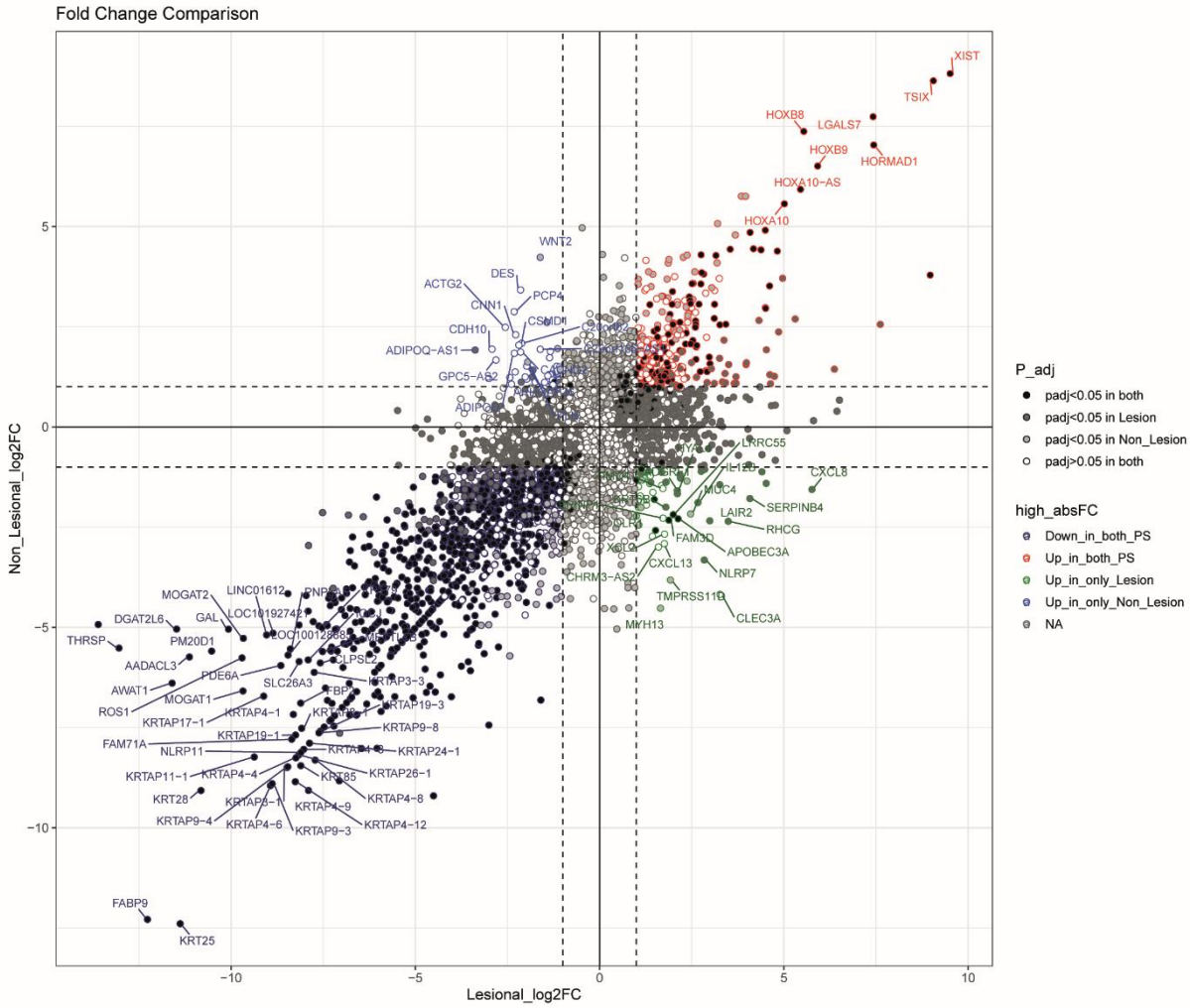


Figure 3.4 Scatter plot untreated psoriasis. X-axis: Log2FC in differential gene expression PS L (untreated) vs HC. Y-axis: Log2FC in differential gene expression PS NL (untreated) vs HC. Log2FC; Log2Fold Change, PS L; lesional psoriasis, PS NL; non-lesional psoriasis.

3.3.3 NB-UVB-treated group

Pairwise analysis of DEG between PS L (NB-UVB), PS R (NB-UVB) and HC:

Downregulated genes also outnumbered upregulated genes for PS L (NB-UVB) and PS R (NB-UVB) compared to HC. There were 654 DEG PS L (NB-UVB) vs HC and 710 DEG PS R (NB-UVB) vs HC following phototherapy (Log2 FC >2, FDR <0.01). Downregulation of genes involved in lipid metabolism was prominent in both PS L (NB-UVB) (**Figure 3.5 (a), Figure 3.6**) and PS R (NB-UVB) (**Figure 3.5 (b), Figure 3.6**) skin.

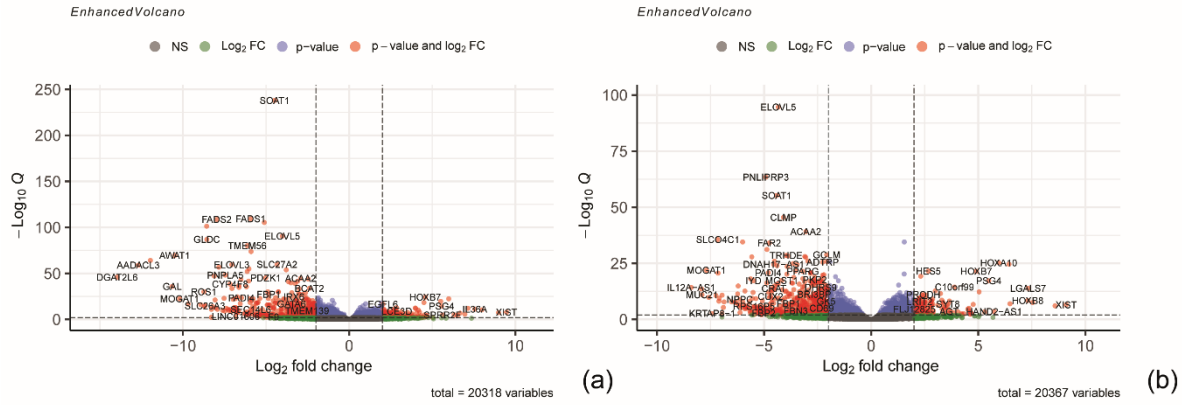


Figure 3.5 Differential gene expression NB-UVB-treated psoriasis (a) PS L (NB-UVB) vs HC (b) PS R (NB-UVB) vs HC (Log2Fold Change>2, BH adjusted p-value <0.01). PS L; lesional psoriasis, PS R; resolved psoriasis, HC; healthy control.

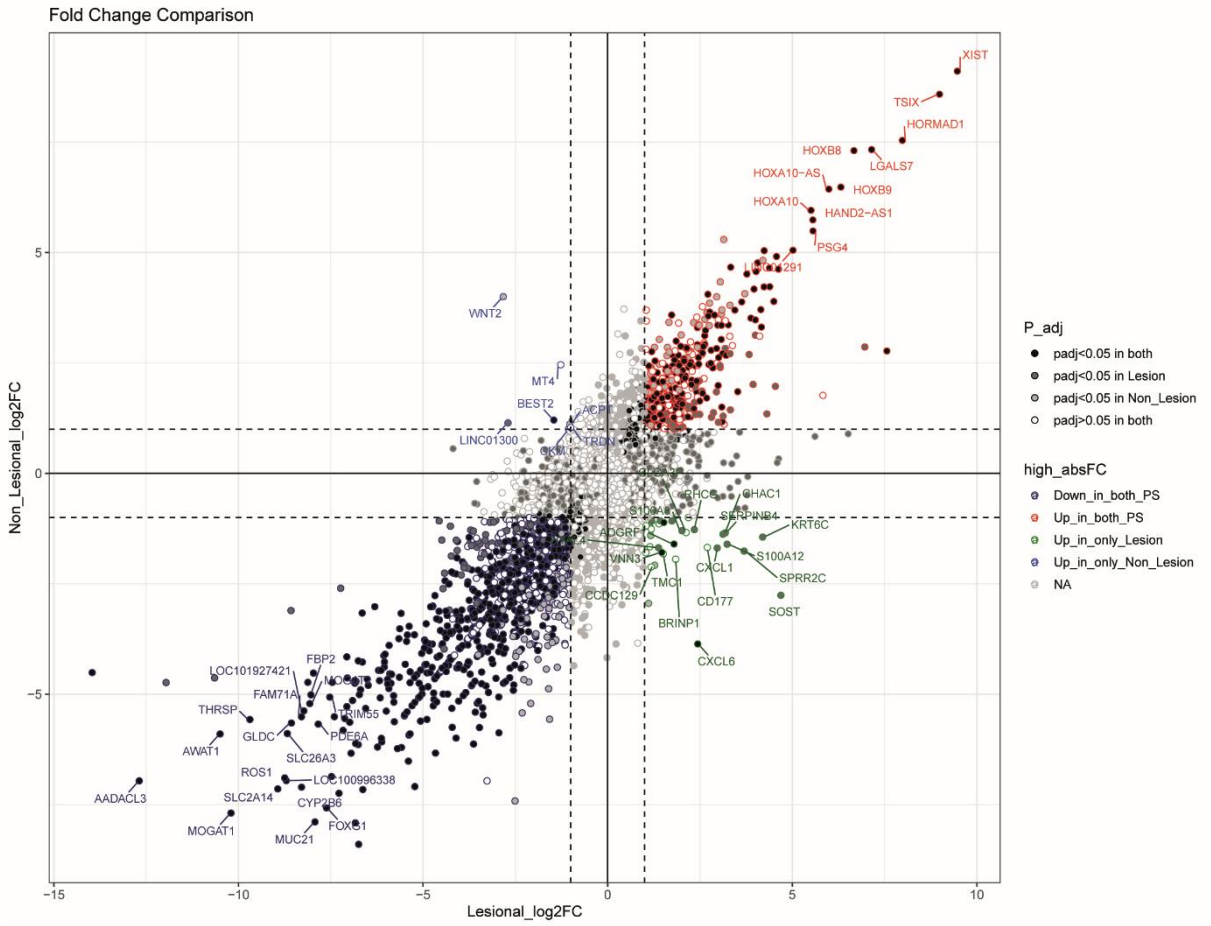


Figure 3.6 Scatter plot NB-UVB-treated psoriasis. X-axis: Log2FC in differential gene expression PS L (NB-UVB) vs HC. Y-axis: Log2FC in differential gene expression PS R (NB-UVB) vs HC. Log2FC; Log2Fold Change, PS L; lesional psoriasis, PS NL; non-lesional psoriasis- here = R (resolved psoriasis).

3.3.4 Secukinumab-treated group

Pairwise analysis of DEG between PS L (Secukinumab), PS R (Secukinumab) and HC:

In the secukinumab-treated group, there were 861 DEG for PS L vs HC and 718 DEG for PS R vs HC (Log2FC>2, FDR <0.01). Again, downregulation of genes involved in lipid metabolism was seen in both PS L (**Figure 3.7 (a)**) and PS R (**Figure 3.7 (b)**) skin, as also illustrated in the scatter plot (**Figure 3.8**).

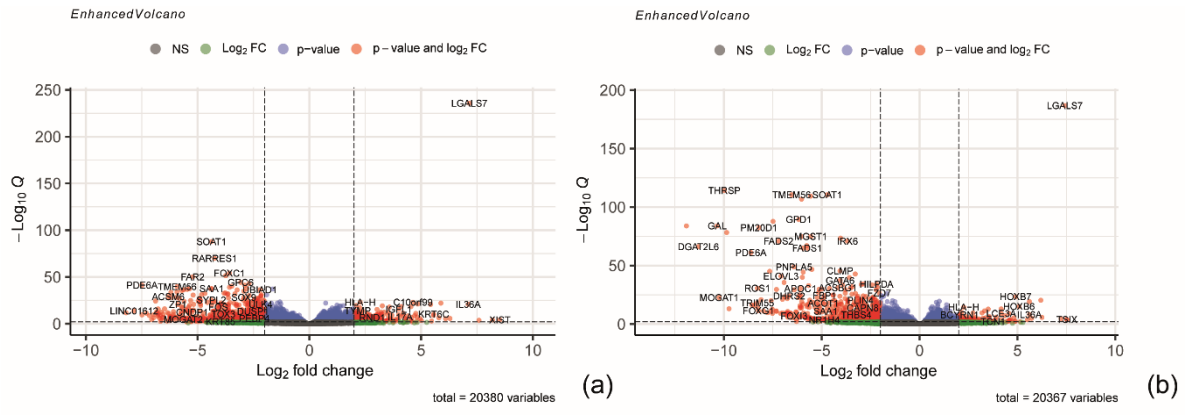


Figure 3.7 Differential gene expression secukinumab-treated psoriasis (a) PS L (Secukinumab) vs HC (b) PS R (Secukinumab) vs HC (Log2Fold Change>2, BH adjusted p-value <0.01). PS L; lesional psoriasis, PS R; resolved psoriasis, HC; healthy control.

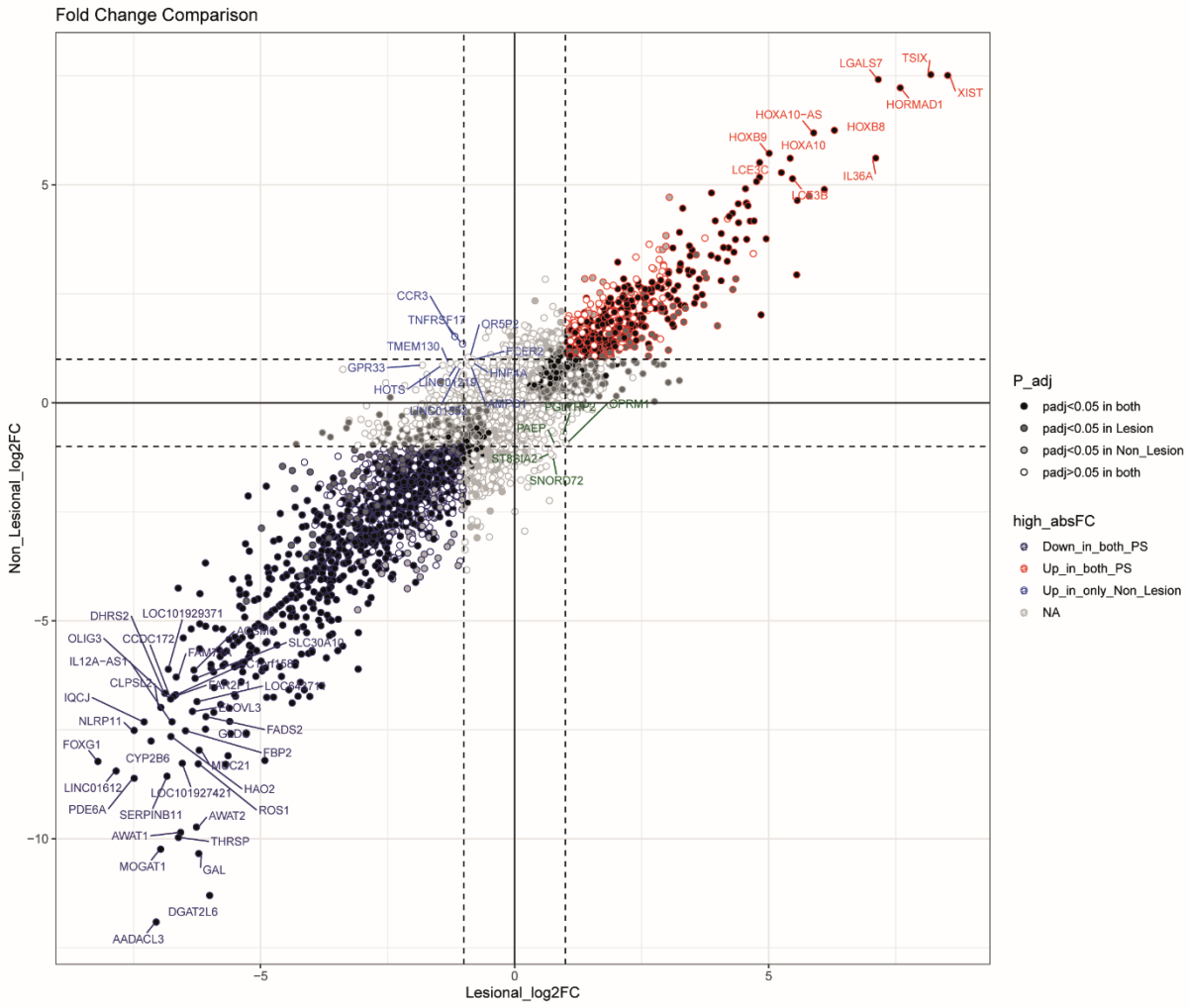


Figure 3.8 Scatter plot secukinumab-treated psoriasis. X-axis: Log2FC in differential gene expression PS L (Secukinumab) vs HC. Y-axis: Log2FC in differential gene expression PS R (Secukinumab) vs HC. Log2FC; Log2Fold Change, PS L; lesional psoriasis, PS NL; non-lesional psoriasis- here = R (resolved psoriasis).

3.3.5 Assessment of DEG in healthy and diseased skin: Venn Diagrams

Using a cut-off of Log2FC>2, further examination of DEG data of our psoriasis cohort vs HC revealed that clinically normal NL/R skin, in the untreated and treated groups, demonstrated an approximately similar number of DEG (**Table 3.3**). For lesional skin, the number of DEG vs HC was highest in untreated PS L skin>PS L (Secukinumab)>PS L (NB-UVB). For all groups, the number of downregulated genes was more than double that of upregulated genes vs HC, except for the NB-UVB-treated samples which demonstrated a lower ratio of downregulated to upregulated genes vs HC.

Table 3.3 Differential gene expression: Psoriasis vs healthy control skin. Log2FC>2. PS L; lesional psoriasis, PS NL; non-lesional psoriasis, PS R; resolved psoriasis, HC; healthy control.

Comparison	DEG (total) vs HC	Upregulated vs HC	Downregulated vs HC
PS L (untreated)	2,749	809	1,940
PS L (NB-UVB)	1,939	705	1,234
PS L (Secukinumab)	2,448	784	1,664
PS NL (untreated)	1,936	598	1,338
PS R (NB-UVB)	2,210	833	1,377
PS R (Secukinumab)	2,043	622	1,421

Venn diagram analysis of DEG in disease vs HC, using a cut-off of log2FC>2, is shown below (**Figure 3.9, Figure 3.10**) and demonstrates overlapping DEG across treatment groups.

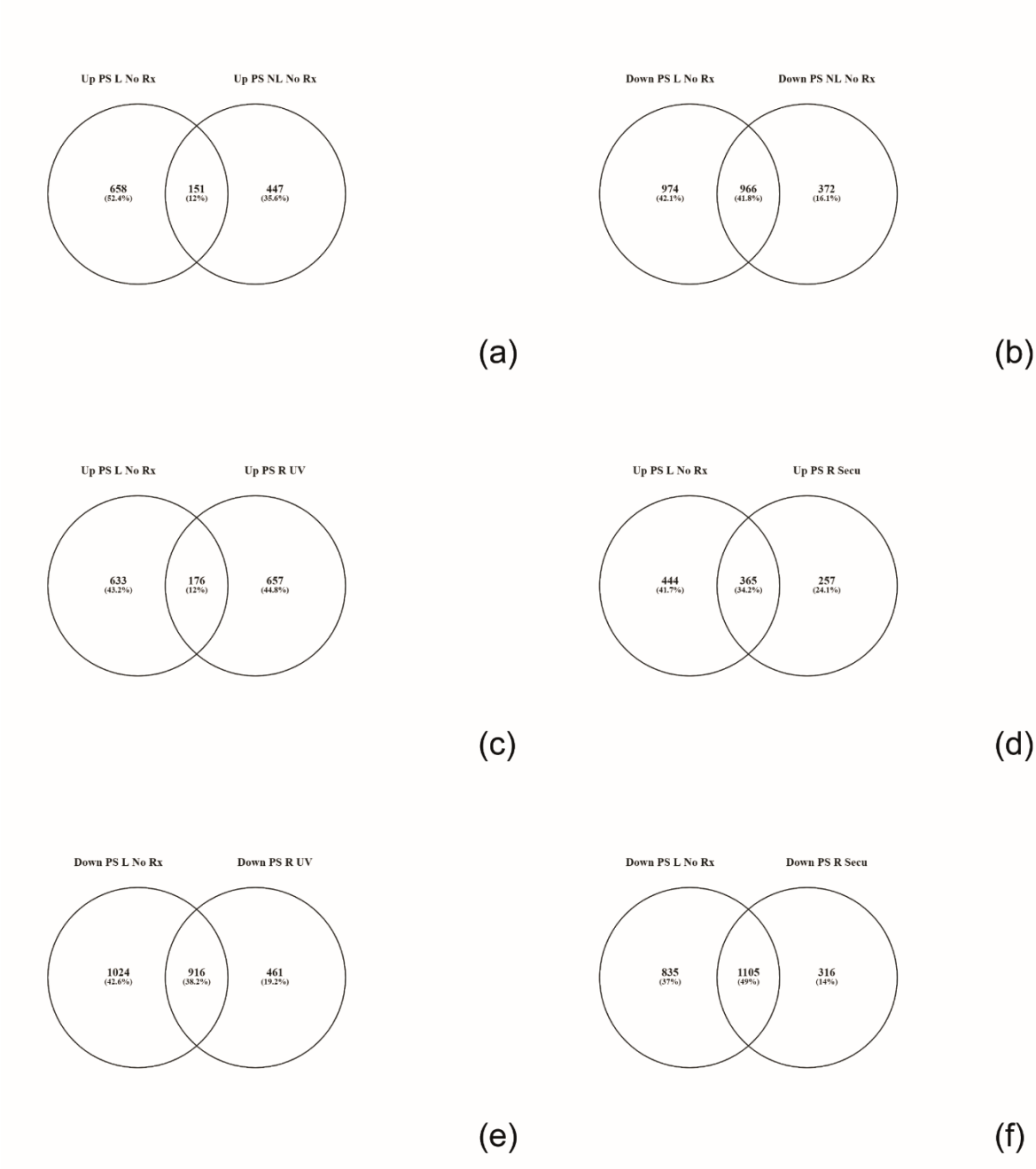


Figure 3.9 Differential gene expression, psoriasis cohort, Log2FC>2 (a) Upregulated genes untreated group, PS L (vs HC) and PS NL (vs HC) (b) Downregulated genes untreated group, PS L (vs HC) and PS NL (vs HC) (c) Upregulated genes in untreated PS L (vs HC) and PS R (NB-

UVB) (vs HC) (d) Upregulated genes in untreated PS L (vs HC) and PS R (Secukinumab) (vs HC) (e) Downregulated genes in untreated PS L (vs HC) and PS R (NB-UVB) (vs HC) (f) Downregulated genes PS L (vs HC) and PS R (Secukinumab) (vs HC). PS L; lesional psoriasis, PS NL; non-lesional psoriasis, PS R; resolved psoriasis, HC; healthy control, No Rx; untreated, UV; NB-UVB, Secu; secukinumab.

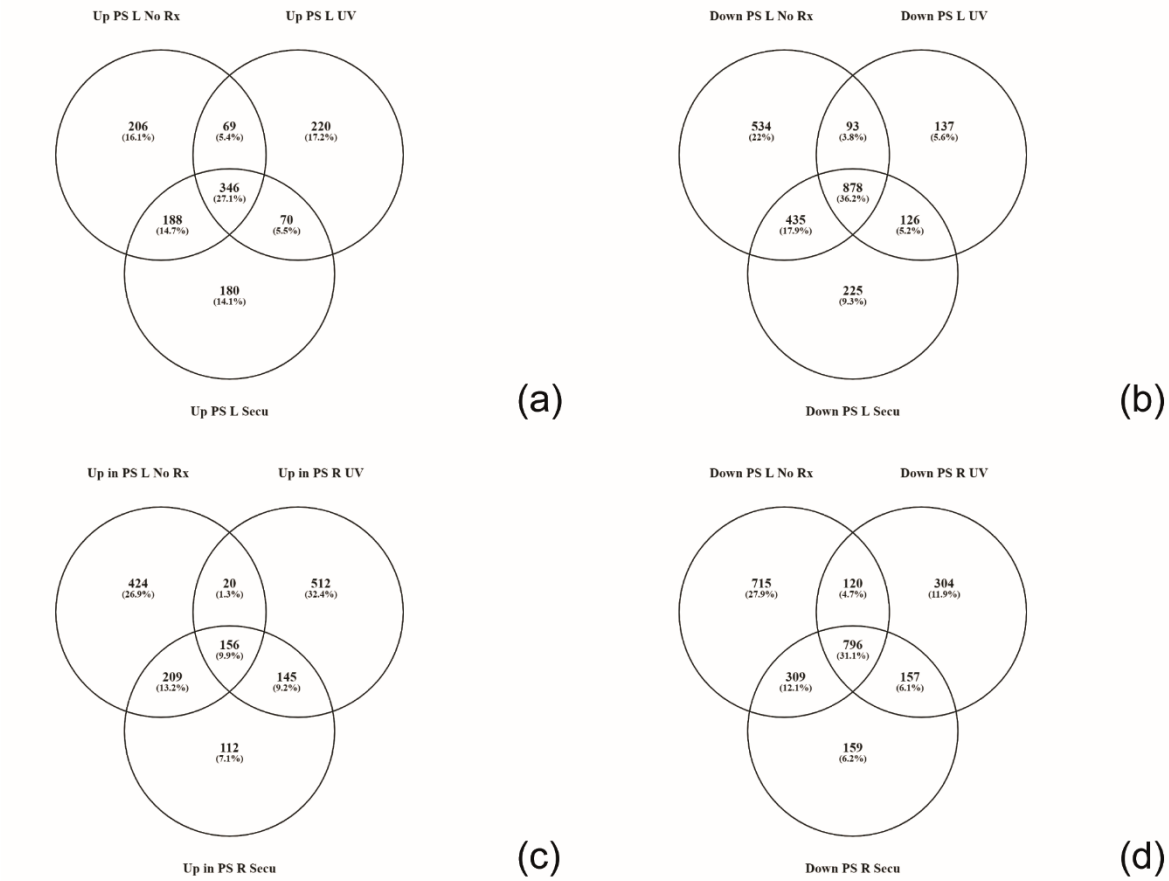


Figure 3.10 Differential gene expression, psoriasis cohort, Log2FC>2 (a) Upregulated genes across PS L skin (each vs HC) (b) Downregulated genes across PS L skin (each vs HC) (c) Upregulated genes untreated PS L skin vs clinically resolved skin following NB-UVB/secukinumab (each vs HC) (d) Downregulated genes untreated PS L skin vs clinically resolved skin following NB-UVB/secukinumab (each vs HC). PS L; lesional psoriasis, PS NL; non-lesional psoriasis, PS R; resolved psoriasis, HC; healthy control, No Rx; untreated, UV; NB-UVB, Secu; secukinumab.

Untreated psoriasis

In the untreated group vs HC, 151 of the upregulated genes (**Figure 3.9 (a)**) and 966 of the downregulated genes were shared (**Figure 3.9 (b)**). Examples of the DEG and their protein products are given in **Table 3.3**.

Table 3.3 Differentially Expressed Genes (vs healthy control): Untreated psoriasis. Shared and exclusively differentially expressed genes (vs healthy control) in untreated lesional and non-lesional psoriasis. Log2FC>2. DEG; Differentially expressed genes, PS L; lesional psoriasis, PS NL; non-lesional psoriasis, HC; healthy control.

Untreated PS L	Untreated PS NL	Differential expression (vs HC)	Examples of DEG and role of encoded proteins
+	+	Upregulated	**Development:** Various *HOX* **Proteostasis:** Various *HSP* **Immune signalling:** *IL36* family (*IL36A*, *IL36B*, *IL36RN*), *IL1F10* **Structural:** Keratins (*KRT1*, *KRT10*, *KRT14*) Late cornified envelope (*LCE*) genes Collagens (*COL4* subtypes) **Lipid pathways:** Enzymes: Lipoxygenases (*ALOX12B*)
+	-	Upregulated	**HLA:** *HLA-C*, *HLA-G* **Psoriasis auto-antigens:** *SERPINB3* and *SERPINB4* **Immune signalling:** *STAT1*, *STAT3*, *FOXP3*, *IL1RN*, *IL2RA*, *IL2RG*, *IL4I1*, *IL4R*, *IL12B*, *IL12RB2*, *IL7R*, *IL17A*, *IL17C*, *IL17F*, *IL17REL*, *IL18RAP*, *IL19*, *IL20*, *IL21R*, *IL23A*, *IL26*, *IL36G* **Antimicrobial peptides:** *DEFB4A*, *S100A7*, *S100A7A*, *S100A8*, *S100A9*, *S100A12* **Structural:** Keratins (*KRT6A*, *KRT6B*, *KRT6C*, *KRT16*, *KRT16P1*, *KRT16P2*, *KRT16P3*, *KRT24*, *KRT37*)

			Late cornified envelope *(LCE3C)* **Lipid pathways:** Enzymes: Phospholipases (*PLA2G4B*, *PLA2G4D*), lipoxygenases (*ALOX5AP*) Binding proteins (*FABP5*) CD1 *(CD1B*, *CD1C)*
+	+	Downregulated	**Immune signalling:** *IL1A*, *IL6*, *IL12A*, *IL17RB* **Structural:** Keratins (*KRT4*, *KRT7*, *KRT8*, *KRT13*, *KRT25*, *KRT26*, *KRT27*, *KRT28*, *KRT32*, *KRT33A*, *KRT33B*, *KRT35*, *KRT38*, *KRT39*, *KRT40*, *KRT71*, *KRT74*, *KRT79*, *KRT82*, *KRT83*, *KRT85*, *KRT86*, *KRT222)* Collagens (*COL6A4P2*, *COL9A1*) **Lipid pathways:** Enzymes (*ACADM*, *ACOX2*, *AWAT1*, *AWAT2*, *ACSL1*, *ACSL3*, *ACSL5, ACSM1*, *ACSM3*, *ACSM6*, *ACACB*, *ACAT2*, *ACOT1*, *ACOT2*, *ACOT4*, *ACSM3*, *ACSM6*, *ALOX12P2*, *ALOX15B, APOC1*, *APOE*, *CRAT*, *DGAT2*, *DGAT2L6*, *ELOVL3*, *ELOVL5*, *FABP1*, *FABP6*, *FABP7*, *FABP9*, *FADS1*, *FADS2*, *FASN*, *LRAT*, *MOGAT1*, *MOGAT2*, *PLA2R1*, *PLA2G7*, *PLA2G16*, *PNPLA3*, *PNPLA5*, *PPARG*, *PPARGC1A*, *TCLD1*) Binding proteins (*RBP1*)
+	-	Downregulated	**Immune signalling:** *IL17B*, *IL17D*, *IL31RA* **Structural:** Keratins (*KRT18*, *KRT19*, *KRT20*, *KRT75*) **Lipid pathways:** Enzymes (*LPL)* Binding proteins (*RBP4*)

All psoriasis groups

DEG across psoriasis subgroups are assessed in **Table 3.4**.

Table 3.4 Differentially Expressed Genes (vs healthy control): Psoriasis. Shared and exclusively differentially expressed genes (vs healthy control) in psoriasis by subgroup. Log2FC>2. N/A; not assessed, DEG; Differentially expressed genes, PS L; lesional psoriasis, PS NL; non-lesional psoriasis, HC; healthy control.

Untreated PS L	**PS L (NB-UVB)**	**PS L (Secukinumab)**	**Untreated PS NL**	**PS R (NB-UVB)**	**PS R (Secukinumab)**	**Differential expression (vs HC)**	**Examples of DEG and role of encoded proteins**
+	+	+	+	+	+	Upregulated	**Immune signalling:** *IL36A*, *IL36RN* **Structural:** Collagens (*COL4* subtypes) **Lipid pathway:** Enzymes (*ALOX12B*)
+	+	+	N/A	N/A	N/A	Upregulated	**Psoriasis auto-antigens:** *SERPINB3* and *SERPINB4* **Immune signalling:** *IL12RB2*, *IL17A*, *IL17F*, *IL36A*, *IL36G*, *IL36RN* **Antimicrobial peptides:** *S100A7, S100A8*, *S100A9*, *S100A12* **Structural:** Keratins *(KRT6C*, *KRT16)* **Lipid pathways:** Enzymes (*PLA2G4D*, *PLA2G4E*, *PLA2G4E-AS1*, *PLA2G2F*, *PLA2G3*) Binding proteins (*FABP5*)
+	-	-	N/A	N/A	N/A	Upregulated	**HLA:**

							HLA-C, *HLA-E* **Immune signalling:** *IL1F10*, *IL12B*, *IL17REL*, *IL21R* **Structural:** Keratins (*KRT6B*)
+	N/A	N/A	N/A	+	+	Upregulated	**Immune signalling:** *IL1F10*, *IL36A*, *IL36RN* **Structural:** Keratins (*KRT1*, *KRT10*, *KRT14*, *KRT37*) Late cornified envelope (*LCE1E*, *LCE1F*, *LCE2A*) **Lipid pathways:** Enzymes (*PLA2G3*, *ALOX12B)*
+	N/A	N/A	N/A	-	+	Upregulated	**Immune signalling:** *IL12RB2*, *IL17A* **Antimicrobial peptides:** *S100A9* **Structural:** Keratins (*KRT6C*, *KRT16*) **Lipid pathways:** Receptors (*PPARD*)
+	N/A	N/A	N/A	-	-	Upregulated	**HLA:** *HLA-C* **Psoriasis autoantigens:** *SERPINB3 and SERPINB4* **Immune signalling:** *JAK3, IL1RN*, *IL2RA*, *IL2RG*, *IL4*, *IL4I1*, *IL7R*, *IL12B*, *IL17C*, *IL17F*, *IL17REL*, *IL18RAP*, *IL19*, *IL20*, *IL21R*, *IL23A*, *IL26* **Antimicrobial peptides:** *S100A7*, *S100A8*, *S100A12*

							Structural: Keratins (*KRT6B*, *KRT24*) **Lipid pathways:** Enzymes (*PLA2G2F*, *PLA2G4B*, *PLA2G4E-AS1*) CD1 (*CD1C*) Binding proteins (*FABP5*)
+	+	-	N/A	N/A	N/A	Upregulated	**Structural:** Keratins (*KRT10*)
+	-	+	N/A	N/A	N/A	Upregulated	**Immune signalling:** *IL17C*, *IL23A* **Structural:** Keratins (*KRT1*, *KRT14*, *KRT24*) **Hypoxia response:** *HIF1A*
-	+	+	N/A	N/A	N/A	Upregulated	**Structural:** Keratins (*KRT2*)
+	+	-	+	+	-	Upregulated	**Immune signalling:** *IL36B*
+	+	+	+	+	+	Downregulated	**Immune signalling:** *IL12A*, *IL17RB* **Structural:** Keratins (*KRT4*, *KRT7*, *KRT79*) Collagens (*COL6A4P2*, *COL9A1*) **Lipid pathways:** Enzymes (*ACAA2, ACACB*, *ACADM*, *ACAT2*, *ACOT1*, *ACOT2*, *ACOT4*, *ACOX2*, *ACSL1*, *ACSL3*, *ACSM3*, *ACSM6*, *AWAT1*, *ELOVL3*, *ELOVL5*, *CRAT*, *DGAT2*, *DGAT2L6*, *RDH11*, *SOAT1*, *FADS1*, *FADS2*, *MOGAT1*,

							MOGAT2, *PNPLA5*, *CYP27A1*, *PLA2R1*, *PLA2G7* , *PLA2G16*, *ALOX12P2*, *ALOX15B*) Binding proteins (*APOC1*, *APOE*, *FABP1*, *FABP7*, *FABP9*, *RBP1*) Receptors (*PPARG*, *PPARGC1A*)
+	-	-	N/A	N/A	N/A	Downregulated	**Immune signalling:** *IL1A*, *IL17B*, *WNT6* **Structural:** Keratins (*KRT33B*, *KRT83*, *KRT86)* **Lipid pathways:** Enzymes (*LPL*, *LRAT*) Binding proteins (*APOB*, *RBP4*) Receptors (*RXRG*)
-	-	-	-	+	-	Downregulated	**Immune signalling:** *IL26* **Structural:** Keratins (*KRT6B*)
-	+	-	-	+	-	Downregulated	**Immune signalling:** *IL22RA2*

3.3.6 RNA-Seq of cytokine mRNA in healthy and diseased skin

Several key cytokines integral to psoriasis pathogenesis demonstrated altered expression patterns across disease and treatment groups (**Figure 3.12, Figure 3.13**). The counts in these figures are normalised to the library size (total read count) of the sequenced sample.

Unsurprisingly, *IL17A* and *IL17F* expression were highest in PS L skin compared to PS NL skin and the AD and HC groups (**Figure 3.11 (a), Figure 3.11 (b)**). *IL12A* was expressed at similar levels in all disease groups but elevated in HC (**Figure 3.11 (c)**), while *IL23A* expression was relatively increased in psoriasis (**Figure 3.11 (d)**). There were no marked differences for *IFNG* (**Figure 3.11 (e)**) but *TNF* expression was increased in skin from PS and AD patients relative to HC (**Figure 3.11 (f)**). The most highly expressed cytokines from the six examined were *IL23A* and *TNF*.

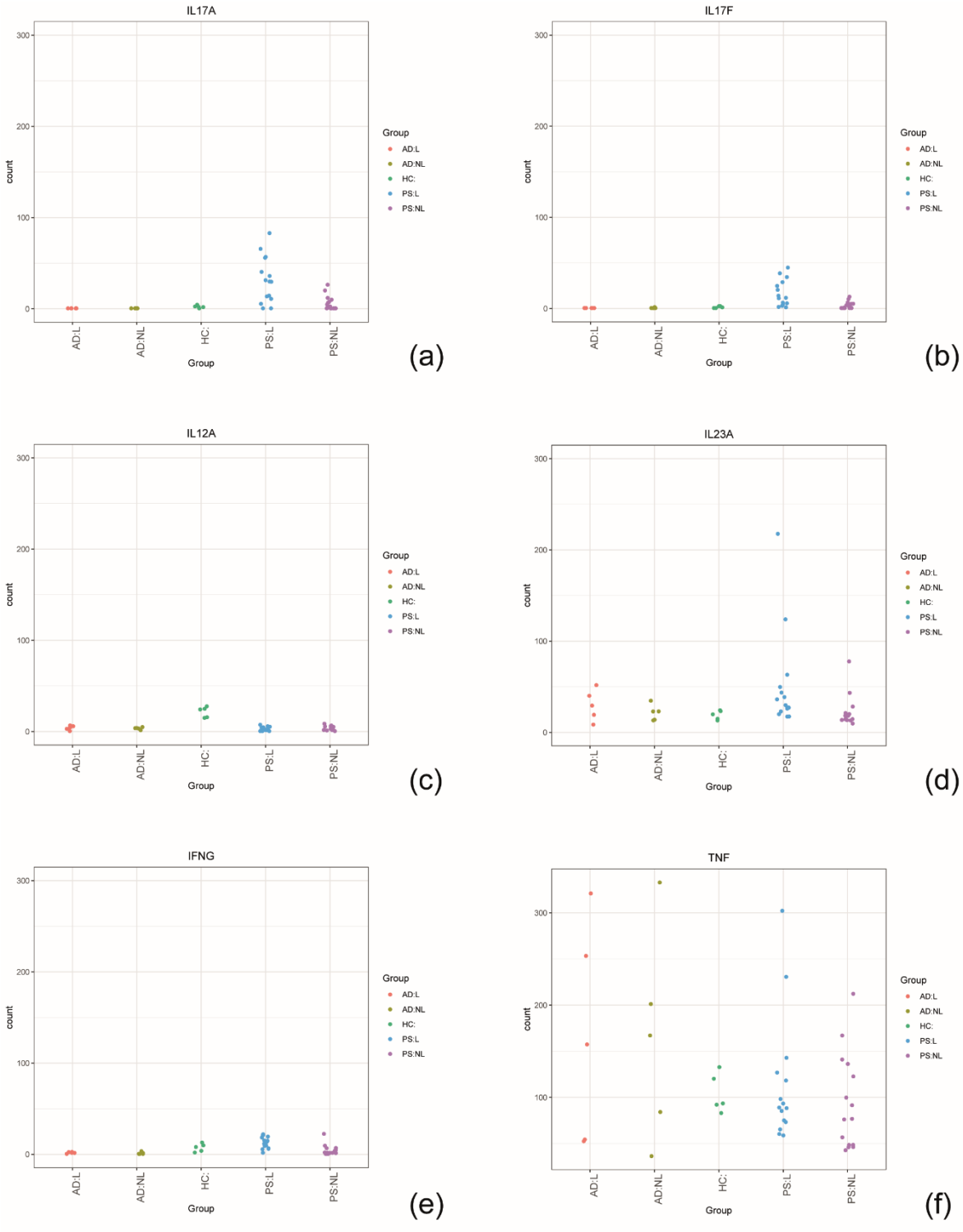


Figure 3.11 Dot plots comparing gene expression of key cytokines across disease groups (a) IL17A (b) IL17F (c) IL-12A (d) IL-23 (e) IFNG (f) TNF. AD; atopic dermatitis, PS; psoriasis, L; lesional, NL; non-lesional (including resolved psoriasis), HC; healthy control.

On analysis of cytokine expression within psoriasis treatment groups, skin that had clinically resolved with NB-UVB showed expression levels of *IL17A* similar to that of untreated PS NL skin, with secukinumab R skin only marginally higher (**Figure 3.12 (a)**). PS NL/R skin had lower levels than PS L skin across all treatment groups. Differences between groups for PS L skin were slight, but showed expression was highest in untreated PS L>PS R (Secukinumab)>PS R (NB-UVB) skin. *IL17F* expression was marginally higher across PS L skin for all treatment groups compared to PS NL/R skin (**Figure 3.12 (b)**). Expression levels of *IL12A* were similar across all groups (**Figure 3.12 (c)**). *IL23A* was increased in untreated, and to a lesser extent, PS L (Secukinumab) skin, while much lower in PS L (NB-UVB) skin (**Figure 3.12 (d)**). Levels in PS R (Secukinumab) skin were higher than those in untreated PS NL and PS R (NB-UVB) skin (**Figure 3.12 (d)**). There were only marginal differences in *IFNG* expression across all treatment groups (**Figure 3.12 (e)**), while *TNF* expression was highest in untreated PS L, both secukinumab samples and of similar levels in untreated PS NL and both NB-UVB samples (**Figure 3.12 (f)**).

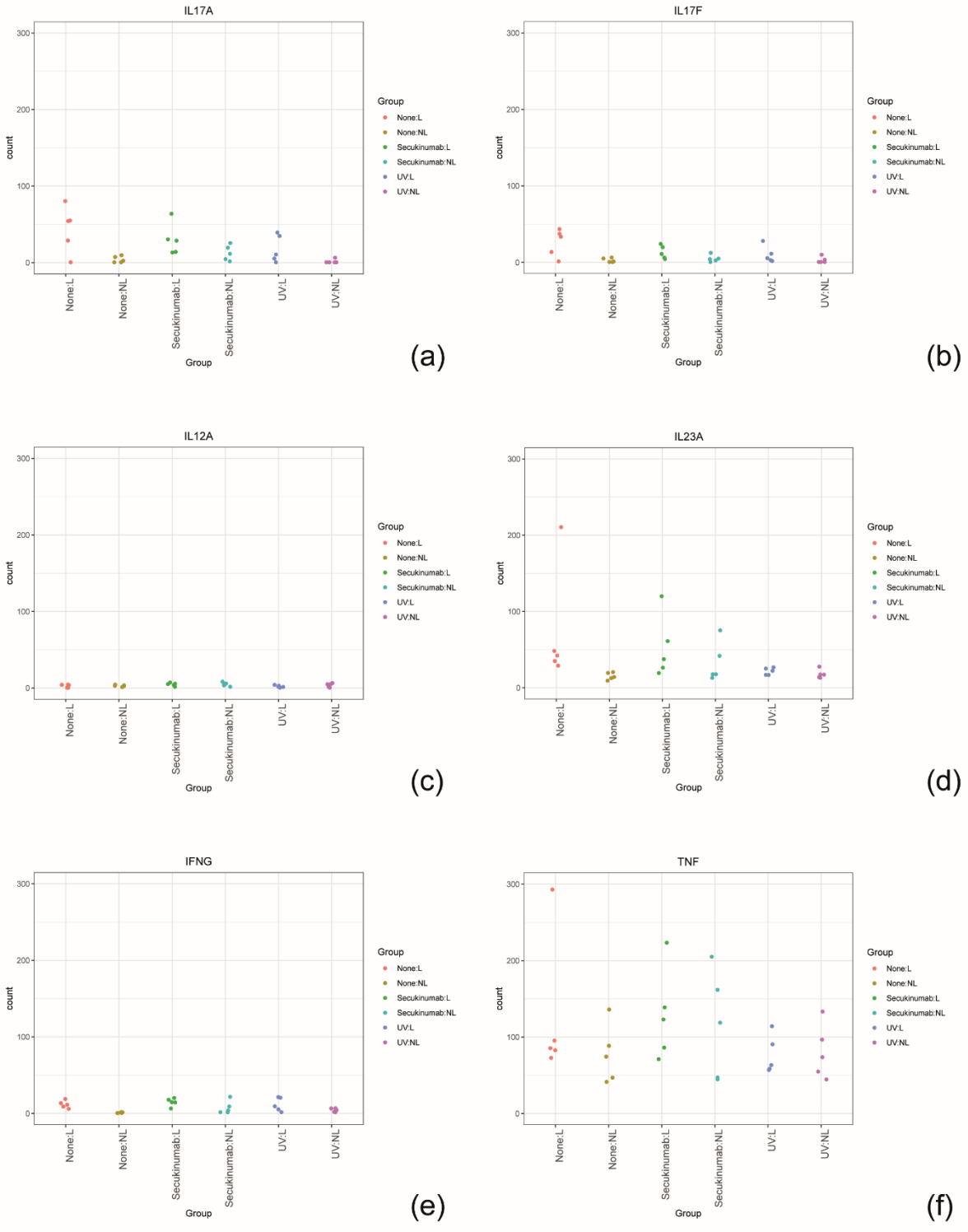


Figure 3.12 Dot plots comparing gene expression of key cytokines between psoriasis treatment groups (a) IL17A (b) IL17F (c) IL-12A (d) IL-23 (e) IFNG (f) TNF. None; untreated, UV; NB-UVB, L; lesional, NL; non-lesional (including resolved psoriasis).

3.3.7 Module-trait relationships and Gene Ontology

To gain deeper understanding of groups of genes that are modulated together, analysis of module-trait relationships was undertaken.

Weighted Gene Co-expression Network Analysis (WGCNA) is a software package for R that is used for weighted correlation network analysis. Analysis was based on a gene list that was filtered by variance and included the 3000 most variable genes for each of eight subgroups. In the diagram below (**Figure 3.13**), within each square there are two numbers. The top number represents the correlation coefficient between the module (clusters of genes that are highly interconnected) and the trait of interest (here; clinical state). The bottom number (in brackets) is the p-value of the association (significance) by Spearman's correlation. Squares where the module is more positively correlated with the trait of interest are redder in colour while squares that are more negatively correlated with the trait are bluer.

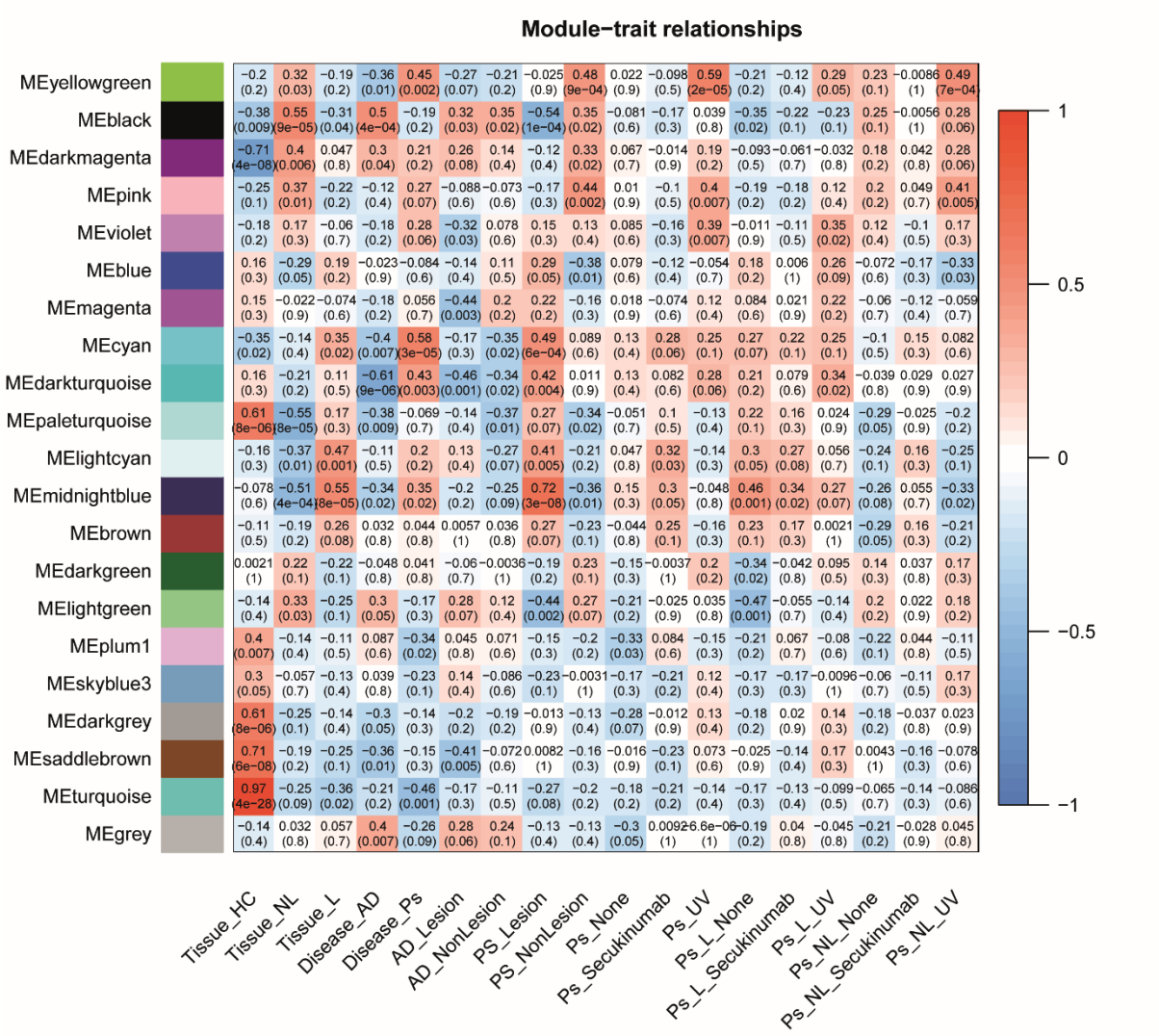


Figure 3.13 Module-Trait Relationships using Weighted Gene Co-expression Network Analysis (WGCNA).

The Turquoise module was most highly correlated with HC skin, with a total of 785 genes, of which 659 were positively correlated with HC status (**Figure 3.14**). Gene Ontology revealed that these genes were involved in metabolic and catabolic processes for cellular lipids, steroids and FA, among others. Enzymatic activity and formation of structures relevant to mitochondria, peroxisomes and lipid droplet formation also featured. Of note, *APOE* featured as a joint point between the steroid metabolic process and the merged small molecule/organic acid/carboxylic acid metabolic process. *ACADM*, *ACAT2*,

ACOT1, *ACOX2*, *ALOX15B*, *AWAT1, ACSL1*, *CRAT*, *DGAT2*, *ELOVL3* and *ELOVL5*, *FADS1* and *FADS2* feature in the FA metabolic process.

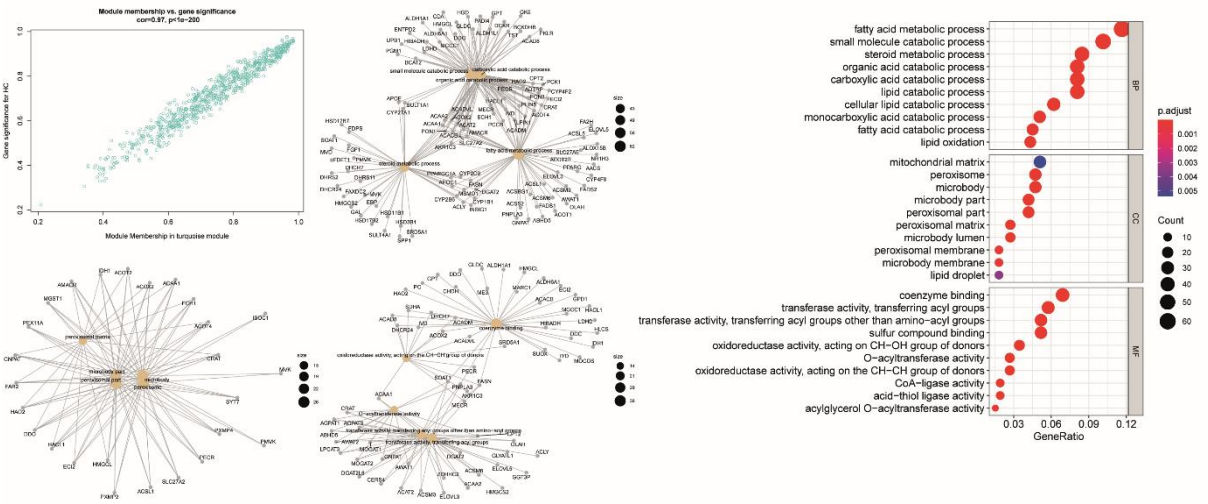


Figure 3.14 Module-Trait relationships: Turquoise module. 659 genes were positively correlated with healthy control status.

126 genes negatively correlated with HC and included multiple *HOX* genes, a few *HLA* subtypes and *WNT3* (**Figure 3.15**). The Wnt pathway has been implicated in psoriasis (Gudjonsson, Johnston, et al., 2010; Reischl et al., 2007).

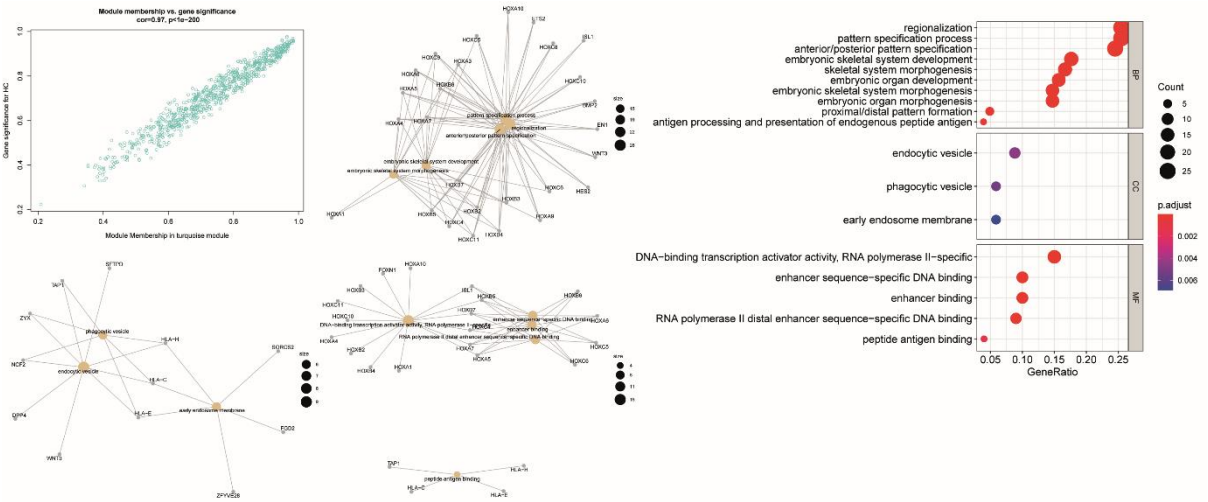


Figure 3.15 Module-Trait relationships: Turquoise module. 126 genes were negatively correlated with healthy control status.

After searching all modules discussed in this section for GO terms pertaining to retinoids, only the Turquoise module (positive correlation with healthy control) showed a positive correlation with GO0001523 (retinoid metabolic process) and GO0032526 (response to retinoic acid), suggesting that normal retinoid metabolism and signalling is a feature of healthy human skin.

On the other hand, the Dark Magenta module was the most negatively correlated with healthy control skin. It showed 17 genes positively correlated with HC status (but no enriched GO terms) and 38 genes negatively correlated with HC status, particularly those involved in cornification including *KRT1* and *KRT10* (data not shown).

The Midnight Blue module was highly correlated with PS L skin for all three treatment groups. 698 genes were positively correlated with PS lesional status and Gene Ontology revealed that those involved in the anti-viral response and type I interferon signalling featured most prominently (**Figure 3.16**). Cytokine and chemokine activity and receptor binding and binding to the Receptor for Advanced Glycation End Products (RAGE) also feature. Network plots showed many known psoriatic cytokines, including *IL1B, L17A*, *IL17C*, *IL17F*, *IL22*, *IL23A*, *IL36A* and more, as well as *WNT5A*, which also featured in the type I interferon-related network (signalling and response). *STAT1*, *STAT3* and *DEFB4* were also part of the chemokine network. *S100A7*, *S100A8*, *S100A9*, *S100A12* were all related to RAGE receptor binding (in network). The response to virus networks also included *IL23A, IL1B* and *LCN2*.

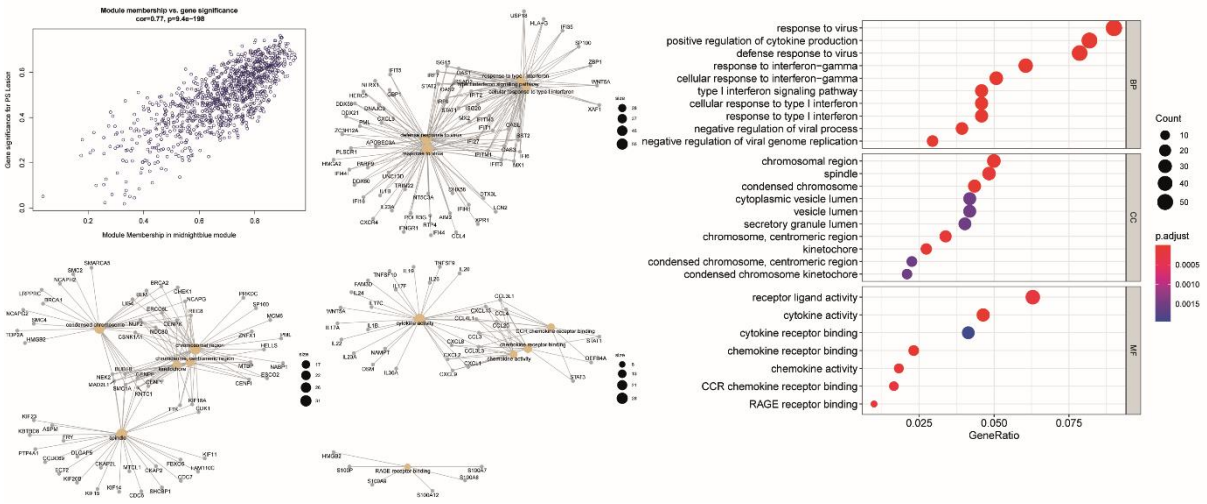


Figure 3.16 Module-Trait relationships: Midnight Blue Module. 698 genes were positively correlated with lesional psoriasis.

306 genes were negatively correlated with PS L skin, with many involved in metabolic processes for organic chemicals and the regulation of the Wnt signalling pathway based on Gene Ontology (**Figure 3.17**).

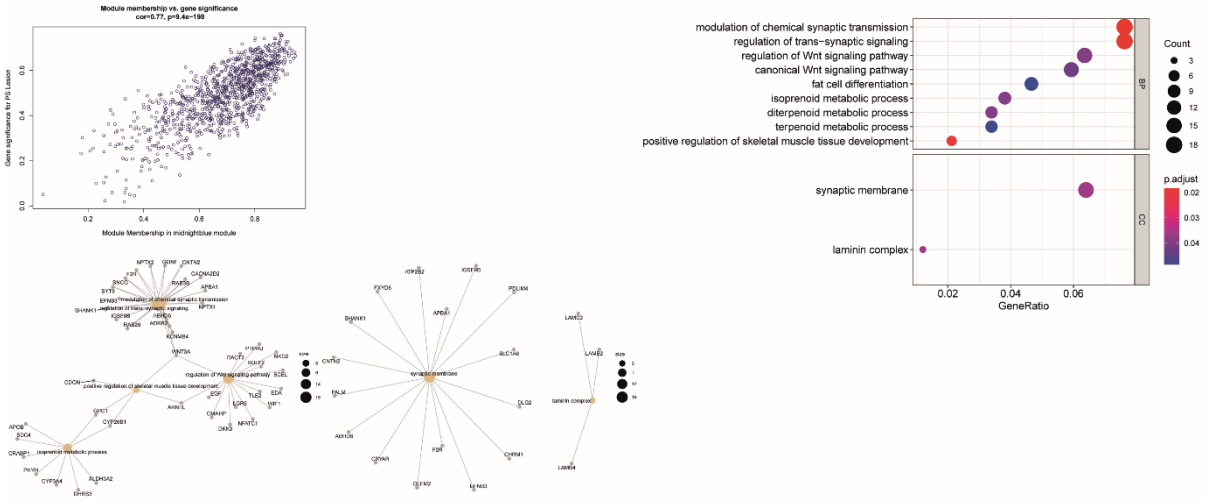


Figure 3.17 Module-Trait Relationships: Midnight Blue Module. 306 genes were negatively correlated with lesional psoriasis.

The Cyan module showed 456 genes that correlated with psoriasis overall, 328 of which were positively correlated with PS status (**Figure 3.18**). Gene Ontology showed

that these were mainly involved in epidermal maturation, including keratinocyte differentiation and keratinisation, as well as lipid biosynthetic, metabolic and catabolic processes, including those related to ceramides, sphingolipids, glycolipids, liposaccharides, membrane and cellular lipids. Lipase and phospholipase activity was also noted, with network genes including *SMPD1* (which encodes sphingomyelinase) and the phospholipases *PLA2G4B*, *PLA2G4D* and *PLA2G2F*. Pertinent genes for GO terms related to epidermis development included *PPARD* and for skin development included *GBA*, *ELOVL1* and *ALOX12B*. Late Cornified Envelope (LCE) genes also featured.

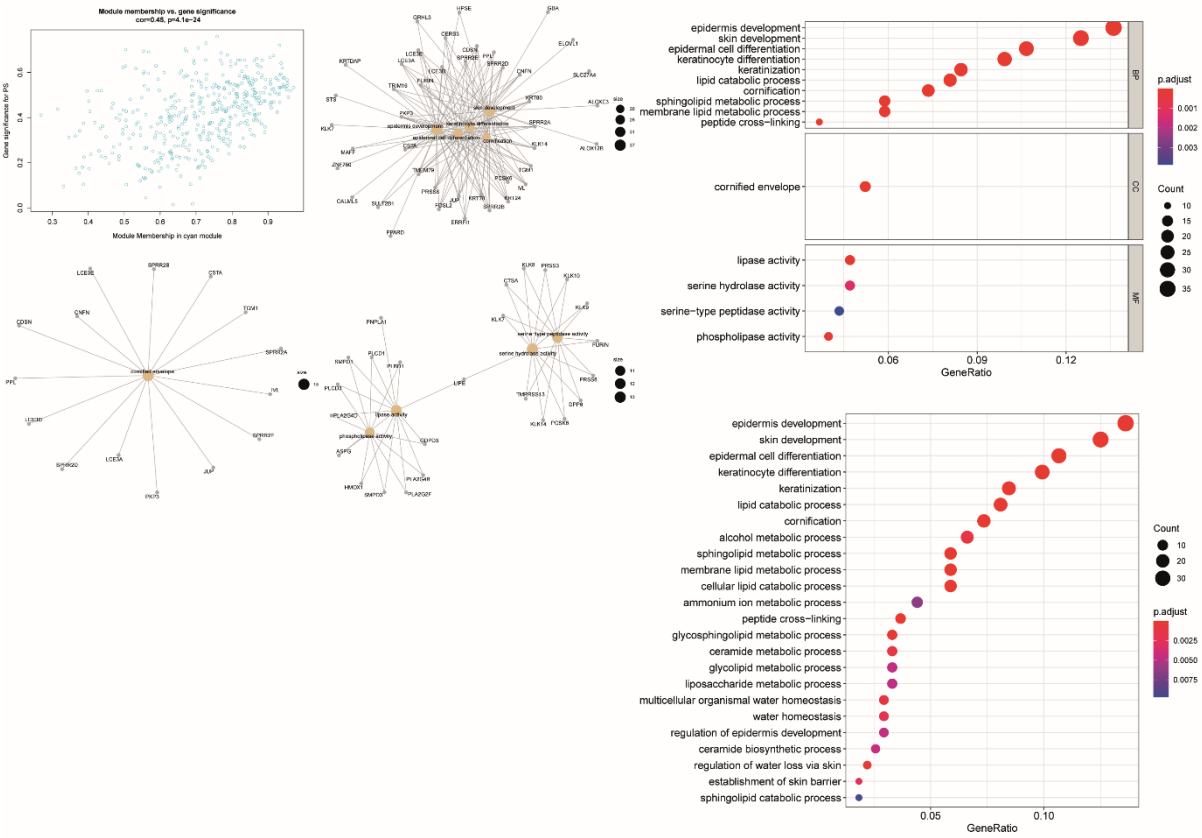


Figure 3.18 Module-Trait relationships: Cyan Module. 328 genes were positively correlated with psoriasis status.

128 genes were negatively correlated with psoriasis status and were mainly related to molecular transport of ions and neurotransmitters and changes in charge across membranes (**Figure 3.19**). The Cyan module negatively correlated with AD.

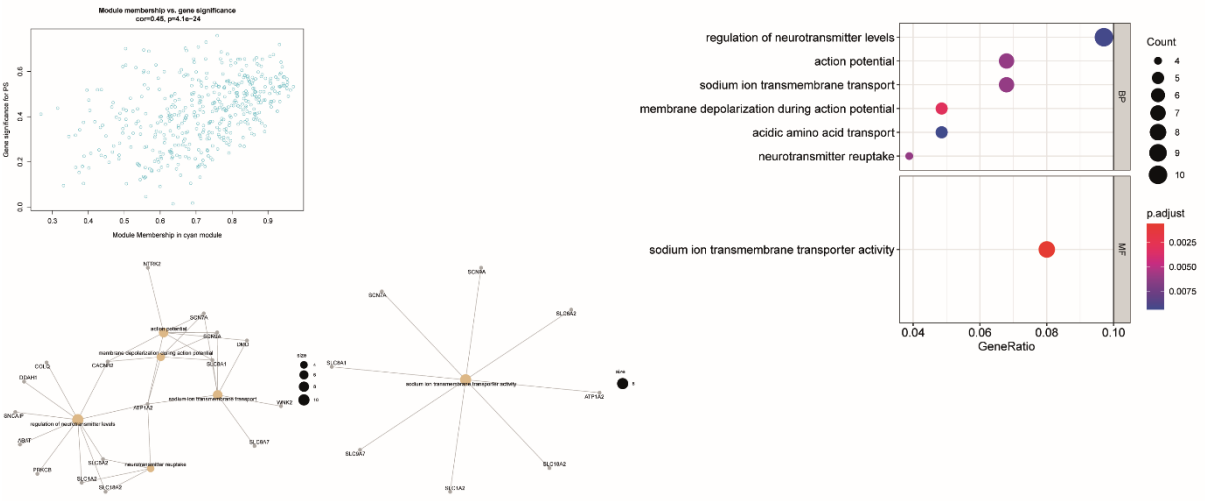


Figure 3.19 Module-Trait relationships: Cyan Module. 128 genes were negatively correlated with PS status.

3.3.8 Co-expression networks

Further analysis of the top 50 driver genes that featured in different modules of interest was performed to identify key genes with the highest correlation with that biopsy subset e.g. HC skin. These are displayed below (**Figure 3.20**- **Figure 3.23**) as co-expression networks and contain a mixture of both positively and negatively correlated genes. The STRING (protein-protein interaction networks and functional enrichment analysis) database covers physiochemical and functional interactions between proteins that are either recognised or predicted. The size of the circles, as for the co-expression networks, corresponds to the number of interactions; proteins in larger circles indicate those that are involved in more interactions. In this way, detection of potential "hub" genes was possible.

The Turquoise module (785 genes) co-expression network showed genes relevant to cutaneous lipid metabolism (**Figure 3.20 (a)**). These included *PDZK1* (cholesterol metabolism) and *MOGAT1* (diacylglycerol (DAG) synthesis- DAG are precursors of triacylglycerols (TAG) and phospholipids) as key genes, as well as *AWAT1* (wax ester production) and *FADS1* (desaturation of ω3- and ω6- PUFA for the formation of eicosapentaenoic and arachidonic acid) deeper in the network.

STRING analysis to assess protein interaction (**Figure 3.20 (b)**) showed ApoE connecting directly to RBP1 and indirectly to ALDH1A1 (both enzymes relevant to retinoid metabolism), indirectly to ACADM and ACAT1 (enzymes of the FA β-oxidation pathway by which NFA are broken down), and peripherally FADS2 and ACSL1 (both involved in linoleic acid metabolism).

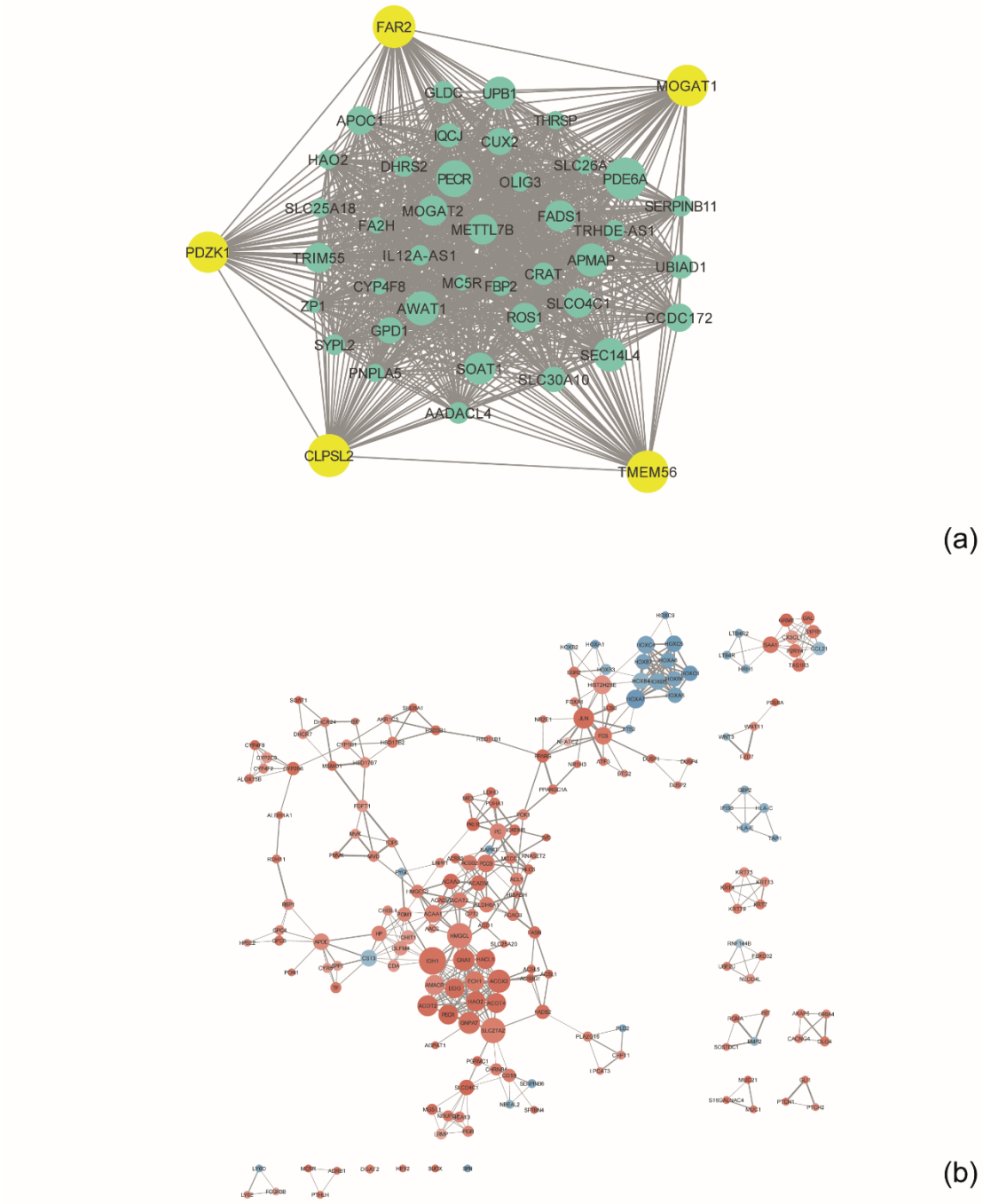


Figure 3.20 Turquoise module WGCNA (a) Co-expression network (b) STRING.

The Midnight Blue module (1004 genes) co-expression network (**Figure 3.21 (a)**), which was highly correlated with PS L skin, included recognised psoriatic genes such as *S100A12*, *DEFB4*, *S100A7A* and *IL36*, *SERPINB3* and *SERPINB4*. STRING analysis (**Figure 3.21 (b)**) also showed a network of several keratins, including KRT6A, KRT6B,

KRT6C and KRT16. STAT3 was a focal point with direct and indirect links to psoriatic cytokines IL-23A, IL-22, IL-17A and IL-17F. This part of the network also contained members of the Wnt pathway including WNT-5A, WNT-10A and WNT-3A.

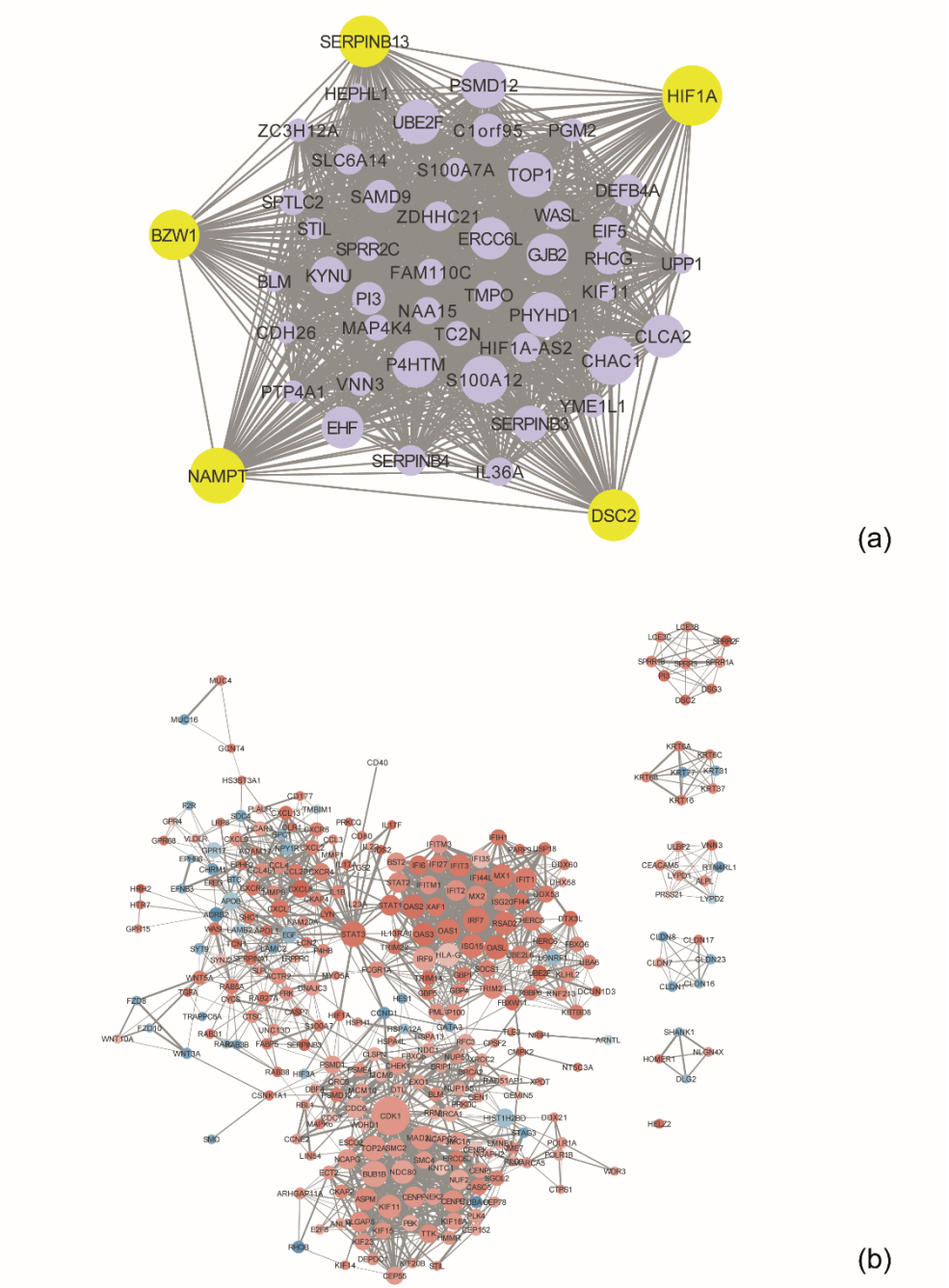


Figure 3.21 Midnight Blue Module WGCNA (a) Co-expression network (b) STRING.

PPARD and *GBA* were two of the cornerstone genes in the co-expression network of the top 50 interconnected genes in the Cyan module (out of 456 genes) (**Figure 3.22**). *IL36RN* (which encodes the interleukin 6 receptor antagonist) and *SPRR2D* and *SPRR2E* also feature within this network. Proteins of interest on STRING prediction include proteins of keratinisation (SPRR2A, SPRR2B, SPRR2D, SPRR2E) and cornification (LCE3A/LCE3D/LCE3E) and peripherally the FA transporter SLC27A4 (for translocation of long chain fatty acids (LCFA) across the plasma membrane), the phospholipase PLA2G4B and CERS3 for ceramide synthesis, the latter linked to enzymes of the sphingolipid metabolic pathway.

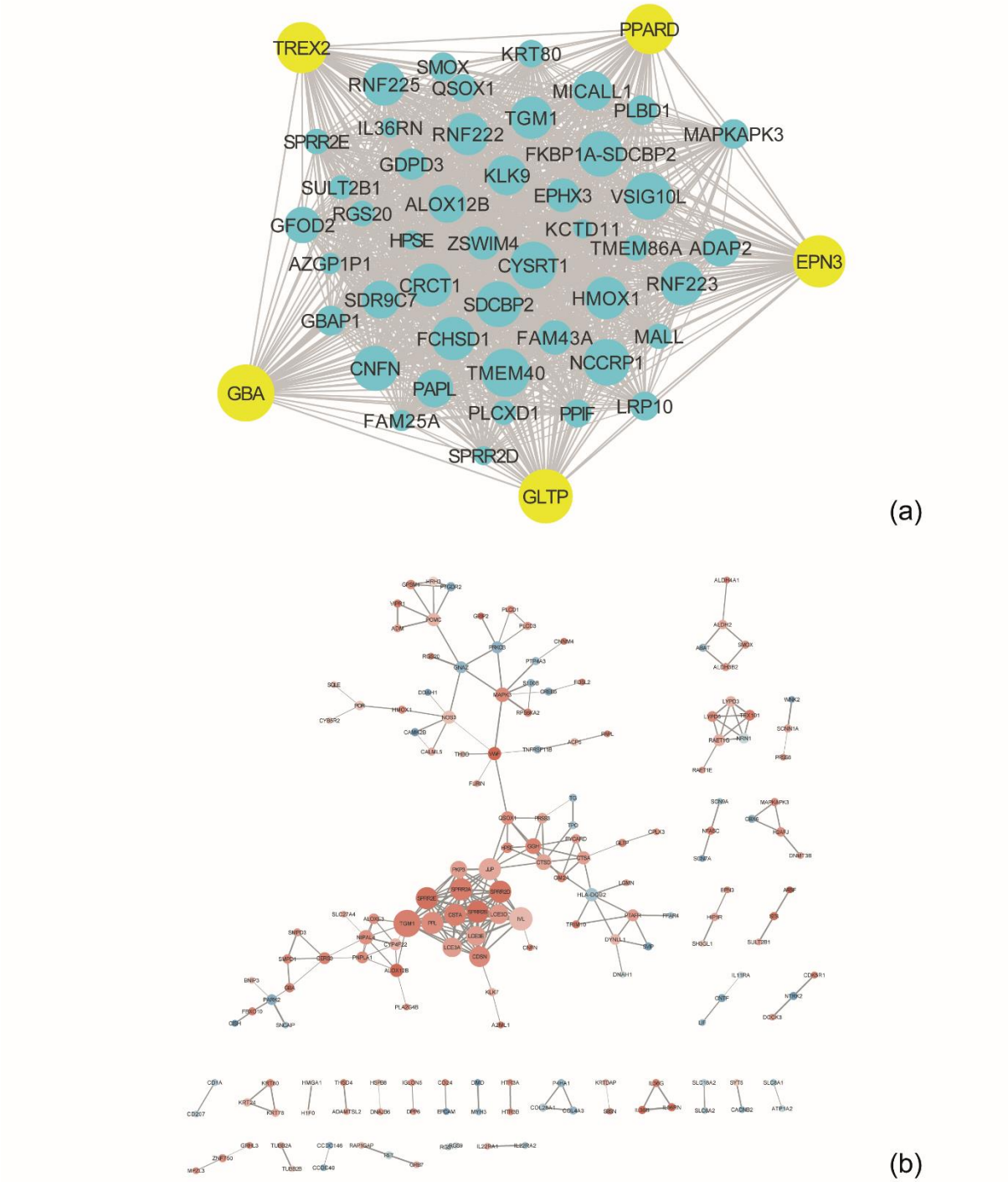


Figure 3.22 Cyan Module WGCNA (a) Co-expression network (b) STRING.

The Black module co-expression network (**Figure 3.23 (a)**) contained *IL17RE* (which encodes IL-17 receptor E). STRING analysis (**Figure 3.23 (b)**) showed WNT family members WNT-2, WNT-4 and WNT-7B.

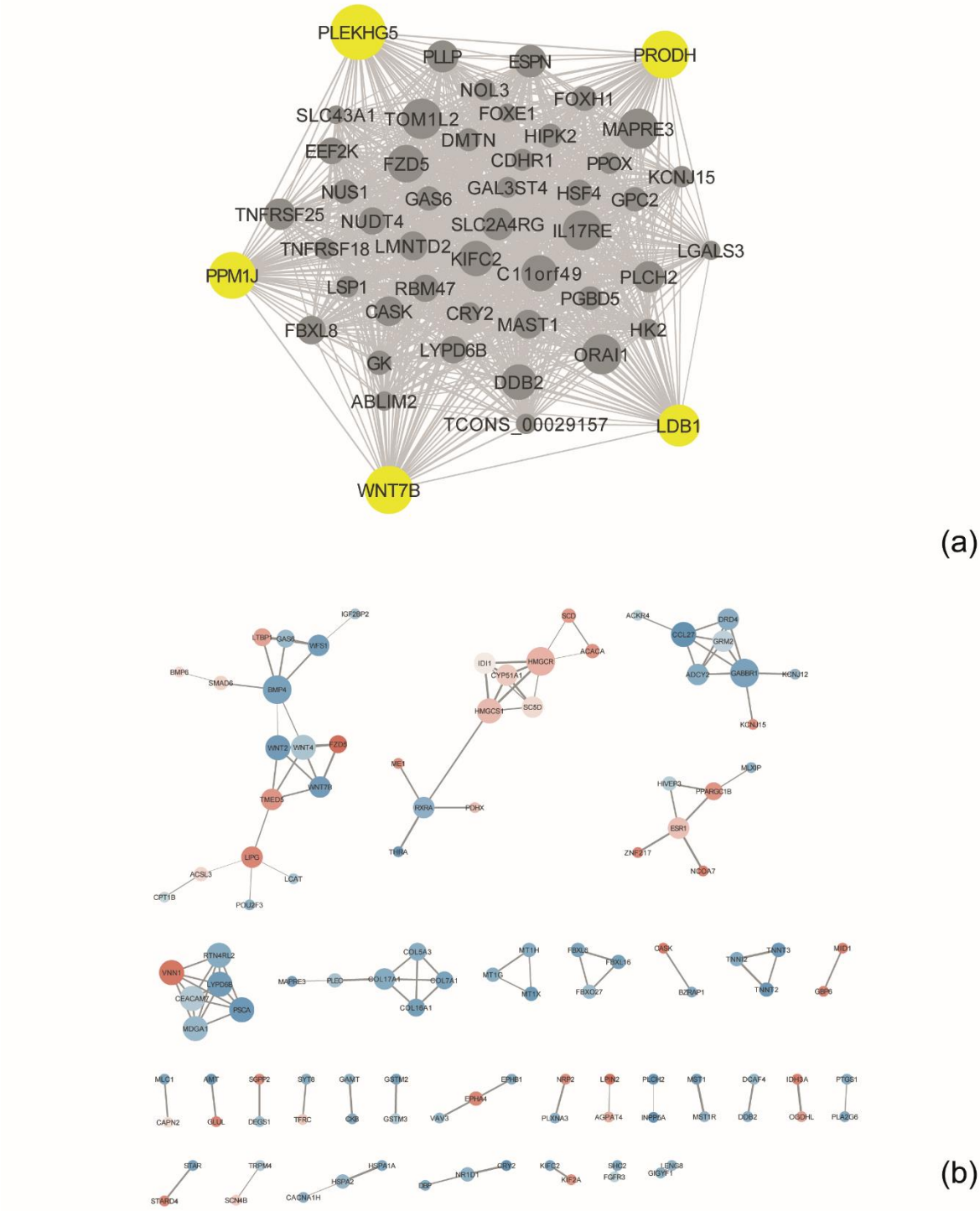


Figure 3.23 Black Module WGCNA (a) Co-expression network (b) STRING.

3.3.9 RNA-Seq results summary

RNA-Seq data supported the findings of published literature with regards to DEG in psoriasis, particularly downregulation of lipid pathways, with alterations in expression of genes relevant to candidate CD1a lipid antigens. New insight was gained into modulation of gene expression by different therapeutic modalities in this disease.

3.4 Discussion

Overall findings

Prior to embarking on analysis of gene expression in psoriasis and the effects of treatment, a review of the literature established a number of points. Specifically, there are significant differences in gene expression in psoriatic lesional compared to non-lesional skin and in psoriatic lesional skin compared to healthy skin. Non-lesional psoriatic skin, although clinically unremarkable, also shows differential gene expression compared to healthy skin. Most studies to date are of psoriatic lesional skin and uninvolved skin which may or may not be adjacent to the lesional skin. Furthermore, studies assessing the psoriatic transcriptome in lesional skin that has become clinically normal following specific treatments are very limited.

RNA-Seq analysis of paired lesional and non-lesional biopsies from a patient cohort consisting of individuals with psoriasis under various treatments was performed: topical therapy (considered untreated), NB-UVB phototherapy and anti-IL17A biologic therapy with secukinumab, as well as atopic dermatitis as an inflammatory disease control group and single biopsies from healthy controls. This is the first analysis of its kind and sheds new light on differential gene expression in untreated psoriatic skin compared to that which has clinically persisted or resolved with common therapeutic modalities. Many of

the findings from our analysis relating to PS L, PS NL and AD skin (vs HC) are supported by previously published work, including clustering of samples by disease group on PCA, upregulation of genes encoding immune signalling proteins, key psoriasis cytokines and antimicrobial peptides and downregulation of genes involved in lipid pathways in psoriatic skin (Bowcock et al., 2001; Deng et al., 2022; Gudjonsson, Ding, et al., 2010; Gudjonsson et al., 2009; Jabbari et al., 2012; Kulski et al., 2005; Oestreicher et al., 2001; Reischl et al., 2007; Suárez-Fariñas et al., 2010, 2012; Yao et al., 2008; Z. Yu et al., 2020; Zhou et al., 2003). A number of genes encoding phospholipases featured as positively correlated with PS overall (WGCNA Cyan module), including *PLA2G4D*, with the role of the protein product already identified by work from this lab as relevant to CD1a antigen presentation in the context of psoriasis (Cheung et al., 2016). STRING analysis of the WGCNA Midnight Blue module (correlating with PS L skin) highlighted the central role of STAT3 with direct and indirect links to IL-23A, IL-22, IL-17A and IL-17F.

Some have suggested that psoriasis is a dysregulated response to infection or physical stress, as summarised in a recent review by Teng et al (Teng et al., 2021). This was supported by Gene Ontology for the Midnight Blue module (correlating with PS L skin) in WGCNA analysis which prominently featured type I interferon signalling and the anti-viral response. Postulated psoriasis autoantigen and potential propagator, Pso p27, is derived from proteins encoded by *SERPINB3* and *SERPINB4*, which were also identified in our data as exclusively upregulated in lesional psoriasis. Iversen et al's comprehensive review reports that cytokines such as TNF may provoke generation of this autoantigen while a number of psoriasis therapies prevent it (Iversen et al., 2017).

Interestingly, clinically normal, PS NL skin is not identical in gene expression to HC skin. This was the case not only for our study, where biopsies were taken across the border of a lesion, but also where biopsies were taken from more distant sites (Gudjonsson et

al., 2009). Many upregulated and downregulated genes were shared between PS L (vs HC) and PS NL (vs HC) (**Figure 3.10**, **Figure 3.11**). This suggests a possible genetic predisposition in patients who go on to develop psoriasis; that the skin has baseline susceptibility to the development of lesions. HLA subtype has been raised as a predisposing factor (Nair et al., 2006). Whether the downregulation of enzymes involved in lipid pathways shared across all psoriatic skin, including non-lesional and clinically resolved skin, may contribute to this susceptibility is, as yet, unknown. GO terms for the WGCNA Turquoise module, which was most correlated with HC skin, included steroid and FA metabolic processes as well as FA and lipid catabolic processes. This module was also positively correlated with retinoid metabolic processes and response to retinoic acid. The downregulation of these genes in disease may alter the lipid environment in the skin to the point that new lipid antigens are generated or inhibitory lipid antigens are displaced. We postulate that retinyl esters are ligands for CD1a (**Chapter 4**). If this is the case in healthy skin, it is conceivable that displacement of these esters by antigenic lipids may occur in diseased skin as a consequence of downregulation of relevant synthetic genes (such as *LRAT*). The second-generation retinoid acitretin, which promotes generation of triglycerides and breakdown of FA, may help to rectify this balance. Co-expression networks again highlighted genes relevant to cutaneous lipid metabolism, including for cholesterol, diacylglycerols and wax esters, and the arachidonic acid pathway.

Differences in gene expression based on therapeutic modality

Given the design of our cohort, we were able to elucidate new data with regards to differential gene expression in skin that has clinically resolved with two common therapeutic modalities, NB-UVB phototherapy and the anti-IL17A therapy secukinumab. Our data revealed that the psoriatic transcriptome differs in lesional skin compared to healthy skin across all three groups (untreated/NB-UVB/secukinumab), albeit to varying

degrees. Differential gene expression between psoriatic treatment groups provided insight on how these treatments work. NB-UVB phototherapy exerts a generalised immunosuppressive effect, whereas the IL-17A antagonist secukinumab is a targeted therapy for one of the key driver cytokines in psoriasis. It would therefore be expected that the effect on mRNA expression would be broader with NB-UVB and this was indeed the case. Many key genes (*KRT6C*, *KRT16*, *S100A8*, *S100A9*, *SERPIN B3, SERPINB4*, *IL17A*, *IL17F*, members of the *IL36* family) were upregulated in PS L skin, whether untreated or undergoing therapy with NB-UVB or secukinumab. However, on clinical resolution, *SERPINB3* and *SERPINB4*, *S100A8* and *IL17F* were no longer upregulated in both PS R groups. Genes that remained upregulated in PS R secukinumab (vs HC) but not PS R UV (vs HC) included *KRT6C*, *KRT16*, *S100A9* and *IL17A*. It is notable that secukinumab is an anti-IL17A antibody but does not affect the upregulation of IL17A in clinically resolved skin. However, it has been shown that expression of IL17-pathway-related genes are downregulated as treatment continues (from six weeks onwards) (J. Wang et al., 2023).

Compared to HC, untreated PS L skin shared 1,092 DEG with PS R (NB-UVB) and 1,470 DEG with PS R (Secukinumab). PS L (NB-UVB) and PS R (NB-UVB) had the lowest ratio of downregulated to upregulated genes compared to HC and the number of DEG compared to HC was also less in PS L (NB-UVB) vs PS L (Secukinumab). This suggests that the broad immunosuppressive effects of phototherapy, rather than the targeted mode of action of secukinumab, is more effective at returning gene expression to a level closer to that seen in HC. The difference in gene expression between these treatment modalities may not only be related to their mode of action, but also the mode of delivery (externally to skin vs subcutaneous injection) and potential additional effects on minor pathways. The more targeted action of secukinumab on downstream cytokine signalling pathways may mean that upstream pathways in psoriasis pathogenesis remain intact, as in untreated skin. It is also interesting to note that patients usually progress to biologic

therapy after having failed phototherapy (non-response) (**Figure 1.1**). Whether phototherapy in months or years prior, and the cumulative exposure, may exert long term effects on gene expression is unknown.

Lipid pathways in psoriasis

Changes in lipid enzyme metabolic pathways were identified, including downregulation of pathways relevant to FA and triglycerides, across all three psoriatic treatment groups compared to healthy controls. WGCNA analysis for the Turquoise module, which correlated highly with HC skin, highlighted pathways relevant to metabolic and catabolic processes for lipids, steroids and FA. Of specific interest for this project, two GO terms pertaining to retinoids, GO0001523 (retinoid metabolic process) and GO0032526 (response to retinoic acid), were found to significantly positively correlate with HC skin (Turquoise module). This lends credence to the idea that intact retinoid metabolism is a feature of healthy skin. Although these three GO terms were not identified in the other modules, even as negatively correlated terms, in **Chapter 4** I will elaborate further on dysfunction of retinoid pathways in psoriatic skin based on experimental data. *LPL*, *RBP4* and *RXRG* were uniquely downregulated in untreated PS L skin (only) vs HC. Lesional or resolved skin subject to NB-UVB or secukinumab did not display downregulation of *LRAT* (downregulated in untreated PS L and PS NL vs HC), a key enzyme for synthesis of retinyl esters. Correction of the downregulation of these genes may suggest a potential therapeutic mode of action for retinoids such as acitretin in psoriasis. STRING analysis of the WGCNA Midnight Blue module (correlated with PS L skin) also identified a network of keratins including KRT6B and KRT16, both suppressed by retinoic acid (Lee et al., 2009).

The downregulation of genes from pathways relevant to the synthesis and metabolism of FA was noted across all psoriasis groups, e.g. *ACACB*, *FADS2* and *FASN*, as were

two of the key enzymes in the β-oxidation pathway, *ACADM* and *ACAA2*. Fatty acids may function as small, headless antigens for CD1a (De Jong et al., 2014). Exogenous FA have been shown to reduce T_H1 differentiation and significantly reduce production of T_H1, T_H2 and T_H17 cytokines but do not negatively impact T_{reg} (Michalek et al., 2011). In fact, it has been suggested that T_{reg} may use exogenous FA to sustain their proliferation (Berod et al., 2014). Disturbances in FA metabolism could therefore theoretically affect T cell activity. Nitrated fatty acids (NFA), which are discussed in detail in **Chapter 5**, have been shown to exert both pro- and anti-inflammatory effects and nitro-conjugated linoleic acid has been found at increased levels in PS L (vs NL) skin (Mathers et al., 2018). Whether this is a protective mechanism or a contributor to the pro-inflammatory state in diseased skin remains to be elucidated. Linoleic acid, a PUFA which was specifically identified in Gene Ontology, is a substrate for nitration for the formation of the NFA, nitro-conjugated linoleic acid. The gene encoding the enzyme FADS2, which converts linoleic acid to highly unsaturated fatty acid (HUFA) is downregulated across psoriasis groups, potentially increasing the amount available as a substrate for nitration. Downregulated genes in NB-UVB-treated skin included those encompassed by GO terms for oxidoreductase activity which could also have a bearing on the formation of NFA. The Turquoise module (correlates with HC skin) showed upregulation of genes involved in the catabolism of FA including linoleic acid. If abnormalities of lipid metabolism are a contributing factor to disease pathogenesis and differential expression of relevant genes is not corrected in skin that has clinically resolved with NB-UVB or secukinumab, this may contribute to the chronicity of disease and explain why these treatments are merely suppressive rather than curative. To investigate, further exploration of genes of interest identified through our data is outlined in **Chapter 7**.

3.5 Chapter Summary

The RNA-Seq data reflects many recognised alterations in gene expression in psoriatic skin, AD skin and healthy control skin. Some findings from skin treated with NB-UVB phototherapy are also supported in the literature, although there are several variables, such as the site and timing of sampling, to consider, as well as our data being initially compared to HC. Our analysis has revealed differences in DEG across two commonly employed therapeutic modalities. Genes relevant to key lipid pathways in psoriasis will be explored in more detail in **Chapter 7**.

4 Chapter 4 Retinyl Esters

4.1 Introduction

Retinoids are compounds derived from vitamin A. There are two groups, Vitamin A1 and Vitamin A2 (dehydroretinoids); the former will be the focus of this thesis. Retinol is oxidised to retinaldehyde (retinal) by a reversible reaction and then irreversibly metabolised to retinoic acid (RA), which, in its *all-trans* form, exerts most of the biological effects associated with these molecules. Retinyl esters (RE) are the storage form of retinol. *All-trans*-retinoic acid (atRA) binds to nuclear receptors (Retinoic Acid Receptors; RAR) to exert both genomic and non-genomic effects with wide-reaching implications for growth, maturation and immunological function. It is also responsible for most of the potential side effects associated with this group of drugs, which are widely used in dermatology.

Many of the clinical and histological features seen in psoriasis are counteracted by the actions of retinoids and synthetic retinoids, notably acitretin, have been employed with therapeutic success (**Chapter 6**). RNA-Seq data demonstrated changes in genes encoding proteins involved in retinoid metabolic pathways in psoriasis compared to healthy controls (**Chapter 3**, **Chapter 8**). Although much research has been done on the physiological effects of retinol, retinal and retinoic acid, the study of RE is more limited. Investigation of RE as potential CD1a ligands and the implications for this in the pathogenesis of cutaneous T-cell mediated inflammation is outlined in this chapter.

4.1.1 Retinyl Ester metabolism

Retinol is essential for life and can only be obtained from exogenous sources, predominantly as RE in meat or as pro-vitamin A carotenoids such as beta-carotene. RE

are hydrolysed to retinol in the small intestine and subsequently absorbed and stored in the liver, predominantly as retinyl palmitate (Blomhoff, 2001; Blomhoff & Blomhoff, 2006; O'Byrne & Blaner, 2013). The transfer of LCFA moieties from the membrane phospholipid phophatidylcholine to retinol, mainly by lecithin retinol acyltransferase (LRAT), results in formation of common esters in the human body such as retinyl palmitate, retinyl oleate, retinyl stearate and retinyl linoleate (O'Byrne & Blaner, 2013). RE can also be formed via ARAT (acyl CoA:retinol acyltransferase) activity, which has been detected in various enzymes including DGAT1, DGAT2 and AWAT2. RE are found at an estimated concentration of ~2,000pmol/g in the skin, about ten times more than *all-trans*-retinol, with atRA undetectable in dermis or epidermis (Sorg et al., 1999). The reported ratio of RE to different retinols in the skin varies by study (Antille et al., 2003; Randolph & Simon, 1996; Sorg et al., 1999; Vahlquist, 1982), but it is clear that these represent a key component of skin lipids. If dietary intake of Vitamin A is reduced, RE are converted back to retinol to maintain serum retinol concentration at 1-2μM (Blomhoff, 2001). Lysosomal acid lipase (LAL) is the principal acid retinyl ester hydrolase in cultured human hepatic stellate (LX-2) cells (Wagner et al., 2020). The retinoid metabolic pathway is linked to the sterol metabolic pathway (**Chapter 6**) by LAL, also known as cholesteryl ester hydrolase (**Figure 4.1**).

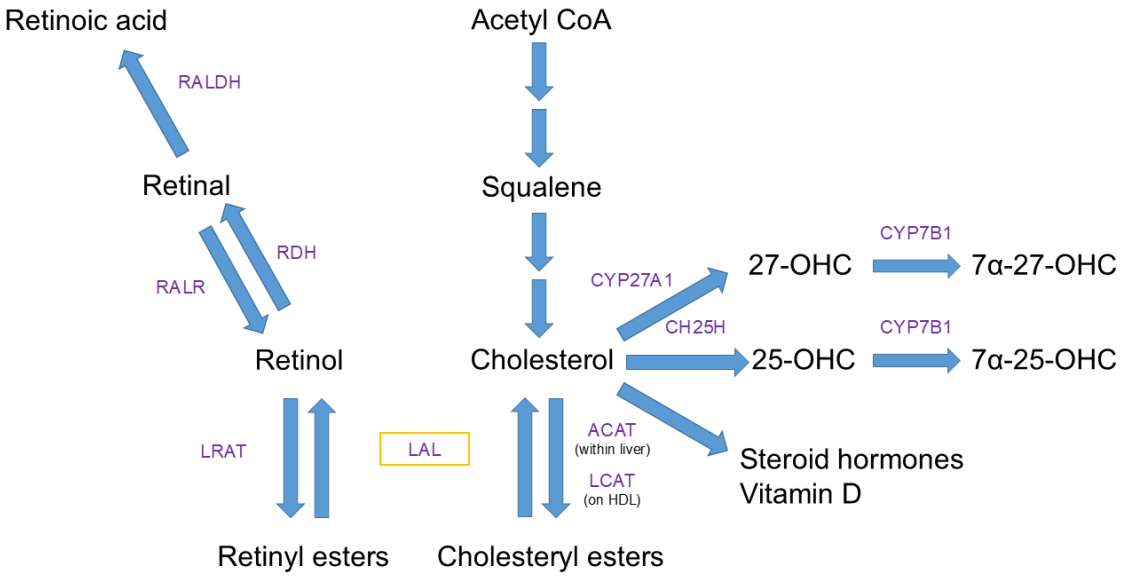


Figure 4.1 Interaction of Sterol and Retinoid pathways. The enzyme Lysosomal Acid Lipase (LAL), also known as cholesteryl ester hydrolase (CEH), links the two pathways. Enzymes in purple text. RALDH; retinaldehyde dehydrogenase, RALR; retinal reductase, RDH; retinol dehydrogenase, LRAT; leicithin:retinol acyltransferase, LAL; lysosomal acid lipase, ACAT; acyl-coenzymeA:cholesterol acyltransferase, LCAT; lecithin:cholesterol acyltransferase, CH25H; cholesterol 25-hydroxylase, CYP27A1; cytochrome P450 family 27 subfamily A member 1, CYP7B1; cytochrome P450 family 7 subfamily B member 1.

4.1.2 Retinyl Esters in healthy skin

RE are a component of healthy human skin(Vahlquist, 1982) and are formed in basal keratinocytes (LRAT) or the supra-basal layers of the epidermis (ARAT). Normal human epidermal keratinocytes (NHEK) in culture esterify exogenous retinol to RE (predominantly retinyl oleate) within hours and gradually hydrolyse it to retinol, with some of that oxidised to RA, over approximately one week (Guo, 2000). atRA added to human keratinocyte cultures increases the rate and amount of RE synthesis and reduces RE utilization while decreasing cellular RA concentration (Randolph & Simon, 1996). Microarray data from Lee et al supports atRA's role in regulating the esterification of

retinol (Lee et al., 2009). When *all-trans* retinoids are applied to human keratinocyte cultures, they (RA>retinaldehyde/retinol) promote esterification of exogenous retinol, mainly via LRAT, with the implication that LRAT activity is induced by retinoids (Kurlandsky et al., 1996). Vehicle-treated cultured keratinocytes were found to produce retinyl stearate, retinyl oleate and retinyl palmitate, whereas those stimulated by RA produced not only larger amounts of these esters, but additional esters including retinyl linoleate and retinyl myristate (Kurlandsky et al., 1996). However, there was no increase in the formation of RE in basal keratinocytes of human skin treated topically with RA *in vivo* and the authors suggest this was due to adequate retinoids already present ensuring maximal esterifying activity (Kurlandsky et al., 1996). Randolph et al found that cultured human epidermal keratinocytes maintained in retinol-containing medium produced esters in the following order of abundance: oleate 54.9%, palmitate 24.6%, palmitoleate 16.1% and stearate 4.4% (Randolph & Simon, 1993). In another study with the same culture protocol, RE detected were palmitoleate 14%, oleate plus palmitate 55% and stearate 10% (Randolph & Simon, 1995).

4.1.3 Retinyl Esters and psoriasis

The use of RE as topical formulations is relatively novel, although they have been included in cosmetic anti-ageing formulations of late. Oral synthetic retinoids are used to treat a range of diseases including psoriasis, hand dermatitis and acne.

Although there is a paucity of studies related to RE and abnormal human skin, evidence from the literature suggests an alteration in genes related to retinoid metabolism in psoriasis. Comparison of atRA-treated and control primary human epidermal keratinocytes revealed that atRA induced the expression of genes involved in its own biosynthesis and metabolism (including esterification), such as *LRAT*, *RDH11*,

ALDH1A3, *CRABP2* and *CYP26B1*, while downregulating genes involved in biosynthesis of cholesterol and steroid and sphingolipid metabolism (Lee et al., 2009). These downregulated genes included *FASN* (whose protein synthesises LCFA) and multiple enzymes of the cholesterol pathway (*HMGCS1*, *HMGCR*, *MVK*, *PMVK*, *MVD*, *FDPS*, *FDFT1*, *LSS*) (Lee et al., 2009). All of these genes were significantly downregulated in our RNA-Seq data for untreated PS L vs HC with the exception of LSS, which was downregulated but not significantly. AtRA also induced *FADS1*(Lee et al., 2009) (whose protein catalyses formation of HUFA), which was downregulated across all psoriasis samples (vs HC) in our data (**Table 3.4**).

In keratinocytes extracted from healthy skin, RE formation is limited by the metabolism of RA (Randolph & Simon, 1997). The expression of enzymes involved in metabolising retinol to RA is linked to keratinocyte terminal differentiation, with a lack of activity in non-differentiated keratinocytes (Siegenthaler, Saurat, et al., 1990). Another study showed that RA is produced from retinol at a higher rate in lesional psoriatic compared to healthy epidermis and this correlated with increased amounts of CRABP (later identified as CRABP2; **Chapter 8**) (Siegenthaler, Gumowski-Sunek, et al., 1990).

RA has been shown to antagonise many of the processes that result in the clinical and histological presentation of plaque psoriasis. Plaque psoriasis is characterised by an acanthotic epidermis due to hyperproliferation of keratinocytes, with hyperkeratosis and parakeratosis due to abnormal cellular differentiation and reduction or loss of the granular layer. The papillary dermis shows tortuous capillaries and a mixed inflammatory infiltrate; neutrophils may migrate to form micro-abscesses in the epidermis. atRA antagonises these changes via a number of mechanisms, including suppression of multiple keratin genes, including *KRT6B* and *KRT16*, promotion of keratinocyte apoptosis and suppression of the gene encoding vascular endothelial growth factor

(VEGF) (Lee et al., 2009). Of relevance to CD1a, it also suppresses several members of the PLA_2 family (Lee et al., 2009). Several studies have described an increase in retinoid transporters, such as LCN2 and RBP4, in psoriasis serum and increased proteins capable of binding RA in PS L skin (**Chapter 8**).

In summary, RE are found in healthy skin, raising the possibility that they may have a homeostatic role. Meanwhile, retinoid metabolism is known to be altered in psoriatic skin and many of the processes that result in the features of this disease are countered by RA. Indeed, synthetic retinoids with RA analogues as their active ingredients are successfully used to treat psoriasis in the dermatology clinic. Whether this could be due to restoration of RE stores is unclear. In this chapter, the potential for RE to act as CD1a ligands was investigated, with three chosen for further experimentation: *all-trans*-retinyl oleate, *all-trans*-retinyl stearate and *all-trans*-retinyl palmitate. The acyl tails of these esters would be predicted to fit in the CD1a binding cleft (**Figure 4.2**), given the length of their carbon chains (De Jong et al., 2014; Huang et al., 2023; Zajonc et al., 2003).

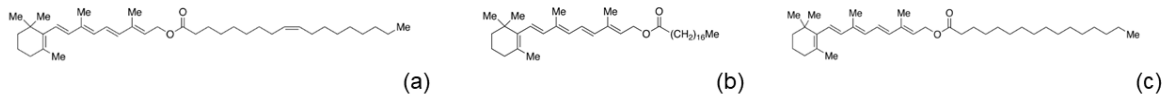


Figure 4.2 Chemical structure of (a) all-trans-retinyl oleate (RO), $C_{38}H_{62}O_2$, (b) all-trans-retinyl stearate (RS), $C_{38}H_{64}O_2$ and (c) all-trans-retinyl palmitate (RP), $C_{36}H_{60}O_2$. Composite of images take from information on products purchased on www.trc-canada.com.

4.2 Results: Retinyl Esters

4.2.1 Interrogation of RNA-Seq data for retinoid-relevant genes

Chapter 3 outlined lipid metabolic pathways altered during psoriasis pathogenesis and following treatment with NB-UVB or anti-IL17A monoclonal antibody therapy. More

detailed analysis of key enzymes of retinoid-specific pathways identified several relevant changes. Given the cross-over with sterol pathways, some of the genes below are also discussed in **Chapter 6**. Genes chosen for validation are discussed in **Chapter 8**.

Downregulation of genes encoding multiple enzymes of the retinoid metabolic pathway was seen in untreated PS L vs HC skin (**Table 4.1**), such as those that synthesise RE from retinol (*LRAT*, *DGAT2* and *AWAT2* whose protein products have ARAT activity). Most genes encoding enzymes promoting formation of RA (alcohol and retinol dehydrogenases, aldehyde dehydrogenases) were also downregulated. Genes encoding retinol binding proteins (RBPs), which with transthyretin (TTR) carry retinol originating from hydrolysed hepatic RE in the blood, were downregulated, while genes encoding proteins with RA binding capabilities, e.g. CRABP2, FABP5 and LCN2, were upregulated.

Table 4.1 Selection of DEG relevant to retinoid pathways: Untreated lesional psoriasis (PS L) versus healthy control (HC) skin.

Gene	Log2FC	p_{adj}
LRAT	-1.681	0.025
LIPA	0.47	0.041
CRABP2	1.004	0.088
FABP5	1.569	0.015
LCN2	1.710	0.099
DGAT1	0.367	0.027
DGAT2	-2.096	8.09×10^{-29}
ACAT1	-0.599	0.001
SCD1	0.315	0.605

NCEH1	-0.062	0.899
PLA2G16	-1.79	5.47×10^{-9}
RBP1	-1.180	0.002
RBP4	-3.064	1.32×10^{-5}
ALDH1A1 (RALDH1)	-2.730	2.31×10^{-15}
ALDH1A2 (RALDH2)	-1.642	0.002
ALDH1A3 (RALDH3)	0.798	0.087
ALDH8A1	-0.493	0.513
ADH1A	0.079	0.931
ADH1B	-0.492	0.779
ADH1C	-0.957	0.605
ADH4	-2.221	0.007
TTR	-1.169	0.528
CYP26A1	-0.534	0.799
RDH5	-0.003	0.996
RDH10	0.251	0.384
RDH11	-1.389	1.55×10^{-9}
RDH12	0.651	0.015
RDH13	0.181	0.382
RDH14	-0.23	0.11
RDH16	0.305	0.369
PPARD	1.138	4.30×10^{-5}
PNPLA2	-0.27	0.109
AWAT2	-13.605	5.10×10^{-48}

Differential expression of retinoid-pertinent genes (vs HC) was milder in skin that had clinically resolved with NB-UVB or secukinumab (**Table 4.2**). The improvement was similar or greater in NB-UVB-treated skin except for CRABP2 and LCN2, where changes were more marked in secukinumab-treated skin. Therapy with both modalities resulted in increased downregulation (vs HC) for *RBP1*, *ALDH8A1* and *RDH11* while more marked downregulation was noted with NB-UVB only for *ALDH1A1*, *ALDH8A1* and *ADH4*. For *ALDH1A3*, *ADH1A* and *RDH10*, which were upregulated in untreated PS L skin, treatment with either NB-UVB or secukinumab resulted in downregulation (although these changes were mild). *CYP26A1* was mildly downregulated in untreated PS L skin and further downregulated by NB-UVB but upregulated by secukinumab.

*Table 4.2 Comparison of DEG in untreated lesional psoriasis (PS L) versus healthy control (HC) skin with DEG in clinically resolved skin following treatment with NB-UVB [PS R (NB-UVB)] or secukinumab [PS R (Secukinumab)] versus healthy control skin. Values represent Log2FC. *p_{adj}<0.05.*

Gene	Untreated PS L Vs HC	PS R (NB-UVB) Vs HC	PS R (Secukinumab) Vs HC
LRAT	-1.681*	-0.909	-1.396
LIPA	0.47*	0.170	0.412
CRABP2	1.004	-0.591	-0.076
FABP5	1.569*	-0.449	0.745
LCN2	1.710	-0.962	-0.185
DGAT1	0.367*	0.524*	0.545*
DGAT2	-2.096*	-1.324*	-1.925*
ACAT1	-0.599*	-0.229	-0.502*
SCD1	0.315	N/A	N/A

NCEH1	-0.062	-0.581	-0.074
PLA2G16	-1.79*	-1.499*	-1.454*
RBP1	-1.180*	-1.478*	-1.306*
RBP4	-3.064*	-0.263	-0.523
ALDH1A1 (RALDH1)	-2.730*	-3.094*	-2.676*
ALDH1A2 (RALDH2)	-1.642*	1.195	-0.904
ALDH1A3 (RALDH3)	0.798	-2.096*	-0.820
ALDH8A1	-0.493	-0.925	-0.587
ADH1A	0.079	-0.346	-0.205
ADH1B	-0.492	0.690	0.905
ADH1C	-0.957	-1.005	-0.749
ADH4	-2.221*	-3.127*	-2.071*
TTR	-1.169	-0.199	-1.318
CYP26A1	-0.534	-2.696	0.571
RDH5	-0.003	0.862	0.746*
RDH10	0.251	-0.428*	-0.337*
RDH11	-1.389*	-1.807*	-1.576*
RDH12	0.651*	0.430	0.579
RDH13	0.181	0.525*	0.091
RDH14	-0.23	-0.276	-0.186
RDH16	0.305	-0.1	0.127
PPARD	1.138*	0.606	1.025
PNPLA2	-0.27	0.269	0.216

AWAT2	-13.605*	-4.736	-9.734

(GO) terms showed that genes encoding enzymes of the retinoid metabolic process and response to RA were downregulated in untreated PS L vs HC skin (**Table 4.3**).

*Table 4.3 Enriched Gene Ontology (GO) terms relevant to retinoid pathways: Untreated lesional psoriasis (PS L) versus healthy control (HC) skin. All GO terms in this table were downregulated in untreated PS L vs HC skin. *Log2FC>2. **Log2FC>4. p_{adj}; adjusted p-value.*

GO Term	Differential expression untreated PS L vs HC	p_{adj}	Genes
GO:0001523** Retinoid metabolic process	Downregulated	0.0005	*GPC6*, *AWAT2*, *DGAT2*, *CYP1B1*, *LPL*, *GPC4*, *ALDH1A1*, *RDH11*, *GPC3*, *STRA6*, *AKR1C3*, *APOE*, *RBP4*, *ABCA4*, *GPC5*, *APOB*, *ALDH1A2*, *RBP1*, *SDC2*, *PNLIP*, *ADH4*, *LRAT*
GO:0032526* Response to retinoic acid	Downregulated	0.0003	*PPARG*, *SLC6A4*, *FZD7*, *HSD17B2*, *PTCH1*, *NTRK3*, *DUSP1*, *FZD4*, *PCK1*, *RXRG*, *BRINP2*, *RBP4*, *BRINP3*, *WNT6*, *SOX9*, *TBX1*, *RORB*, *ALDH1A2*, *EPHA3*, *WNT11*, *IGFBP2*, *LRAT*, *STRA8*
GO:0071300*	Downregulated	0.0018	*PPARG*, *SLC6A4*, *FZD7*, *NTRK3*, *FZD4*, *PCK1*, *BRINP2*, *BRINP3*,

Cellular response to retinoic acid			*WNT6*, *SOX9*, *TBX1*, *RORB*, *ALDH1A2*, *EPHA3*, *WNT11*, *STRA8*

4.2.2 Optimisation of Retinyl Ester solubility

All the RE dissolved satisfactorily in DMSO, particularly after sonication, although there was some mild variation between esters, with retinyl palmitate more likely to precipitate at room temperature.

4.2.3 Investigation of Retinyl Ester binding to CD1a

In 2-day IEF gels, all RE caused a shift in the pI for CD1a (**Figure 4.3**). This was most marked for retinyl oleate and retinyl stearate (**Figure 4.3 (a), Figure 4.3 (b)**), with retinyl palmitate showing more subtle changes (**Figure 4.3 (c)**). However, results for retinyl palmitate varied slightly from assay to assay, which may be due to batch variation and/or its increased susceptibility to precipitation at room temperature.

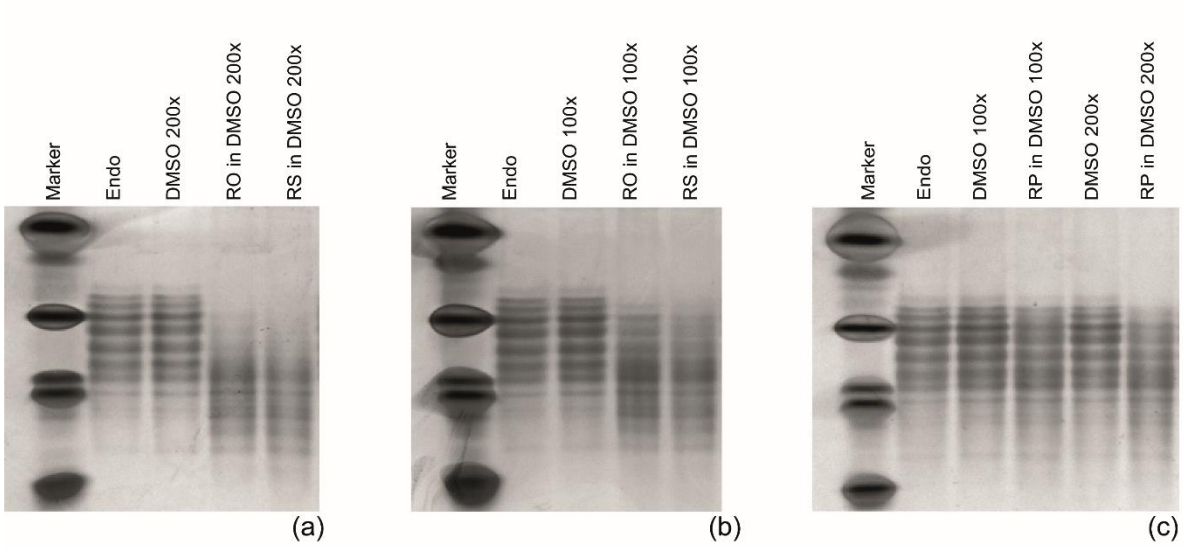


Figure 4.3 IEF gels: CD1a loaded overnight with lipid/vehicle then diluted 1:1 with IEF sample buffer and 18µL/well loaded to IEF gel. Endo (endogenous lipids): CD1a loaded with PBS only, 200x: 8µL CD1a:2µL lipid/vehicle, 100x: 9µL CD1a: 1µL lipid/vehicle (a) RO; Retinyl Oleate (b) RS; Retinyl Stearate (c) RP; Retinyl Palmitate. Lipid stocks: Retinyl E all at 40mM. DMSO; dimethyl sulfoxide.

For gels pre-loaded with GD3 and LPC, the shift produced by each combination differed from RE alone for GD3 (**Figure 4.4**), but the difference was subtle and most convincing for retinyl oleate. Using LPC, all three esters caused a mild shift, with the patterns similar to RE in DMSO only (**Figure 4.5**).

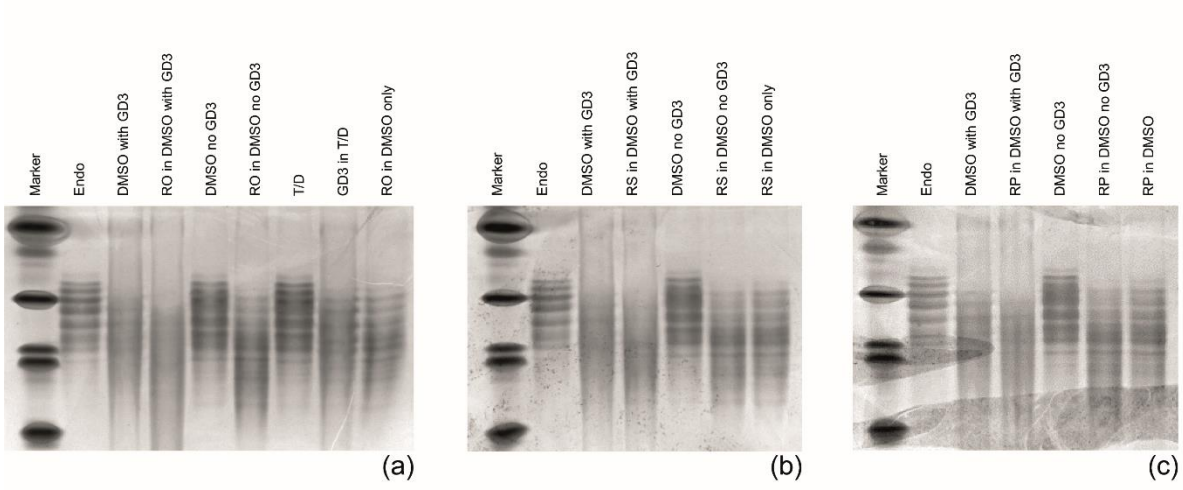


Figure 4.4 Pre-loaded IEF gels (GD3): 1µL of GD3 was pre-loaded to CD1a and incubated overnight at RT, then loaded with 1µL of RE overnight, diluted 1:1 with IEF sample buffer and 18µL/well loaded to IEF gel. (a) Retinyl Oleate (b) Retinyl Stearate (c) Retinyl Palmitate. Lipid stocks: RE at 40mM, GD3 at 13.3mM. RO; Retinyl Oleate, RS; Retinyl Stearate, RP; Retinyl Palmitate, DMSO; dimethyl sulfoxide.

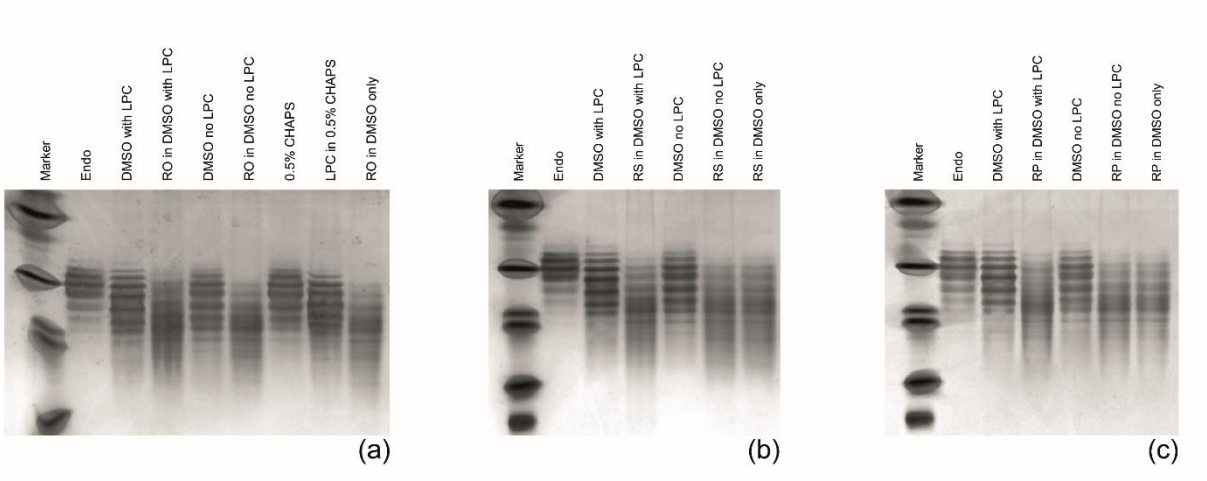


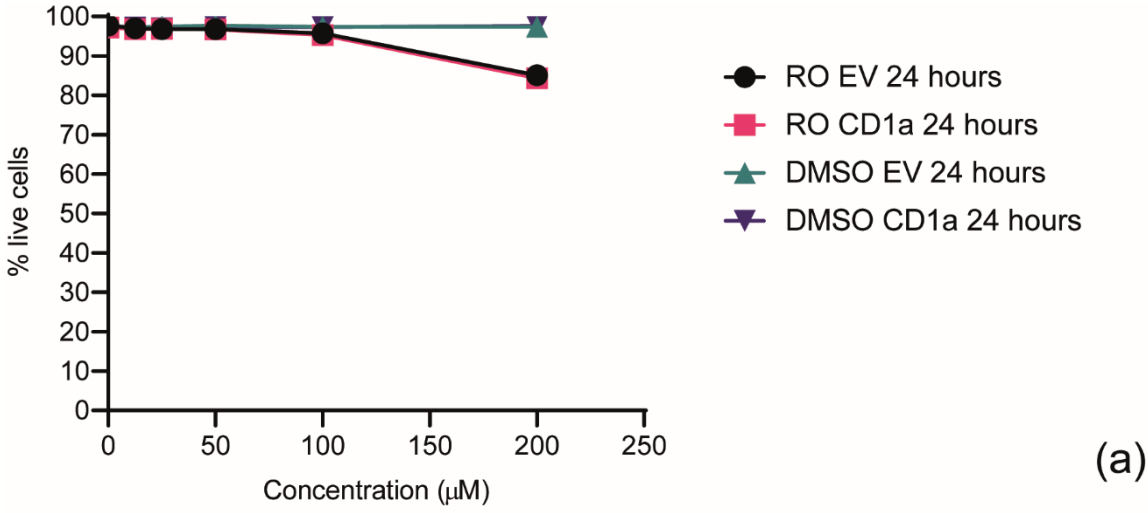
Figure 4.5 Pre-loaded IEF gels (LPC): 1µL of LPC was pre-loaded to CD1a and incubated overnight at RT, then loaded with 1µL of RE overnight, diluted 1:1 with IEF sample buffer and 18µL/well loaded to IEF gel. (a) Retinyl Oleate (b) Retinyl Stearate (c) Retinyl Palmitate. Lipid stocks: RE at 40mM, LPC at 13.3mM. RO; Retinyl Oleate, RS; Retinyl Stearate, RP; Retinyl Palmitate, DMSO; dimethyl sulfoxide.

4.2.4 Assessment of toxicity of K562 cells by Retinyl Esters

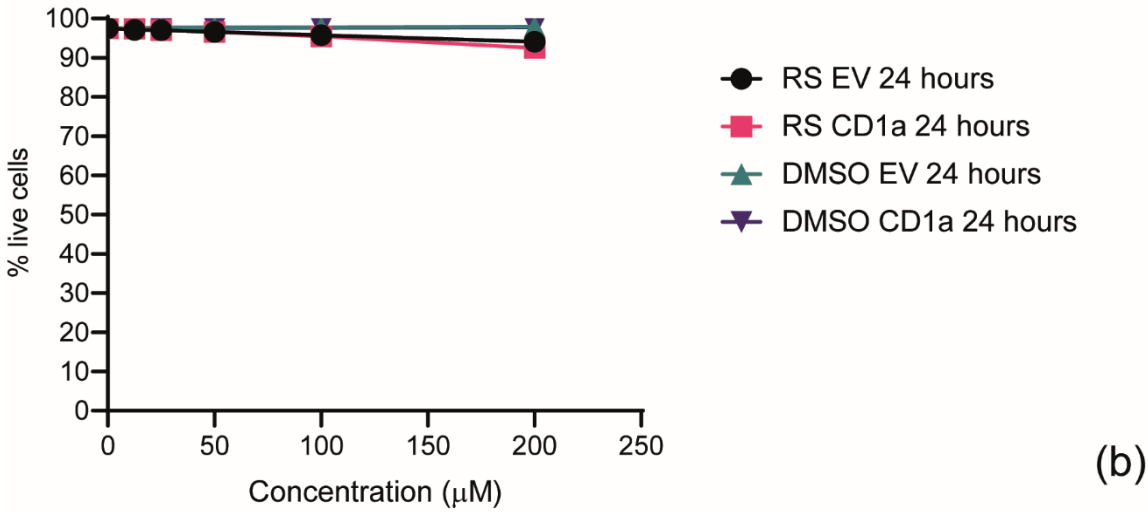
Initially, toxicity testing was performed using very low maximum final concentrations of RE in solution (2µM). This was based on published reports that a 0.2µM concentration of RE in the blood indicated systemic retinol toxicity (Blomhoff et al., 2003). There was no evidence of toxicity to K562 cells using this concentration or one ten times higher (data not shown), so some initial ELISpot experiments were performed using final concentrations of 2µM and 0.2µM. Later, testing was repeated to assess how high a concentration of RE could be feasibly used in future experiments.

Repeat testing using serial dilutions demonstrated up to 13.2% reduction in viability for retinyl oleate (**Figure 4.6 (a)**), 5.1% for retinyl stearate (**Figure 4.6 (b)**) and 2.2% for retinyl palmitate (**Figure 4.6 (c)**) in the K562-CD1a group at the maximum final concentration of 200µM. Changes in K562-EV were similar or milder and there was

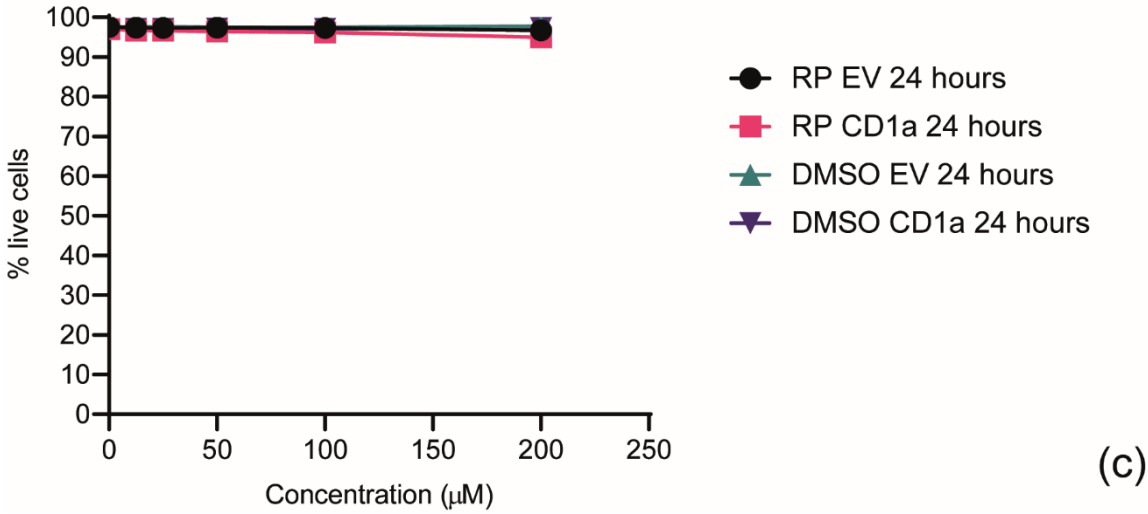
minimal toxicity from vehicle control (DMSO). There was some minor impact on viability (<2.1%) at 100μM which was minimal thereafter, so it was decided to proceed with a final concentration in solution of 50μM for K562 experiments. Given that moDC are less robust, a final concentration of 25μM was used for those experiments.


% live cells
100
90
80
70
60
50
40
30
20
10
0
0
50
100
150
200
250
Concentration (μM)
RO EV 24 hours
RO CD1a 24 hours
DMSO EV 24 hours
DMSO CD1a 24 hours

(a)


% live cells
100
90
80
70
60
50
40
30
20
10
0
0
50
100
150
200
250
Concentration (μM)
RS EV 24 hours
RS CD1a 24 hours
DMSO EV 24 hours
DMSO CD1a 24 hours

(b)


% live cells
100
90
80
70
60
50
40
30
20
10
0
0
50
100
150
200
250
Concentration (μM)
RP EV 24 hours
RP CD1a 24 hours
DMSO EV 24 hours
DMSO CD1a 24 hours

(c)

Figure 4.6 K562 Toxicity Testing: K562 pulsed for 24 hours with serial dilutions of lipid/vehicle and media only and cell viability measured using Live-Dead Aqua by flow cytometry (a) Retinyl Oleate (b) Retinyl Stearate and (c) Retinyl Palmitate. RO; Retinyl Oleate, RS; Retinyl Stearate, RP; Retinyl Palmitate, DMSO; dimethyl sulfoxide. EV; Empty vector-transduced K562 cells, CD1a; CD1a-transduced K562 cells.

4.2.5 Tetramer and dextramer staining with Retinyl Esters

There were technical issues with tetramer staining using polyclonal T cells from healthy donors and T cell clones (data not shown). Later, a new protocol for dextramer staining was used. Using frozen PBMC from healthy donors (3) and psoriasis patients (3), there was evidence of an increase in binding of RE-loaded dextramers (retinyl oleate>retinyl stearate>retinyl palmitate) compared to those containing endogenous lipids and dextran negative control for both healthy control (**Figure 4.10**) and psoriasis samples (**Figure 4.11**). Binding was more pronounced in $CD3^{+}CD4^{+}$ T cells vs $CD3^{+}CD8a^{+}$ T cells and was higher in psoriasis compared to healthy control.

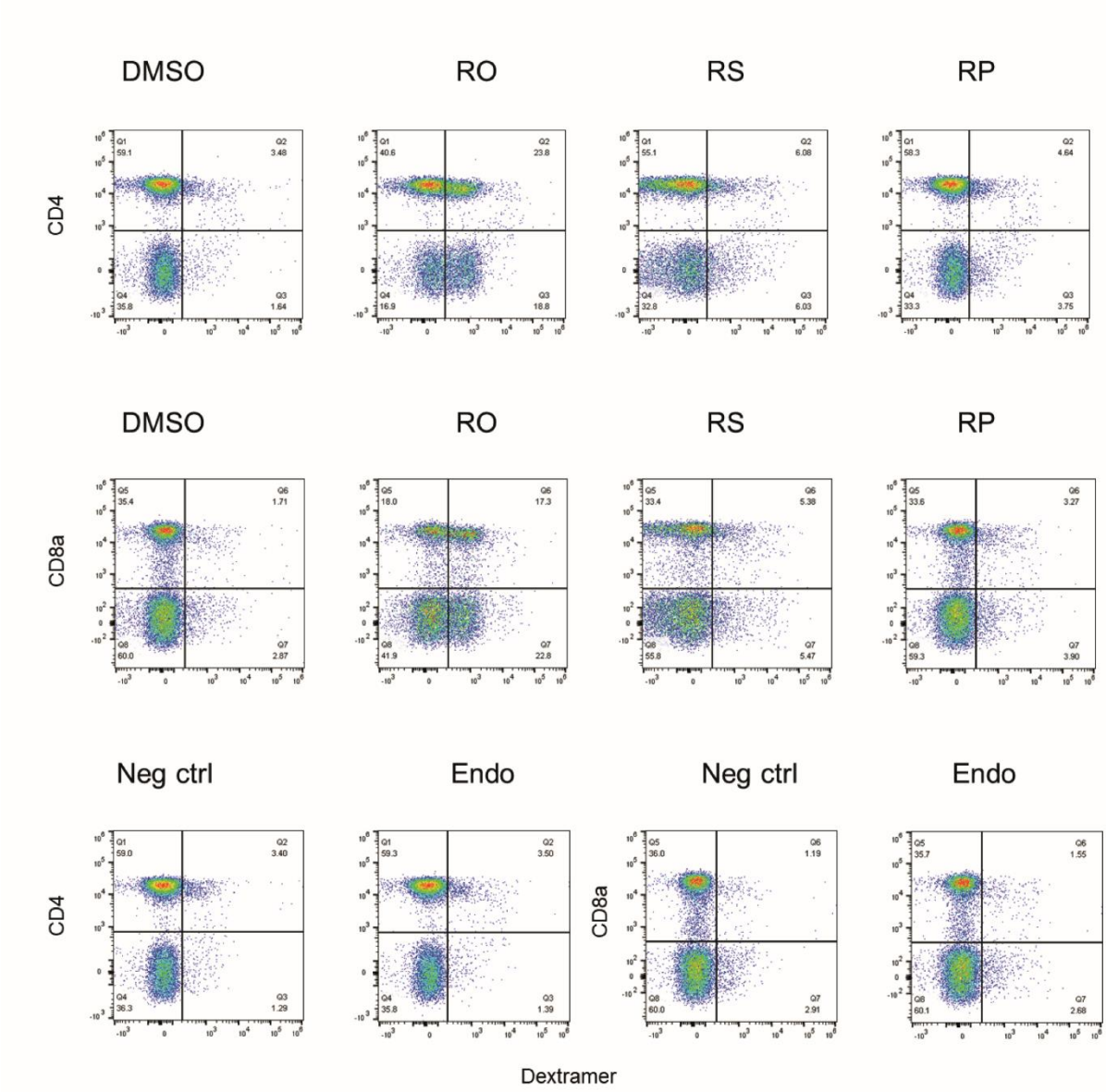


Figure 4.7 Dextramer staining (Healthy control C2933): Biotinylated CD1a was loaded with RE/DMSO overnight, then assembled into dextramers using Streptavidin PE. Frozen PBMC were stained with dextramers and analysed by flow cytometry. RO; Retinyl Oleate, RS; Retinyl Stearate, RP; Retinyl Palmitate, DMSO; dimethyl sulfoxide (vehicle control); Neg ctrl; negative (dextran only) control; Endo; endogenous lipid within cleft of biotinylated in-house CD1a.

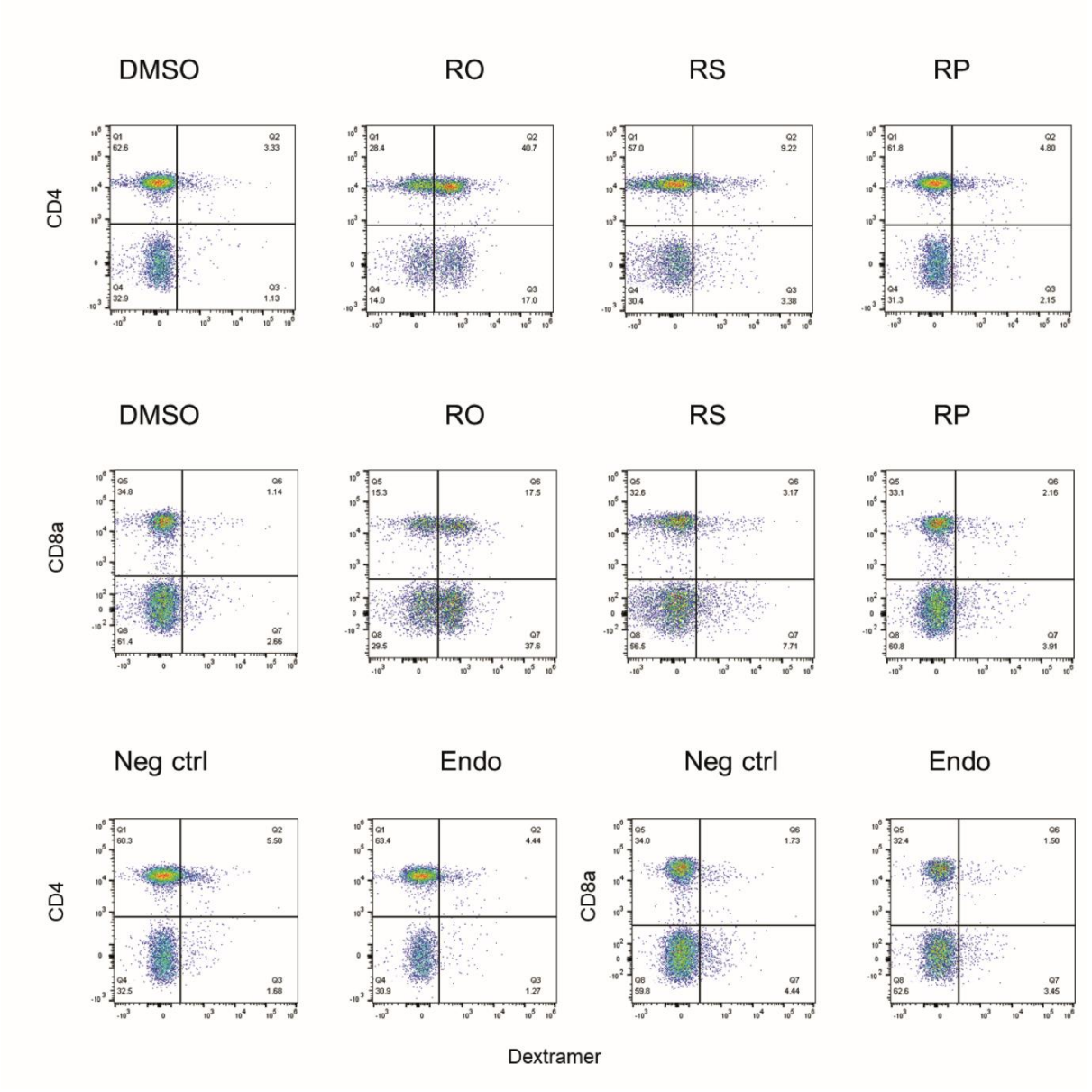


Figure 4.8 Dextramer staining (Psoriasis PS2650). Biotinylated CD1a was loaded with RE/DMSO overnight, then assembled into dextramers using Streptavidin PE. Frozen PBMC were stained with dextramers and analysed by flow cytometry. RO; Retinyl Oleate, RS; Retinyl Stearate, RP; Retinyl Palmitate, DMSO; dimethyl sulfoxide (vehicle control); Neg ctrl; negative (dextran only) control; Endo; endogenous lipid within cleft of biotinylated in-house CD1a.

4.2.6 The effect of Retinyl Esters on CD1a expression on moDC and K562 cells

MoDC showed a slight reduction in CD1a expression when pulsed with RE on day three of differentiation (**Figure 4.12**), but this was not statistically significant, except for retinyl palmitate (p=0.003) (**Figure 4.12 (c)**). Decreased CD1a expression was not related to a reduction in cell viability (**Figure 4.12 (d)**). The effect was not as marked on day five of differentiation and lost significance, but several donors did not produce enough cells to enable both day three and day five analysis.

In summary, retinyl palmitate may reduce CD1a expression on moDC when administered during differentiation, in the absence of any significant toxic effect.

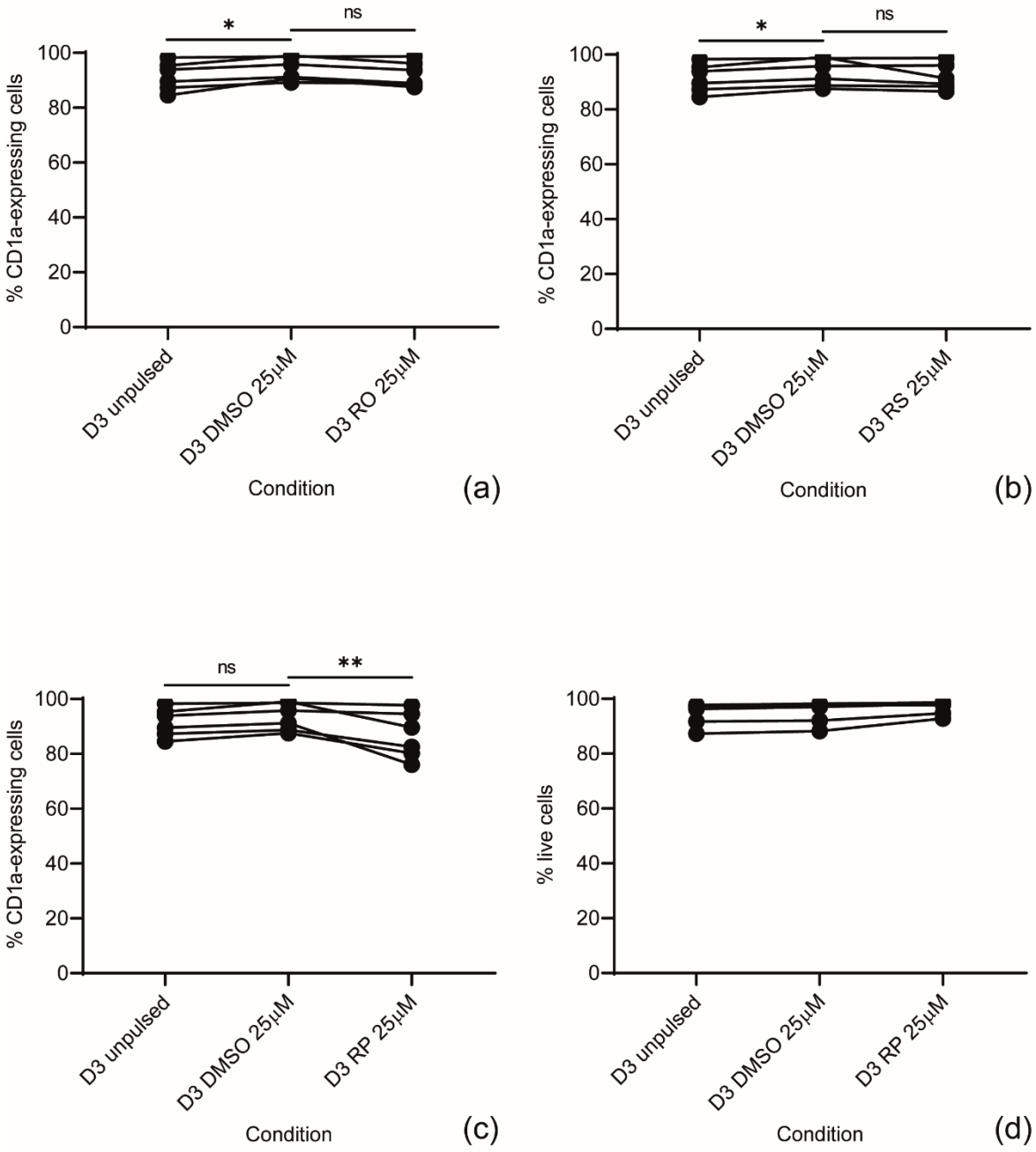


*Figure 4.9 CD1a expression on moDC from HC blood following Day 3 pulsing with lipid/vehicle (a) RO; Retinyl Oleate 25µM (b) RS; Retinyl Stearate 25µM (c) RP; Retinyl Palmitate 25µM (d) % live cells at 25µM Retinyl Palmitate. Only cells that showed good differentiation (>80% CD1a expression in unpulsed condition) were included in the analysis. Friedman non-parametric one-way ANOVA with post-hoc Dunn test. *p<0.05 **p<0.005.*

Assessment of expression of CD1a on K562 following pulsing with RE for 24 hours was assessed during toxicity testing (**Section 4.3.4**). Surface CD1a expression as assessed by flow cytometry showed a maximum reduction of 1.9% in CD1a expression for RO at 200μM (0.002% for RS and 0.003% for RP) while changes in CD1a expression for solvent (DMSO) were <0.1% (data not shown). Effects on CD1a expression were minimal at the final concentrations of RE chosen for use in further experiments.

4.2.7 Assessment of cytokine production by CD1a-reactive T cells

Polyclonal experiments

Initial polyclonal ELISpot experiments were performed using relatively low final concentrations (2μM and 0.2μM) of retinyl oleate and retinyl stearate. No relevant significant difference in IFN-γ secretion was detected for K562-CD1a pulsed with lipid or vehicle control in either healthy control (**Figure 4.10**) or psoriasis patients (**Figure 4.11**). However, frozen PBMC were used as a source of psoriasis T cells which may have affected the results.

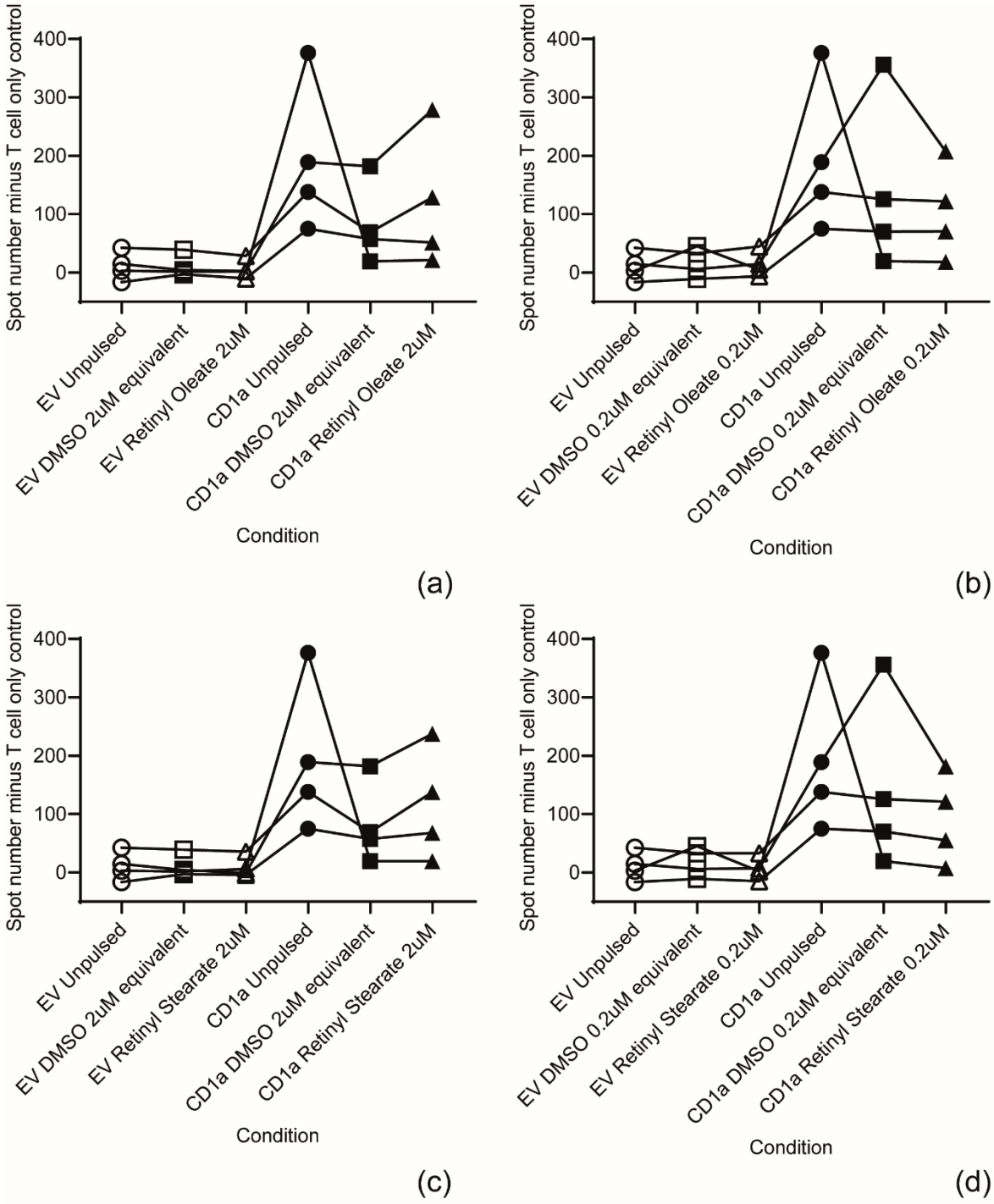


Figure 4.10 IFN-γ ELISpot (Healthy controls): K562 cells were pulsed with lipid/vehicle overnight then co-cultured with polyclonal T cells extracted from healthy donors (T cells from either frozen CD3+ or PBMC) in the ratio 25,000:75,000 cells. ELISpot readout: Each spot represents a cell secreting IFN-γ (a) RO; Retinyl Oleate 2μM (b) RO; Retinyl Oleate 0.2μM (c) RS; Retinyl Stearate 2μM (d) RS; Retinyl Stearate 0.2μM. DMSO; dimethyl sulfoxide. EV; Empty vector-transduced

K562 cells, CD1a; CD1a-transduced K562 cells. Friedman non-parametric one-way ANOVA with post-hoc Dunn test.

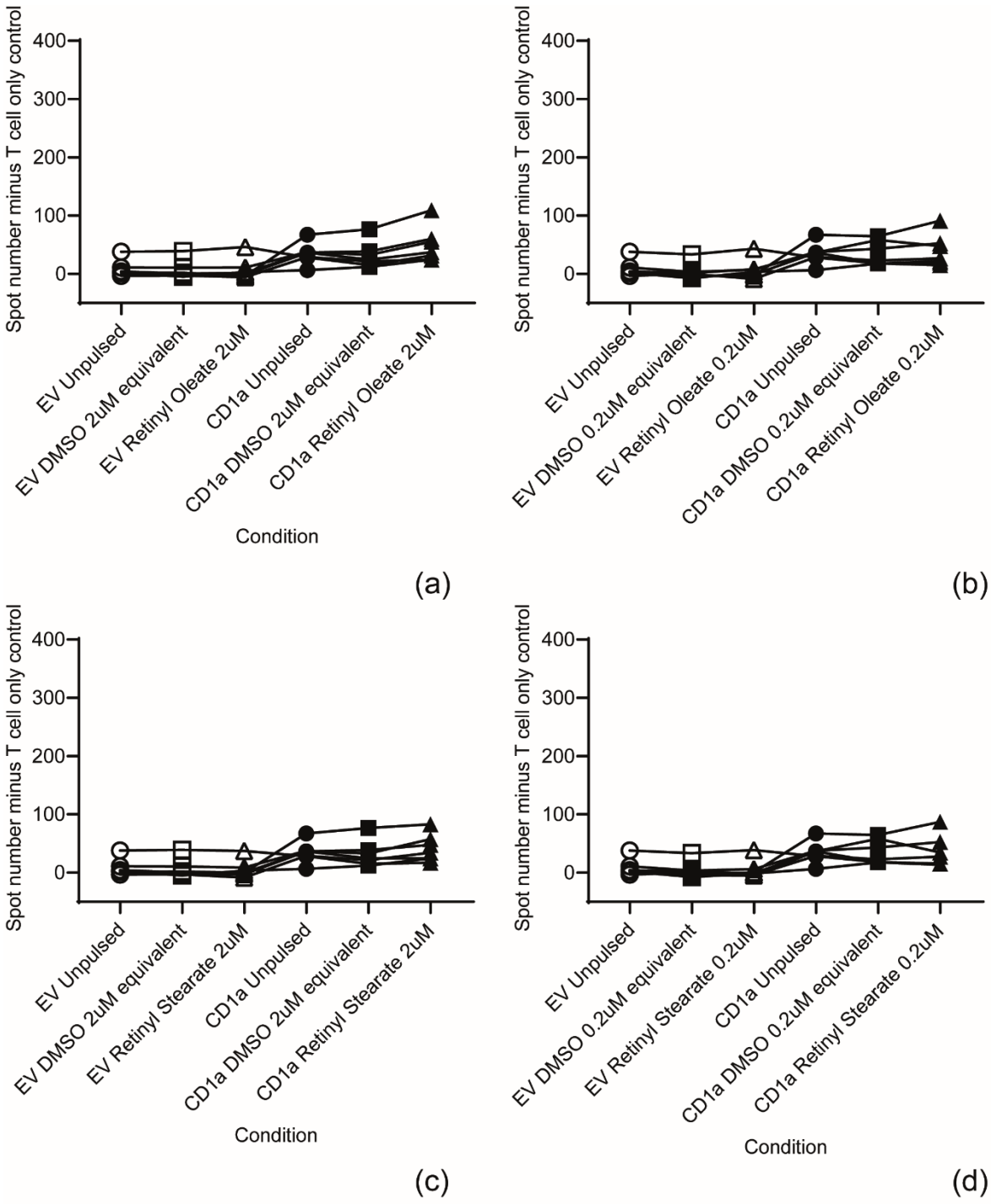


Figure 4.11 IFN-γ ELISpot (Psoriasis): K562 cells were pulsed with lipid/vehicle overnight then co-cultured with polyclonal T cells extracted from psoriasis samples (T cells from frozen PBMC) in the ratio 25,000:75,000 cells. ELISpot readout: Each spot represents a cell secreting IFN-γ (a)

RO; Retinyl Oleate 2μM (b) RO; Retinyl Oleate 0.2μM (c) RS; Retinyl Stearate 2μM (d) RS; Retinyl Stearate 0.2μM. DMSO; dimethyl sulfoxide. EV; Empty vector-transduced K562 cells, CD1a; CD1a-transduced K562 cells. Friedman non-parametric one-way ANOVA with post-hoc Dunn test.

Later ELISpot experiments were performed using higher K562 pulsing concentrations of all three RE (50μM final concentration). However, again, no relevant significant changes in IFN-γ secretion were detected for lipid-pulsed conditions compared to vehicle controls, even using T cells extracted from fresh donor blood in all cases (**Figure 4.12**). However, overall spot number was generally low, which limits the interpretation of these results.

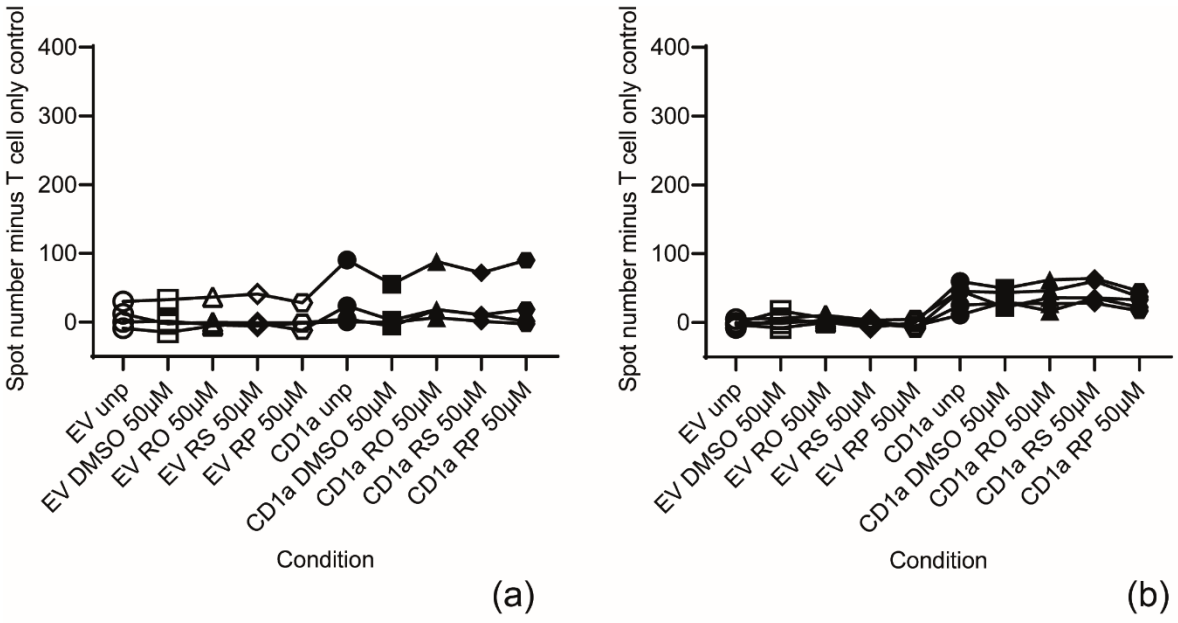


Figure 4.12 IFN-γ ELISpot (RE): K562 cells were pulsed with lipid/vehicle overnight then co-cultured with polyclonal T cells extracted from fresh blood of donor samples in the ratio 25,000:75,000 cells. ELISpot readout: Each spot represents a cell secreting IFN-γ (a) Healthy controls (4 donors) (b) Psoriasis (5 donors). RO; Retinyl Oleate, RS; Retinyl Stearate, RP; Retinyl Palmitate, DMSO; dimethyl sulfoxide. EV; Empty vector-transduced K562 cells, CD1a; CD1a-transduced K562 cells. Friedman non-parametric one-way ANOVA with post-hoc Dunn test.

Clonal experiments

Given the encouraging results from IEF gels that RE were potential ligands for CD1a, it was considered that CD1a-reactive T cells that bound them may be of too limited a number in peripheral blood to be detectable by ELISpot. Therefore, IFN-γ ELISA using CD1a-reactive T cell clones, sorted and cultured from healthy donors by Dr Yi-Ling Chen, was performed. In some cases the same clone was used in different experiments weeks apart (marked as replicates in **Figure 4.13**) and did not always demonstrate a reproducible response, which may reflect differences in activation state. When taking all clones together as individuals, a small but statistically significant increase in IFN-γ secretion was demonstrated with retinyl stearate only (**Figure 4.13**).

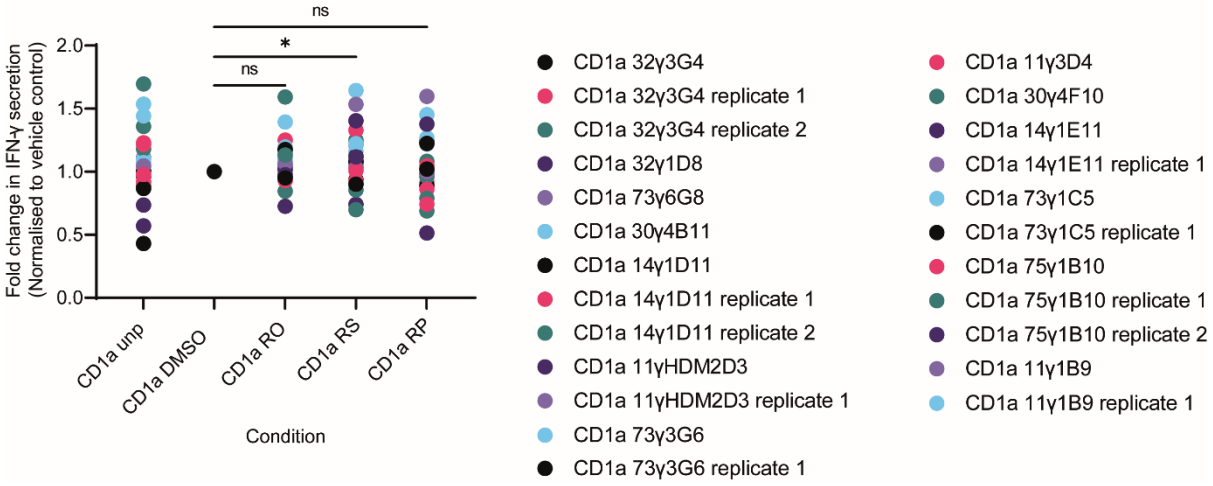


*Figure 4.13 IFN-γ ELISA: RE. K562 cells were pulsed with lipid/vehicle for 21-22 hours then co-cultured with CD1a-reactive T cell clones in a ratio of 150,000:100,000 cells for 24 hours. Co-culture supernatants were processed using IFN-γ ELISA Max™ Deluxe set. Clone cytokine secretion normalised to vehicle control (100% DMSO) by Friedman non-parametric one-way ANOVA and post-hoc Dunn's Test, *p-value <0.05. CD1a; CD1a-transduced K562 cells.*

ELISA using GM-CSF (for IL-17A and TNF-α) and IL-22 clones was also performed to assess effects on TNF-α, IL-17A and IL-22, but was inconclusive, with most clones failing to reach the respective assays' threshold for detection.

4.2.8 Clonal assay using the CD1a-autoreactive BK6 TCR

Although autoreactivity of the BK6 clone was detected, this was not statistically significant and there was no significant difference in CD69 expression between pulsed and unpulsed conditions for K562-CD1a (**Figure 4.18**), suggesting that the BK6 TCR does not specifically bind to these lipids.

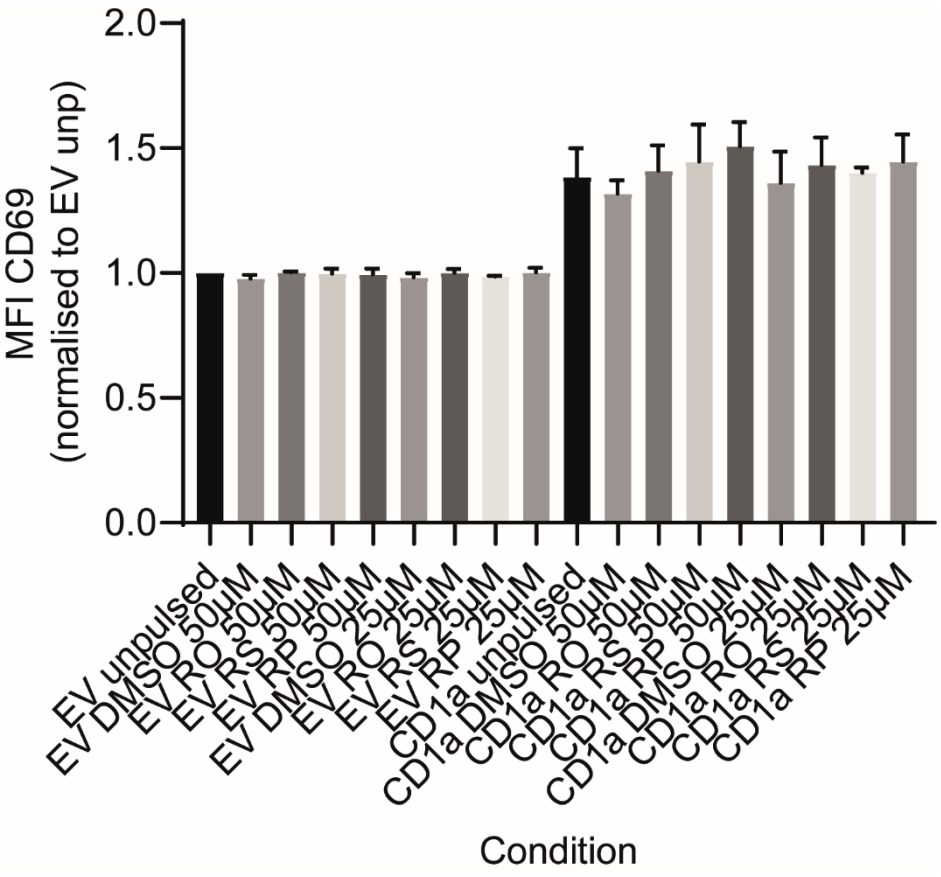


Figure 4.14 BK6 functional assay (3 experiments): K562 cells were pulsed with lipid/vehicle overnight then co-cultured with BK6 Jurkat T cells 25,000:75,000 cells. Surface expression of CD69 on BK6 Jurkat T cells was measured by flow cytometry. MFI; median fluorescence intensity.

RO; all-trans-retinyl oleate, RS; all-trans-retinyl stearate, RP; all-trans-retinyl palmitate, EV; Empty vector-transduced K562 cells, CD1a; CD1a-transduced K562 cells.

4.2.9 Retinyl Esters results summary

Retinoid pathways were altered in RNA-Seq data in psoriasis. IEF gels and dextramer staining results supported RE as potential CD1a lipid antigens and indicated that retinyl palmitate may slightly reduce CD1a expression on moDC. Clonal T cell assays suggested a small but significant increase in IFN-γ with retinyl stearate.

4.3 Discussion

RNA-Seq results and the background literature supported the role of retinoid pathways in psoriasis, while their structure suggested that they may be suitable ligands for CD1a.

Lee et al(Lee et al., 2009) found that atRA modulated several genes known to be upregulated in psoriasis, including suppression of *SERPINB3*, *SERPINB4*, *ALOX12B*, *HMOX1*, *KRT16*, *S100A8* and *WNT5A* and induction of *S100A7*, *S100A12* and *STAT1*. All of these genes were also significantly upregulated in untreated PS L skin (vs HC) in our RNA-Seq data (**Chapter 3**), except for *WNT5A*, which was upregulated but not significantly. Three of the four genes we chose for validation (**Chapter 8**) are also modulated by atRA in human keratinocytes; *CRABP2* (upregulated at 4h, suppressed after 24h), *FABP5* and *LCN2*, no doubt related to their RA binding capacities (Lee et al., 2009). atRA induces *FADS1* (HUFA biosynthesis), which was significantly downregulated in untreated PS L skin (vs HC) in our data.

RNA-Seq findings suggested that there may be a dearth of retinoic acid in lesional psoriatic skin. Multiple GO terms related to retinoid metabolism and cellular response

were downregulated in untreated PS L skin (vs HC) in our data. mRNA for *LIPA* and *LRAT* were significantly altered in untreated PS L skin, implying reduced synthesis of RE and increased RE hydrolysis to supply more RA, along with increased expression of genes encoding binding proteins (CRABP2, FABP5) for RA, which may influence receptor binding. Most retinoid-related DEG were less markedly altered in skin that had resolved with NB-UVB or secukinumab therapy, although in some cases differential expression was altered in an opposing manner by these therapies. Although intuitively synthetic retinoids such as acitretin may restore retinoid homeostasis in psoriatic skin with concomitant clinical improvement, other treatments may also indirectly exert an effect on the retinoid pathway. There is a possibility that resolution of psoriasis and return to healthy skin may in itself restore retinoid balance in the skin, although the differing results noted in our data for PS R (NB-UVB) and PS R (Secukinumab) suggest that this may not be the case. That some of the changes in differential gene expression were more marked with NB-UVB may be related to the broader immunosuppressive effects of this treatment or other modes of action such as promotion of vitamin D formation; the VDR, like RAR, forms heterodimers with RXR, linking both pathways (Schräder et al., 1993). NB-UVB wavelength is 311-313nm. Maximum absorption of UV by retinol and RE is 325nm, with a range of 300nm-350nm crossing UVB and UVA spectra (Antille et al., 2003). In a murine study with a single exposure, RE were degraded by UVB more completely than retinol at 315nm (UVB), albeit with both showing partial recovery at 24 hours (Sorg et al., 1999). Topical application of retinyl palmitate to mice and humans exerts a photoprotective effect (Antille et al., 2003).

If RE bind the CD1a cleft, then the pertinent question is whether they are activatory or inhibitory to T cells secreting pro-inflammatory cytokines. The evidence from this chapter suggests they are more likely to be inhibitory ligands and part of healthy skin homeostasis. Disruption of retinoid metabolism in psoriasis may lead to a deficit of RE in

the skin. Synthetic retinoids result in improvement in psoriasis and studies discussed in **Chapter 1** illustrate that atRA induces the enzymes of its own biosynthesis and metabolism, notably increasing the activity of *LRAT* for formation of RE.

Initial results with IEF gels were promising, with a change in the pI of CD1a seen for all esters, with some variation for retinyl palmitate. This may be due to batch variation, contamination or related to how the esters were made up, with retinyl oleate and retinyl stearate dissolved in chloroform in their original vials, aliquoted, dried down and dissolved in DMSO, while retinyl palmitate was weighed as a solid then dissolved. The results of 3-day gels suggested that all RE may partially displace LPC and retinyl oleate may partially displace the known CD1a ligand GD3 from the CD1a binding cleft. Dextramer staining demonstrated some binding of all esters, most pronounced for retinyl oleate and greater in psoriasis than healthy control. Although this raises the possibility that some polyclonal CD1a-reactive T cells in health and disease may recognise RE bound to CD1a to a greater extent than those bound to endogenous lipids, due to the small sample number, further experiments to assess the reproducibility of these effects across a larger number of donors are needed.

MoDC data suggested that pulsing on Day 3 with retinyl palmitate results in alteration of CD1a expression on these cells. Although this is an artificial system, this idea would fit with the role of retinoids in psoriasis therapeutics, particularly given that CD1a-reactive T cells have been identified among the Th22 subgroup (De Jong et al., 2010). IL-22 is a wound-healing cytokine responsible for many of the clinical features, such as epidermal acanthosis, seen in psoriasis (**Chapter 1**). Disruption of CD1a expression in human DC could therefore theoretically negatively influence this signalling pathway. However, an alternative explanation is that this reduction in surface marker expression may be a sign of cellular stress. Although cell viability was not affected, Live-Dead Aqua staining does

not detect apoptotic cells and re-assessment with an alternative such as Annexin V would be warranted to determine this with certainty.

Results of experiments assessing the effect of RE on IFN-γ were conflicting. Polyclonal experiments did not detect any significant changes in cytokine secretion but overall, were limited by concentration and/or donor number, as well as some technical issues resulting in low spot numbers in some cases, making the elucidation of small differences in effect undiscernible. Secondly, although CD1a-reactive T cells have been identified as a minor component (0.02-0.4%) of the circulating memory T cell population (De Jong et al., 2010), the number of TCR that recognise these esters bound to CD1a may be much more limited, particularly in blood. Although ELISpot is a sensitive technique, it may not be able to detect cytokine secretion within the limits of the parameters (such as cell number per well) that were used.

ELISA demonstrated a significant increase in IFN-γ secretion by retinyl stearate only. ELISA is a sensitive technique but is open to potential variation from experiment to experiment- hence why the data included here are replicates. Although the same clones were used, they had been in culture for different periods of time on testing, with differences in activation states. T cell clones downregulate their TCR after feeding and although feeding was performed at consistent intervals (every 2 days) in an attempt to mitigate this, with co-culture performed 2 days after last feeding on each occasion, multiple factors may influence the cells' responsiveness to pulsed K562 cells, which themselves may be open to variation based on passage number and other influences.

If RE are in fact CD1a ligands, the next step is identification of the TCR that binds this complex, with generation of the crystal structure. Unfortunately, BK6 clonal experiments

did not show a difference in activation when co-cultured with RE-pulsed K562 cells, refuting the possibility that this TCR recognises RE bound to CD1a.

The complexities of interpretation of the above data notwithstanding, a case remains for RE as CD1a ligands. Acknowledging the therapeutic effects of retinoids in the context of psoriasis, RE may act as homeostatic lipids, with inhibitory effects on CD1a signalling pathways when bound to its cleft.

4.4 Chapter Summary

There is substantial support for a role for retinoids in psoriasis pathogenesis, not least due to RNA-Seq data showing these metabolic pathways are altered in disease. Retinoid-based therapeutics also alleviate clinical and histological features of disease. Although preliminary, the findings outlined in these experiments suggest that RE may act as ligands for CD1a. However, more work is required to untangle the complexity of their actions in different cell types and environments.

5 Chapter 5 Nitro-Fatty Acids

5.1 Introduction

5.1.1 Nitro-fatty acid pathways

Nitro-fatty acids (NO_2-FA, NFA) arise from non-enzymatic reactions between unsaturated FA and nitric oxide (NO), nitrite (NO_2^-) or reactive oxygen species (Mathers et al., 2018). Substrates for nitration include the non-essential MUFA, oleic acid, and the essential PUFA, linoleic acid. Oleic acid is non-essential as it can be synthesised endogenously by the enzyme SCD1. *In vivo*, NFA fall into nitroalkene or nitrohydroxy groups (Freeman et al., 2008). Nitroalkenes (dehydrated) are in equilibrium with their derivative nitrohydroxy counterparts in aqueous solution (Schopfer et al., 2005).

NFA nitroalkenes are electrophilic and can react rapidly with thiols to form Michael adducts, with roles in Nrf2 (nuclear factor erythroid 2-related factor 2) anti-oxidant signalling via Keap1 (Kelch-like ECH-associating protein 1) (Koutoulogenis & Kokotos, 2021). As summarised by Freeman et al, in addition to modulation of *Nrf2* dependent gene transcription, NFA actions include antagonising the activity of inflammatory cells, increasing *HMOX1* mRNA and protein expression, inhibition of NFκB signalling and PPAR agonism (Freeman et al., 2008). They can also modulate the enzymes 5-lipoxygenase, soluble epoxide hydrolase and microsomal prostaglandin E synthase 1 (mPGES1) as well as prostaglandin endoperoxide H synthases 1 and 2 (COX-1 and COX-2), all of which are involved in inflammation (Piesche et al., 2020).

The microbiome plays a key role in the generation of NFA as human cells cannot metabolise nitrate, whereas commensal bacteria can convert nitrates (from exogenous sources such as the diet/pollutants and endogenous sources such as the L-arginine-NO

pathway) to nitrites and in an acidic environment, such as the stomach, further reaction to NO may occur (Lundberg et al., 2004). Reactive nitrogen species may also be generated during inflammation and ischaemia-reperfusion (Schopfer & Khoo, 2019).

5.1.2 Nitro-fatty acids *in vivo*

Most experimental studies to date have been done using animal models and exogenous NFA; relatively little is known about endogenous NFA and its formation/metabolism in humans (Buchan et al., 2018). There is some controversy regarding plasma levels of NFA in humans, with wide variation in reported studies in part attributable to measurement technique (Baker et al., 2004, 2005; Tsikas, Zoerner, Mitschke, & Gutzki, 2009; Tsikas, Zoerner, Mitschke, Homsi, et al., 2009). The nitro-oleic acid isomers 9-NO_2-OA and 10-NO_2-OA were initially thought to exist at a mean concentration of 1nM in human plasma but were subsequently re-calibrated to concentrations in the picomolar range (Tsikas, Zoerner, Mitschke, & Gutzki, 2009; Tsikas, Zoerner, Mitschke, Homsi, et al., 2009). 9-NO_2-OA and 10-NO_2-OA are found at a molar ratio of approximately 1:1 in healthy human plasma (Tsikas, Zoerner, Mitschke, Homsi, et al., 2009). The most commonly formed NFA *in vivo* is nitro-conjugated linoleic acid (NO_2-CLA) (rather than NO_2-OA or NO_2-LA) with a human plasma concentration of 0.3nM to 1.3nM of NO_2-CLA with an average of 0.72nM across seven healthy donors (Bonacci et al., 2012).

Synthetic nitro-oleic acid is made up of 2 regioisomers (9-and 10-nitro-9-*cis*-octadecenoic acids) (Baker et al., 2005), both of which were used in experiments, along with nitro-conjugated linoleic acid (**Figure 5.1**). For clarity, 9-NO, 10-NO and NO2-CLA will be used as abbreviations for these chemicals throughout. They will be referred to collectively as NFA.

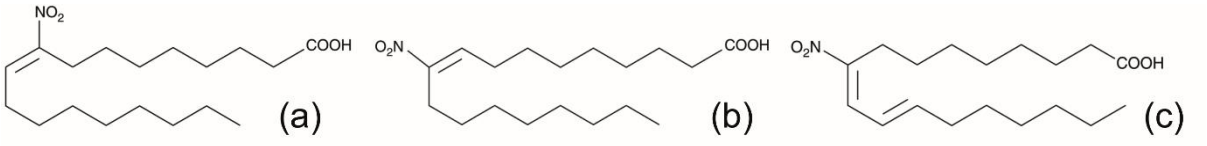


Figure 5.1 Chemical structures of (a) 9-nitrooleate (9-NO) (b) 10-nitrooleate (10-NO) and (c) nitro-conjugated linoleic acid (NO2-CLA). Composite of images taken from information on products purchased on www.caymanchem.com.

5.1.3 Nitro-Fatty Acids and inflammation

Multiple studies in rodents have demonstrated an anti-inflammatory effect of NFAs across a range of disease models, including atherosclerosis, hypertension, diabetic nephropathy, inflammatory bowel disease and non-alcoholic fatty liver disease, as summarised by Schopfer et al (Schopfer & Khoo, 2019). However, the mode of administration appears to be significant, with anti-inflammatory effects observed following systemic administration, but exacerbation of inflammation following topical application noted in some studies. Reduction of contact hypersensitivity (CHS), *IL1B* and *IL6* mRNA expression and increased *FOXP3* and *IL10* transcripts and T_{reg} accumulation are seen when OA-NO_2 (nitro-oleic acid, including 10-NO) is administered subcutaneously in mice 18 hours prior to both sensitisation and elicitation with the contact sensitiser 2,4- dinitrofluorobenzene (DNFB) (Mathers et al., 2017). OA-NO_2 also abrogated established murine CHS (Mathers et al., 2017). However, the same group found that OA-NO_2 augments DNFB-induced CHS and *IL17* mRNA expression when topically applied to mice at the elicitation phase (Mathers et al., 2018), demonstrating that in the presence of other inflammatory stimuli, NFA can exacerbate inflammation. In these experiments, the combination of OA-NO_2 and DNFB resulted in murine ear swelling and neo-angiogenesis consistent with a psoriasiform dermatitis (Mathers et al., 2018).

Although nitric oxide synthase (NOS) inhibitors reduced CHS in a murine model using picryl chloride, NO itself was unlikely to be critical to the delayed type hypersensitivity reaction of CHS as modulation of inflammation only occurred at the time of elicitation rather than sensitisation (Morita et al., 1996). A significant increase in dermal inducible NOS (iNOS) was also noted in both allergic and irritant contact dermatitis (Ormerod, Dwyer, Reid, et al., 1997).

OA-NO2 activates all PPAR (α, γ, δ) in a dose-dependent manner, with the greatest effect for PPARγ (Baker et al., 2005). This is of particular interest as PPARγ agonism (where ligands are added from the first day of moDC differentiation) has been shown to downregulate CD1a on human moDC (Nencioni et al., 2002; Szatmari et al., 2004). PPARγ activation also reduced moDC production of inflammatory cytokines including TNF-α, IL-6, IL-12 and IL-15 (Nencioni et al., 2002).

CXA-10, an NO2-OA (10-nitro-octadec-9-enoic acid) regioisomer, is currently under evaluation as a potential therapy in inflammatory and fibrotic disease, with Phase I trials completed (Garner et al., 2019).

5.1.4 Nitro-Fatty Acids and psoriasis

Skin commensals such as *Staphylococcus epidermidis* and *Staphylococcus aureus* contain nitrate reductases which may act on nitrates in sweat to generate nitrites and subsequently NO (Weller et al., 1996), suggesting NFA may occur naturally in healthy skin. Inducible NOS is significantly increased in PS L vs PS NL/HC skin and correlated with CD3 and Ki67 staining (Ormerod et al., 1998). NO is also significantly increased in PS L vs PS NL skin (Ormerod et al., 1998). Analysis of paired human skin samples

demonstrated that nitro-conjugated linoleic acid was significantly increased by 56% in PS L vs PS NL skin (Mathers et al., 2018).

IFN-γ can induce the production of nitric oxide by human keratinocytes (Bécherel et al., 1994). Imiquimod, rmIL-23 and transgenic K14-VEGF murine models of psoriasis developed less ear inflammation with pre-emptive oral administration of electrophilic NFA (OA-NO2); *IL1B*, *IL17A* and *IL6* mRNA were all significantly reduced in treated mice versus those that received vehicle (P. Wang et al., 2021). OA-NO2 also abrogated STAT3 phosphorylation and reduced cutaneous IL-6 protein expression in the IMQ and K14-VEGF models (P. Wang et al., 2021). *In vitro*, OA-NO2 also demonstrates dose and time-dependent suppression of NFκB phosphorylation due to TNF-α in HaCaT cells, impairs their growth and antagonises T_H1 and T_H17 differentiation (P. Wang et al., 2021).

Many psoriasis therapies reduce NO in lesional skin; topically these include steroids, coal tar, dithranol and calcipotriol (Ormerod, Dwyer, Weller, et al., 1997). Retinoids (including atRA and isotretinoin) inhibit production of nitrites and TNF-α by human keratinocytes (Bécherel et al., 1994, 1996). Dimethyl fumarate (Fumaderm®) is a drug used for the treatment of psoriasis in Germany, although it is not licensed in the UK and has fallen out of favour due to potential side effects. Like NFA, it is also electrophilic, is a Michael acceptor and can alkylate Keap1 and inhibit NFκB as summarised by Piesche et al (Piesche et al., 2020). Topically applied dimethyl fumarate elicits cutaneous inflammation on patch testing in patients with a history of furniture dermatitis (allergic contact dermatitis to chemicals in furniture, of which dimethyl fumarate was found to be a component) (Lammintausta et al., 2010). Dimethyl fumarate impedes human moDC differentiation *in vitro*, including upregulation of CD1a (Zhu & Mrowietz, 2001).

5.2 Results: Nitro-Fatty Acids

5.2.1 Interrogation of RNA-Seq data for Nitro-Fatty Acid-relevant genes

Most genes involved in NFA metabolism and signalling were downregulated in untreated PS L vs HC skin, except *PTGR1* (**Table 5.1**). *PTGR1* is a Nrf2-regulated gene that encodes prostaglandin reductase 1, an enzyme involved in FA catabolism.

Downstream targets of NFA include *NFE2L2* (which encodes Nrf-2) and *KEAP1* which were both marginally, but not significantly, upregulated in PS L vs HC skin. *PPARG* encodes the nuclear receptor PPARγ, which regulates differentiation of adipocytes, was significantly downregulated in untreated PS L skin. Genes encoding heat shock proteins (HSPs) and other anti-inflammatory molecules which have been shown to be increased >10-fold following exposure to nitro-oleic acid were mostly minimally and non-significantly upregulated in untreated PS L vs HC skin.

*Table 5.1 Selection of DEG relevant to NFA pathways: Untreated lesional psoriasis (PS L) versus healthy control (HC) skin. p_{adj}; adjusted p-value. *>10-fold change on exposure to nitro-oleic acid vs oleic acid* (Kansanen et al., 2009).

Gene	Log2FC	p_{adj}
Genes involved in NFA metabolism:		
PNPLA2	-0.270	0.109
ACADM	-1.788	2.30×10^{-11}
ECHS1	-0.123	0.551
HADH	-0.742	0.003
ACAT1	-0.599	0.001
ACSL1	-1.986	6.94×10^{-29}
PTGR1	0.228	0.697

Action of NFA via:		
NFE2L2	0.186	0.549
KEAP1	0.288	0.101
PPARG	-3.695	8.42×10^{-31}
Genes induced by OA-NO2:		
*HSPA6**	1.043	0.001
*HSPA1A**	0.295	0.464
*HSPA1B**	-0.174	0.672
*DNAJA4**	0.197	0.563
*DNAJB1**	0.642	0.006
*HMOX1**	1.251	0.001
GCLM	-0.927	0.0002
NQO1	-1.079	0.0230

GO terms related to FA biosynthesis, metabolism and catabolism, including linoleic acid metabolic process, were all downregulated in untreated PS L vs HC skin (**Table 5.2**). Most of these genes remained downregulated despite clinical resolution with either NB-UVB or anti-IL-17A monoclonal antibody therapy.

*Table 5.2 Enriched Gene Ontology (GO) terms relevant to NFA pathways: Untreated lesional psoriasis (PS L) versus healthy control (HC) skin. All GO terms in this table were downregulated in untreated PS L vs HC skin. *Log2FC>2. **Log2FC>4. p_{adj} ; adjusted p-value.*

GO Term	Differential expression untreated PS L vs HC	p_{adj}	Genes
GO:0043651** linoleic acid metabolic process	Downregulated	0.0041	*FADS2*, *FADS1*, *ELOVL3*, *ELOVL5*, *ACSL1*, *GSTA1*, *ALOX15B*
GO:0006631** fatty acid metabolic process	Downregulated	8.49×10^{-13}	*FADS2*, *FADS1*, *ELOVL3*, *PPARGC1A*, *ELOVL5*, *AWAT1*, *INSIG1*, *CRAT*, *HAO2*, *PECR*, *CYP4F8*, *ACAA2*, *ACSM6*, *OLAH*, *PPARG*, *FA2H*, *FASN*, *ACSL1*, *DGAT2*, *ACOX2*, *ACSM3*, *PNPLA3*, *ACSBG1*, *APOC1*, *CYP1B1*, *MSMO1*, *ACOT1*, *LPL*, *ABHD5*, *ACOT2*, *MECR*, *HACL1*, *LPIN1*, *ACOT4*, *SLC27A2*, *ACACB*, *GNPAT*, *AACS*, *AMACR*, *ACADM*, *IVD*, *ACSL3*, *ACSS2*, *CYP2B6*, *PRKAA2*, *ACSL5*, *GSTA1*, *ECH1*, *ACAT2*, *NR1H3*, *ADTRP*, *PCK1*, *AKR1C3*, *ECI2*, *FADS6*, *ALOX15B*, *PRKAG3*, *PON3*,

			ACSF2, *CEACAM1*, *PHYH*, *PDK4*, *FADS3*, *IRS1*, *ATP6V1B1*, *PLIN5*, *CYP4F2*, *SCD5*, *TWIST1*, *SLC27A6*, *ACSM1*, *ACOT6*, *PON1*, *MLXIPL*, *FABP1*, *PTGS2*, *CYP2C19*, *ANGPTL3*
GO:0055089 fatty acid homeostasis**	Downregulated	0.0086	*DGAT2*, *PRKAA2*, *APOE*, *NR1H4*, *MLXIPL*
GO:0019395* fatty acid oxidation	Downregulated	8.32×10^{-6}	*PPARGC1A*, *CRAT*, *HAO2*, *PECR*, *ACAA2*, *PPARG*, *DGAT2*, *ACOX2*, *MECR*, *HACL1*, *SLC27A2*, *ACACB*, *AMACR*, *ACADM*, *IVD*, *ECH1*, *ACAT2*, *ECI2*, *PHYH*, *PDK4*, *IRS1*, *PLIN5*, *TWIST1*, *ACSM1*, *FABP1*
GO:0009062* fatty acid catabolic process	Downregulated	0.0001	*CRAT*, *HAO2*, *PECR*, *ACAA2*, *ACOX2*, *MECR*, *HACL1*, *LPIN1*, *SLC27A2*, *ACACB*, *AMACR*, *ACADM*, *IVD*, *ECH1*, *ACAT2*, *ADTRP*, *PCK1*, *ECI2*, *PHYH*, *IRS1*, *PLIN5*, *CYP4F2*, *TWIST1*, *FABP1*
GO:0001676** long-chain fatty acid metabolic process	Downregulated	0.0001	*FADS2*, *FADS1*, *ELOVL3*, *ELOVL5*, *AWAT1*, *ACSL1*, *PNPLA3*, *ACSBG1*, *CYP1B1*, *ACOT1*, *ACOT2*, *ACOT4*, *SLC27A2*, *ACSL3*, *CYP2B6*, *ACSL5*, *GSTA1*, *ADTRP*, *AKR1C3*, *ALOX15B*, *CYP4F2*,*SLC27A6*, *PTGS2*, *CYP2C19*

GO:0006633** fatty acid biosynthetic process	Downregulated	0.0002	*FADS2*, *FADS1*, *ELOVL3*, *ELOVL5*, *INSIG1*, *PECR*, *ACSM6*, *OLAH*, *FA2H*, *FASN*, *ACSM3*, *APOC1*, *LPL*, *MECR*, *ACOT4*, *ACACB*, *ACSL3*, *ACSS2*, *PRKAA2*, *NR1H3*, *AKR1C3*, *FADS6*, *ALOX15B*, *PRKAG3*, *CEACAM1*, *PDK4*, *FADS3*, *SCD5*, *ACSM1*, *MLXIPL*, *PTGS2*
GO:0070542* response to fatty acid	Downregulated	0.0003	*PPARGC1A*, *P2RY4*, *PPARG*, *ACSL1*, *DGAT2*, *GLDC*, *LPL*, *GNPAT*, *AACS*, *PRKAA2*, *SFRP1*, *AKR1C3*, *TGFBR3*, *NR1H4*, *APOB*, *PDK4*, *IRS1*, *CPS1*, *PON1*, *PTGS2*
GO:1901568** fatty acid derivative metabolic process	Downregulated	0.0005	*FAR2*, *FADS1*, *ELOVL3*, *ELOVL5*, *AWAT1*, *AWAT2*, *CYP4F8*, *ACSS3*, *FASN*, *ACSL1*, *DGAT2*, *ACSBG1*, *CYP1B1*, *AACS*, *ACSL3*, *CYP2B6*, *ACSL5*, *GSTA1*, *HMGCS2*, *AKR1C3*, *ALOX15B*, *PON3*, *ATP6V1B1*, *CYP4F2*, *SCD5/DPEP1*, *GGT3P*, *PON1*, *PTGS2*, *CYP2C19*
GO:0006635* fatty acid β-oxidation	Downregulated	0.0027	*CRAT*, *ACAA2*, *ACOX2*, *MECR*, *SLC27A2*, *ACACB*, *AMACR*, *ACADM*, *IVD*, *ECH1*, *ACAT2*, *ECI2*, *IRS1*, *PLIN5*, *TWIST1*, *FABP1*
GO:0000038**	Downregulated	0.0067	*ELOVL3*, *ELOVL5*, *ACSBG1*, *ACOT1*, *ACOT2*, *ACOT4*, *SLC27A2*, *CYP4F2*, *SLC27A6*

very long-chain fatty acid metabolic process			
GO:0046320* regulation of fatty acid oxidation	Downregulated	0.0067	*PPARGC1A*, *PPARG*, *DGAT2*, *ACACB*, *PDK4*, *IRS1*, *PLIN5*, *TWIST1*, *FABP1*
GO:0071398* cellular response to fatty acid	Downregulated	0.0068	*PPARGC1A*, *P2RY4*, *PPARG*, *DGAT2*, *LPL*, *PRKAA2*, *SFRP1*, *AKR1C3*, *NR1H4*, *APOB*, *PDK4*, *IRS1*, *CPS1*
GO:0045923* positive regulation of fatty acid metabolic process	Downregulated	0.0077	*PPARGC1A*, *ELOVL5*, *PPARG*, *NR1H3*, *IRS1*, *PLIN5*, *TWIST1*, *MLXIPL*, *FABP1*, *PTGS2*
GO:1901570* fatty acid derivative biosynthetic process	Downregulated	0.0095	*FAR2*, *FADS1*, *ELOVL3*, *ELOVL5*, *AWAT1*, *AWAT2*, *ACSS3*, *FASN*, *ACSL1*, *ACSBG1*, *AACS*, *ACSL3*, *ACSL5*, *HMGCS2*, *AKR1C3*, *SCD5*, *GGT3P*, *PTGS2*

5.2.2 Investigation of Nitro-Fatty Acid binding to CD1a

Results from 2-day gels using in-house CD1a showed a marked shift in the pI for all NFA tested, more prominent at higher molar excesses (**Figure 5.2**). Loading of 9-NO to NIH CD1b and CD1c also showed a shift for both. When nanomolar "physiological" concentrations of NO based on the literature were used rather than 20mM stocks, no shift was evident on IEF using in-house CD1a (data not shown).

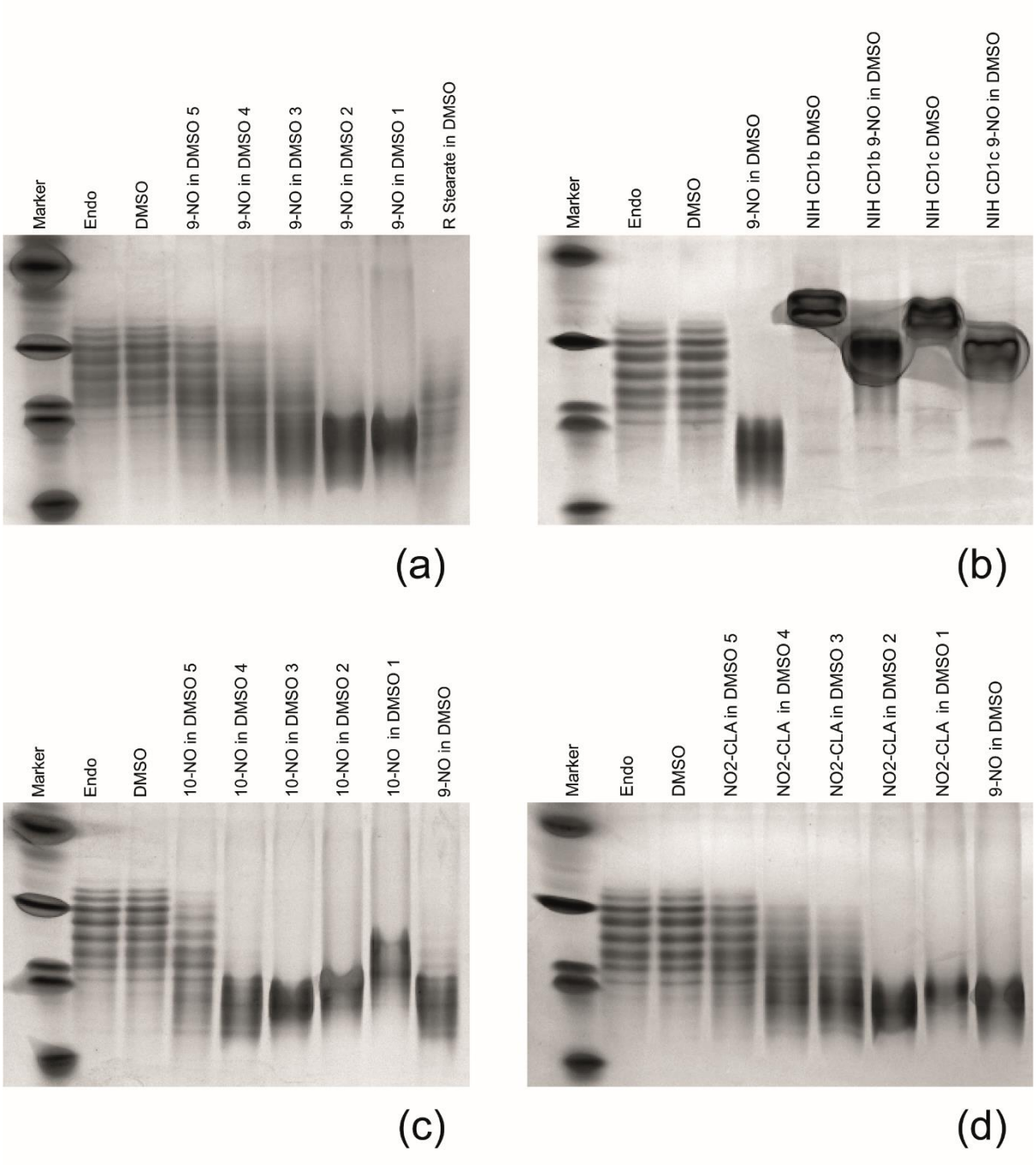


Figure 5.2 IEF gels: CD1a loaded overnight with lipid/vehicle then diluted 1:1 with IEF sample buffer and 18μL/well loaded to IEF gel. Endo (endogenous lipids); CD1a loaded with PBS only, 200x; 8μL CD1a:2μL lipid/vehicle, 100x; 9μL CD1a:1μL lipid/vehicle. (a)9-NO serial dilutions (b) 9-NO NIH CD1b/CD1c (c) 10-NO serial dilutions and (c) NO2-CLA serial dilutions. Lipid stocks: NFA all at 20mM. All serial dilution IEFs were 8μL CD1a + 2μL lipid where lipid was 1=20mM, 2=10mM, 3=5mM, 4=3.33mM, 5=1mM. 9-NO; 9-nitrooleate, 10-NO; 10-nitrooleate, NO2-CLA;

9(E),11(E)-9-nitro conjugated linoleic acid, DMSO; dimethyl sulfoxide, NIH; National Institutes of Health.

3-day gels showed at least partial displacement of GD3, with a smudging of all bands, and full displacement of LPC, with bands identical to NFA alone, by all three NFA tested (**Figure 5.3**).

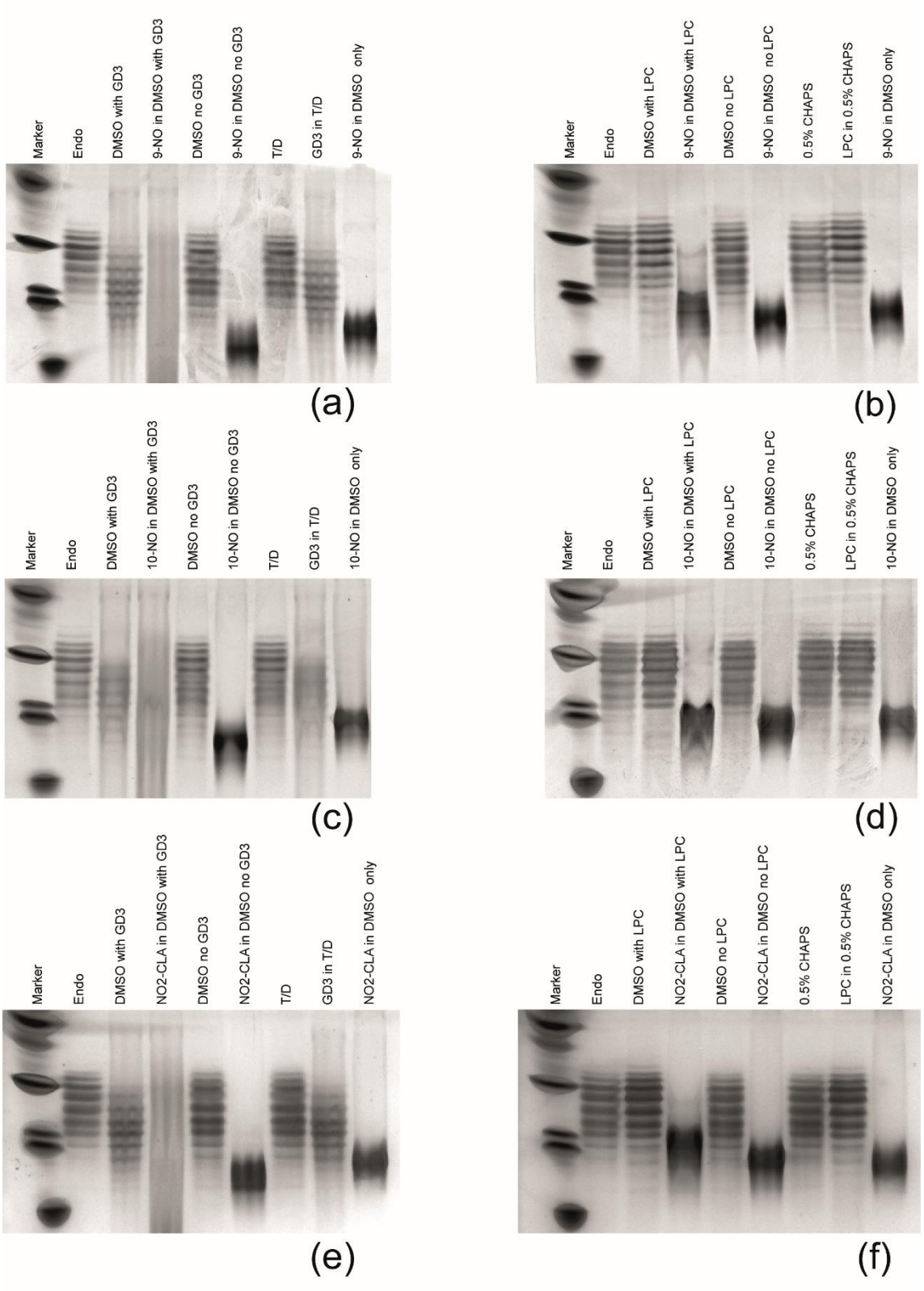
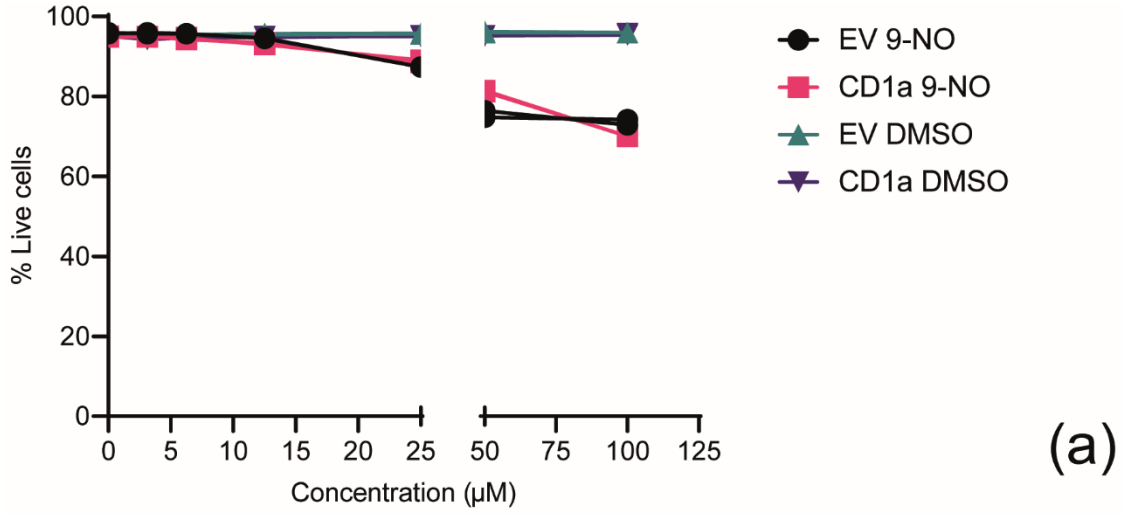


Figure 5.3 Pre-loaded IEF gels: 1μL of GD3 or LPC was pre-loaded to CD1a and incubated overnight at RT, then loaded with 1μL of 100x NFA overnight, diluted 1:1 with IEF sample buffer and 18μL/well loaded to IEF gel. (a) GD3 + 9-NO (b) LPC + 9-NO (c) GD3 + 10-NO (d) LPC + 10-NO (e) GD3 + NO2-CLA (f) LPC + NO2-CLA. Lipid stocks: NFA all at 20mM, GD3/LPC at 13.3mM. 9-NO; 9-nitrooleate, 10-NO; 10-nitrooleate, NO2-CLA; 9(E),11(E)-9-nitro conjugated linoleic acid, GD3; ganglioside GD3, LPC; lysophosphatidylcholine, DMSO; dimethyl sulfoxide, T/D; 0.25% tyloxapol/2% DMSO.

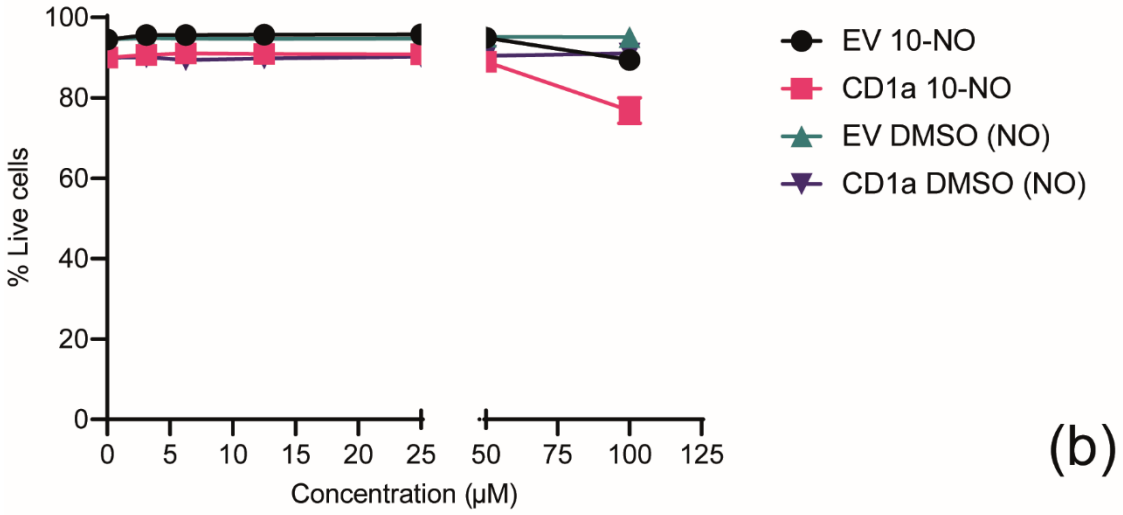
5.2.3 Assessment of toxicity on K562 cells by Nitro-Fatty Acids

Toxicity testing using serial dilutions demonstrated up to 26.3% reduction in viability of K562-CD1a cells for 9-NO (**Figure 5.4 (a)**), 14.6% for 10-NO (**Figure 5.4 (b)**) and 11.3% for NO2-CLA (**Figure 5.4 (c)**) at the maximum final concentration of 100μM. K562-EV cells were less affected and changes in viability for the vehicle were negligible. Frozen 10-NO was used for these tests but a comparison experiment between fresh and frozen 9-NO and NO2-CLA showed similar results (data not shown).

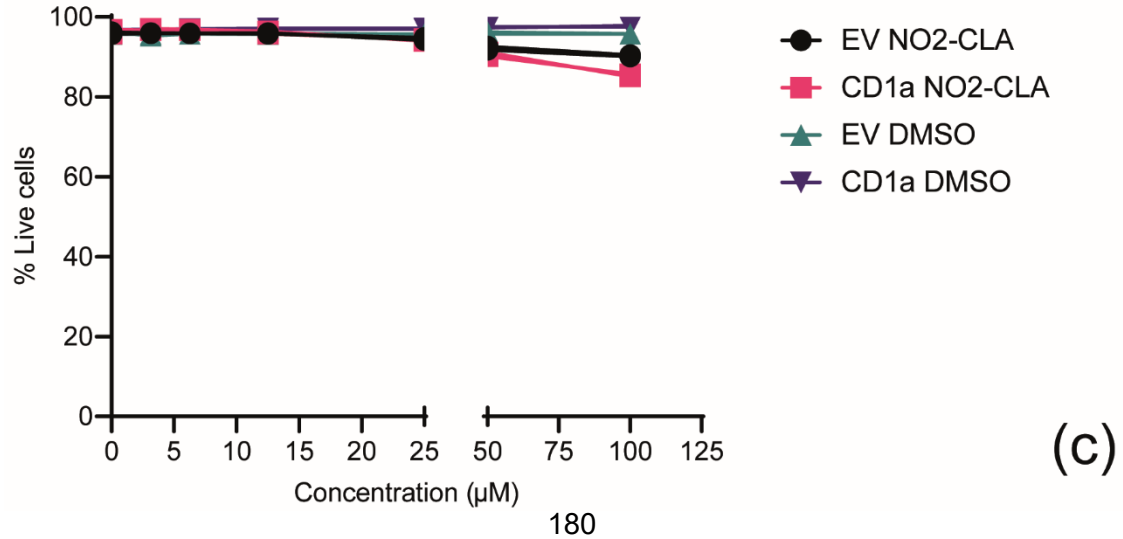
It was decided to proceed with a final concentration in solution of 5μM for 9-NO and 10-NO and 10μM for NO2-CLA for both K562 and moDC experiments.


100
80
60
40
20
0
% Live cells
0 5 10 15 20 25 50 75 100 125
Concentration (μM)
EV 9-NO
CD1a 9-NO
EV DMSO
CD1a DMSO

(a)


100
80
60
40
20
0
% Live cells
0 5 10 15 20 25 50 75 100 125
Concentration (μM)
EV 10-NO
CD1a 10-NO
EV DMSO (NO)
CD1a DMSO (NO)

(b)

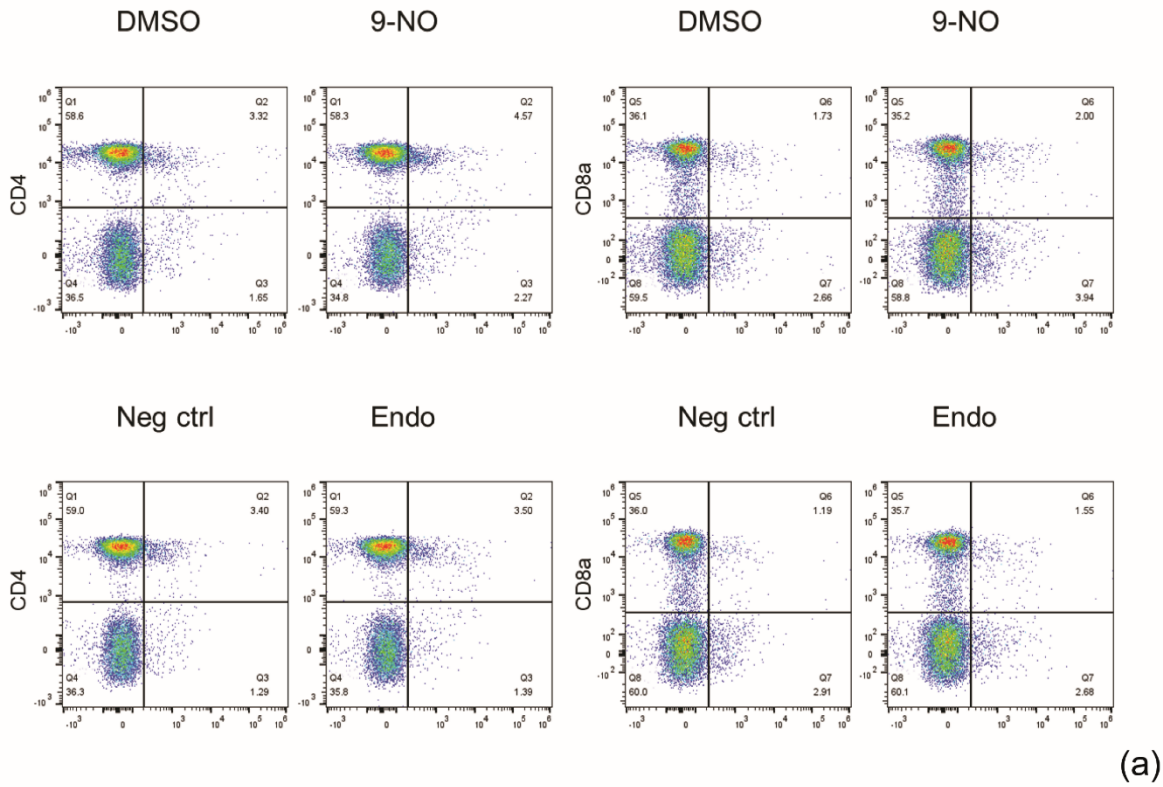

100
80
60
40
20
0
% Live cells
0 5 10 15 20 25 50 75 100 125
Concentration (μM)
EV NO2-CLA
CD1a NO2-CLA
EV DMSO
CD1a DMSO

(c)

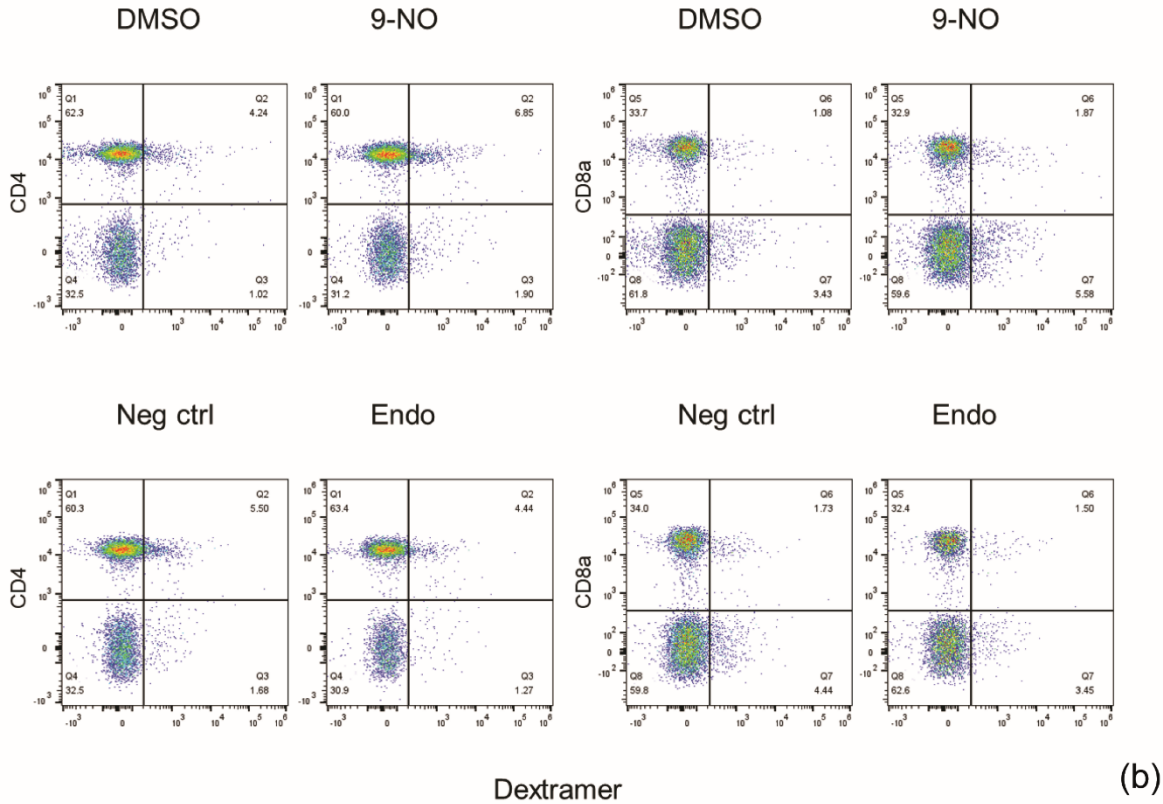
Figure 5.4 K562 Toxicity Testing: K562 pulsed for 24 hours with serial dilutions of lipid/vehicle and media only and cell viability measured using Live-Dead Aqua by flow cytometry. (a) 9-NO (b) 10-NO and (c) NO2-CLA. 9-NO; 9-nitrooleate, 10-NO; 10-nitrooleate, NO2-CLA; 9(E),11(E)-9-nitro conjugated linoleic acid, DMSO; dimethyl sulfoxide.

5.2.4 Tetramer and Dextramer staining with Nitro-Fatty Acids

Tetramer staining with 9-NO was performed using fresh healthy control polyclonal T cells and several T cell clones. No marked differences were seen compared to endogenous CD1a control (data not shown). Dextramer staining using a new protocol was later performed for all NFA, this time using frozen PBMC from healthy controls (**Figure 5.5 (a)**) and psoriasis patients (**Figure 5.5 (b)**). There was slightly increased binding to 9-NO for $CD3^+CD4^+$ and $CD3^+CD8a^+$ cells compared to vehicle, negative control and endogenous CD1a, all of which were similar. Binding was higher in psoriasis compared to healthy control. These results suggest that some polyclonal T cells may bind to 9-NO, particularly in an inflammatory milieu.


DMSO
9-NO
DMSO
9-NO
CD4
CD8a
Q1 58.6
Q2 3.32
Q4 36.5
Q3 1.65
Q1 58.3
Q2 4.57
Q4 34.8
Q3 2.27
Q5 36.1
Q6 1.73
Q8 59.5
Q7 2.66
Q5 35.2
Q6 2.00
Q8 58.8
Q7 3.94
Neg ctrl
Endo
Neg ctrl
Endo
Q1 59.0
Q2 3.40
Q4 36.3
Q3 1.29
Q1 59.3
Q2 3.50
Q4 35.8
Q3 1.39
Q5 36.0
Q6 1.19
Q8 60.0
Q7 2.91
Q5 35.7
Q6 1.55
Q8 60.1
Q7 2.68

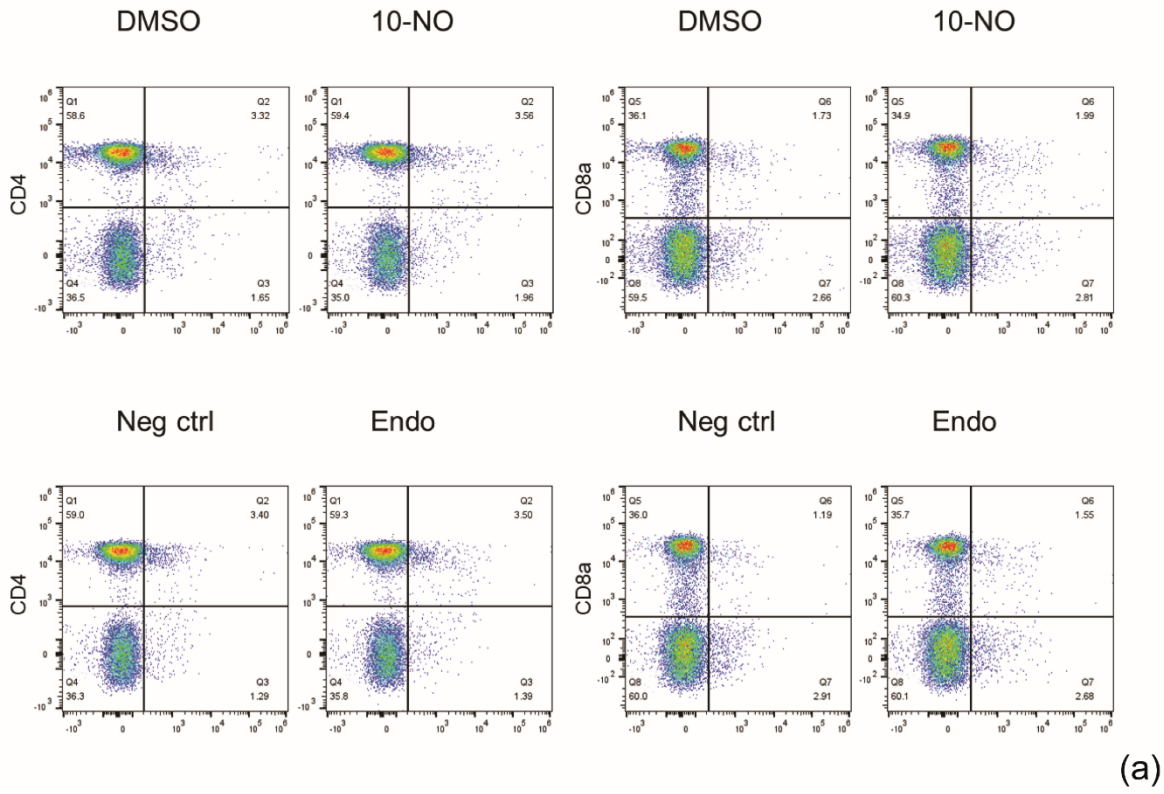
(a)


DMSO
9-NO
DMSO
9-NO
CD4
CD8a
Q1 62.3
Q2 4.24
Q4 32.5
Q3 1.02
Q1 60.0
Q2 6.85
Q4 31.2
Q3 1.90
Q5 33.7
Q6 1.08
Q8 61.8
Q7 3.43
Q5 32.9
Q6 1.87
Q8 59.6
Q7 5.58
Neg ctrl
Endo
Neg ctrl
Endo
Q1 60.3
Q2 5.50
Q4 32.5
Q3 1.68
Q1 63.4
Q2 4.44
Q4 30.9
Q3 1.27
Q5 34.0
Q6 1.73
Q8 59.8
Q7 4.44
Q5 32.4
Q6 1.50
Q8 62.6
Q7 3.45
Dextramer

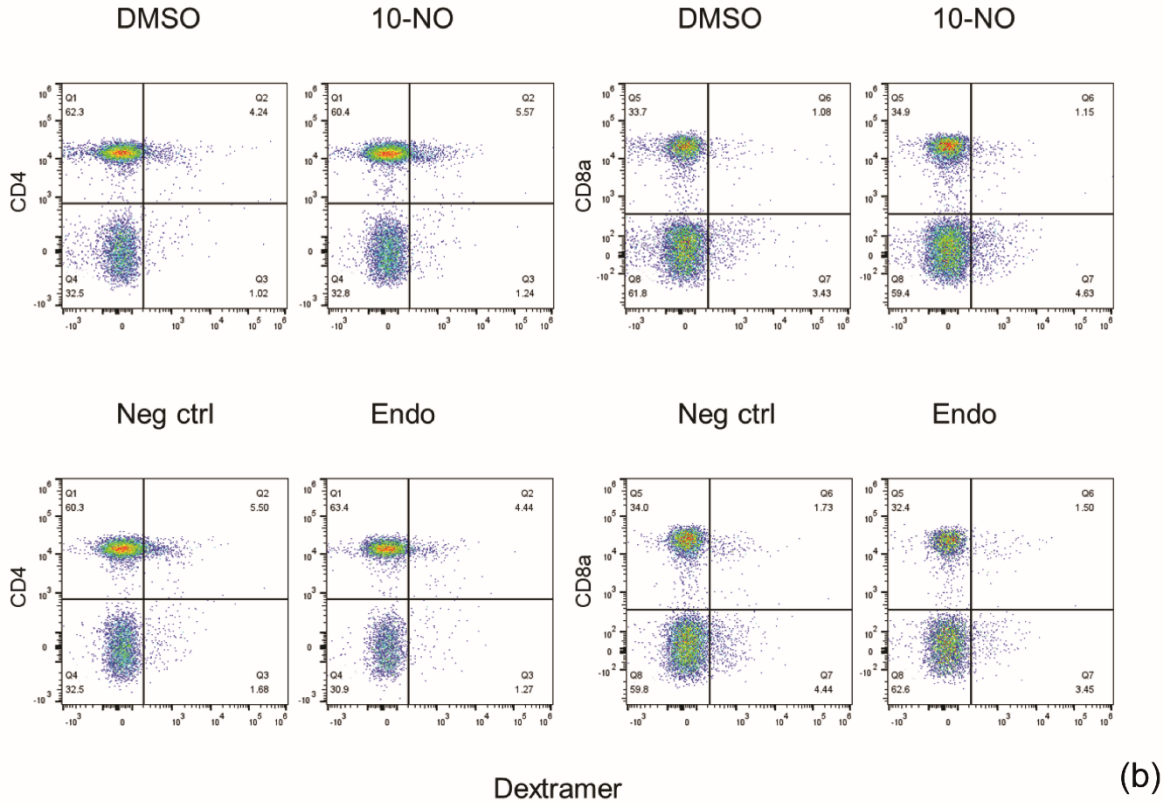
(b)

Figure 5.5 Dextramer staining 9-NO: Biotinylated CD1a was loaded with 9-NO/DMSO overnight, then assembled into dextramers using Streptavidin PE. Frozen PBMC were stained with dextramers and analysed by flow cytometry. (a) Healthy Control C2933 (b) Psoriasis PS2650. 9-NO; 9-nitrooleate, DMSO; dimethyl sulfoxide.

10-NO showed similar levels of dextramer binding to 9-NO for $CD3^+CD8a^+$ cells in healthy control but the psoriasis sample showed less binding than negative control/endogenous, which may be due to assay variability. There was no notable increase in $CD3^+CD4^+$ dextramer binding for 10-NO in either sample (**Figure 5.6**).



(a)



(b)

Dextramer

Figure 5.6 Dextramer staining 10-NO: Biotinylated CD1a was loaded with 10-NO/DMSO overnight, then assembled into dextramers using Streptavidin PE. Frozen PBMC were stained with dextramers and analysed by flow cytometry. (a) Healthy Control C2933 (b) Psoriasis PS2650. 10-NO; 10-nitrooleate, DMSO; dimethyl sulfoxide.

Dextramer staining of NO2-CLA samples showed markedly increased binding in healthy control for polyclonal $CD3^+CD4^+$ and $CD3^+CD8a^+$ cells. Dextramer binding was also increased, albeit to a much lower degree, in the psoriasis sample (**Figure 5.7**).

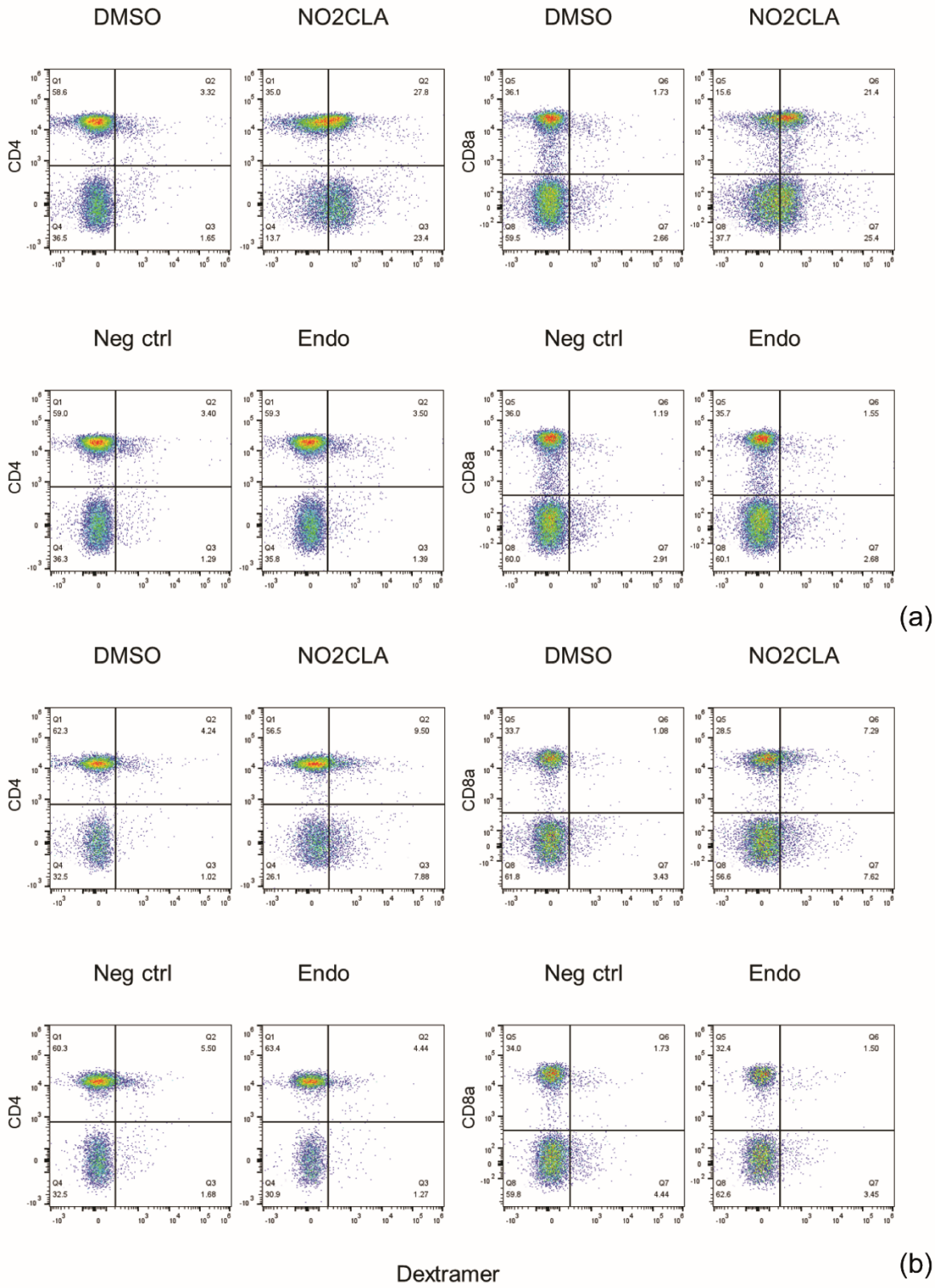

DMSO
NO2CLA
DMSO
NO2CLA
CD4
CD8a
Q1 58.6
Q2 3.32
Q4 36.5
Q3 1.65
Q1 35.0
Q2 27.8
Q4 13.7
Q3 23.4
Q5 36.1
Q6 1.73
Q8 59.5
Q7 2.66
Q5 15.6
Q6 21.4
Q8 37.7
Q7 25.4
Neg ctrl
Endo
Neg ctrl
Endo
Q1 59.0
Q2 3.40
Q4 36.3
Q3 1.29
Q1 59.3
Q2 3.50
Q4 35.8
Q3 1.39
Q5 36.0
Q6 1.19
Q8 60.0
Q7 2.91
Q5 35.7
Q6 1.55
Q8 60.1
Q7 2.68
(a)
DMSO
NO2CLA
DMSO
NO2CLA
Q1 62.3
Q2 4.24
Q4 32.5
Q3 1.02
Q1 56.5
Q2 9.50
Q4 26.1
Q3 7.88
Q5 33.7
Q6 1.08
Q8 61.8
Q7 3.43
Q5 28.5
Q6 7.29
Q8 56.6
Q7 7.62
Neg ctrl
Endo
Neg ctrl
Endo
Q1 60.3
Q2 5.50
Q4 32.5
Q3 1.68
Q1 63.4
Q2 4.44
Q4 30.9
Q3 1.27
Q5 34.0
Q6 1.73
Q8 59.8
Q7 4.44
Q5 32.4
Q6 1.50
Q8 62.6
Q7 3.45
Dextramer
(b)

Figure 5.7 Dextramer staining NO2-CLA: Biotinylated CD1a was loaded with NO2-CLA/DMSO overnight, then assembled into dextramers using Streptavidin PE. Frozen PBMC were stained with dextramers and analysed by flow cytometry. (a) Healthy Control C2933 (b) Psoriasis PS2650. NO2-CLA; 9(E),11(E)-9-nitro conjugated linoleic acid, DMSO; dimethyl sulfoxide.

5.2.5 The effect of Nitro-Fatty Acids on CD1a expression on moDC and K562 cells

Pulsing of moDC on Day 3 with 9-NO or 10-NO did not show any change in CD1a expression compared to vehicle control (**Figure 5.8 (a)** and **(b)**). However, day 3 pulsing with NO2-CLA showed a statistically significant reduction in CD1a expression compared to vehicle control, p_{adj} 0.008 (**Figure 5.8 (c)**). This appeared to be unrelated to toxicity (**Figure 5.8 (d)**).

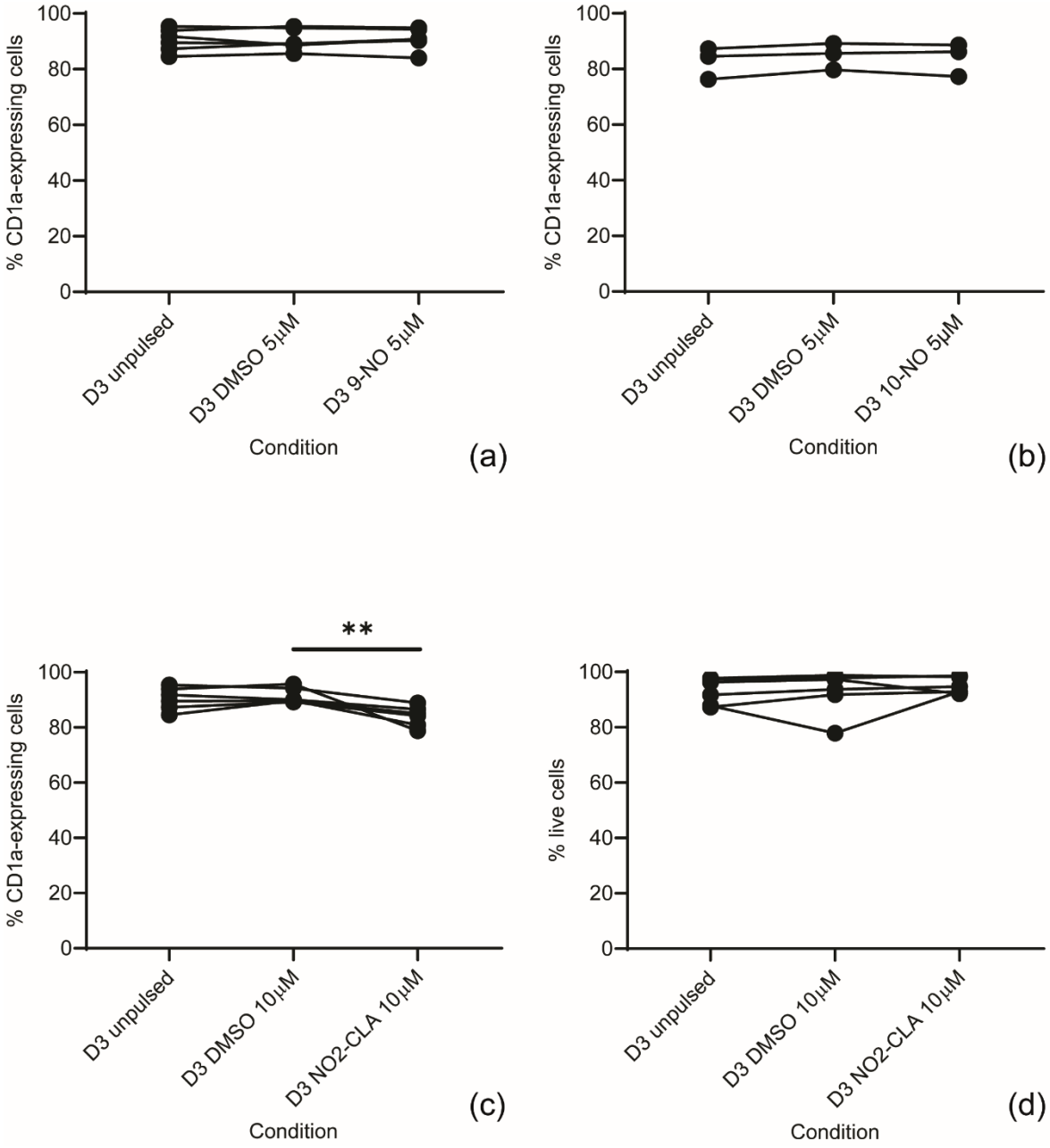


*Figure 5.8 CD1a expression on moDC following Day 3 lipid pulsing vs vehicle control (a) 9-NO 5µM (b) 10-NO 5µM (c) NO2-CLA 10µM and % Live cells (d) NO2-CLA. Only cells that showed good differentiation (>80% CD1a expression in unpulsed condition) were included in the analysis, apart from 10-NO, where a 75% cut-off was employed. Friedman non-parametric ANOVA with post-hoc Dunn test. **p-value <0.05.*

K562 toxicity testing (**Section 5.2.3**) also demonstrated a reduction in CD1a expression out of proportion to toxicity for NO2-CLA. There was a 13.8% reduction in CD1a expression at 100μM for NO2-CLA versus 4.2% for 9-NO and 4.42% for 10-NO. There was a maximum 2% change in CD1a expression for the final concentrations chosen for future experiments.

5.2.6 Assessment of cytokine production by CD1a-reactive T cells

Polyclonal experiments

Polyclonal assays using IFN-γ ELISpot did not demonstrate any significant changes in cytokine secretion for T cells co-cultured with NFA-pulsed K562 cells (data not shown). Unfortunately, these experiments were limited by technical issues and a batch of 9-NO without shift on IEF gel was inadvertently used for two of these experiments.

Clonal experiments

Polyclonal T cells comprise a mixed population of cells which can reduce sensitivity and specificity. Therefore, IFN-γ ELISA using CD1a-reactive T cell clones, sorted and cultured from healthy donors by Dr Yi-Ling Chen, was performed. In some cases the same clone was used in different experiments weeks apart (marked as replicates in **Figure 5.9**) and did not always demonstrate a reproducible response, which may reflect differences in activation state. When taking all clones together as individuals, a small but significant inhibitory effect on IFN-γ secretion was demonstrated with 10-NO only (**Figure 5.9**).

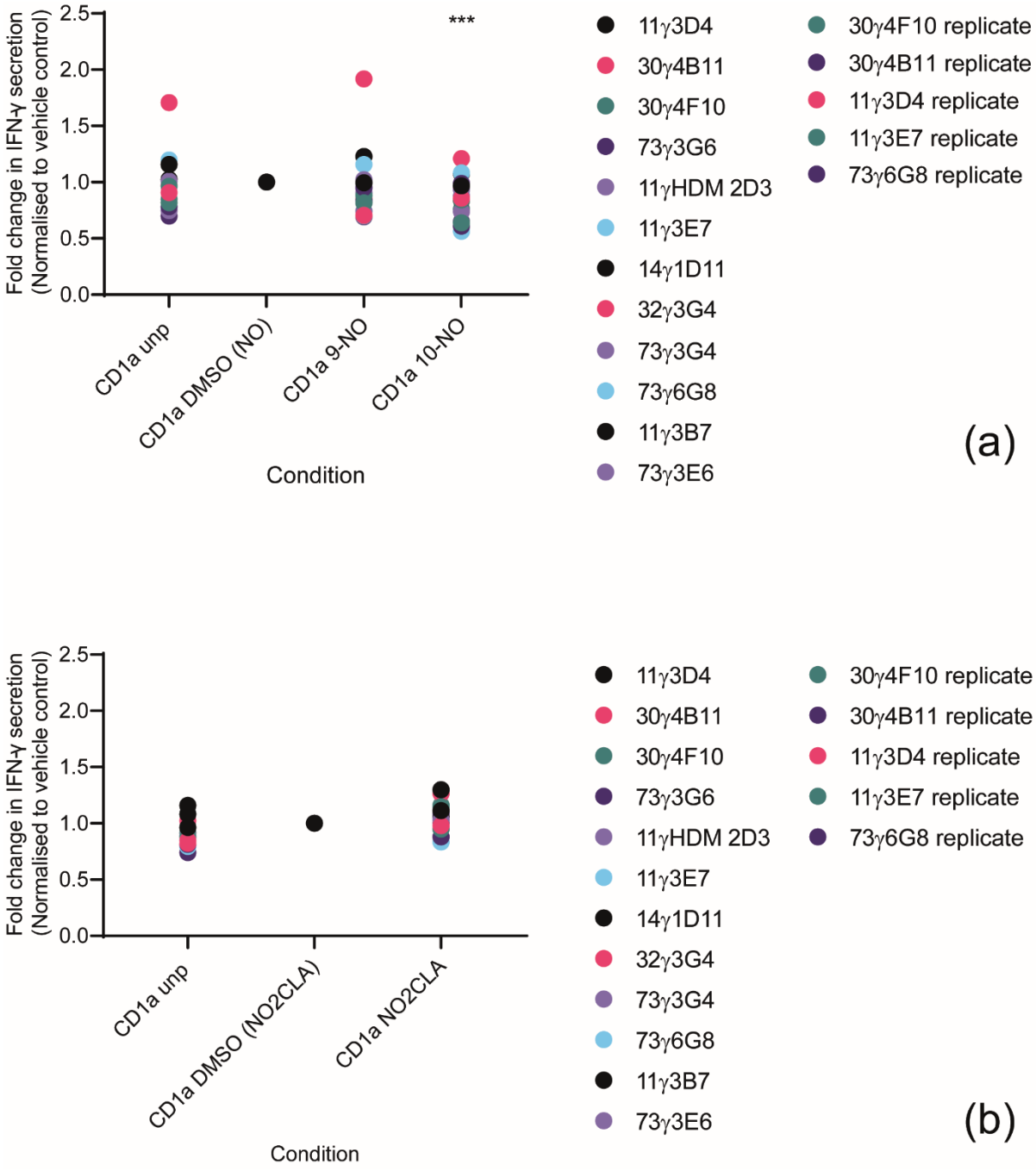


Figure 5.9 IFN-γ ELISA: NFA. K562 cells were pulsed with lipid/vehicle for 21-22 hours then co-cultured with CD1a-reactive T cell clones in a ratio of 150,000:100,000 cells for 24 hours. Co-culture supernatants processed using IFN-γ ELISA Max™ Deluxe set. Clone cytokine secretion normalised to vehicle control (DMSO) by Friedman non-parametric one-way ANOVA with Dunn test. CD1a; CD1a-transduced K562 cells, unp; unpulsed, DMSO; dimethyl sulfoxide.

ELISA using GM-CSF (for IL-17A and TNF-α) and IL-22 clones were also performed but only 2-3 clones reached the detection limit of the assay for TNF-α and IL-22 while none did for IL-17A so interpretation of results was limited.

5.2.7 Clonal assay using the CD1a-autoreactive BK6 TCR

Although CD69 autoreactivity was detected across most K562-CD1a conditions vs K562-EV unpulsed in a clonal assay using Jurkat BK6 cells, no statistically significant difference between lipid- pulsed conditions and their vehicles were detected within the K562-CD1a cohort (data not shown).

5.2.8 Nitro-Fatty Acids results summary

RNA-Seq data demonstrated differential expression of some genes linked to NFA pathways in psoriasis. IEF gels supported the role of NFA as CD1a ligands and dextramer staining supported this for NO2-CLA, which was also suggested to downregulate CD1a expression on moDC. Cell-based assays showed a possible inhibitory effect on IFN-γ secretion for 10-NO. Further studies are required to fully assess NFA as CD1a ligands.

5.3 Discussion

Alterations in FA metabolism occur in psoriasis, as supported by RNA-Seq data (**Chapter 3**). Some genes involved in NFA metabolism and signalling were downregulated in psoriatic skin vs HC skin. *PPARG* was significantly downregulated across all psoriasis groups vs HC; as discussed in the introduction, NFA may act as ligands for PPARγ on moDC and dampen the production of cytokines implicated in psoriatic inflammation, such as TNF-α. Substrates for nitration, unsaturated FA

(including oleic and linoleic acid) are increased in psoriatic scale compared to healthy stratum corneum (Wertz et al., 1989).

NFA all produced a marked shift on IEF gels, suggesting binding to the CD1a cleft. This was also shown to be the case for the isoforms CD1b and CD1c provided by the NIH. Potential explanations include a broad specificity of binding to multiple CD1 isoforms or attachment of the NFA to the exterior of the CD1 molecule resulting in a shift. However, pre-loaded 3-day gels suggested that 9-NO, 10-NO and NO2-CLA can at least partially displace the known CD1a ligands GD3 and LPC, lending credence the possibility they bind to the CD1a cleft. However, CD1b and CD1c structurally differ from each other and CD1a and would not necessarily be presumed to bind the same lipid. Also, if binding is not specific to CD1a, this would have further ramifications for the role of these lipids in psoriasis, although CD1b is also important in this disease (Bagchi et al., 2017).

Tetramer staining was limited to 9-NO and did not show anything conclusive. Dextramer staining was variable, although NO2-CLA appeared to show greater binding to polyclonal T cells than 9-NO and 10-NO and this was particularly evident in the HC sample. In total three psoriasis and three healthy control samples were tested and all showed similar patterns of marked binding for NO2-CLA. Whether this is down to a technical issue is unclear. The cells from both donors were >90% live for all conditions but were stained with Live-Dead Aqua rather than an apoptotic marker. On toxicity testing, although K562-CD1a toxicity was less marked with NO2-CLA compared to the nitro-oleates, NO2-CLA had a greater impact on CD1a expression on K562 cells, even at apparently non-toxic concentrations. This effect reduced to <2% at 12.5μM and 0.7% at 6.25μM, which informed the choice of the final concentration for use as 10μM. A similar effect was noted with lipid-pulsed moDC, despite viability remaining high on flow cytometry. However, again, without an apoptotic marker, it cannot be ruled out that these apparent reductions

in CD1a expression may be a reaction to cellular stress, particularly in the case of the less robust moDC. NO2-CLA is thought to be the most physiologically relevant NFA (based on CLA being the preferential substrate)(Bonacci et al., 2012) and it therefore makes sense that it, and not 9-NO or 10-NO, would influence CD1a expression. If it is indeed a true effect, reduction in CD1a expression may be anti-inflammatory by reducing binding of phospholipase-generated ligands that activate pro-inflammatory T cells, which has been shown to be the case in psoriasis (Cheung et al., 2016).

It is unclear how much of these NFA would be produced in the skin during inflammation and in particular psoriasis. Studies are limited to mouse models who have received subcutaneous injection or topical application of NFA and then serum levels are measured (Mathers et al., 2017, 2018). More recently, concerns have been raised that NFA may not be present in the skin to a degree capable of influencing physiological processes (Tsikas, Zoerner, Mitschke, Homsi, et al., 2009). IEF gels using these "physiological" concentrations of 9-NO did not show any shift. However, the formation of NFA is dynamic and they may be produced in much larger quantities local to a site of inflammation *in vivo*.

ELISpot experiments assessing polyclonal T cell response to NFA lacked a consistent pattern but interpretation was hampered by overall low spot number. Clonal experiments suggested a mild inhibition of IFN-γ secretion with 10-NO. Although statistically significant, the fold change here was so mild as to be unlikely to be of clinical relevance. It is perhaps surprising that the 9-NO isoform would not have similar effects given its identical carbon tail length. However, notably there was an issue with one batch of 9-NO being used for some of the clonal and polyclonal experiments that subsequently did not produce a shift on IEF, which may have affected these results. Experiments using GM-

CSF and IL-22 clones did not produce conclusive results for the effects of NFA on the secretion of TNF-α, IL-17A or IL-22.

These data suggest NFA act to reduce inflammation. Murine studies have demonstrated that NFA are anti-inflammatory when administered systemically but may be pro-inflammatory when applied topically in the context of contact hypersensitivity (Mathers et al., 2017, 2018). CD1a has also been implicated in human contact hypersensitivity (allergic contact dermatitis) (Nicolai et al., 2020). Mathers et al also found that a statistically significant increase in ear thickness was induced by topical application of 1% OA-NO2 at 24 and 48 hours compared to naïve ear skin which the authors attributed to an irritant effect (Mathers et al., 2018). Thereafter 0.1% OA-NO2, which had no significant impact on ear thickness, was used for the experiments in combination with DNFB. These effects seem contradictory as NFA activate downstream pathways that antagonise oxidative stress (Freeman et al., 2008). However, Nrf2 mRNA and protein are upregulated in PS L vs HC skin and can be upregulated in human keratinocytes by IL-17 and IL-22 (L. Yang et al., 2017). In HaCaT cells and primary human keratinocytes, Nrf2 increases expression of *KRT6*, *KRT16* and *KRT17* and in an IMQ mouse model of psoriasis, topical application of Nrf2 siRNA ameliorates inflammation and downregulates *IL17* and *TNF* mRNA, as well as mRNA and protein for KRT6, KRT16 and KRT17, suggesting the Nrf2 pathway, may also have pro-inflammatory effects in the skin (L. Yang et al., 2017). Therefore, it remains to be determined in the context of a disease such as psoriasis, where presumably NFA may be produced in relatively large amounts, whether NFA may aggravate or antagonise the disease process.

Overall, the experimental results detailed in this chapter, particularly IEF and dextramer staining, suggest that NFA may act as ligands for CD1a. Based on ELISA, their role may potentially include dampening of the T-cell inflammatory response. Further *in vitro*

studies are needed to elucidate their effects before considering *in vivo* assessment. There are numerous challenges to further investigating the role of NFA in human cutaneous disease given their transitory formation and uncertainty around their quantities and location in the skin in an inflammatory context. It is also not clear how sample processing may affect detection and the sensitivity of these measurements.

5.4 Chapter summary

NFA are formed from unsaturated FA in inflammatory, acidic environments. Their physiological effects in humans are yet to be fully elucidated. However, studies in the literature suggest potential effects in cutaneous inflammation in psoriasis and allergic contact dermatitis. Both of these conditions involve Th1/Th17 signalling and there are early indications that CD1a may have a role in these diseases. Experiments delineated in this chapter suggest a potential role for NFA in CD1a-mediated signalling, with their relevance in human inflammatory skin disease requiring further examination.

6 Chapter 6 Sterols and other CD1a candidate lipid ligands

6.1 Sterols: Molecules of the cholesterol pathway

A large number of studies investigating changes in the lipid milieu in psoriasis have been conducted and are summarised by Nowowiejska et al (Nowowiejska et al., 2021). As for RE and NFA, genes encoding enzymes for synthesis and metabolism of cholesterol and related molecules were altered in PS versus HC skin by RNA-Seq analysis (**Chapter 3**). Cholesterol is an integral component of the membrane of all animal cells and is required for the synthesis of steroid hormones, vitamin D and bile acids.

In this chapter, investigation of cholesterol and cholesteryl esters (CE) as potential CD1a ligands was undertaken to assess whether the changes identified in psoriasis had relevance for CD1a-mediated lipid antigen presentation. Several other lipid candidates were assessed for potential binding to CD1a, including some licensed and more anecdotally successful treatments for psoriasis where the exact mode of action is unknown.

6.1.1 Sterol pathways and psoriasis pathogenesis

Cholesterol biosynthesis occurs via a multi-step pathway (**Figure 6.1**). Precursors include farnesyl pyrophosphate and squalene. Cholesterol is further metabolised to immunoactive oxysterols, 25-hydroxysterol and 27-hydroxysterol and their 7α-dihydroxysterol derivatives, as summarised by Willinger (Willinger, 2019), which have mixed effects, including modulation of T_h17 differentiation. CE are the storage form of cholesterol. Cholesteryl oleate (18:1) is the predominant CE found in adult epidermis (Tachi & Iwamori, 2008).

The sterol and retinol pathways share the enzyme lysosomal acid lipase (LAL), also known as cholesteryl ester hydrolase (CEH), which hydrolyses RE to retinol and converts CE to cholesterol, linking the two pathways.

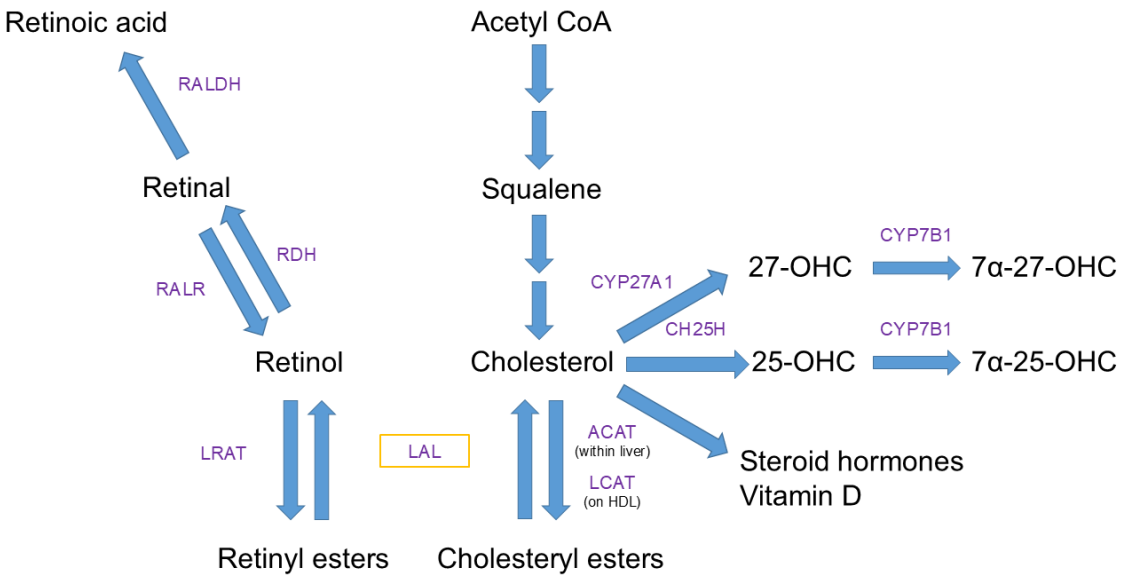


Figure 6.1 Interaction of Sterol and Retinoid pathways. The enzyme Lysosomal Acid Lipase (LAL), also known as cholesteryl ester hydrolase (CEH), links the two pathways. Enzymes in purple text. RALDH; retinaldehyde dehydrogenase, RALR; retinal reductase, RDH; retinol dehydrogenase, LRAT; leicithin:retinol acyltransferase, LAL; lysosomal acid lipase, ACAT; acyl-coenzymeA:cholesterol acyltransferase, LCAT; lecithin:cholesterol acyltransferase, CH25H; cholesterol 25-hydroxylase, CYP27A1; cytochrome P450 family 27 subfamily A member 1, CYP7B1; cytochrome P450 family 7 subfamily B member 1.

Downstream cholesterol metabolites form part of the bile acid synthetic pathway (the main cholesterol catabolic pathway). Aramchol (arachidyl amido cholanoic acid) is a synthetic fatty acid-bile acid conjugate (FABAC) (Gilat et al., 2001) being developed by Galmed pharmaceuticals. It has been shown to downregulate *SCD1* (encoding stearoyl CoA desaturase 1) in hepatic stellate cells, the principal location of RE storage, while increasing *PPARG*, with similar effects on protein expression (Bhattacharya et al., 2021).

Aramchol also increases expression of *ABCA1* (ATP-binding cassette transporter 1) and *ABCG1* (ATP Binding Cassette Subfamily G Member 1) expression, which encode proteins that act as cholesterol efflux pumps, and downregulates *ACAT2*, which encodes a catalysing enzyme for CE as well as other gene sets that regulate cholesterol biosynthesis (Bhattacharya et al., 2021). A phase three RCT (ARMOR) to assess the efficacy and safety of aramchol as a treatment for non-alcoholic steatohepatitis (clinicaltrials.gov identifier NCT04104321) is currently underway.

SCD1 catalyses the rate-limiting step of monounsaturated fatty acid (MUFA) synthesis; as there is an equilibrium between FA and cholesterol synthesis, skin-specific *SCD1* knockout mice have dry skin, alopecia and sebaceous gland hypoplasia, with alterations in cutaneous lipids including reduced sebaceous lipids but significantly increased free cholesterol (but not CE) and retinoids (including a 2.4-fold increase in RE) (Flowers et al., 2011; Sampath et al., 2009). Murine full *SCD1* knockouts show downregulation of *SREBP1* (also known as *SREBF1*) (Sterol Regulatory Binding Proteins/Sterol Regulatory Element Binding Transcription Factors), which encodes a transcription factor involved in the regulation of cholesterol and FA metabolism (Ntambi et al., 2002). *SREBP2*/*SREBF2*, as well as *FDPS* (farnesyl diphosphate synthase) and *FDFT1* (farnesyl-diphosphate farnesyltransferase 1) are suppressed by RA (Lee et al., 2009).

Psoriasis is associated with the metabolic syndrome (Rodríguez-Zúñiga & García-Perdomo, 2017), which includes dyslipidaemia, denoted as increased triglyceride and reduced HDL cholesterol levels in the blood. Patients with psoriasis have an altered serum FA profile compared to HC, with increased % MUFA and reduced % PUFA (Myśliwiec et al., 2017). There are also local changes to lipid metabolism seen in the skin even in the absence of clinical lesions. Historical publications have suggested that the ratio of CE to total cholesterol is significantly reduced in the surface lipid film of non-

lesional psoriatic chest and back skin compared to healthy control skin(Rothman, 1950) and cholesterol esterifying ability in non-lesional psoriatic skin is approximately one tenth that of healthy control skin (Gara et al., 1964). CE content varies depending on keratinization, with cholesterol in the basal layers of the epidermis almost all in a free (uncombined) form (98.2% vs 81.9% in the stratum corneum), while just under a fifth (approximately 18%) is esterified with free FA as CE in the stratum corneum (Kooyman, 1932). Although the stratum corneum is thickened in psoriasis and increased CE content would be expected, a study by Schmidt et al reported reduced CE and increased free cholesterol in PS vs HC skin of the legs and back, while both CE and free cholesterol were increased in the skin of the sole in PS vs HC (Schmidt et al., 1977). This study also showed that body site influenced the CE content of healthy skin, with increased levels found in non-plantar skin compared to that of sole, while free cholesterol content was similar (Schmidt et al., 1977).

Genes encoding proteins of FA metabolism including *ALOX15B*, *FADS1* and *ELOVL3* have been demonstrated to be reduced in even non-lesional psoriatic skin compared to healthy control skin and synthesis of lipids, LCFA and CE are downregulated, while uptake of arachidonic acid, eicosanoid and lipid is increased (Gudjonsson et al., 2009). ELOVL (ELongation-Of-Very-Long-chain-fatty-acids) elongases are ubiquitous enzymes required for the synthesis of very long chain fatty acids (VLCFA), which are in turn components of sphingolipids, glycerophospholipids, triacylglycerols, sterol and wax esters (Jakobsson et al., 2006). Saturated and mono-unsaturated FA are elongated by ELOVL1, 3 and 6, while elongation of PUFA is performed by ELOVL 2, 4 and 5 (Jakobsson et al., 2006). The rate of epidermal lipogenesis is increased in PS L versus PS NL skin and this correlates with increased free sterol: monoester (sterol esters plus wax esters) ratios (Cooper et al., 1976). Of note, wax esters have been identified as lipid ligands for CD1a (De Jong et al., 2014).

As discussed in **Chapter 1**, type I and type II interferons are implicated in upstream pathways of psoriasis and both have been shown to upregulate expression of *CH25H* (K. Park & Scott, 2010). Its protein product, 25-Hydroxycholesterol, has been shown to antagonise virus infection in cultured cells and mice (Liu et al., 2013).

Although cholesterol is not typical in structure for CD1a ligands discovered to date, other members of the cholesterol biosynthetic pathway such as squalene (De Jong et al., 2014) and farnesol (Nicolai et al., 2020) have been shown to bind CD1a.

Taken together, the above studies implicate sterols and their esters in skin homeostasis and psoriasis pathogenesis and CD1 biology: this pathway is investigated below using cholesterol and two of its esters (**Figure 6.2**).

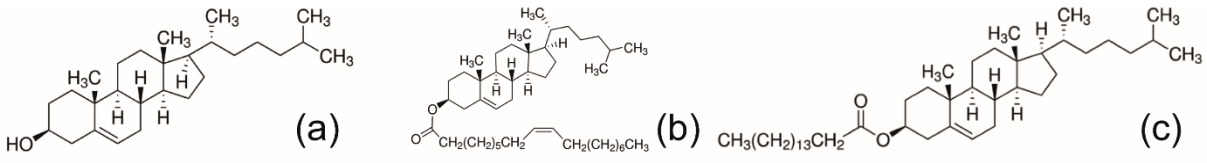


Figure 6.2 Chemical structures of sterols examined further following IEF screening (a) Cholesterol, $C_{27}H_{46}O$ (b) Cholesteryl oleate, $C_{45}H_{78}O_2$ (c) Cholesteryl palmitate, $C_{43}H_{76}O_2$. Composite of images taken from information on products used for experiments at www.sigmaaldrich.com.

6.2 Lipid pathways and psoriasis treatment – coal tar derivatives and acitretin

Topically applied coal tar derivatives and oral acitretin are longstanding treatments for psoriasis, but little is known regarding their exact mode of action. The possibility that their therapeutic effect could be exerted via CD1a was considered.

6.2.1 Coal tar derivatives

Coal tar and its derivatives have been used topically for many years as a treatment for psoriasis. The mechanism of action is poorly understood but is thought to include anti-inflammatory, anti-proliferative and anti-microbial effects (Roelofzen et al., 2007). Coal tar derivatives have been shown to atrophy viable epidermis when used for prolonged periods (40 days) in healthy controls, although hyperplasia may occur in the initial treatment period (Lavker et al., 1981). In the current NICE guidelines (www.nice.org.uk/psoriasis), they are third line topical therapy for body and scalp psoriasis after steroids and vitamin D analogues. This is partly related to the carcinogenic properties of topically applied polyaromatic hydrocarbons in animal studies (Bickers & Lowy, 1989), although a comprehensive review of studies in humans using topical dermatological preparations (Pion et al., 1995) and a more recent large cohort study (Roelofzen et al., 2010) have not confirmed this link. Occupational exposure to coal tar has also been associated with malignancy and although human carcinogenicity in the realm of dermatological usage remains unproven, the World Health Organisation (WHO) recommends it is used at a concentration of <5%.

Evidence of efficacy is also limited. Young found that tar formulations were superior to vehicle in a paired comparison study over fifty years ago (Young, 1970). The small number of studies that have been performed since showed no difference compared to

placebo and inferiority to vitamin D analogues when examined by systematic review (Mason et al., 2013; Samarasekera et al., 2013). There are many formulations available in the form of ointments, shampoos and bath additives, with distilled coal tar as the active ingredient. However, as coal tar contains over 10,000 excipients, variability between preparations may be significant. The coal tar derivatives used in the current study were a coal tar solution (distilled coal tar with 81-86% ethyl alcohol, Alfa Aesar, 43671) and a 40% w/v bath additive containing distilled coal tar (Psoriderm™, by Dermal™), which is available over the counter.

6.2.2 Acitretin

Synthetic retinoids have been used by dermatologists for decades, both topically and systemically, to treat a range of cutaneous diseases, including inflammatory (e.g. acne, psoriasis, chronic hand dermatitis, pityriasis rubra pilaris), malignant (e.g. cutaneous T cell lymphoma) and hereditary (e.g. Darier disease) conditions and more recently to modify physiological processes (skin ageing).

Topical retinoid formulations such as tazarotene are used for psoriasis alone or in combination with topical steroids in Europe and the US but are not included in NICE guidelines in the UK. Efficacy is similar to Vitamin D analogues (Mason et al., 2013; Weinstein et al., 1997, 2003).

The second-generation oral retinoid Acitretin (**Figure 6.3**) selectively binds the retinoic acid receptor (RAR). It is a third-line option for patients who require systemic treatment for plaque psoriasis in the absence of psoriatic arthritis, if methotrexate and/or ciclosporin are ineffective or contraindicated. It is favoured in cases where immunosuppression is unsuitable and is also used to manage pustular psoriasis (NICE). However, it cannot be used in women of child-bearing age due to teratogenicity and has a host of potential side

effects including dyslipidaemia, hepatic and ocular dysfunction, neuropsychiatric effects and abnormal ossification with long term use. Many patients also find it difficult to tolerate higher doses that may be more effective due to secondary cutaneous dryness. The mode of action is not well understood, but is thought to involve effects on cell proliferation, differentiation and keratinisation, along with immunomodulatory and anti-inflammatory actions (Gollnick, 1996). There are few efficacy studies, including RCT, but a network meta-analysis of nine trials of acitretin vs placebo and four trials of acitretin versus another acitretin dose or treatment (ciclosporin, etanercept), concluded that it had moderate efficacy (between that of methotrexate and ciclosporin) in attaining PASI 75 (75% improvement in psoriasis), although the confidence interval was wide (Sbidian et al., 2017). Acitretin may be used as an adjunct to phototherapy (Re-PUVA or Re-UVB) to increase efficacy, particularly for the treatment of plaque psoriasis (Sbidian et al., 2011).

The potential for acitretin (**Figure 6.3**) to engage the CD1a pathway or even be a novel ligand was tested in the experiments below.

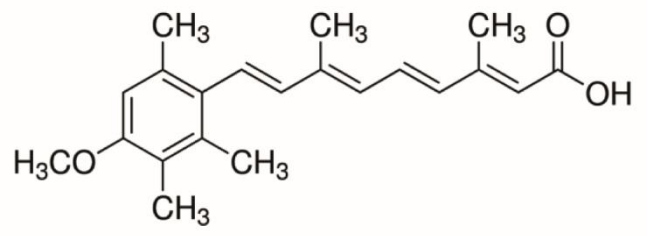


Figure 6.3 Chemical structure of acitretin, $C_{21}H_{26}O_3$. Image taken from information on product used for experiments at www.sigmaaldrich.com.

6.3 Other lipids of interest

Some published studies suggest benefits from substances more commonly considered foodstuffs in the treatment of psoriasis. Curcumin, from turmeric, reduces cellular production of IFN-γ and IL-17 *in vitro*(Skyvalidas et al., 2020) and RCT have shown

benefit in psoriasis patients (Patel et al., 2024). Oral mustard seed (Sinapis Alba Linn) reduces imiquimod-induced psoriasiform inflammation in a murine model, with statistically significant reduction in *IFNA*, *IL17A*, *IL17F* and *IL22* mRNA (R. Yang et al., 2013). Topical application of black seed (black cumin) oil (Nigella sativa) reduces inflammation in an IMQ mouse model of psoriasis (Okasha et al., 2018). Its bioactive component, thymoquinone, has anti-inflammatory effects, including induction of HMOX1/HO1 (mRNA and protein) in human keratinocytes (HaCaT cells) (Kundu et al., 2014), part of the anti-oxidant response with downstream pathways overlapping with those of NFA. Bakuchiol is derived from Psoralea Corylifolia, a plant that also contains psoralens, whose components have long been used in herbal remedies (Shamsi, 2019) and has recently become popular as a retinoid-alternative in anti-ageing products. The gene expression profile of bakuchiol was similar to retinol and was also shown to dramatically upregulate *LRAT* (82-fold vs vehicle) compared to retinol (12.3-fold vs vehicle) in EpiDerm FT skin substitutes, possibly suggesting a role in RE formation (Chaudhuri & Bojanowski, 2014). In a study using psoriasis surrogate keratinocytes and skin substitutes, bakuchiol's salicylic acid ester, bakusylan, modulated transcription in a similar way to retinoids, including downregulation of genes of the type I interferon response and response to virus (S. Ma et al., 2017). GO terms enriched with genes downregulated by bakusylan included steroid and cholesterol biosynthesis and triglyceride biosynthesis and catabolic processes (S. Ma et al., 2017).

6.4 Results I: Sterols and related molecules

6.4.1 Interrogation of RNA-Seq data for sterol-relevant genes

Chapter 3 outlined lipid metabolic pathways that were altered (compared to healthy skin) in psoriasis and following treatment with NB-UVB or anti-IL17A monoclonal antibody therapy. More detailed analysis of key enzymes of sterol-specific pathways identified

relevant changes, albeit relatively small in magnitude and often not reaching significance (**Table 6.1**).

Table 6.1 Selection of DEG relevant to sterol pathways: Untreated lesional psoriasis (PS L) versus healthy control (HC) skin. p_{adj}; adjusted p-value.

Gene	Log2FC	p_{adj}
LIPA	0.470	0.041
ACAT1	-0.599	0.001
ACAT2	-1.560	1.54×10^{-7}
LCAT	0.268	0.689
CH25H	0.347	0.554
CYP27A1	-2.746	2.07×10^{-30}
CYP7A1	0.428	0.742
CYP7B1	1.196	0.066
CYP8B1	2.253	0.004
HMGCR	-0.480	0.108
DHCR7	-1.346	2.43×10^{-9}
DHCR24	-1.193	1.56×10^{-11}
SREBF2	0.225	0.115
FDPS	-1.400	6.93×10^{-6}
FDFT1	-0.540	0.007
GPR183	0.419	0.352
ELOVL3	-7.615	4.64×10^{-81}
ELOVL5	-3.651	1.95×10^{-65}
NR1H3	-1.678	1.76×10^{-7}

HMGCR encodes the enzyme 3-Hydroxy-3-Methylglutaryl-CoA Reductase (HMG Co-A reductase) which catalyses the rate-limiting step in cholesterol biosynthesis. It was downregulated in untreated PS L vs HC skin. This was also the case for genes encoding other enzymes of the cholesterol biosynthetic pathway such as *FDPS*, *FDFT1* and *DHCR7*/*DHCR24*, which encode proteins that catalyse the final steps in cholesterol biosynthesis. These results were in keeping with Gene Ontology (GO) results, where GO terms encoding sterol and cholesterol biosynthetic and metabolic processes were downregulated in untreated PS L vs HC skin (**Table 6.2**). There was significant upregulation of *LIPA*, the gene encoding LAL/CEH, which breaks down CE and triglycerides, and reciprocal downregulation of *ACAT*, which catalyses the formation of CE using acyl CoA chains. However, *LCAT*, which encodes a protein that catalyses the formation of CE on HDL, was minimally (and non-significantly) upregulated.

For the oxysterol pathway, *CYP7B1*, which encodes an enzyme that converts cholesterol to bile acids outside of the liver, was upregulated (although not significantly), suggesting some formation of inflammatory dihydroxy oxysterols. However, *CYP27A1* was markedly downregulated, while *CH25H* was slightly upregulated, indicating predisposition to the formation of 25-hydroxycholesterol and 7α, 25- dihydroxysterol. Of interest, *CYP27A1* was only slightly downregulated compared to HC in skin that had resolved with NB-UVB (Log2FC -1.573, p_{adj} 0.0001), while in skin that had resolved with secukinumab, downregulation vs HC was similar to that of untreated PS L skin (Log2FC -2.181, p_{adj} 8.23 x 10^{-12}). Some oxysterols, including 25-hydroxycholesterol and 27-hydroxycholesterol, can bind LXRα, a Liver X Receptor that heterodimerises with Retinoid X Receptors (RXR) (Janowski et al., 1996). The role of these receptors in psoriasis is of interest; downregulation of this receptor has been identified in PS L compared with NL and HC skin (Gupta et al., 2010). Our RNA-Seq data also supports this finding (*NR1H3* encodes LXRα) (**Table 6.1**). This group further found that

knockdown of this receptor in healthy human keratinocytes resulted in increased *IFNG* and *IL8* and reduced *PPARG* and *VDR* (vitamin D receptor) mRNA expression, a pattern similar to that observed in lesional PS keratinocytes (Gupta et al., 2010). *GPR183*, which encodes an oxysterol receptor, was slightly upregulated in untreated PS L skin. *CYP7A1* encodes the enzyme catalysing the rate-limiting step for conversion of cholesterol to bile acids and was also slightly upregulated in untreated PS L skin. There was significant downregulation of the genes encoding the VLCFA elongases ELOVL3 and ELOVL5, suggesting impaired VLCFA synthesis, with implications for the manufacture of a range of lipids, including the CE. Other ELOVL genes were more mildly upregulated (*7*, *2*, *6*) or downregulated (*1*, *4*).

*Table 6.2 Enriched Gene Ontology (GO) terms relevant to sterol pathways: Untreated lesional psoriasis (PS L) skin versus healthy control (HC) skin. All GO terms in this table were downregulated in untreated PS L vs HC skin. *Log2FC>2. **Log2FC>4. p_{adj}; adjusted p-value.*

GO Term	Differential expression untreated PS L vs HC	p_{adj}	Genes
GO:0016126* Sterol biosynthetic process	Downregulated	0.0005	*INSIG1*, *ACAA2*, *FASN*, *MSMO1*, *FGF1*, *ACACB*, *FAXDC2*, *DHCR24*, *SC5D*, *PRKAA2*, *DHCR7*, *MVD*, *HMGCS2*, *ACAT2*, *PMVK*, *APOE*, *FDPS*, *APOB*, *HMGCS1*
GO:0016125**	Downregulated	2.79×10^{-5}	*SOAT1*, *INSIG1*, *ACAA2*, *CYP27A1*, *FASN*, *DGAT2*, *APOC1*, *CYP1B1*, *MSMO1*, *FGF1*, *CYP11A1*, *ACACB*,

Sterol metabolic process			*FAXDC2*, *DHCR24*, *SC5D*, *PRKAA2*, *DHCR7*, *MVD*, *HMGCS2*, *ACAT2*, *SCARB1*, *PMVK*, *APOE*, *FDPS*, *CUBN*, *NR1H4*, *APOB*, *HMGCS1*, *AKR1D1*, *SORL1*, *CYP21A2*, *PON1*, *ANGPTL3*
GO:0006695* Cholesterol biosynthetic process	Downregulated	0.0005	*INSIG1*, *ACAA2*, *FASN*, *MSMO1*, *FGF1*, *ACACB*, *DHCR24*, *SC5D*, *PRKAA2*, *DHCR7*, *MVD*, *HMGCS2*, *ACAT2*, *PMVK*, *APOE*, *FDPS*, *APOB*, *HMGCS1*
GO:0008203** Cholesterol metabolic process	Downregulated	7.42×10^{-5}	*SOAT1*, *INSIG1*, *ACAA2*, *CYP27A1*, *FASN*, *DGAT2*, *APOC1*, *MSMO1*, *FGF1*, *CYP11A1*, *ACACB*, *DHCR24*, *SC5D*, *PRKAA2*, *DHCR7*, *MVD*, *HMGCS2*, *ACAT2*, *SCARB1*, *PMVK*, *APOE*, *FDPS*, *CUBN*, *NR1H4*, *APOB*, *HMGCS1*, *AKR1D1*, *SORL1*, *PON1*, *ANGPTL3*

6.4.2 Optimisation of sterol solubility

The main challenge in executing the following experiments was the difficulty in successfully dissolving cholesterol and its esters, necessary to facilitate loading to CD1a. For the oxysterols and aramchol, solubility in DMSO or mixtures containing it were largely successful. However, for cholesterol and its esters, a large range of frequently-used solvents were initially trialled with variable success and additional, more unusual solvents were tested later (**Table 6.3**). Cholesterol and its esters were provided as solids

(powders for cholesterol and cholesteryl oleate and flakes for cholesteryl palmitate), with cholesterol and cholesteryl palmitate packaged in plastic rather than glass. These chemicals were all weighed out then transferred to a glass vial for dissolving. In many cases, a balance between solubility and the challenges of handling powders/flakes with a volatile solvent with relevant safety precautions, such as fume cupboard usage, was difficult to reach.

Table 6.3 Solubility of cholesterol and cholesteryl esters in a variety of solvents post sonication. Ch Oleate; cholesteryl oleate, Ch Palmitate; cholesteryl palmitate.

Solvent	Cholesterol	Ch Oleate	Ch Palmitate
100% DMSO	No	No	No
0.25% Tyloxapol/2% DMSO	Yes	Partial	Partial
100% Methanol	No	No	No
100% Ethanol	Partial	No	No
Ethanol: Dichloromethane 1:1	Yes	Yes	Yes
100% Dichloromethane	Yes	Yes	Yes
0.5% CHAPS	Partial	Partial	No
2% CHAPS	Partial	Partial	Partial
Chloroform/Methanol/Milli-Q water	Yes	Partial	Partial

Ultimately, to maximise solubility, the solvent used varied for each lipid. The figure legends below indicate the relevant solvent for each experiment.

6.4.3 Investigation of cholesterol and cholesteryl ester binding to CD1a

While some initial IEF gels did suggest a subtle shift in pI with cholesterol (e.g. thickened fifth band, **Figure 6.4 (a)**) and cholesteryl oleate (e.g. loss of fifth band, **Figure 6.4 (b)**),

these results were not reproducible. Cholesteryl palmitate did not show any shift (**Figure 6.4 (c)**).

There was no shift noted for 25-hydroxycholesterol and 27-hydroxycholesterol (**Figure 6.4 (c)**) while aramchol showed partial loss of the upper four bands (**Figure 6.4(d)**). Aramchol demonstrated precipitation in some circumstances which limited interpretation and further work.

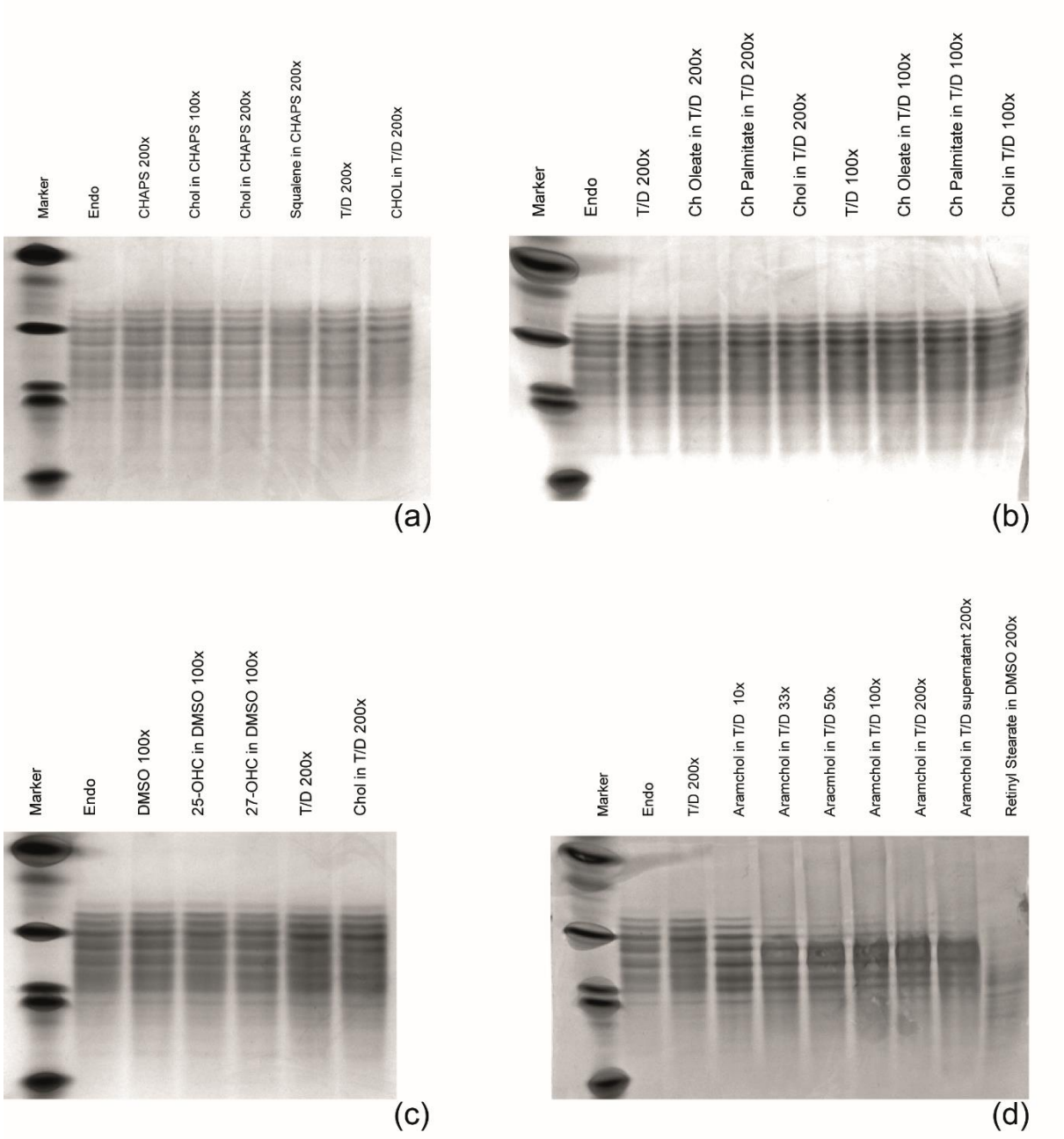


Figure 6.4 IEF gels: CD1a loaded overnight with lipid/vehicle then diluted 1:1 with IEF sample buffer and 18µL/well loaded to IEF gel. Endo (endogenous lipids); CD1a loaded with PBS only, 200x; 8µL CD1a:2µL lipid/vehicle, 100x; 9µL CD1a:1µL lipid/vehicle. (a) Cholesterol (b) Cholesteryl esters (c) Hydroxycholesterols (d) Aramchol. Lipid stocks: Cholesterol, cholesteryl esters and aramchol all at 40mM, hydroxycholesterols at 20mM. Chol; cholesterol, Ch Oleate; cholesteryl oleate, Ch Palmitate; cholesteryl palmitate, 25-OHC; 25-hydroxycholesterol, 27-OHC;

27-hydroxycholesterol, DCM; dichloromethane, DMSO; dimethyl sulfoxide, CHAPS; 0.5% CHAPS, T/D; 0.25% tyloxapol/2% DMSO.

Although unlikely, it was considered that the lack of shift on IEF may reflect a successfully loaded lipid with an identical iso-electric point. To exclude this possibility, CD1a was first loaded with the known ligand GD3 and subsequently incubated with the test lipids to assess displacement. Neither cholesterol nor its esters showed evidence of displacing GD3 from the binding cleft (**Figure 6.5**).

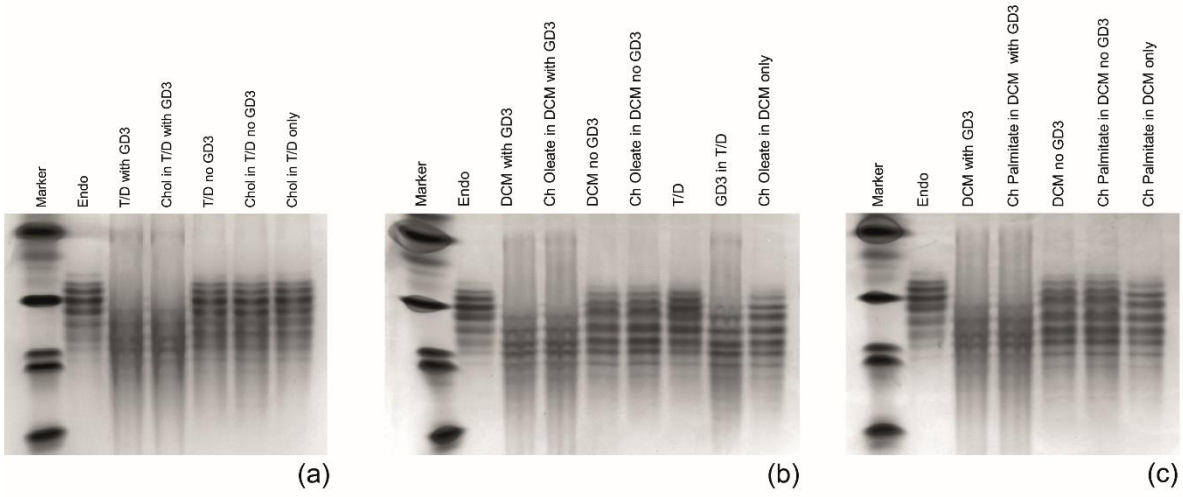
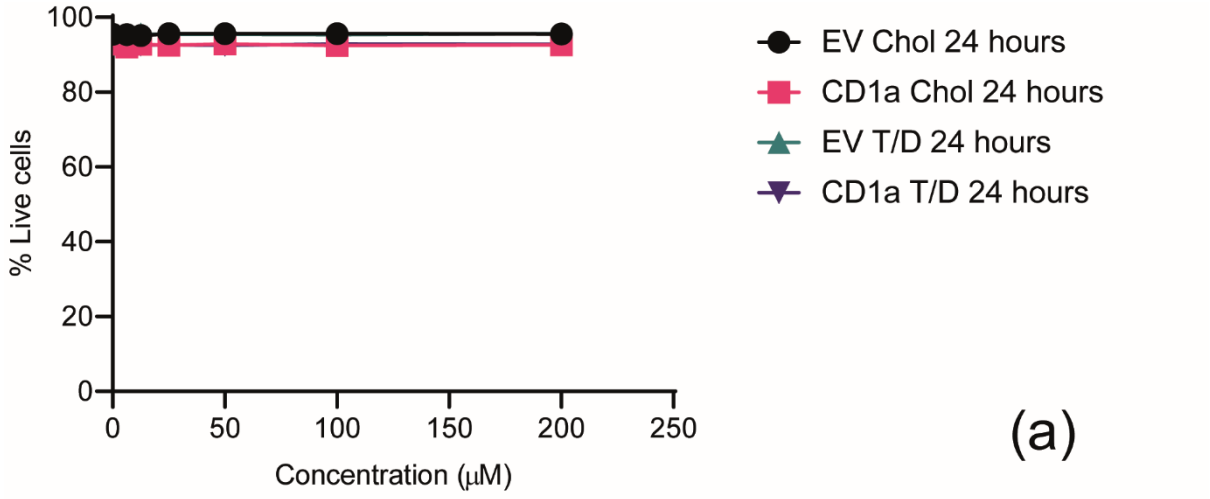


Figure 6.5 Pre-loaded IEF gels (GD3): 1µL of GD3 was pre-loaded to CD1a and incubated overnight at RT, then loaded with 1µL of 100x cholesterol/esters overnight, diluted 1:1 with IEF sample buffer and 18µL/well loaded to IEF gel. (a) Cholesterol (b) Cholesteryl oleate (c) Cholesteryl palmitate. Lipid stocks: Cholesterol and cholesteryl esters all at 40mM, GD3 at 13.3mM. Chol; cholesterol, Ch Oleate; cholesteryl oleate, Ch Palmitate; cholesteryl palmitate, GD3; ganglioside GD3, DCM; dichloromethane, T/D 0.25% tyloxapol/2% DMSO.

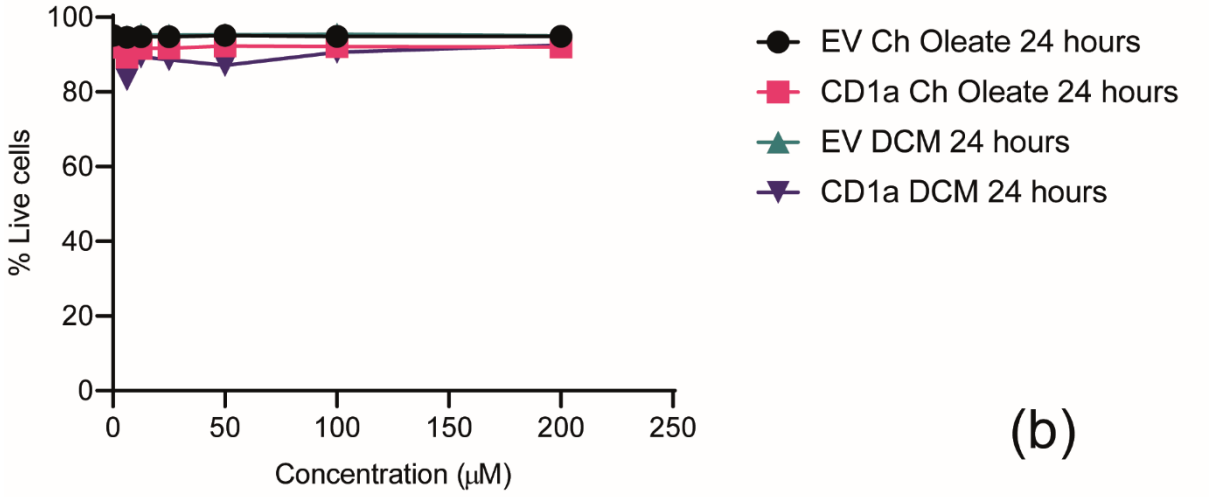
Overall, IEF data suggested challenges in assessing these specific sterol molecules for direct CD1a binding, but prior to ruling out specific CD1a-ligand activity, functional experiments were undertaken. These mainly focussed on cholesterol and, where possible, CE, although solubility issues limited their interpretation.

6.4.4 Assessment of toxicity and effects on CD1a expression on K562 cells by cholesterol and cholesteryl esters

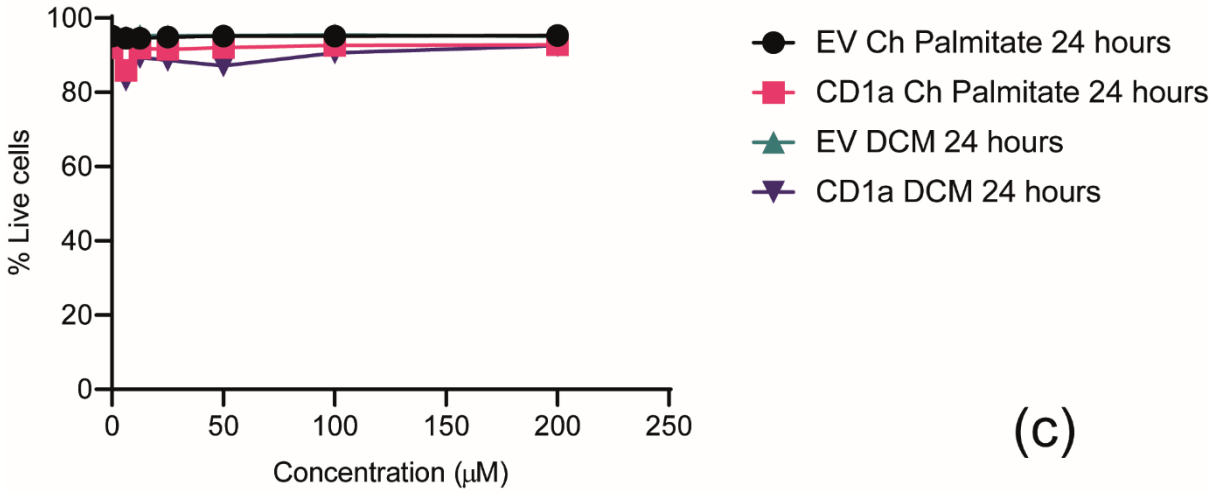
Toxicity testing showed good viability of both K562-EV and K562-CD1a to a final concentration of 200μM of cholesterol and its esters, including in the presence of different solvents (**Figure 6.6**). These findings supported the use of a final concentration in solution of 200μM for further cell-based experiments.


100
80
60
40
20
0
% Live cells
0
50
100
150
200
250
Concentration (μM)
EV Chol 24 hours
CD1a Chol 24 hours
EV T/D 24 hours
CD1a T/D 24 hours

(a)


100
80
60
40
20
0
% Live cells
0
50
100
150
200
250
Concentration (μM)
EV Ch Oleate 24 hours
CD1a Ch Oleate 24 hours
EV DCM 24 hours
CD1a DCM 24 hours

(b)


100
80
60
40
20
0
% Live cells
0
50
100
150
200
250
Concentration (μM)
EV Ch Palmitate 24 hours
CD1a Ch Palmitate 24 hours
EV DCM 24 hours
CD1a DCM 24 hours

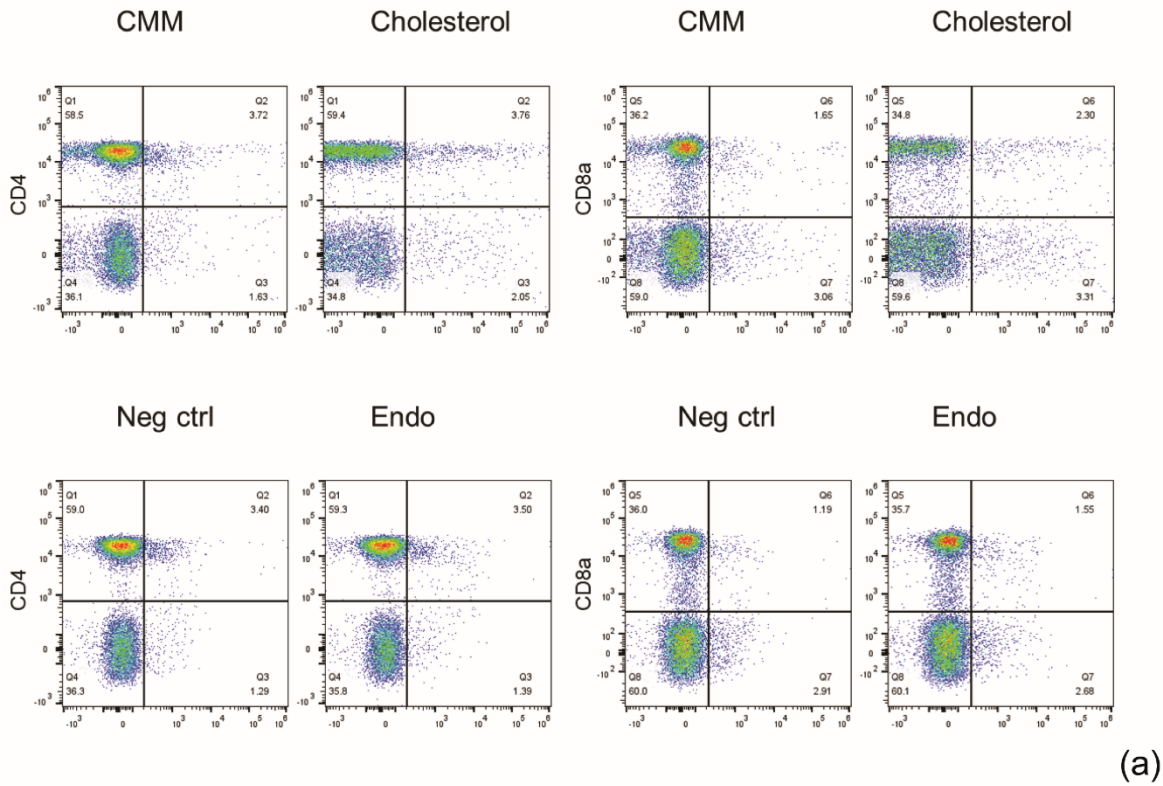
(c)

Figure 6.6 K562 Toxicity Testing: K562 cells were pulsed for 24 hours with serial dilutions of lipid/vehicle and media only and cell viability measured using Live-Dead Aqua by flow cytometry. (a) Cholesterol, (b) Cholesteryl oleate (c) Cholesteryl palmitate. DCM, Dichloromethane; T/D, 0.25% Tyloxapol/2% DMSO. EV; Empty vector-transduced K562 cells, CD1a; CD1a-transduced K562 cells.

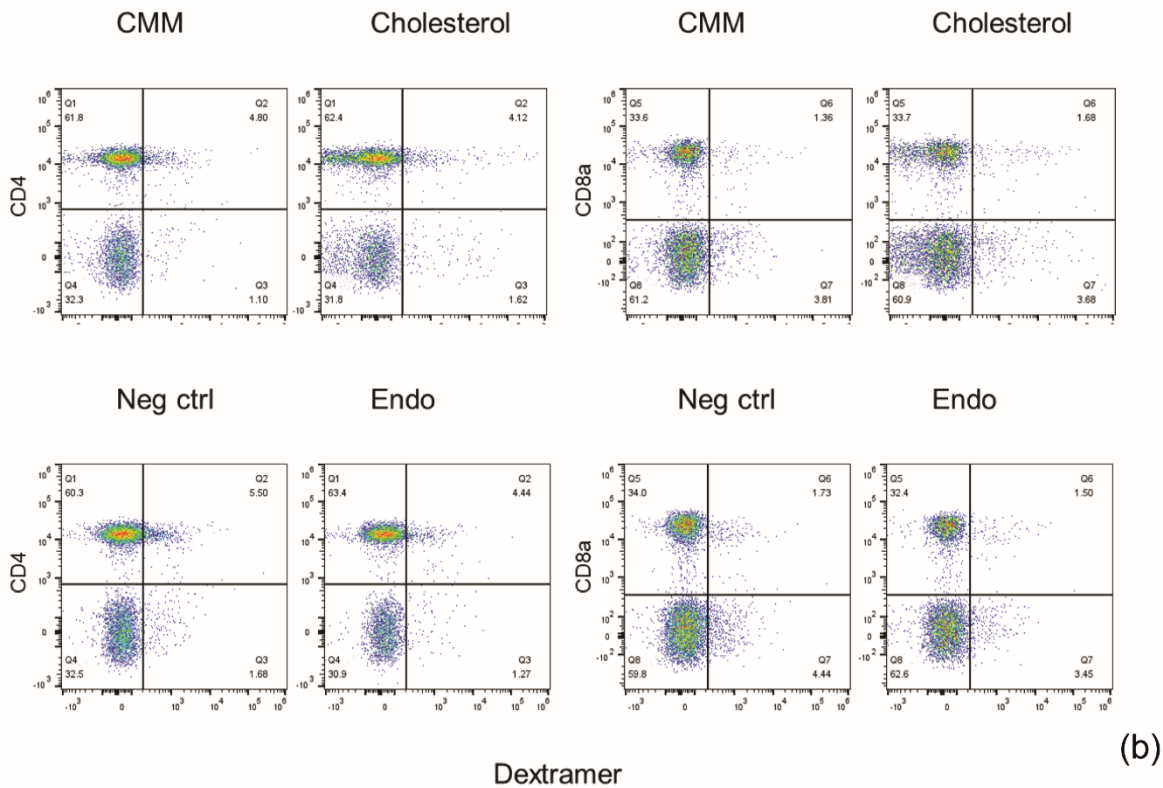
6.4.5 Tetramer and Dextramer staining with cholesterol

CD1a-based multimers have been used to detect CD1a-reactive T cells and tetramer and dextramer staining were performed for a range of lipids in this project (**Chapter 4**, **Chapter 5**). CD1a-based dextramer staining using frozen PBMC from psoriatic (3) and healthy donors (3) was performed as for other candidate CD1a-ligands. To avoid precipitation that could create artefact on the flow cytometer, help was sought from collaborator and biochemist Professor Gurdyal Besra at the University of Birmingham, who advised using a solvent mixture of Methanol:Chloroform:MilliQ water (ratio 10:10:3). This successfully dissolved cholesterol but issues remained with the esters which were therefore not included in the experiment.

Toxicity of the cholesterol-loaded dextramers was negligible, with live cells analysed demonstrating >99% viability (data not shown). However, the degree of binding of $CD3^{+}CD4^{+}$ cells in both healthy and psoriatic donors was similar to that of CD1a loaded with endogenous lipids and with the dextran-only control (**Figure 6.7**). Interpretation of dextramer staining was challenging due to the high level of staining of the dextran-only control.



(a)



(b)

Dextramer

Figure 6.7 Dextramer staining Cholesterol: Biotinylated CD1a was loaded with Cholesterol/CMM overnight, then assembled into dextramers using Streptavidin PE. Frozen PBMC were stained with dextramers and analysed by flow cytometry. (a) Healthy Control C2933 (b) Psoriasis PS2650. CMMM; Chloroform/Methanol/Milli-Q water (vehicle control), Neg ctrl; negative (dextran only) control, Endo; endogenous lipid within cleft of biotinylated in-house CD1a. Representative examples from 3 psoriatic and 3 healthy control donors.

6.4.6 The effect of cholesterol and cholesteryl esters on CD1a expression on K562 cells

CD1a expression on K562 cells was also assessed as part of the toxicity experiment, with no consistent change in CD1a expression across a range of concentrations up to 200μM for cholesterol and its esters at 24 hours (data not shown).

6.4.7 Assessment of cytokine production by CD1a-reactive T cells

Polyclonal experiments

The interpretation of IFN-γ production by healthy control peripheral blood-derived T cells by ELISpot was limited by donor number (1) and precipitation of lipids at the K562 pulsing stage.

Clonal experiments

IFN-γ ELISA using CD1a-reactive T cell clones, sorted and cultured from healthy donors by Dr Yi-Ling Chen was performed. In some cases the same clone was used in different experiments weeks apart (marked as replicates in **Figure 6.8**) and did not always demonstrate a reproducible response, which may reflect differences in activation state.

Although a significant autoreactive IFN-γ response was seen when comparing T cell clones co-cultured with K562-CD1a vs K562-EV cells for all conditions, there was no significant difference in cytokine secretion for T cell clones co-cultured with lipid-pulsed vs vehicle control-pulsed K562-CD1a (data not shown).

ELISA using GM-CSF (for IL-17A and TNF-α) and IL-22 clones were inconclusive, mainly because most of these clones did not reach the respective assays' threshold for detection (data not shown).

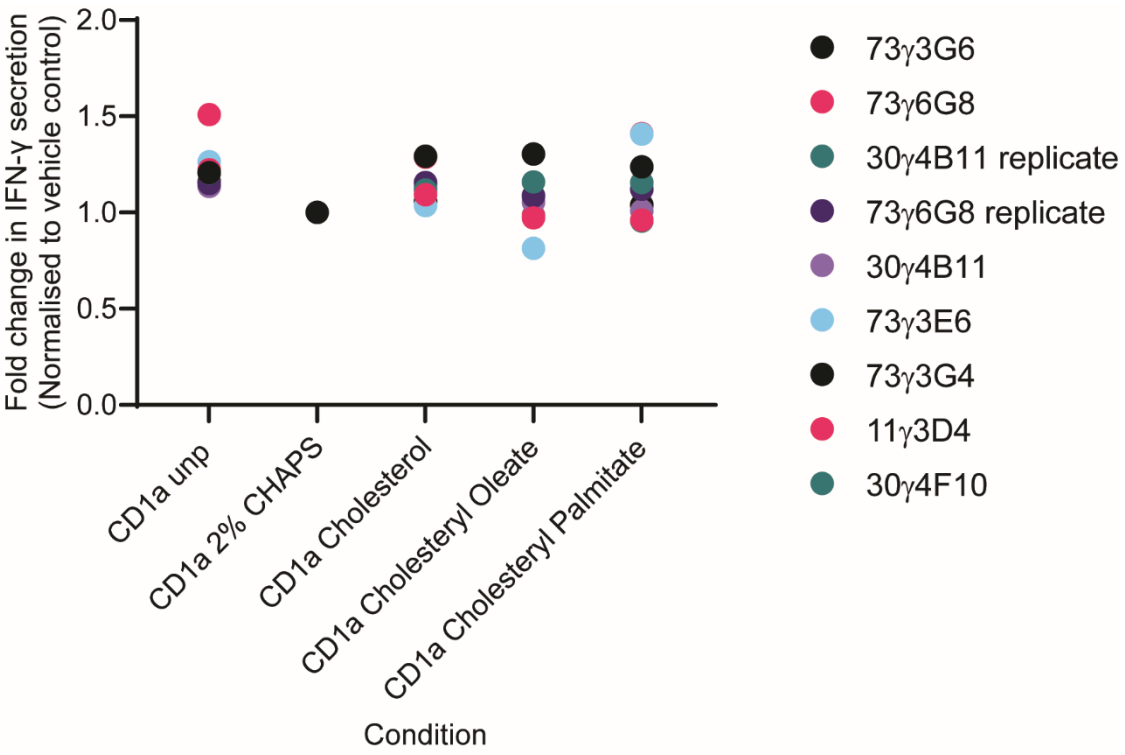


Figure 6.8 IFN-γ ELISA: Cholesterol and Esters. K562 cells were pulsed with lipid/vehicle for 21-22 hours then co-cultured with CD1a-reactive T cell clones in a ratio of 150,000:100,000 cells for 24 hours. Co-culture supernatants processed using IFN-γ ELISA Max™ Deluxe set. Clone

cytokine secretion normalised to vehicle control (2% CHAPS) by Friedman non-parametric one-way ANOVA with Dunn test. CD1a; CD1a-transduced K562 cells, unp; unpulsed.

6.4.8 Cholesterol and cholesteryl esters: Results Summary

Overall, although the literature and data from RNA-Seq promoted a potential role for cholesterol and its esters in psoriasis, investigation of these molecules as CD1a ligands in the context of this thesis was limited by issues with solubility.

6.5 Results II: Coal Tar Derivatives and Acitretin

6.5.1 Optimisation of solubility for coal tar derivatives and acitretin

The results that follow should be interpreted in the context of the chemical composition of the lipids assessed. Distilled coal tar (DCT) was purchased as a solution in 81-86% ethanol. Given that coal tar contains over 10,000 excipients, it was not possible to calculate a molar concentration. However, it was calculated that there were 14g of coal tar per 100mL of solution assuming an ethanol content of 86%, with 7.14mL equivalent to 1g. Psoriderm™ is a 40% w/v solution in ethanol with polysorbate 20, trolamine, phenoxyethanol and purified water (Summary of Product Characteristics on medicines.ie, https://www.medicines.ie/medicines/psoriderm-emulsion-40-w-v-bath-additive-33485/spc) and it was calculated that 2.5mL should equate to approximately 1g. Coal tar derivatives were added to brown glass vials, dried with a nitrogen stream and dissolved. DCT dried down to a smaller volume compared to Psoriderm™, likely due to the latter's excipients. Given the known solubility of these chemicals based on their formulations, ethanol was initially favoured as a solvent, but DMSO gave clearer results on IEF gels. For IEF gels, stocks of 25mg/mL were used so that 1µL loaded to CD1a was equivalent to the final amount of coal tar derivative during pulsing for ELISpot (250µL

of 100µg/mL antigen solution plus 250µL K562 cells), 50µg/mL (final concentration), 25µg (final amount).

Acitretin is a yellow powder with an inherent risk of teratogenicity and was handled in a fume cupboard or hood. Ethanol was not used as a solvent as physiologically it can increase the toxicity of acitretin. Acitretin dissolved in DMSO but residue was frequently apparent at the neck of the vial following sonication, suggesting ready precipitation, and its distinctive colour was sometimes persistently visible on addition to media.

6.5.2 Investigation of coal tar derivatives and acitretin binding to CD1a

2-day IEF gels showed a thickened 6th band for DCT and Psoriderm™ with thinning and loss of the lower band for Psoriderm™ (**Figure 6.9(a)**). Pre-loading with GD3 resulted in a different band pattern for DCT compared to GD3 or DCT in DMSO alone (**Figure 6.9 (b)**) and no change with Psoriderm™ (data not shown). 3-day gels with pre-loaded LPC and Psoriderm™ showed additional lower bands that were seen with Psoriderm™ plus 0.5% CHAPS (LPC mock) suggesting potential partial displacement (**Figure 6.9 (c)**), but this was not the case with DCT (data not shown), implying one of the excipients in the Psoriderm™ formulation may have been responsible.

Acitretin did not demonstrate any clear shift on 2-day gels using in-house CD1a, although IEF gels using NIH CD1a had previously suggested a very subtle shift (data not shown). Some precipitation was evident using 40mM concentration (**Figure 6.9 (d)**) so serial dilutions with lower molar excesses were tried (**Figure 6.9 (e)**). There was no apparent displacement of GD3 by acitretin (data not shown). Pre-loading with LPC resulted in thickening of some of the lower bands with acitretin (**Figure 6.9 (f)**) suggesting a possible partial displacement of LPC from the CD1a binding cleft.

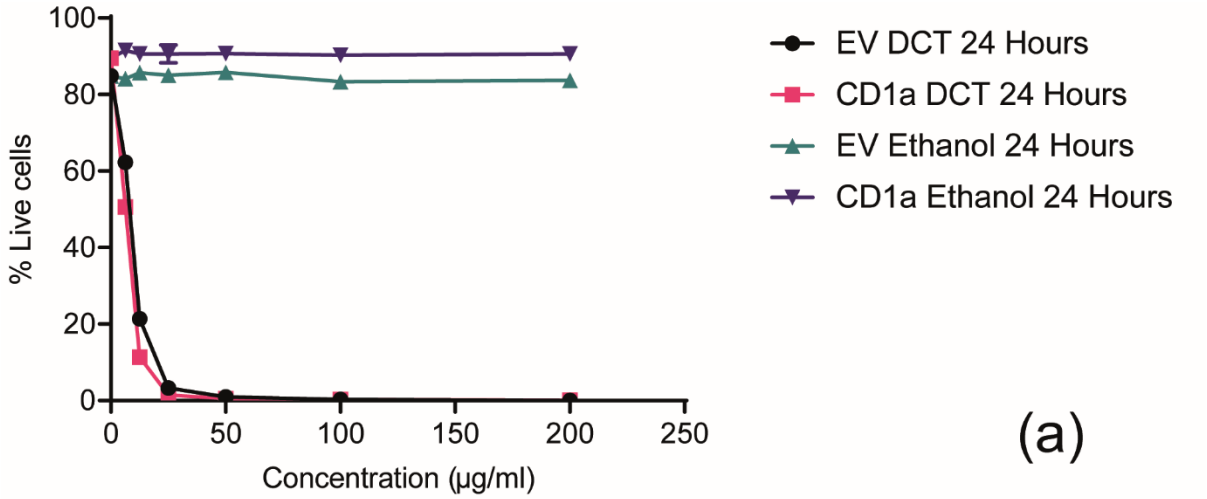
Overall, changes were generally subtle and complicated to a degree by issues with precipitation, making definitive conclusions regarding CD1a binding of these chemicals elusive.

Marker
Endo
DMSO 100x
DCT in DMSO 100x
Psoriderm™ in DMSO 100x
DMSO 200x
DCT in DMSO 200x
Psoriderm™ in DMSO 200x
R Oleate 200x
(a)
Marker
Endo
DMSO with GD3
DCT in DMSO with GD3
DMSO no GD3
DCT in DMSO no GD3
T/D
GD3 in T/D
DCT in DMSO
R Oleate in DMSO
(b)
Marker
Endo
DMSO with LPC
Psoriderm™ in DMSO with LPC
DMSO no LPC
Psoriderm™ in DMSO no LPC
0.5% CHAPS
LPC in 0.5% CHAPS
Psoriderm™ in DMSO
R Oleate in DMSO
(c)
Marker
Endo
DMSO 100x
Acitretin in DMSO 100x
DMSO 200x
Acitretin in DMSO 200x
R Oleate 200x
R Stearate 200x
R Palmitate 200x
(d)
Marker
Endo
DMSO 100x
Acitretin in DMSO 0.0625x
Acitretin in DMSO 0.125x
Acitretin in DMSO 0.25x
Acitretin in DMSO 2.5x
Acitretin in DMSO 25x
Acitretin in DMSO 50x
R Stearate in DMSO 100x
(e)
Marker
Endo
DMSO with LPC
Acitretin in DMSO with LPC
DMSO no LPC
Acitretin in DMSO no LPC
0.5% CHAPS
LPC in 0.5% CHAPS
Acitretin in DMSO
R Oleate in DMSO
(f)

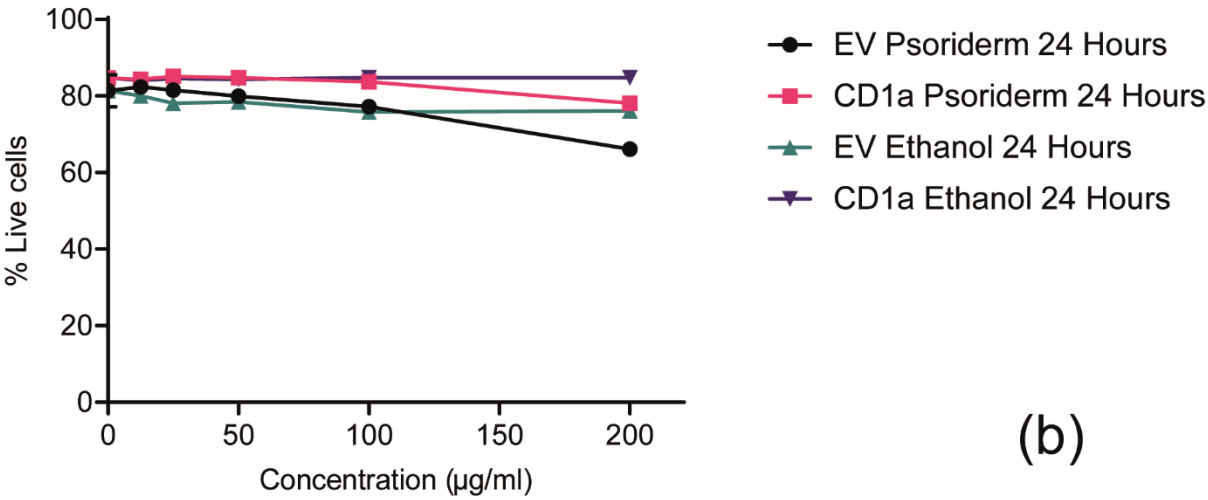
Figure 6.9 IEF (a) DCT and Psoriderm™ (b) DCT and GD3 (c) Psoriderm™ and LPC (d) Acitretin (e) Acitretin serial dilutions (f) Acitretin and LPC. DCT; Distilled Coal Tar, DMSO; dimethyl sulfoxide, GD3; GD3 Ganglioside ammonium salt from bovine milk, LPC; lysophosphatidylcholine, R Oleate; retinyl oleate, R stearate; retinyl stearate, R palmitate; retinyl palmitate.

6.5.3 Assessment of toxicity on K562 cells by coal tar derivatives and acitretin

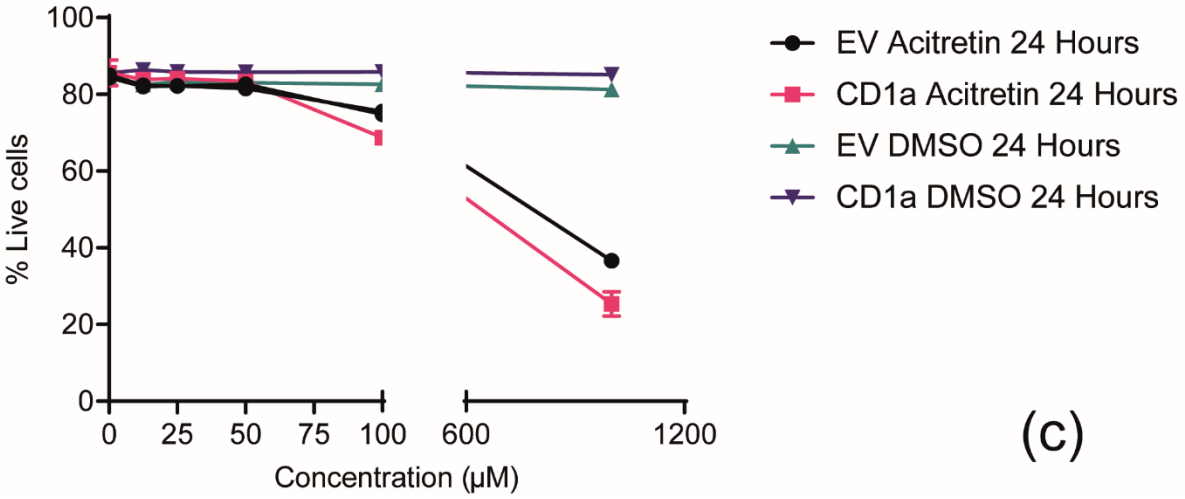
Autofluorescence of DCT in the violet channel was an issue for flow cytometry experiments which meant DCT-containing conditions demonstrated extremely low viability when assessed by this method (**Figure 6.10 (a)**). Therefore, toxicity testing was repeated manually using trypan blue (data not shown). Suitable final concentration was determined to be 50µg/mL for cellular experiments. For Psoriderm™ (**Figure 6.10 (b)**) and Acitretin (**Figure 6.10 (c)**), 50µg/mL and 50µM respectively were used based on toxicity testing results.


100
80
60
40
20
0
% Live cells
0
50
100
150
200
250
Concentration (µg/ml)
EV DCT 24 Hours
CD1a DCT 24 Hours
EV Ethanol 24 Hours
CD1a Ethanol 24 Hours

(a)


100
80
60
40
20
0
% Live cells
0
50
100
150
200
Concentration (µg/ml)
EV Psoriderm 24 Hours
CD1a Psoriderm 24 Hours
EV Ethanol 24 Hours
CD1a Ethanol 24 Hours

(b)


100
80
60
40
20
0
% Live cells
0
25
50
75
100
600
1200
Concentration (µM)
EV Acitretin 24 Hours
CD1a Acitretin 24 Hours
EV DMSO 24 Hours
CD1a DMSO 24 Hours

(c)

Figure 6.10 K562 Toxicity Testing: K562 cells were pulsed for 24 hours with serial dilutions of lipid/vehicle and media only and cell viability measured using Live-Dead Aqua by flow cytometry (a) Distilled Coal Tar (b) Psoriderm™ (c) Acitretin. EV; Empty vector-transduced K562 cells, CD1a; CD1a-transduced K562 cells.

6.5.4 The effect of coal tar derivatives and acitretin on CD1a expression by moDC

To assess whether these treatments may modulate antigen presentation, moDC were cultured and pulsed with DCT, Psoriderm™ and Acitretin on Day 3 to assess how differentiation was affected, with particular reference to surface CD1a expression. Final concentrations of 50µg/mL and 25µg/mL were assessed for DCT and Psoriderm™ and 50µM and 25µM for acitretin.

There was no significant effect on the expression of CD1a with any of the lipids tested (**Figure 6.11**). Acitretin-pulsed conditions for several donors showed debris separate from the main cell population characterised by very low FSC and high SSC on flow cytometry, suggesting possible chemical precipitation/cell death; Annexin V staining suggested these were apoptotic cells. This mainly affected donors where differentiation was poor in the unpulsed condition and these were therefore not included for analysis.

The effect of coal tar derivatives and acitretin on CD1a expression on K562 cells was not assessed.

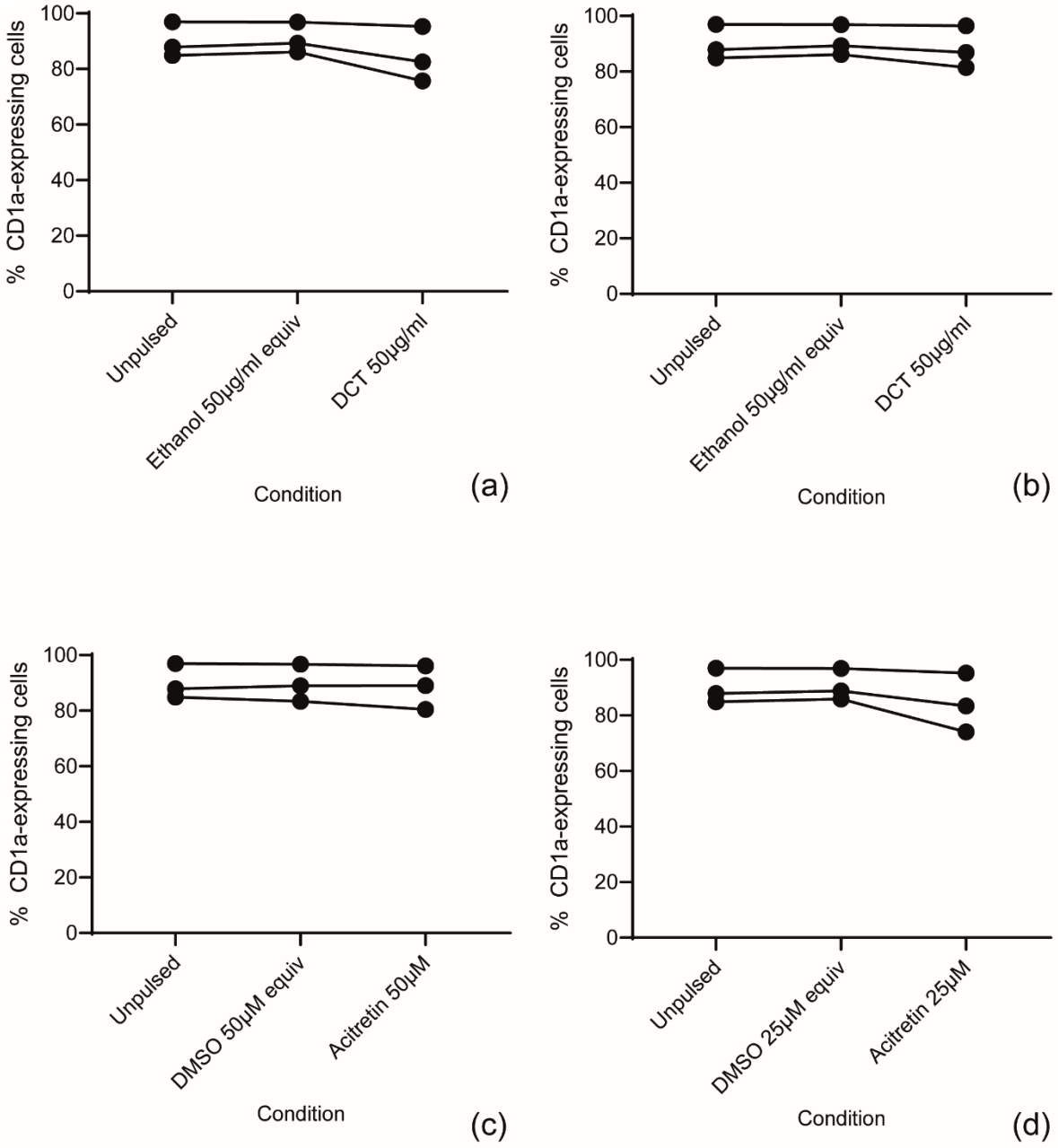


Figure 6.11 CD1a expression on moDC following Day 3 pulsing with lipid/vehicle (a) DCT 50µg/mL (b) Psoriderm 50µg/mL (c) Acitretin 50µM (d) Acitretin 25µM. Equiv; equivalent. Only cells that showed good differentiation (>80% CD1a expression in unpulsed condition) were included in the analysis. Friedman non-parametric one-way ANOVA with post-hoc Dunn test.

6.5.5 Investigation of effect of coal tar derivatives and acitretin on CD1a-reactive T cell responses

To investigate whether K562 cells pulsed with coal tar derivatives or acitretin were recognised by polyclonal CD1a-reactive T cells, IFN-γ ELISpot experiments were performed. Healthy control and psoriasis peripheral blood samples were used but are not directly comparable as T cells extracted from the former were from fresh blood and the latter from frozen samples.

For healthy control samples, there was no statistically significant difference in IFN-γ secretion from polyclonal T cells with coal tar derivatives or acitretin despite a notable CD1a-reactive response (**Figure 6.12**).

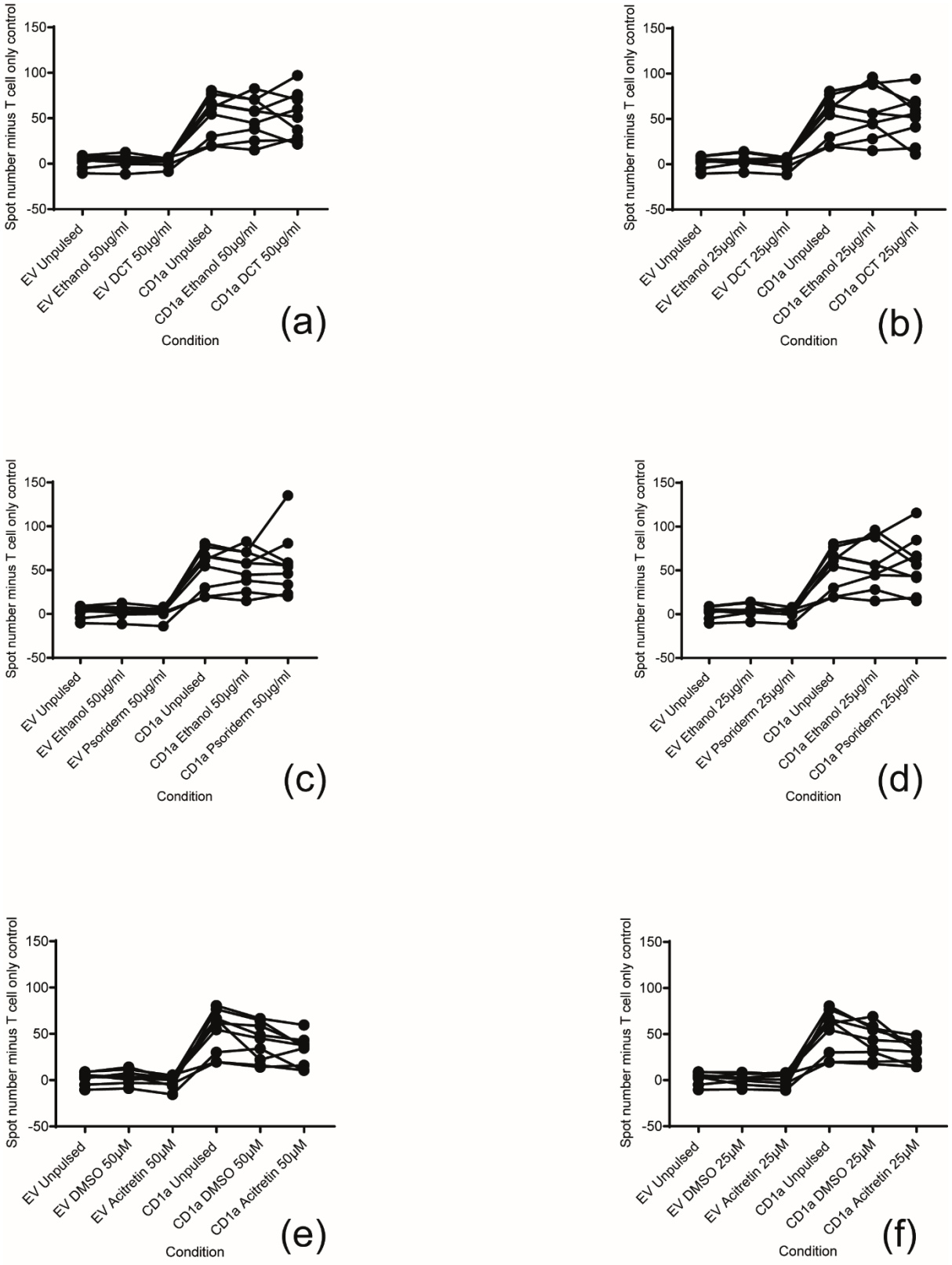
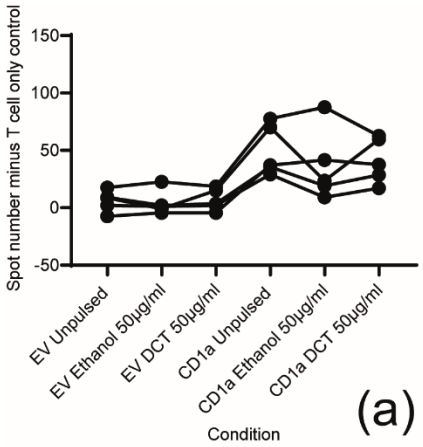
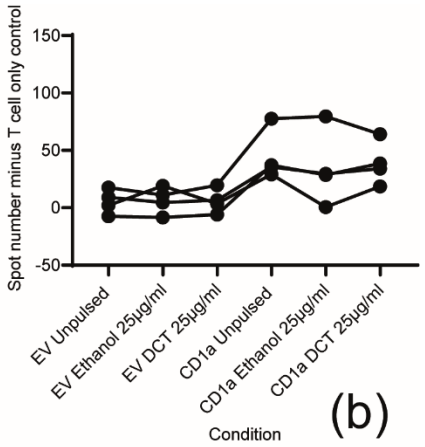


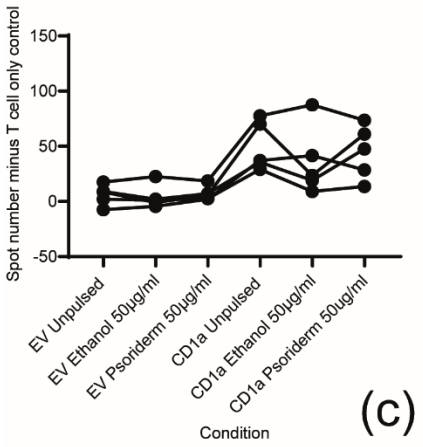
Figure 6.12 IFN-γ ELISpot: K562 cells were pulsed with lipid/vehicle overnight then co-cultured with polyclonal T cells extracted from the fresh blood of nine healthy donors in the ratio

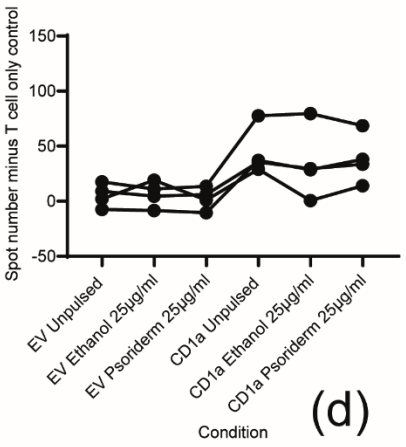
25,000:75,000 cells. ELISpot readout: Each spot represents a cell secreting IFN-γ (a) DCT 50µg/mL (b) DCT 25µg/mL (c) Psoriderm™ 50µg/mL (d) Psoriderm™ 25µg/mL (e) Acitretin 50µM (f) Acitretin 25µM. EV; Empty vector-transduced K562 cells, CD1a; CD1a-transduced K562 cells. Friedman non-parametric one-way ANOVA with post-hoc Dunn test.

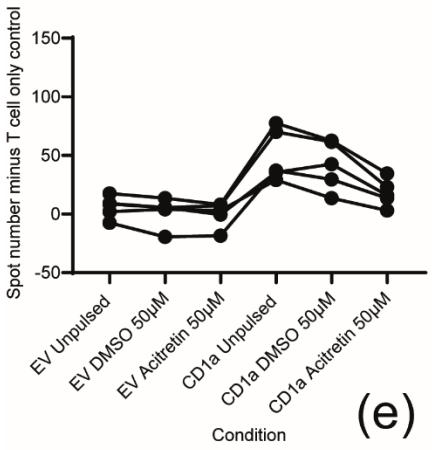
There was no significant difference in IFN-γ response for pulsed vs unpulsed conditions in psoriasis samples (**Figure 6.13**). Spot number was also generally much lower for this cohort, possibly due to the use of frozen samples.


Spot number minus T cell only control
150
100
50
0
-50
EV Unpulsed
EV Ethanol 50µg/ml
EV DCT 50µg/ml
CD1a Unpulsed
CD1a Ethanol 50µg/ml
CD1a DCT 50µg/ml
Condition
(a)


Spot number minus T cell only control
150
100
50
0
-50
EV Unpulsed
EV Ethanol 25µg/ml
EV DCT 25µg/ml
CD1a Unpulsed
CD1a Ethanol 25µg/ml
CD1a DCT 25µg/ml
Condition
(b)


Spot number minus T cell only control
150
100
50
0
-50
EV Unpulsed
EV Ethanol 50µg/ml
EV Psoriderm 50µg/ml
CD1a Unpulsed
CD1a Ethanol 50µg/ml
CD1a Psoriderm 50µg/ml
Condition
(c)


Spot number minus T cell only control
150
100
50
0
-50
EV Unpulsed
EV Ethanol 25µg/ml
EV Psoriderm 25µg/ml
CD1a Unpulsed
CD1a Ethanol 25µg/ml
CD1a Psoriderm 25µg/ml
Condition
(d)


Spot number minus T cell only control
150
100
50
0
-50
EV Unpulsed
EV DMSO 50µM
EV Acitretin 50µM
CD1a Unpulsed
CD1a DMSO 50µM
CD1a Acitretin 50µM
Condition
(e)

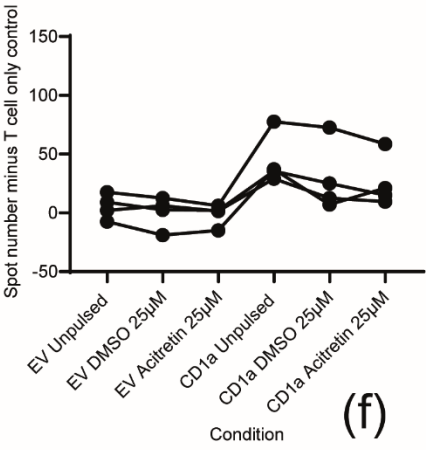

Spot number minus T cell only control
150
100
50
0
-50
EV Unpulsed
EV DMSO 25µM
EV Acitretin 25µM
CD1a Unpulsed
CD1a DMSO 25µM
CD1a Acitretin 25µM
Condition
(f)

Figure 6.13 IFN-γ ELISpot: K562 cells were pulsed with lipid/vehicle overnight then co-cultured with polyclonal T cells extracted from frozen PBMC/T cells of up to five psoriasis patients in the ratio 25,000:75,000 cells. ELISpot readout: Each spot represents a cell secreting IFN-γ (a) DCT 50µg/mL (b) DCT 25µg/mL (c) Psoriderm™ 50µg/mL (d) Psoriderm™ 25µg/mL (e) Acitretin 50µM (f) Acitretin 25µM. EV; Empty vector-transduced K562 cells, CD1a; CD1a-transduced K562 cells. Friedman non-parametric one-way ANOVA with post-hoc Dunn test.

6.5.6 Coal tar derivatives and acitretin: Results summary

Although there was some suggestion that coal tar derivatives and acitretin may bind CD1a based on IEF results, this was not borne out by a limited number of functional experiments. The use of these chemicals was impeded by difficulties with handling and analysis due to the nature of their composition and toxicity and in the end further experiments were abandoned due to the challenges posed.

6.6 Other lipids

Several other lipids were screened for CD1a binding using IEF gels. These were components of traditional remedies for psoriasis such as curcumin (found in turmeric) and thymoquinone (from blackseed oil) and bakuchiol, a plant-derived terpenoid with functional similarity to retinol.

IEF assays showed subtle changes for bakuchiol, with shift and partial loss of the upper band and increased prominence of the lowest band (**Figure 6.14**). No such changes were seen for thymoquinone or curcumin. The latter had to be loaded at reduced molarity due to precipitation in 40mM solution.

This gel was also loaded with cholesterol dissolved using the new solvent mixture suggested by Prof Besra, which resulted in some blurring of bands but no clear shift to suggest binding to the CD1a cleft. 10-NO was used as a positive control.

Due to time limitations, no further experiments were performed to explore the effects of bakuchiol but this molecule remains a candidate of interest as a CD1a ligand.

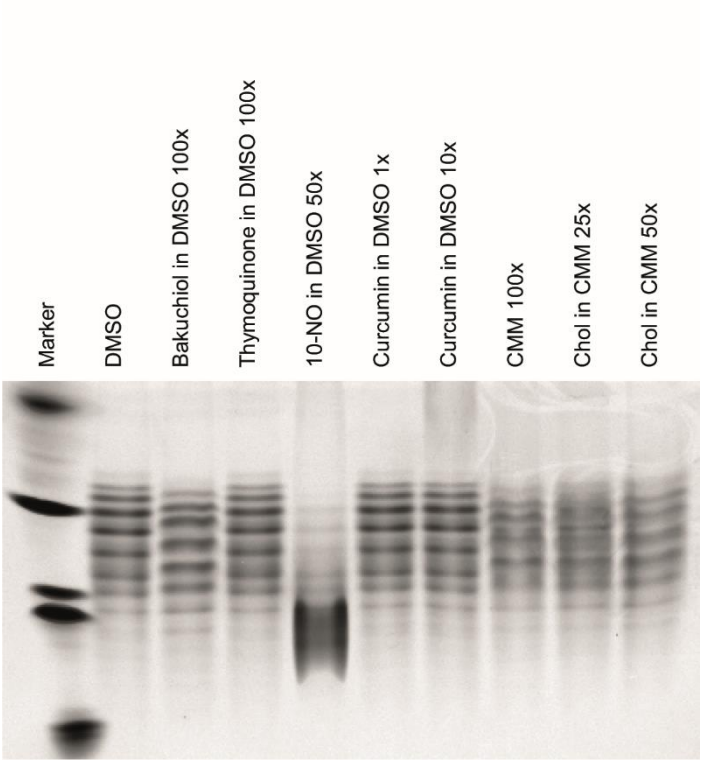


Figure 6.14 IEF gels: CD1a loaded overnight with lipid/vehicle then diluted 1:1 with IEF sample buffer and loaded to IEF gel. 200x 8μL CD1a:2μL lipid/vehicle, 100x 9μL CD1a: 1μL lipid/vehicle, 50x 9μL CD1a:1μL lipid/vehicle. Lipid stocks 40mM, lower molar excess based on further dilutions of stock before loading to CD1a. DMSO; dimethyl sulfoxide, CMM; chloroform:methanol:MilliQ water.

6.7 Discussion

6.7.1 Sterols

Considering the hypothesis put forth in **Chapter 4**, if the retinyl esters are depleted in PS L skin and the enzyme responsible for their breakdown (LAL) is also involved in the breakdown of CE, it would be assumed that cutaneous cholesterol would be increased. This corresponds with Schmidt's findings of increased cholesterol in psoriasis from the legs and back (Schmidt et al., 1977). Viewed in isolation, the mild upregulation of *LIPA* (encoding LAL/CEH), in PS L skin observed in our data would support this. However, our RNA-Seq data showed that genes for GO terms for sterol and cholesterol biosynthetic and metabolic processes were downregulated in untreated PS L vs HC skin and examination of individual genes showed overall downregulation of cholesterol and CE synthesis and upregulation of cholesterol conversion to bile acids. PS L skin is structurally different from healthy skin, not just due to effects of inflammation but also fewer, smaller sebaceous glands (Headington et al., 1989; Rittié et al., 2016; Werner et al., 2008). This may influence differences in gene expression in sterol pathways. Treatments may also affect the quantity of cholesterol in the skin. A single UVB exposure in mice increased synthesis of cholesterol, FA and ceramides at 72 hours (Holleran et al., 1997) and in humans UVB significantly increased squalene, triglycerides and free FA in the stratum corneum (Wefers et al., 1991). Skin biopsy depth may influence how much fat is included; a thicker epidermis in lesional psoriasis may result in a thinner layer of adipose tissue with a punch biopsy compared to healthy or AD skin. Sebaceous gland size and subcutaneous adiposity may also be influenced by age, sex and body site, although the use of paired L and NL/R samples in our study, is of some help in limiting this confounding factor.

Based on these findings and existing CD1a literature, a number of candidate lipid antigens from the sterol pathway were investigated as CD1a lipid antigens. The results of experiments were unable to further clarify this role, although it is important to consider potential technical limitations prior to discarding them as candidate lipid ligands for CD1a.

Solubility was the most pertinent issue encountered when working with these molecules. Despite the use of a range of solvents, precipitation was a prominent feature and readily visible, particularly for cholesterol and cholesteryl palmitate, following lipid pulsing of K562 cells. Solvents in which some or all of these molecules dissolved, such as the chloroform:methanol:MilliQ water 10:10:3 solution suggested by Prof Besra or dichloromethane, entailed their own difficulties due to toxicity and their volatile nature, which was exacerbated by the requirement for fume cupboard and hood usage.

The only changes seen on IEF assays were subtle and aside from cholesterol, which initially appeared reproducible, were not consistent. This may have been due to variation from batch to batch, storage, solubility or contaminants. Even using a new batch of cholesterol each time did not overcome this. It is also important to consider that even if these molecules were CD1a ligands, a change in pI may not be detectable if cholesterol and/or its esters already form part of the endogenous lipids present in the CD1a cleft. However, given the lack of evidence for cholesterol's displacement of the known ligands GD3 and LPC, it is likely that inadequate loading explains the lack of shift on IEF.

The cholesterol and esters were found to be non-toxic to K562 cells based on the concentrations used for toxicity testing. Although this would be expected given their ubiquity in cells, solubility issues may also have affected these results. There was no detectable effect on K562 CD1a expression, interpretation of dextramer binding was

limited and definitive conclusions could not be made regarding effects on T cell IFN-γ secretion by these lipids.

In conclusion, experimental data suggested that cholesterol and its esters were unlikely to be CD1a ligands. However, absolute exclusion of this possibility is difficult due to technical challenges related to solubility, precipitation and loading.

6.7.2 Coal Tar Derivatives and Acitretin

The above results should be interpreted in the context of the challenges posed due to the composition of the lipids assessed; their toxicity, solubility and characteristics such as autofluorescence on flow cytometry (for DCT).

Although there was some suggestion of a shift on IEF assays with the coal tar derivatives, this effect was complicated by the fact that distilled coal tar contains up to 10,000 chemicals. Psoriderm™, in addition to 40% w/v distilled coal tar, also contains excipients. This makes it difficult to assess which component is responsible for changes in experimental assays and separation of reactive fractions would be necessary for identification.

IEF data suggested that acitretin does not load to CD1a, although solubility issues may be a confounding factor. Retinoids act through a broad range of physiological processes and this screening method may be too crude to detect what may be a minor mode of action. Acitretin, at concentrations determined as non-toxic to K562 cells, was toxic to moDC. In general, there were many issues with acitretin due to safety, toxicity and its poor solubility in media.

For the psoriasis treatments examined, ELISpot with polyclonal T cells did not show any changes in IFN-γ secretion from healthy donors or psoriasis patients. However, donor numbers were limited and more robustly powered experiments are required to definitively determine whether there is any effect, particularly from acitretin.

Although the above investigations failed to determine that coal tar derivatives and acitretin are ligands for CD1a, due to the technical challenges posed by these chemicals, this possibility should still be considered.

6.8 Chapter summary

RNA-Seq data suggested that sterol biosynthetic and metabolic pathways were altered in lesional psoriasis and that the differential expression of certain key genes of these pathways such as *CYP27A1* was affected by treatment with NB-UVB. Unfortunately, the exploration of sterols as potential CD1a ligands and experiments to identify their effects on T cells were hampered by practical difficulties such as solubility. There were similar issues attempting to define possible CD1a-related mechanisms for long-established treatments such as the coal tar derivatives and acitretin. However, these challenges do not exclude these substances as potentially relevant to CD1a-pathways in psoriasis, rather indicate a need for the development of new methods for further investigation.

7 Chapter 7 Confirmatory analysis of expression of relevant lipid pathway genes and proteins in inflammatory skin disease

7.1 Background

Analysis of RNA-Seq data from our biopsy cohort revealed trends in DEG in lipid and retinoid pathways. The next step was to confirm our findings and identify genes encoding key proteins of these pathways relevant to our potential CD1a candidate ligands and validate expression of their protein products in diseased and healthy human skin.

Firstly, DEG in diseased versus healthy skin in humans and murine models reported in the literature were identified and compared with our RNA-Seq data, then subsequently corroborated using publicly available genomics data from the Gene Expression Omnibus. Finally, the cutaneous cell type expressing the relevant mRNA was identified using the Human Cell Atlas (Reynolds et al., 2021). Assessment of protein expression using immunofluorescence immunohistochemistry (IF IHC) and imaging mass cytometry with Hyperion™ were then performed.

7.2 Specific materials and methods

7.2.1 GEO Profiles

GEO (Gene Expression Omnibus) Profiles is a publicly available archive of individual gene expression datasets that have been submitted by international researchers (Edgar et al., 2002). Analysis of genomic data using GEO2R (Barrett et al., 2013) was performed for five human GEO DataSets comparing human PS L skin to PS NL skin and HC skin

(**Table 7.1**) and used to assess the robustness of our RNA-Seq data while clarifying the consistency of expression of key genes of the pathways of interest.

Table 7.1 GEO Profiles: GEO DataSet data for psoriatic and healthy human skin. Plaque psoriasis unless otherwise specified. Some GEO Profiles and GEO DataSet data did not correlate with published analyses and information; where this was the case, the GEO Profiles/GEO DataSet information was favoured for inclusion in this table.

GDS/GSE	Type of study	PS	HC	Main associated primary paper
2518/6710	[HG-U133A] Affymetrix Human Genome U133A Array	13 PS L and NL (paired)	None	Rieschl et al(Reischl et al., 2007)
3539/14905	[HG-U133_Plus_2] Affymetrix Human Genome U133 Plus 2.0 Array	26 PS L and NL (paired) plus additional 5 PS L (3 NL excluded from data analysis)	21	Yao et al(Yao et al., 2008)
4602/13355	[HG-U133_Plus_2] Affymetrix Human Genome U133 Plus 2.0 Array	58 PS L and NL (paired)	64	Nair et al(Nair et al., 2009)
4600/30999	[HG-U133_Plus_2] Affymetrix Human	85 PS L and NL (81 paired L/NL,	None	Suárez-Fariñas(Suárez-

	Genome U133 Plus 2.0 Array	4 x L only, 4 x NL only)		Fariñas et al., 2012)
5392/50790	[HG-U133_Plus_2] Affymetrix Human Genome U133 Plus 2.0 Array	4 PS L and NL (paired)	None	Swindell et al(Swindell et al., 2012)

7.2.2 Single Cell Database

The Human Cell Atlas established by Haniffa and colleagues(Reynolds et al., 2021) permits assessment of the expression of particular genes in the skin of healthy adults, psoriasis and atopic dermatitis. Using this resource, the expression of genes of interest in healthy and diseased skin were compared with regards to strength of expression and cellular location. Unsupervised Uniform Manifold Approximation and Projection (UMAP) plots demonstrate the different cell types for PS L and healthy skin (**Figure 7.1**).

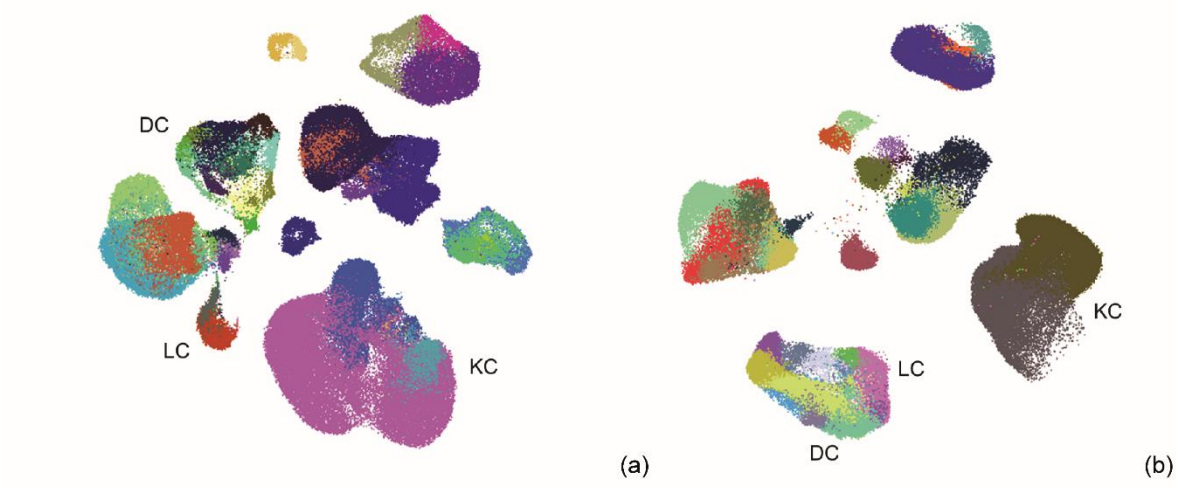


Figure 7.1 Unsupervised Uniform Manifold Approximation and Projection (UMAP) plot of single cell mRNA expression clustered by cell type(Reynolds et al., 2021) *(each cell subtype represented by a different colour) with a focus on cell types with candidate roles in processing*

and/or presentation of lipid antigens to T cells. (a) Psoriasis (b) Healthy skin. LC; Langerhans cells, DC; dendritic cells, KC; keratinocytes.

7.2.3 Immunofluorescence Immunohistochemistry

Adjacent sections from the same block used for RNA-Seq analyses were stained for analysis by IF IHC and Hyperion™ imaging mass cytometry. The same antibodies were used for IF IHC and Hyperion™ staining (**Table 7.2**). Antibodies were diluted in Tris Buffered Saline (TBS; GTX, 48886) and staining was first optimised using a titration of dilutions. Slides were incubated in a humidified slide chamber.

Table 7.2 Antibodies for RNA-Seq validation.

Primary Antibody	Type	Company/ Cat #	Optimised dilution for IF IHC	Secondary Antibody kit
Anti-CRABP2	Anti-rabbit	Abcam ab181255 [EPR14256(B)]	1 in 250	VectaFluor Excel Amplified Kit (Vector, DK-1594)
Anti-FABP5	Anti-rabbit	Abcam ab255276 [EPR22552-64]	1 in 400	VectaFluor Excel Amplified Kit (Vector, DK-1594)
Anti-Apolipoprotein E	Anti-rabbit	Abcam ab52607	1 in 100	VectaFluor Excel

		[EP1374Y]		Amplified Kit (Vector, DK-1594)
Anti-Lipocalin-2/ NGAL	Anti-mouse	Abcam ab23477 [5G5]	1 in 200	VectaFluor Excel Amplified Kit (Vector, DK-1594)

Frozen sections were individually delineated using a hydrophobic barrier pen and rinsed with TBS, then blocked with 2.5% horse serum at RT for 10 minutes. They were then tapped dry and primary antibody in the appropriate dilution (100µL/section) applied and incubated at 4°C overnight. Slides were rinsed twice in TBS with shaking for 5 minutes each time, tapped dry, secondary amplifier antibody (one drop/section) applied and incubated at RT for 15 minutes. Slides were rinsed in TBS, tapped dry and secondary antibody-fluorophore conjugate (one drop/section) applied and incubated at RT for 30 minutes, protected from light for this and all future steps. Slides were rinsed twice in TBS with shaking for 5 minutes each time, then tapped dry and Antifade Mounting Medium with DAPI (Vectashield®, H-1200) applied (10µL/section). A cover slip was placed carefully over the sections, bubbles removed and edges sealed with nail varnish. Following curing at RT for 20 minutes, slides were read on the ECHO Revolve microscope. Slides were stored at 4°C.

IF IHC was performed on one patient from each group of the biopsy cohort, matched for gender (male) and site (lower back) with an attempt to match age and co-morbidities as

closely as possible. There were no available HC samples remaining following RNA-Seq, so lower back biopsies of healthy intact skin from a wound healing study were used.

7.2.4 Hyperion™

Mass cytometry (CyTOF®) with Helios™ permits separation of molecules by mass rather than by wavelength as is the case for staining with fluorophore-conjugated antibodies. This permits the use of more than 50 metal tags and their isotopes in 135 channels. It also circumvents the issue of autofluorescence (which is particularly relevant in cutaneous tissue), variable staining, background signal and fluorescent spillover inherent to fluorophore-conjugated antibodies. Imaging mass cytometry using the Hyperion™ module on fresh frozen sections allows 200Hz UV laser ablation of 1μm^2 of tissue at a time. This aerosolised pixel (plume) is lifted by helium gas then transferred by argon gas to Helios™, where it is ionised, filtered and all particles with a single positive charge and an isotopic mass above 75kDa then pass through the time-of-flight chamber. Ions of lower weight are detected first, followed by those of higher isotopic mass. A final histological image is generated based on the number of ions detected. An antibody panel with preferred metal conjugates was designed by Dr Rachel Etherington (**Table 7.3**).

*Table 7.3 Hyperion™ Panel. *CD11c, FceR1a, CD123.*

Marker	Metal	Clone
CD45	89Y	HI30
aSMA	141Pr	1A4
CD56	142Nd	RNL-1
LCN2	143Nd	5G5
c-kit	144Nd	CC11/370
CCR6	145Nd	G034E3

CD16	146Nd	EPR16784
CRTH2	147Sm	Polyclonal
Keratin 10	148Nd	BC2F5
CD15	149Sm	W6D3
Keratin 14	150Nd	LL002
IL-7R (CD127)	151Eu	EPR2955(2)
IL-17A	152Sm	BL168
IL-13	153Eu	JES10-5a2
CD11b	154Sm	ICRF44
FOXP3	155Gd	236A/E7
CD4	156Gd	RPA-T4
IL-17F	158Gd	EPR17830-169
CRABP2	159Tb	EPR14256(B)
TCRγδ	160Gd	B1
CD20	161Dy	H1
CD8a	162Dy	RPA-T8
CD14	163Dy	SP192
CD161	164Dy	HP-3G10
ApoE	165Ho	EP1374Y
AOAH	166Er	Polyclonal
Granzyme B	167Er	EPR20129-217
CD1a	168Er	HI149
IFNγ	169Tm	IFNG/466
CD3	170Er	Polyclonal
RORγt	171Yb	R1F3
IL-22	172Yb	BL35175

Langerin	173Yb	4CF
HLA-DR	174Yb	L243
CD34	175Lu	581
Myeloid dump*	176Yb	3.9

Conjugation of antibodies for validation in this study was performed using the same antibodies as for IF IHC at dilutions outlined in **Table 7.4**, filter tips, low-bind Eppendorf tubes and the relevant Abcam Lightning-Link® metal conjugation kit. Antibodies were vortexed at 12000xg for 5 minutes to remove aggregates, then 40µL pipetted to a 50kDa filter, followed by 200µL of Maxpar® PBS. The Eppendorf tube was then centrifuged at 12000xg for ten minutes. The filter was inverted into a new Eppendorf tube and centrifuged at 1000xg for 2 minutes. 10µL of the filtered liquid was removed for storage at -20°C. 1µL of LL-Rapid Modifier was added to the residual, which was then transferred to the metal conjugate vial and mixed well. The vial was placed on a shaker at 120rpm for one hour, 1µL of LL-Quencher FD added and replaced on the shaker at 120rpm for a minimum of 20 minutes. Antibody stabiliser was added in a ratio of 1:1 and the conjugated antibody was stored at 4°C pending use.

*Table 7.4 Antibody conjugation for Hyperion™. *FABP5 did not demonstrate any detectable signal during optimisation at dilutions of 1 in 50, 1 in 100 or 1 in 200 so was replaced in the Hyperion™ panel by ApoE.*

Primary Antibody	**Optimised dilution for Hyperion™**	**Metal conjugate**
Anti-CRABP2	1 in 50	159Tb
Anti-FABP5*	N/A	165Ho
Anti-Apolipoprotein E	1 in 50	165Ho

Anti-Lipocalin-2/NGAL	1 in 50	143Nd

Of note, the remaining antibodies in this panel were either conjugated in the same way (AOAH) or using the Maxpar® X8 antibody labelling kit according to the manufacturer's instructions if not available in pre-conjugated form (Fluidigm antibodies).

Hyperion™ images were processed by Dr Rachel Etherington using a macro with FIJI software (Despeckle, Gaussian blur (sigma 1) and Sharpen tools).

7.3 Results I: Selection of candidate genes for validation

7.3.1 Candidate genes of interest

Four genes were chosen for further research and validation based on the methods described (**Figure 7.2**).

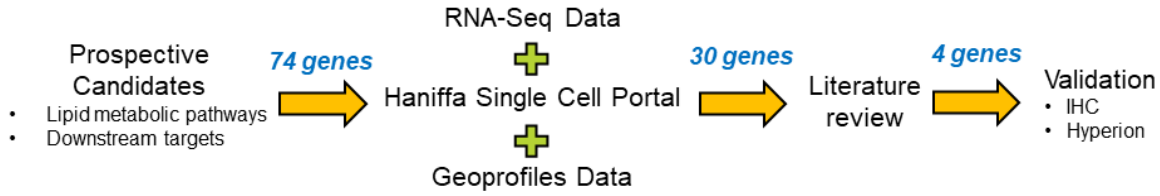


Figure 7.2 Pathway for choosing candidate genes for validation.

The chosen genes were *CRABP2*, *FABP5*, *LCN2* and *APOE*. The RNA-Seq data demonstrated differential expression of these genes in untreated psoriatic skin (**Table 7.5**), which were compared with GEO Profiles/GEO DataSets (**Table 7.6**).

Table 7.5 RNA-Seq: Differential expression of candidate genes of interest in untreated psoriasis group: PS L vs PS NL . PS L; lesional psoriasis, PS NL; non-lesional psoriasis.

Gene	Log2FC	p_{adj}
CRABP2	+1.8313	2.33×10^{-6}
FABP5	+1.9036	1.82×10^{-8}
LCN2	+2.9774	1.52×10^{-9}
APOE	-0.914	0.00805

Examination of the top 250 DEG (PS L vs PS NL skin) for the GEO DataSets of interest (**Table 7.1**) featured *CRABP2* and *LCN2* in four out of five studies, *FABP5* in three out of five and *APOE* in none (**Table 7.6**). However, all genes of interest were differentially expressed to some degree in all five studies.

Table 7.6 GEO Profiles: GEO DataSet Top 250 DEG vs candidate genes of interest: PS L vs PS NL skin. PS L; lesional psoriasis, PS NL; non-lesional psoriasis. Full list refers to the complete list of all DEG in the dataset.

GEO DataSet	***CRABP2***	***FABP5***	***LCN2***	***APOE***
GDS2518 GSE6710	Yes LogFC 1.491 p_{adj} 5.75 x 10^{-8}	No but in full list LogFC 1.082 p_{adj} 2.97 x 10^{-4}	Yes LogFC 3.809 p_{adj} 1.81 x 10^{-9}	No but in full list LogFC -0.907 p_{adj} 4.34 x 10^{-4} (212884_x_at) LogFC -0.86 p_{adj} 1.51 x 10^{-2} (203381_s_at) LogFC -1.053 p_{adj} 8.63 x 10^{-5} (203382_s_at)
GDS3539	No but in full list	Yes	Yes	No but in full list

GSE14905	LogFC 2.28 p_{adj} 7.03 x 10^{-13}	LogFC 1.803 p_{adj} 7.75 x 10^{-17}	LogFC 5.69 p_{adj} 6.28 x 10^{-19}	LogFC -7.46 x 10^{-1} p_{adj} 2.39 x 10^{-11} (212884_x_at) LogFC -1.28 p_{adj} 2.13 x 10^{-5} (203381_s_at) LogFC -1.47 p_{adj} 2.95 x 10^{-10} (203382_s_at)
GDS4602 GSE13355	Yes LogFC 1.812 p_{adj} 5.66 x 10^{-43}	Yes LogFC 1.276 p_{adj} 1.90 x 10^{-49}	Yes LogFC 4.021 p_{adj} 1.19 x 10^{-44}	No but in full list LogFC -7.29 x 10^{-1} p_{adj} 3.05 x 10^{-20} (212884_x_t)

				LogFC -1.02 p_{adj} 9.57 x 10^{-22} (203381_s_at) LogFC -1.05 p_{adj} 1.28 x 10^{-23} (203382_s_at)
GDS4600 GSE30999	Yes LogFC 1.732 p_{adj} 1.35 x 10^{-47}	Yes LogFC 1.467 p_{adj} 2.63 x 10^{-41}	No but in full list LogFC 5.52 p_{adj} 1.10 x 10^{-36}	No but in full list LogFC -6.74 x 10^{-1} p_{adj} 3.24 x 10^{-16} (212884_x_at) LogFC -9.01 x 10^{-1} p_{adj} 4.98 x 10^{-11} (203381_s_at)

				LogFC -7.75 x 10^{-1} p_{adj} 7.34 x 10^{-16} (203382_s_at)
GDS5392 GSE50790	Yes LogFC 1.047 p_{adj} 0.0007224	No but in full list LogFC 0.60685 p_{adj} 0.0048	Yes LogFC 3.811 p_{adj} 0.0008	No but in full list LogFC -0.874 p_{adj} 0.033 (212884_x_t) LogFC -0.674 p_{adj} 0.1038 (203381_s_at) LogFC -1.0104 p_{adj} 0.012 (203382_s_at)

Only two of the GEO DataSets above also had a control group (**Table 7.7**). For the top 250 DEG for these GEO DataSets (PS L vs HC skin), *FABP5* and *LCN2* featured in both and *CRABP2* and *APOE* in neither (**Table 7.7**). However, all genes were differentially expressed to some degree in both GEO DataSets.

Table 7.7 GEO Profiles: GEO DataSet Top 250 DEG vs candidate genes of interest: PS L vs HC skin. PS L; lesional psoriasis, HC; healthy control. Full list refers to the complete list of all DEG in the DataSet.

GEO DataSet	***CRABP2***	***FABP5***	***LCN2***	***APOE***
GDS4602 GSE13355	No but in full list LogFC 1.66 p_{adj} 4.29×10^{-43}	Yes LogFC 1.463 p_{adj} 1.46×10^{-57}	Yes LogFC 4.085 p_{adj} 2.30×10^{-48}	No but in full list LogFC -7.18×10^{-1} p_{adj} 1.06×10^{-20} (212884_x_at) LogFC -1.01 p_{adj} 3.57×10^{-24} (203381_s_at) LogFC -1.06 p_{adj} 9.13×10^{-26} (203382_s_at)

GDS3539 GSE14905	No but in full list LogFC 2.27 p_{adj} 9.04 x 10^{-10}	Yes LogFC 2.41 p_{adj} 7.91 x 10^{-16}	Yes LogFC 5.491 p_{adj} 1.73 x 10^{-14}	No but in full list LogFC -8.92 x 10^{-1} p_{adj} 5.62 x 10^{-13} (212884_x_at) LogFC -1.16 p_{adj} 1.58 x 10^{-3} (203381_s_at) LogFC -1.75 p_{adj} 1.72 x 10^{-11} (203382_s_at)

7.3.2 *CRABP2*: Cellular Retinoic Acid Binding Protein 2

Background: CRABP2 (RBP6) binds *all-trans* retinoic acid (atRA) with high affinity, which it delivers to the nucleus where it binds Retinoic Acid Receptors (RAR). RAR form heterodimers with RXR and bind the retinoic acid response element (RARE) to regulate target gene transcription.

Expression (mRNA): *CRABP2* mRNA is widespread but mainly found in the oesophagus, female genital tract, skin, brain and breast (proteinatlas.org). *CRABP2* mRNA is upregulated in murine skin following application of either topical atRA or a synthetic RARγ agonist (Gericke et al., 2013) and in human moDC by a synthetic PPARγ ligand (Gyöngyösi et al., 2013), while Wnt/β-catenin signalling may downregulate it (Collins & Watt, 2008). Topical retinaldehyde can also induce *CRABP2* mRNA and protein expression in human skin (Saurat et al., 1994).

Location (protein): CRABP1 (RBP5) is found mainly in embryonic tissues, whereas CRABP2 is the dominant isomer in differentiating and non-differentiating human keratinocytes *in vivo* and *in vitro* and particularly in psoriatic epithelium (CRABP2:CRABP1= 17:1) and the oral mucosa (CRABP2:CRABP1= 8.5:1), with a reduced ratio in normal skin (CRABP2: CRABP1= 1.4:1) (Siegenthaler, Tomatis, Chatellard-Gruaz, et al., 1992). CRABP2 protein is also found in the mouth and oesophagus, bladder, breast, female genital tract and prostate (proteinatlas.org).

Previous studies assessing *CRABP2* mRNA expression in psoriatic skin

CRABP2 mRNA is overexpressed in PS L compared to NL and HC skin (Siegenthaler, Tomatis, Didierjean, et al., 1992; Törmä et al., 1994). Expression of *CRABP2* mRNA is

most marked in the supra-basal layers of PS L epidermis and gene expression increases in coordination with the appearance of histological features of psoriasis at the plaque border (Algermissen et al., 1996). *CRABP2* is downregulated in skin that has clinically resolved with NB-UVB phototherapy (vs the previous PS L) (Rácz et al., 2011; Vacharanukrauh et al., 2021). Increased *CRABP2* in PS L (vs PS NL skin) reverted to levels of expression found in uninvolved skin following clinically and histopathologically successful therapy with ciclosporin A (Oestreicher et al., 2001).

Previous studies assessing CRABP2 protein expression in psoriasis

No data were found on serum CRABP2 levels in psoriasis. An increased CRABP2:CRABP1 ratio has been demonstrated in PS L (20.3:1) and PS NL (4.9:1) skin compared with HC (1.5:1) (Siegenthaler, Tomatis, Didierjean, et al., 1992). CRABP2 expression by IHC is significantly increased in PS L compared to PS NL/HC skin and was reduced by a mean of 50-54% vs baseline in clinical responders to 12 weeks of anti-TNF-α therapy (adalimumab, etanercept, infliximab) (Bianchi et al., 2018).

RNA-Seq Data

CRABP2 was upregulated in all treatment groups for PS L skin (vs HC), especially in untreated PS L, but downregulated in PS NL/R skin and AD skin (vs HC), although only PS NL and AD results were significant (**Table 7.8**).

Table 7.8 CRABP2: Differential gene expression in the skin of psoriasis and atopic dermatitis compared to healthy control. p_{adj}; adjusted p-value. PS L; lesional psoriasis, PS NL; non-lesional psoriasis, PS R; resolved psoriasis, AD L; lesional atopic dermatitis, AD NL; non-lesional atopic dermatitis.

CRABP2	**Log2FC**	**p_{adj}**

Untreated PS L	1.004	0.088
PS L (NB-UVB)	0.559	0.269
PS L (Secukinumab)	0.313	0.274
AD L	-1.502	2.27×10^{-9}
Untreated PS NL	-1.034	0.008
PS R (NB-UVB)	-0.591	0.173
PS R (Secukinumab)	-0.076	0.903
AD NL	-1.952	1.45×10^{-14}

GEO Profiles Data

CRABP2 featured in the top 250 DEG for four out of the five GEO DataSets examined and was consistently significantly upregulated in PS L vs PS NL skin (**Table 7.6**). It was significantly upregulated in both GEO DataSets examining PS L vs HC (**Table 7.7**), despite not featuring among the top 250 DEG.

Single Cell Atlas

In psoriatic skin, *CRABP2* expression was seen predominantly in keratinocytes (proliferating>differentiated) and fibroblasts, with lower expression in Schwann cells and undifferentiated keratinocytes. Very low expression was detected in pericytes, type 2 macrophages, lymphatic endothelium, melanocytes, type 2 DC, vascular endothelial cells and type 1 LC (**Figure 7.3**). In healthy skin, expression was lower than that of psoriatic skin and localised more sparsely to fibroblasts and differentiated keratinocytes, with lower amounts in many other cell types.

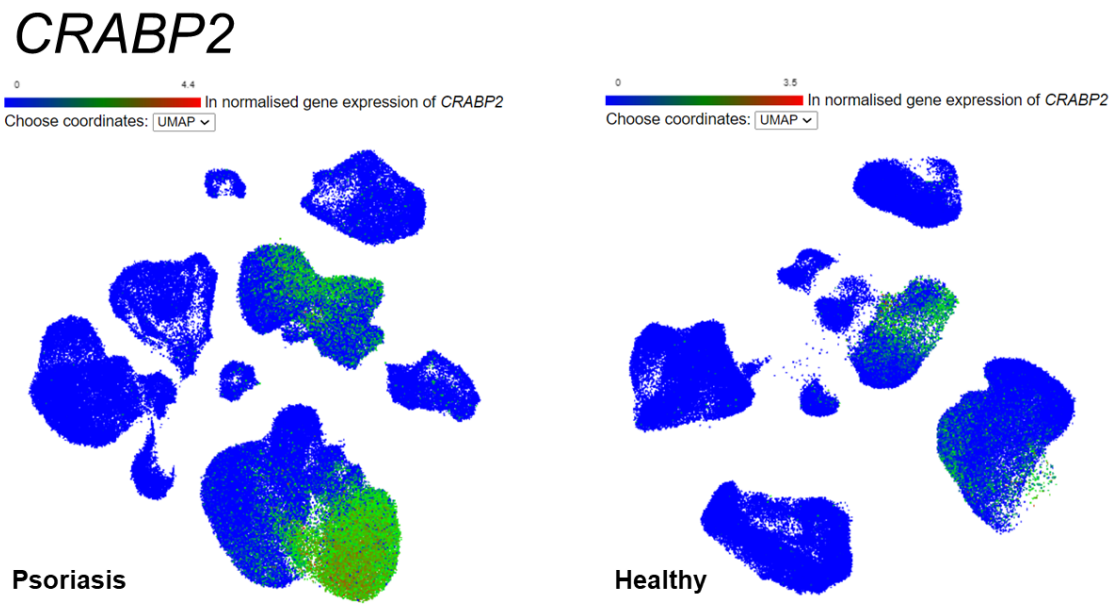


Figure 7.3 Single Cell Atlas: UMAP plots of mRNA expression of CRABP2 in psoriasis and healthy skin.

7.3.3 *FABP5*: Fatty Acid Binding Protein 5/Epidermal Fatty Acid Binding Protein

Background: FABP5 binds LCFA and RA, delivering the latter to PPARβ/δ. Fatty acids of chain length 18:0, 18:1 and 18:2 have the highest affinity for FABP5, including stearic acid and oleic acid (Siegenthaler et al., 1994). Older studies suggested that FABP5 was unable to bind retinoid acid (Siegenthaler et al., 1993, 1994), but this has since been refuted (Schug et al., 2007) and FABP5 acts as a competitor of CRABP2 for RA signalling. PPARβ/δ is a FA receptor that is ubiquitously expressed, but particularly so in keratinocytes/epidermis and although expression is not affected by differentiation, it can be increased by inflammation and trauma to the epidermis (Feingold & Jiang, 2011). FABP5 has also been postulated to have a role in neutrophil chemotaxis and TNF-α/NFκB signalling in human keratinocytes (Hao et al., 2023).

Expression (mRNA): *FABP5* mRNA expression is most prominently found in the proximal digestive tract, female genital tract and brain (proteinatlas.org). It is also found in skin and in smaller amounts in several other tissues (proteinatlas.org). Like *CRABP1* and *CRABP2*, *FABP5* is upregulated by RA or Notch signalling and possibly downregulated by Wnt/β-catenin signalling (Collins & Watt, 2008).

Location (protein): A cytosolic protein originally identified in normal and psoriatic keratinocytes (Madsen et al., 1992), FABP5 is also mostly found in the female genital tract, lung, gastrointestinal (GI) tract, brain and bone marrow/lymphoid tissues, with smaller amounts in the bladder, gallbladder and testis (proteinatlas.org). FABP5 is expressed mainly in the epidermis in both normal and psoriatic skin (Hao et al., 2023).

Previous studies assessing *FABP5* mRNA expression in psoriasis

FABP5 expression is increased in PS L vs HC skin (Bowcock et al., 2001) and in psoriatic peripheral blood T cells (Li et al., 2015). It is also increased in PS L vs PS NL skin lysates (Dallaglio et al., 2013). Treatment with topical steroid (hydrocortisone 17-butyrate; Locoid®) reduced *FABP5* mRNA but did not affect protein expression in PS L skin despite clinical improvement (Kuljpers et al., 1997). Increased *FABP5* in PS L vs PS NL skin reverted to levels of expression found in uninvolved skin following clinically and histopathologically successful therapy with ciclosporin A (Oestreicher et al., 2001).

Previous studies assessing FABP5 protein expression in psoriasis

There are conflicting data on serum FABP5 levels in PS vs HC; it has been reported as similar (Miyake et al., 2012) and significantly elevated, with positive correlation with PASI score and the ω-6/ω-3 PUFA ratio (Kozłowska et al., 2021).

FABP5 expression is increased on IHC of PS L vs HC skin (Chamcheu et al., 2016), with PS L>PS NL>HC (Miyake et al., 2012). FABP5 protein expression is increased in

differentiated keratinocytes in psoriatic vs healthy epidermis (Hao et al., 2023). FABP5 protein levels are highest in psoriatic scales>psoriatic lesions>differentiating keratinocytes>undifferentiated keratinocytes>normal skin (Siegenthaler et al., 1994). PPARβ/δ expression is also increased on IHC in PS L vs control skin (Chamcheu et al., 2016; Romanowska et al., 2010). FABP5 may form a complex with the anti-microbial peptide S100A7, as they purify and precipitate together and are both overexpressed in psoriatic scales (Hagens et al., 1999). Increased expression of FABP4/FABP5 proteins and uptake of exogenous FFA was found in human skin $CD8^+$ T_{RM} (considered the $CD8^+$ T cell phenotype found in PS L skin) compared to blood T_N, T_{CM} and T_{EM} cells (Pan et al., 2017).

There was a significant reduction in the median serum FABP5 value in patients treated with NB-UVB (Kozłowska et al., 2021). A small (10 patients) tape stripping study demonstrated reduction in FABP5 protein expression at 4-6 weeks in clinical responders to anti-TNF-α or NB-UVB (5/7 anti-TNF-α, 2/3 NB-UVB) (Miyake et al., 2012).

RNA-Seq data

FABP5 was significantly upregulated for all PS L samples vs HC, slightly more so in untreated PS L, and was significantly downregulated in AD NL skin (**Table 7.9**). FABP5 was identified as directly linked to SERPINB3 and S100A7 in STRING analysis of the Midnight Blue module (correlated with PS L) by WGCNA (**Chapter 3**).

Table 7.9 FABP5: Differential gene expression in the skin of psoriasis and atopic dermatitis compared to healthy control. p_{adj}; adjusted p-value. PS L; lesional psoriasis, PS NL; non-lesional psoriasis, PS R; resolved psoriasis, AD L; lesional atopic dermatitis, AD NL; non-lesional atopic dermatitis.

FABP5	Log2FC	p_{adj}

Untreated PS L	1.569	0.0149
PS L (NB-UVB)	1.042	0.0193
PS L (Secukinumab)	1.017	0.0052
AD L	-0.541	0.3947
Untreated PS NL	-0.298	0.7556
PS R (NB-UVB)	-0.449	0.5013
PS R (Secukinumab)	0.745	0.2821
AD NL	-1.398	0.0048

GEO Profiles data

FABP5 featured as one of the top 250 DEG in three out of the five GEO DataSets analysed and was consistently significantly upregulated (**Table 7.6**). It also featured as a significantly upregulated gene in the top 250 DEG of both GEO DataSets comparing PS L and HC skin (**Table 7.7**).

Single cell atlas

As seen in **Figure 7.4**, *FABP5* mRNA expression in psoriatic skin was localised mainly to keratinocytes (proliferating>differentiated), lymphatic endothelium, moDC and type 2 DC. Lower expression was found in many other cell types. In healthy skin, *FABP5* expression was mainly in lymphatic endothelium, moDC and monocyte-macrophages.

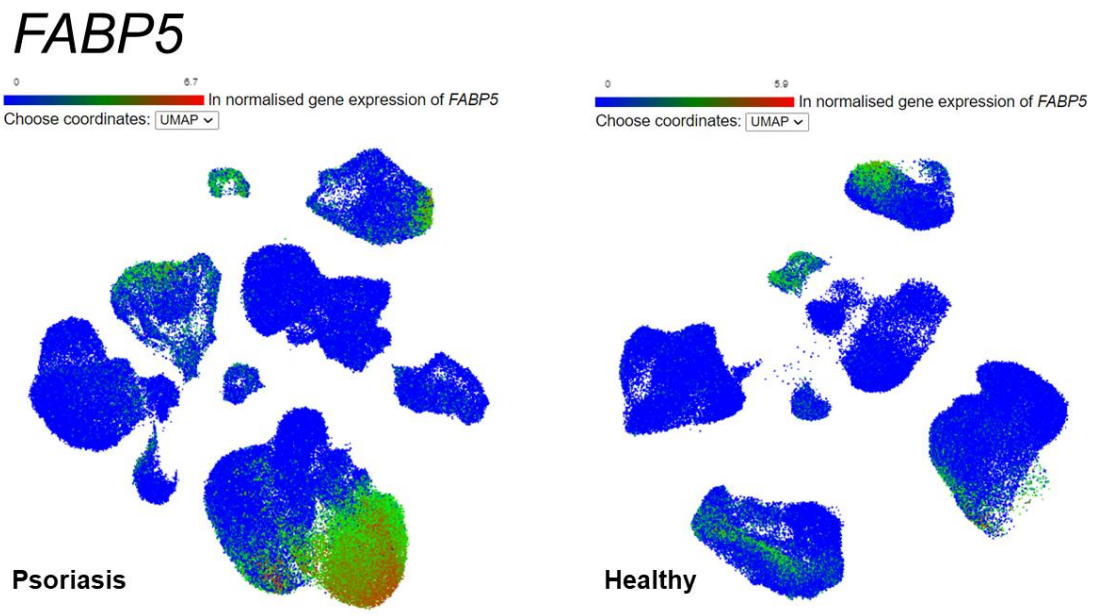


Figure 7.4 Single Cell Atlas: UMAP plots of mRNA expression of FABP5 in psoriasis and healthy skin.

7.3.4 *LCN2*: Lipocalin 2/Neutrophil gelatinase-associated lipocalin (NGAL)/24p3

Background: LCN2 is a pro-inflammatory, iron sequestering, anti-bacterial adipokine involved in cell growth, migration and invasion. It is also able to bind RA. LCN2 provokes increased mRNA expression of several cytokine-encoding genes in neutrophils, including *TNF* (*TNFA*) (Shao et al., 2016). Increased expression of the LCN2 receptor 24p3R (mRNA and protein) has been demonstrated in PS L epidermis (J. Ma et al., 2022). LCN2-stimulated keratinocytes showed upregulation of genes of the cholesterol biosynthetic pathway and elevated cellular cholesterol, postulated to be via SREBP2 activation (J. Ma et al., 2022). A separate, cholesterol-independent, LCN2-induced pathway of inflammasome activation via SREBP2 was also suggested (J. Ma et al., 2022).

Expression (mRNA): *LCN2* mRNA is predominantly found in the bone marrow and lymphoid tissues, gallbladder, bladder, salivary gland and oesophagus, with smaller amounts in other organs including the GI tract and skin (proteinatlas.org). *LCN2* mRNA is significantly increased in circulating neutrophils from psoriasis patients compared with HC (Shao et al., 2016).

Location (protein): LCN2 protein is located mainly in the kidney, bone marrow, spleen and cervix, with smaller amounts in the respiratory and GI tracts, salivary gland and skin (proteinatlas.org). Staining suggests LCN2 is localised to the granules (lamellar bodies) in primary human keratinocytes (Sørensen et al., 2003). LCN2 mRNA and protein expression is solely localised to hair follicle epithelium in the healthy skin of adults, however, it is found in the interfollicular epidermis in disorders of abnormal differentiation with parakeratosis, such as psoriasis (Mallbris et al., 2002). It has been suggested that activated keratinocytes and infiltrated neutrophils are the main source of LCN2 in PS L skin (Shao et al., 2016). Growth factors involved in the wound healing response, including insulin-like growth factor I and TGF-α (both individually and in combination/synergistically), induce antimicrobial peptides including LCN2 (both mRNA and protein) in human primary keratinocytes; IL-1β also induced LCN2 protein (Sørensen et al., 2003). IL-17A, IL-22, TNF-α and H_2O_2 promote LCN2 secretion from HaCaT cells (Shao et al., 2016).

Previous studies assessing *LCN2* mRNA expression in psoriasis

There is some variation between studies in the fold change of *LCN2* between PS L and HC skin;(Bowcock et al., 2001; Dou et al., 2017; Gudjonsson, Ding, et al., 2010) *LCN2* is significantly upregulated in PS L vs NL skin (FC 45.74) (Suárez-Fariñas et al., 2012). *LCN2* expression is significantly increased in PS L vs AD L skin (Guttman-Yassky et al.,

2008; Nomura et al., 2003). LCN2 mRNA and protein are highly expressed in PS L skin (epidermis and dermis) and IMQ induced similar expression (mRNA/protein) in mice (Shao et al., 2016).

LCN2 is downregulated in skin that has clinically resolved with NB-UVB phototherapy (vs the previous PS L) (Rácz et al., 2011; Vacharanukrauh et al., 2021) and has been shown to trend towards downregulation in PS L skin of patients clinically responsive to ciclosporin (Haider, Lowes, et al., 2008).

Previous studies assessing LCN2 protein expression in psoriasis

Most studies report a significant increase in serum LCN2 levels in PS vs HC (Ataseven et al., 2014; Baran et al., 2017; Kamata et al., 2012; Romaní et al., 2013), although there are some exceptions (El-Hadidi et al., 2014). Positive correlations have been reported between serum LCN2 and Retinol Binding Protein 4 (RBP4) (Baran et al., 2017) (which is itself significantly elevated in the serum of PS vs HC) (Romaní et al., 2013), IL-6 (Kamata et al., 2012) and TNF-α (Kamata et al., 2012), with conflicting results for LDL-Cholesterol (Baran et al., 2017; Kamata et al., 2012). A study not focused on psoriasis found a positive correlation between serum LCN2 and body mass index (BMI), plus other markers of cardiovascular risk, possibly confounding psoriasis study results, while also identifying an independent (of BMI) correlation between serum LCN2 and high-sensitivity c-reactive protein (CRP) (Y. Wang et al., 2007). Along with hBD-2, LCN2 is induced by IL-17 and has been suggested as a proxy measurement for this cytokine in serum, as is difficult to accurately measure otherwise (Turina et al., 2017). Data are conflicting on whether serum LCN2 levels change with NB-UVB phototherapy (Kamata et al., 2012; Romaní et al., 2013).

Tissue LCN2 is significantly higher in PS vs HC (El-Hadidi et al., 2014), in both PS L and PS NL skin (Abdel Hay et al., 2020). LCN2 is increased in the upper spinous and granular layers of the epidermis of PS NL skin vs HC skin (Chiricozzi et al., 2016). LCN2 in both PS L and PS NL skin was reduced following NB-UVB (PASI 75 achieved or max 36 sessions) but remained significantly higher than healthy control (Abdel Hay et al., 2020).

RNA-Seq data

LCN2 was upregulated in all treatment groups for PS L, again most marked in untreated PS L, but no results were significant aside from downregulation in AD skin (**Table 7.10**). *LCN2* featured as part of the WGCNA Midnight Blue module (highly correlated with PS L skin for all three treatment groups) Gene Ontology "response to virus". LCN2 was identified in STRING analysis of the Midnight Blue module (correlated with PS L), directly linked to STAT3, a key transcription factor in psoriasis (**Chapter 3**).

Table 7.10 LCN2: Differential gene expression in the skin of psoriasis and atopic dermatitis compared to healthy control. p_{adj}; adjusted p-value. PS L; lesional psoriasis, PS NL; non-lesional psoriasis, PS R; resolved psoriasis, AD L; lesional atopic dermatitis, AD NL; non-lesional atopic dermatitis.

LCN2	Log2FC	P_{adj}
Untreated PS L	1.710	0.0986
PS L (NB-UVB)	1.052	0.0779
PS L (Secukinumab)	0.476	0.3127
AD L	-2.417	0.0007
Untreated PS NL	-0.727	0.6606
PS R (NB-UVB)	-0.962	0.1336
PS R (Secukinumab)	-0.185	0.8156

AD NL	-2.492	0.0016

GEO Profiles

LCN2 was one of the top 250 DEG in four out of five GEO DataSets (PS L vs PS NL) analysed and was consistently significantly upregulated (**Table 7.6**). It also featured as a significantly upregulated gene in the top 250 DEG of both GEO DataSets comparing PS L and HC skin (**Table 7.7**).

Single cell atlas

Expression patterns for *LCN2* mRNA were more subtle than those for the other three candidate genes of interest (**Figure 7.5**). However, once again, the main site of expression was in psoriatic keratinocytes (differentiated>proliferating>undifferentiated, with negligible amounts in lymphatic endothelium). There was negligible expression detectable in healthy skin (localised to lymphatic endothelium), however, the study sample size is small.

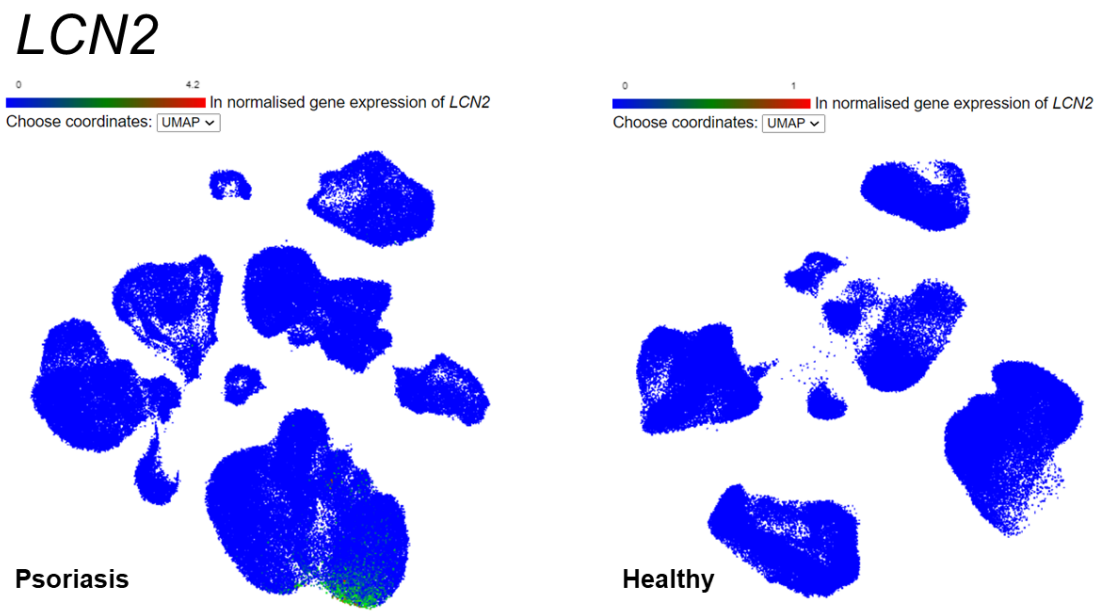


Figure 7.5 Single Cell Atlas: UMAP plots of mRNA expression of LCN2 in psoriasis and healthy skin.

7.3.5 *APOE*: Apolipoprotein E

Background: ApoE is a component of several lipoproteins, which transport lipids. ApoE binds the low-density lipoprotein receptor (LDL), the LDL receptor-related proteins (LRP) LRP1, LRP2 and LRP8 and the very low-density lipoprotein receptor (VLDLR). Aside from lipid transport and homeostasis, it has immunomodulatory functions including maintenance of Th1/Th2 balance, cytokine and NO production, as summarised by Zhang et al (Zhang et al., 2011). *APOE* is found on chromosome 19 and consists of 3 alleles, ε2, ε3 and ε4 in humans, with 6 potential genotypes resulting from combinations of these alleles. Genotype may influence protein function.

Expression: *APOE* mRNA is widely expressed, with the largest amounts in the brain, liver and adrenal gland (proteinatlas.org).

Location (protein): ApoE is synthesised and secreted by human keratinocytes in culture (Gordon et al., 1989). As well as in the skin, this protein is found in the brain, liver, adrenal gland, kidney, endometrium and bone marrow (proteinatlas.org).

Previous studies assessing *APOE* mRNA expression in psoriasis

APOE is downregulated in PS L vs HC skin (Log2FC of -1.41 ($p<0.001$))(Dou et al., 2017) and PS L vs PS NL skin (Reischl et al., 2007). *APOE* is upregulated in skin that has clinically resolved with NB-UVB phototherapy (vs the previous PS L) (Rácz et al., 2011; Vacharanukrauh et al., 2021). Reduced *APOE* in PS L vs NL skin reverted to levels of expression found in uninvolved skin following clinically and histopathologically successful therapy with ciclosporin A (Oestreicher et al., 2001).

The evidence for the association of certain ApoE alleles and genotypes with psoriasis is conflicting and incomplete. A meta-analysis of seven case-control studies suggested that ε2 (increased risk) and ε3 (decreased risk) are ApoE risk alleles for PS, while ε4 may be a risk factor in European populations (Han et al., 2013).

Previous studies assessing ApoE protein expression in psoriasis

There are limited data on serum ApoE levels and psoriasis. One study found a significantly elevated median ApoE level in psoriasis patients (all on some form of treatment) versus HC (Paiva-Lopes et al., 2020). Serum ApoE levels have been found to be significantly positively correlated with BMI, which may be a confounding factor in psoriasis (Miao et al., 2019). Psoriasis patients have significantly higher mean and median serum titres of anti-ApoE IgG antibodies compared to HC and mean titres are significantly higher in severe (PASI >10) disease (Paiva-Lopes et al., 2020).

RNA-Seq data

Compared to HC skin, *APOE* expression was downregulated in all treatment groups for PS L skin to a similar degree and downregulated to lesser degree in PS NL and AD skin (**Table 7.11**). *APOE* was less downregulated in skin that had resolved with NB-UVB but was differentially expressed almost to a similar level as PS L in skin that had resolved with Secukinumab. *APOE* featured in WGCNA Gene Ontology of the Turquoise module (positively correlating with healthy control status) (**Chapter 3**). APOE was also identified on STRING analysis of the Turquoise module as connecting to enzymes of retinoid metabolism and FA (including NFA) metabolism (**Chapter 3**).

Table 7.11 APOE: Differential gene expression in the skin of psoriasis and atopic dermatitis compared to healthy control. p_{adj}; adjusted p-value. PS L; lesional psoriasis, PS NL; non-lesional

psoriasis, PS R; resolved psoriasis, AD L; lesional atopic dermatitis, AD NL; non-lesional atopic dermatitis.

APOE	Log2FC	p_{adj}
Untreated PS L	-2.532	3.50×10^{-6}
PS L (NB-UVB)	-2.406	2.46×10^{-19}
PS L (Secukinumab)	-2.645	2.89×10^{-14}
AD L	-1.698	4.43×10^{-5}
Untreated PS NL	-1.804	1.51×10^{-5}
PS R (NB-UVB)	-1.487	0.0005
PS R (Secukinumab)	-2.313	1.41×10^{-10}
AD NL	-1.604	1.14×10^{-6}

GEO Profiles

APOE did not feature as one of the top 250 DEG in any of the five GEO DataSets analysed. However, in the full lists of DEG from these studies, it was downregulated in PS L vs PS NL (significantly except for one study) (**Table 7.6**) and PS L vs HC (significantly) (**Table 7.7**).

Single cell atlas

As seen in **Figure 7.6**, *APOE* mRNA expression in psoriatic skin was mainly localised to melanocytes, fibroblasts, keratinocytes (differentiated>proliferating), Schwann cells, pericytes and undifferentiated keratinocytes in psoriatic skin. In healthy skin, expression was predominantly found in melanocytes, fibroblasts, differentiated keratinocytes, type 1 macrophages and pericytes, with smaller amounts in other cells.

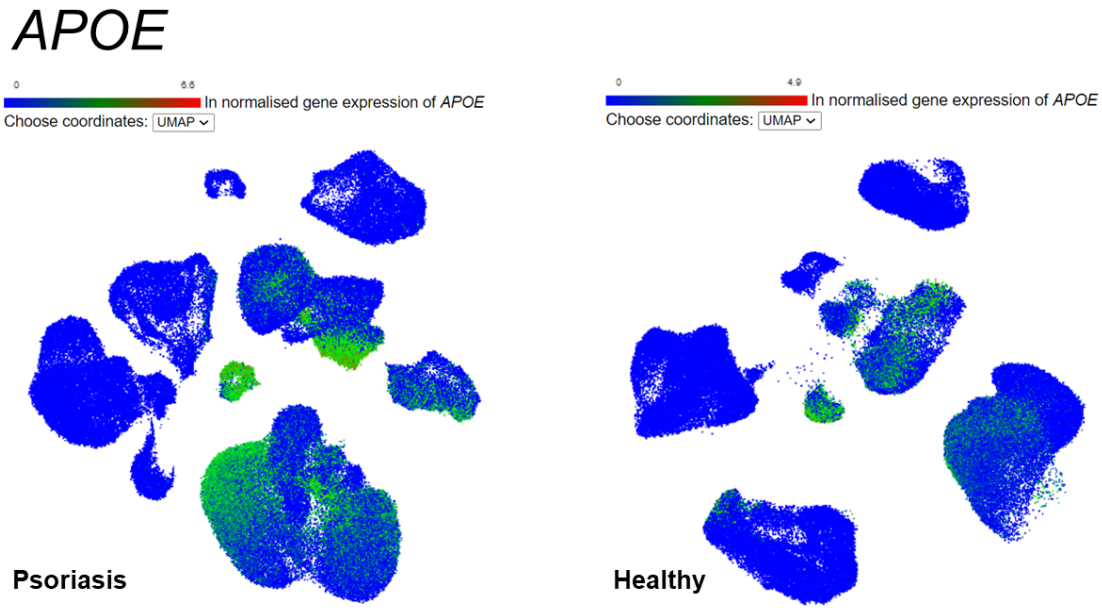


Figure 7.6 Single Cell Atlas: UMAP plots of APOE mRNA expression in psoriasis and healthy skin.

7.4 Results II: Validation of candidate genes of interest

Validation of genes of interest was performed using IF IHC for all four genes and imaging mass cytometry (Hyperion™) for *CRABP2*, *LCN2* and *APOE*. The same skin samples were used for both analyses where possible:

- PS2784 (untreated)
- PS2501 (NB-UVB-treated)
- PS2510 (secukinumab-treated)
- AD2634 (inflammatory control)

Regarding control samples, DER008 was used for IF IHC and DER006 was used for Hyperion™. For sebaceous gland staining, surplus skin DE536 was used.

7.4.1 Immunofluorescence Immunohistochemistry

IF IHC of HC skin demonstrated some epidermal staining with CRABP2 and ApoE (**Figure 7.7**), although this was predominantly localised to the stratum corneum for CRABP2 and may be non-specific.

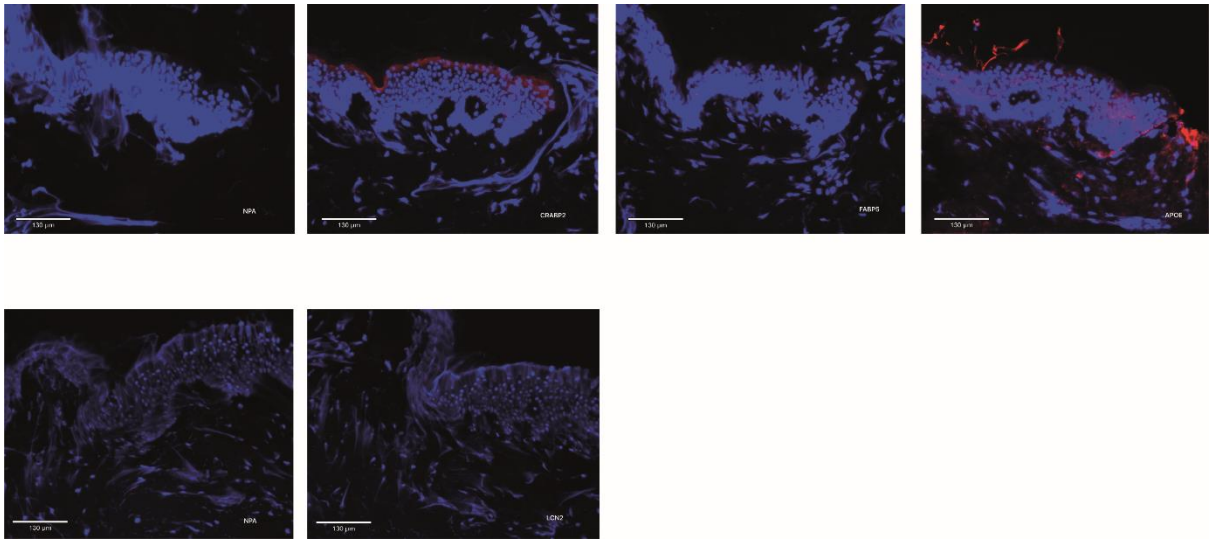


*Figure 7.7 Immunofluorescence immunohistochemistry: Healthy Control DER008B. Frozen sections were stained with primary antibody specific to the target antigen, then stained with a secondary antibody-fluorophore conjugate (**Table 7.2**). Top row (L-R): NPA, CRABP2, FABP5, ApoE. Bottom row (L-R): NPA, LCN2.*

IF IHC of AD skin was similar to HC, with some additional stratum corneum staining for LCN2 (**Figure 7.8**). The PS NL section for ApoE contained a follicle that stained, in keeping with its known predilection for the pilo-sebaceous unit. Hyperion™ imaging mass cytometry (**Figure 7.19**) corroborated this, suggesting staining is not autofluorescent in nature.

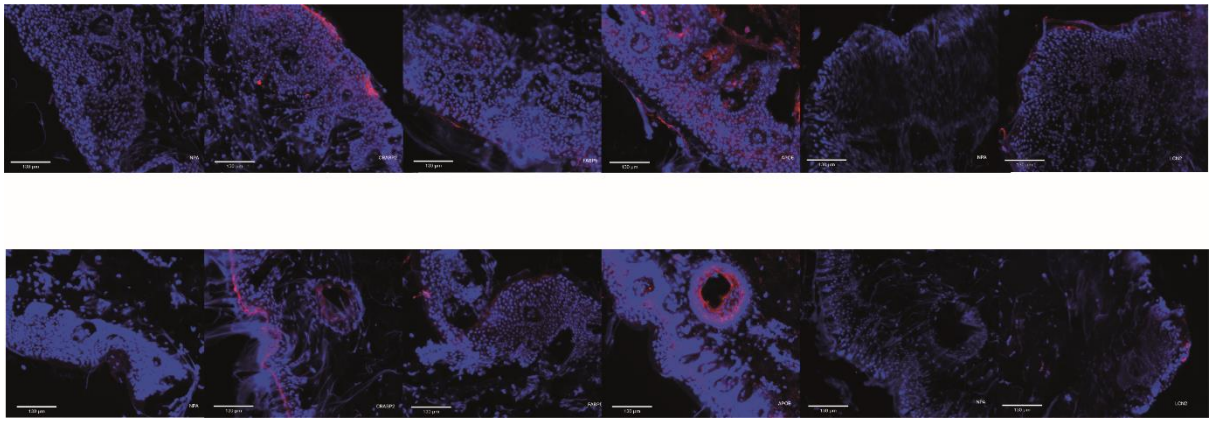


*Figure 7.8 Immunofluorescence immunohistochemistry: AD2634. Frozen sections were stained with primary antibody specific to the target antigen, then stained with a secondary antibody-fluorophore conjugate (**Table 7.2**). Top row: Lesional (L-R): NPA, CRABP2, FABP5, ApoE, NPA, LCN2. Bottom row: Non-Lesional (L-R): NPA, CRABP2, FABP5, ApoE, NPA, LCN2.*

PS L (untreated) skin showed non-specific stratum corneum staining only (**Figure 7.9, Figure 7.10**). There was no epidermis on the lesional section for LCN2 for this donor.

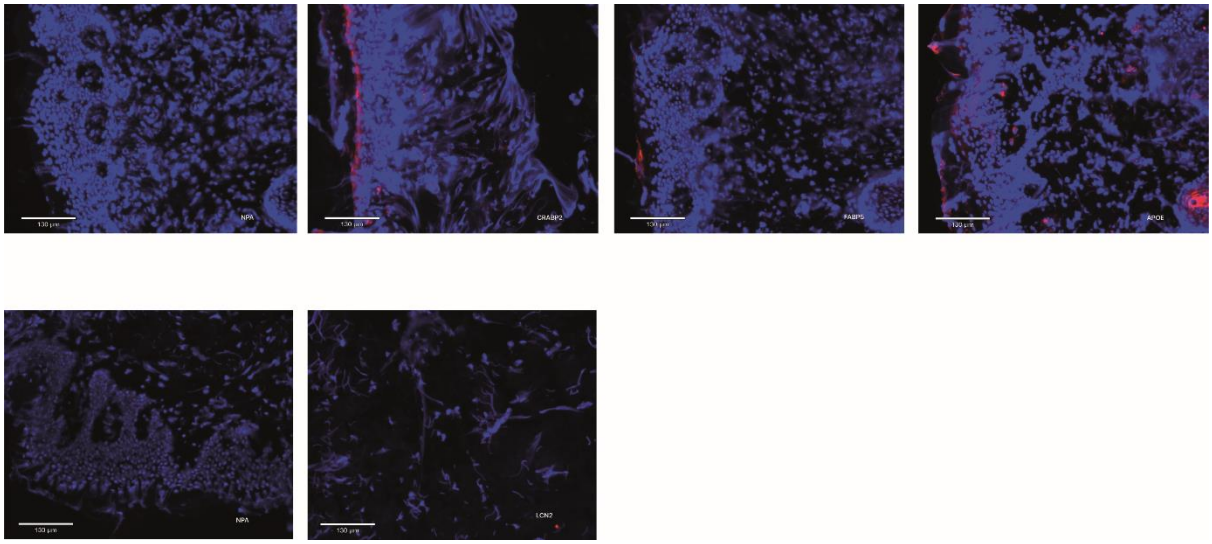


*Figure 7.9 Immunofluorescence immunohistochemistry: PS2784 L (untreated). Frozen sections were stained with primary antibody specific to the target antigen, then stained with a secondary antibody-fluorophore conjugate (**Table 7.2**). Top row (L-R): NPA, CRABP2, FABP5, ApoE. Bottom row (L-R): NPA, LCN2. L; lesional.*

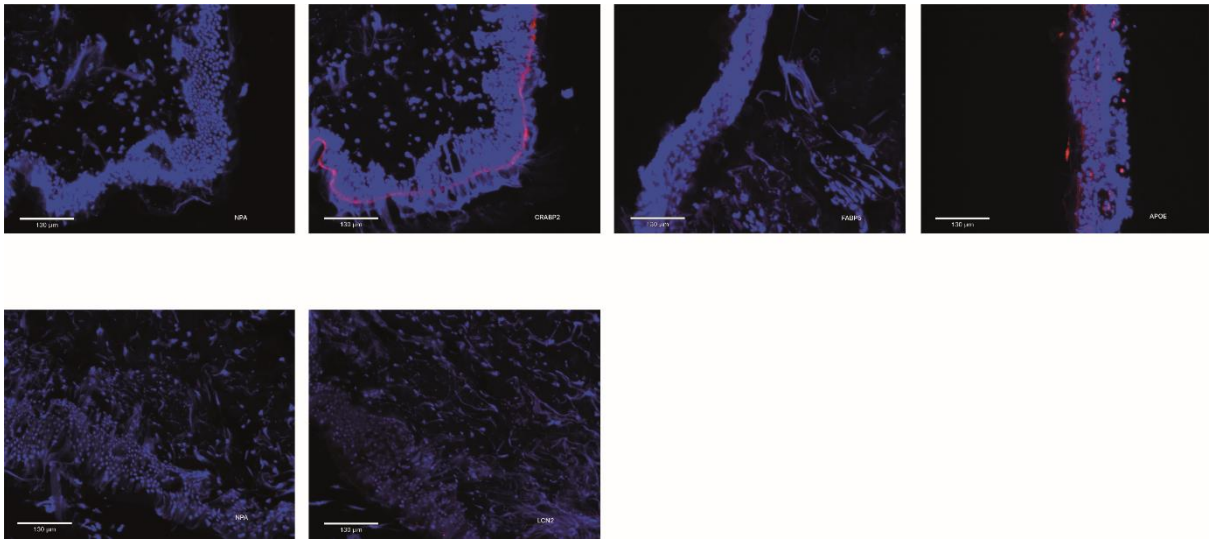


*Figure 7.10 Immunofluorescence immunohistochemistry: PS2684 NL (untreated). Frozen sections were stained with primary antibody specific to the target antigen, then stained with a secondary antibody-fluorophore conjugate (**Table 7.2**). Top row (L-R): NPA, CRABP2, FABP5, ApoE. Bottom row (L-R): NPA, LCN2. NL; non-lesional.*

Results for NB-UVB-treated psoriatic skin were similar to those for HC and AD, although the increased stratum corneum on PS L skin, in keeping with the hyperproliferation of keratinocytes seen in psoriasis, attracted more (likely non-specific) staining for all antibodies (**Figure 7.11, Figure 7.12**).

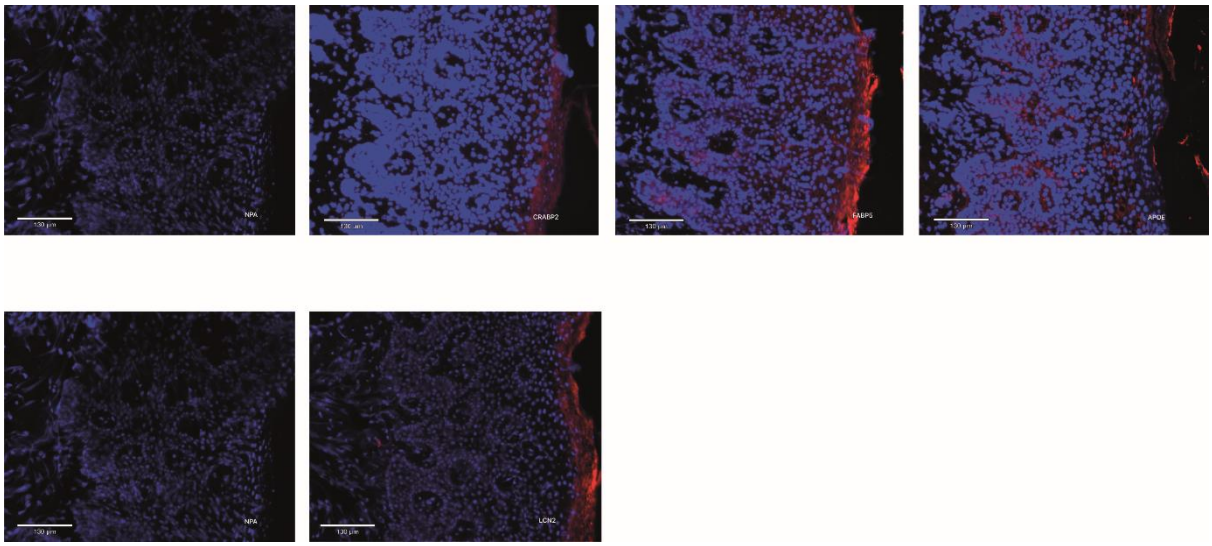


*Figure 7.11 Immunofluorescence immunohistochemistry: PS2501 L (NB-UVB). Frozen sections were stained with primary antibody specific to the target antigen, then stained with a secondary antibody-fluorophore conjugate (**Table 7.2**). Top row (L-R): NPA, CRABP2, FABP5, ApoE. Bottom row (L-R): NPA, LCN2. L; lesional.*

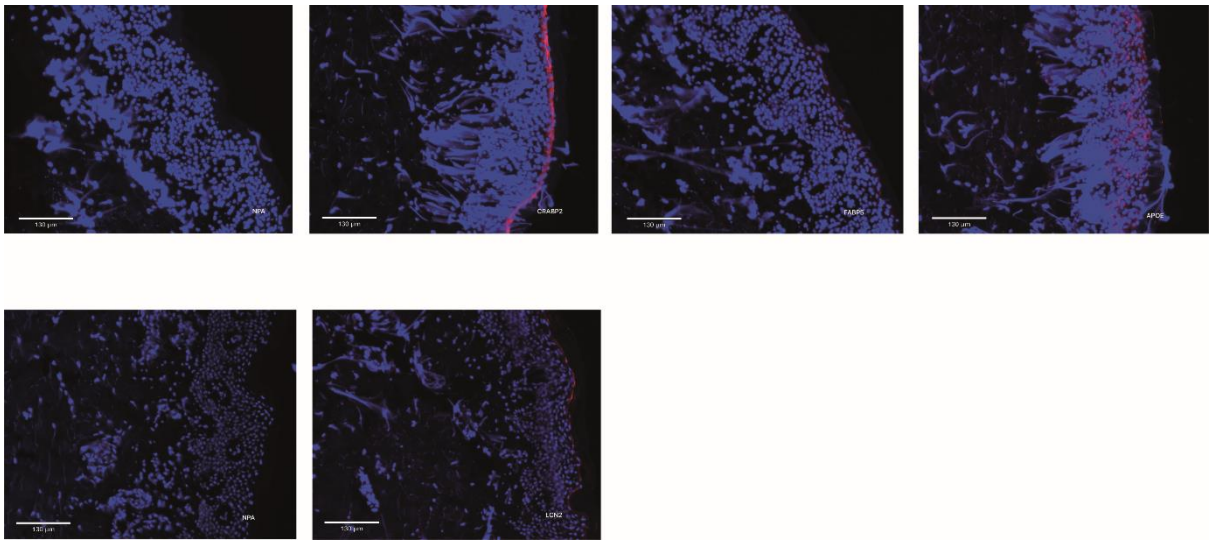


*Figure 7.12 Immunofluorescence immunohistochemistry: PS2501 NL (NB-UVB). Frozen sections were stained with primary antibody specific to the target antigen, then stained with a secondary antibody-fluorophore conjugate (**Table 7.2**). Top row (L-R): NPA, CRABP2, FABP5, ApoE. Bottom row (L-R): NPA, LCN2. NL; non-lesional (resolved).*

IF IHC of secukinumab-treated skin was akin to that of NB-UVB-treated skin (**Figure 7.13, Figure 7.14**), with substantial stratum corneum staining for all antibodies.

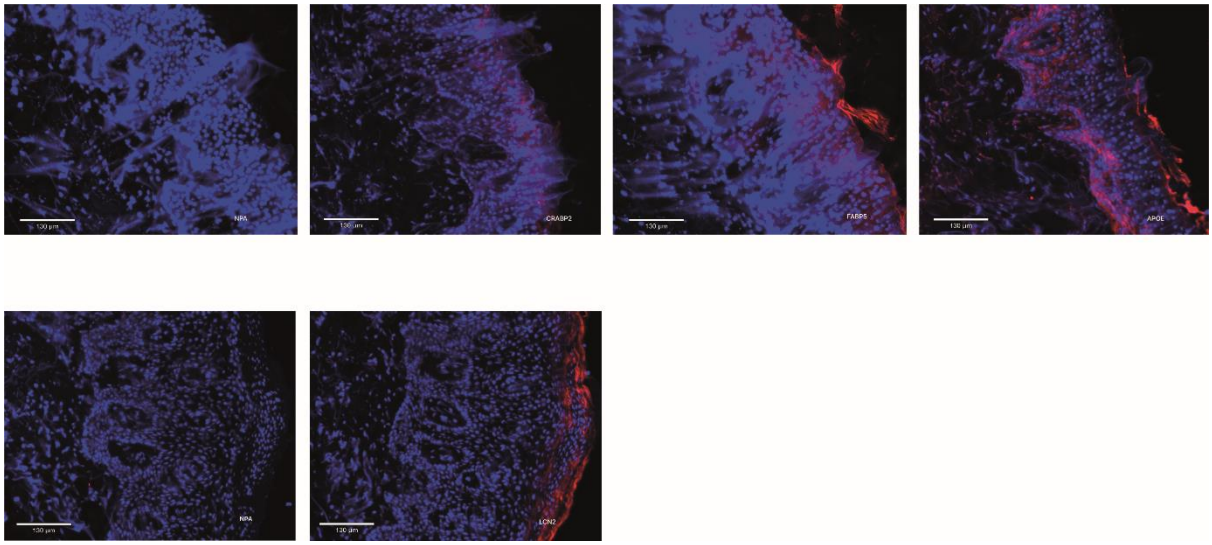


*Figure 7.13 Immunofluorescence immunohistochemistry: PS2510 L (Secukinumab). Frozen sections were stained with primary antibody specific to the target antigen, then stained with a secondary antibody-fluorophore conjugate (**Table 7.2**). Top row (L-R): NPA, CRABP2, FABP5, ApoE. Bottom row (L-R): NPA, LCN2. L; lesional.*

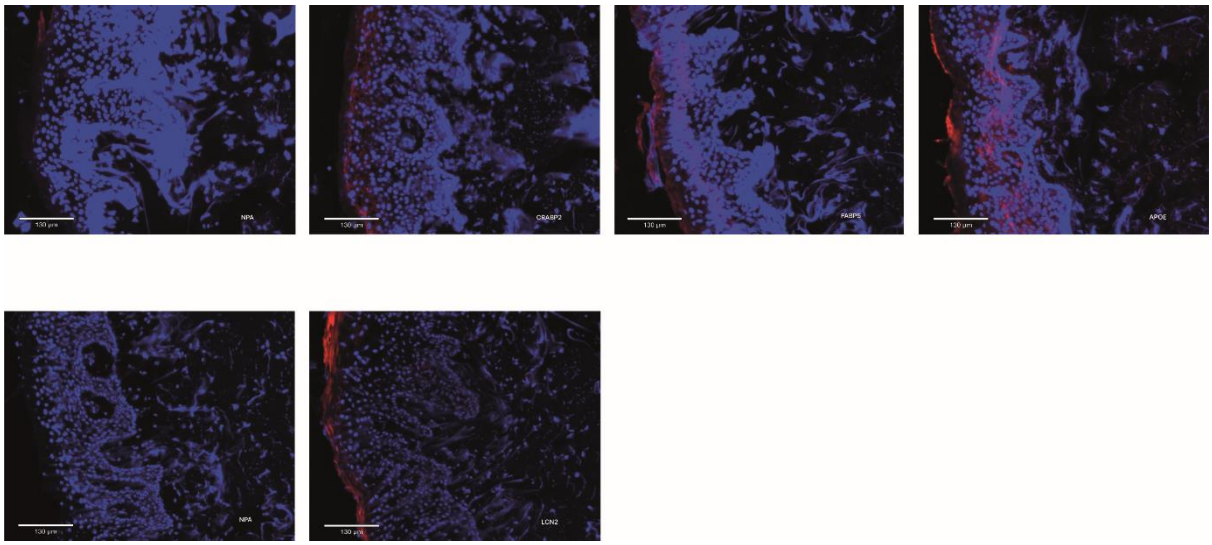


*Figure 7.14 Immunofluorescence immunohistochemistry: PS2510 NL (Secukinumab). Frozen sections were stained with primary antibody specific to the target antigen, then stained with a secondary antibody-fluorophore conjugate (**Table 7.2**). Top row (L-R): NPA, CRABP2, FABP5, ApoE. Bottom row (L-R): NPA, LCN2. NL; non-lesional (resolved).*

7.4.2 Hyperion™

Architecture of lesional vs non-lesional psoriasis

Initial comparison was made between untreated PS L vs PS NL skin. Classic histological features of psoriatic epidermis were visible (**Figure 7.15 (a)**), with acanthosis (hyperproliferation of keratinocytes) evident in the lesional but not the non-lesional sample (**Figure 7.15 (b)**). Keratin 14 staining is prominent in the basal and supra-basal layers for both samples, although appearing to extend more superficially in the PS L sample, possibly due to cross-cut sectioning, with keratin 10 predominating in the stratum granulosum and stratum corneum. Keratin 10 staining was more pronounced in the PS NL and HC samples (**Figure 7.5 (b) and (c)**). Infiltrating haematopoetic ($CD45^+$) cells were visible coalescing in the dermis of lesional skin but were sparse in non-lesional skin.

Untreated PS NL had similar architecture to HC skin (**Figure 7.15 (c)**) with minimal infiltrate by immune cells. Epidermal acanthosis was visible in PS L skin treated with NB-UVB (**Figure 7.15 (d)**) and secukinumab (**Figure 7.15 (e)**) and in AD L skin (**Figure 7.15 (f)**). AD L skin also showed increased $CD45^+$ infiltrates compared to PS and HC skin.

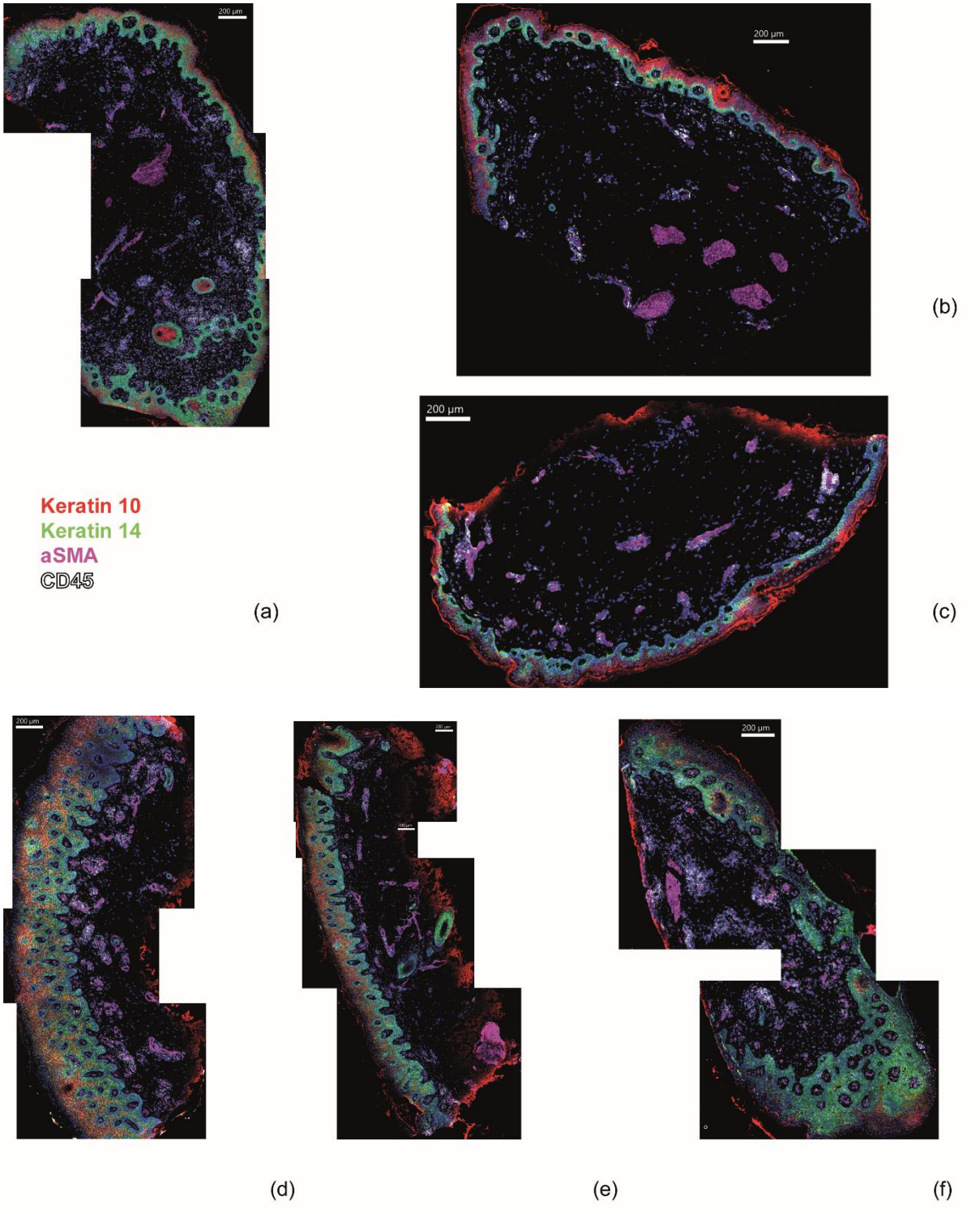


Figure 7.15 Hyperion: Tissue architecture. (a) PS L (untreated) (b) PS NL (untreated) (c) HC (d) PS L (NB-UVB) (e) PS L (Secukinumab) (f) AD L. L; lesional, NL; non-lesional.

In psoriasis and healthy control skin, CD1a is expressed mainly on LC, but in AD there is another population of cells staining for CD1a that does not stain for langerin (**Figure 7.16**). Among PS L subgroups, PS L (NB-UVB) appeared to express CD1a at a lower frequency and intensity.

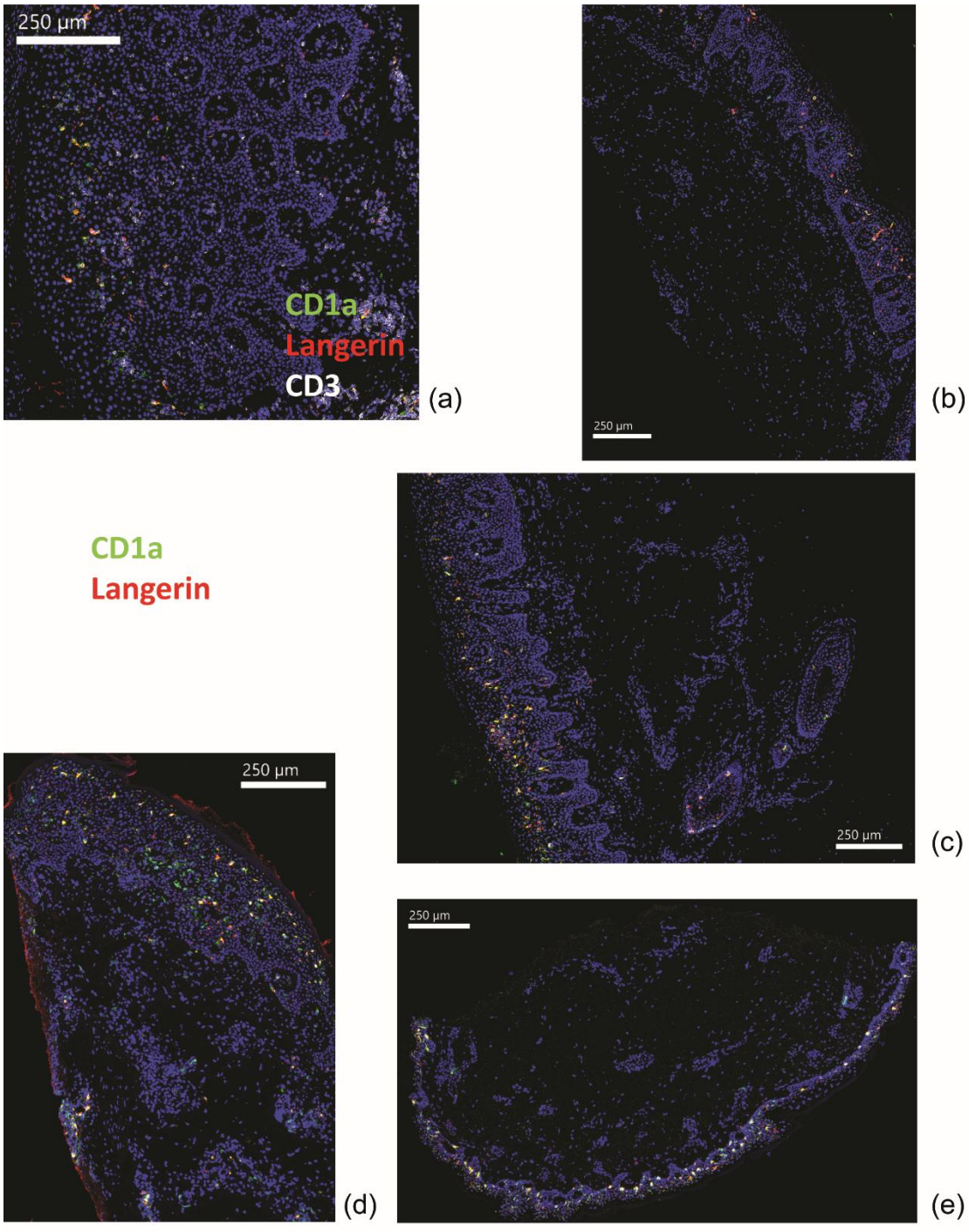


Figure 7.16 Hyperion: CD1a expression. (a) PS L (untreated) (b) PS L (NB-UVB) (c) PS L (Secukinumab) (d) AD (e) HC. Additional CD3 staining performed in PS L (untreated). L; lesional.

Expression of candidate genes of interest

CRABP2

Diffuse epidermal, with some dermal, staining with CRABP2 was evident in all samples (**Figure 7.17**).

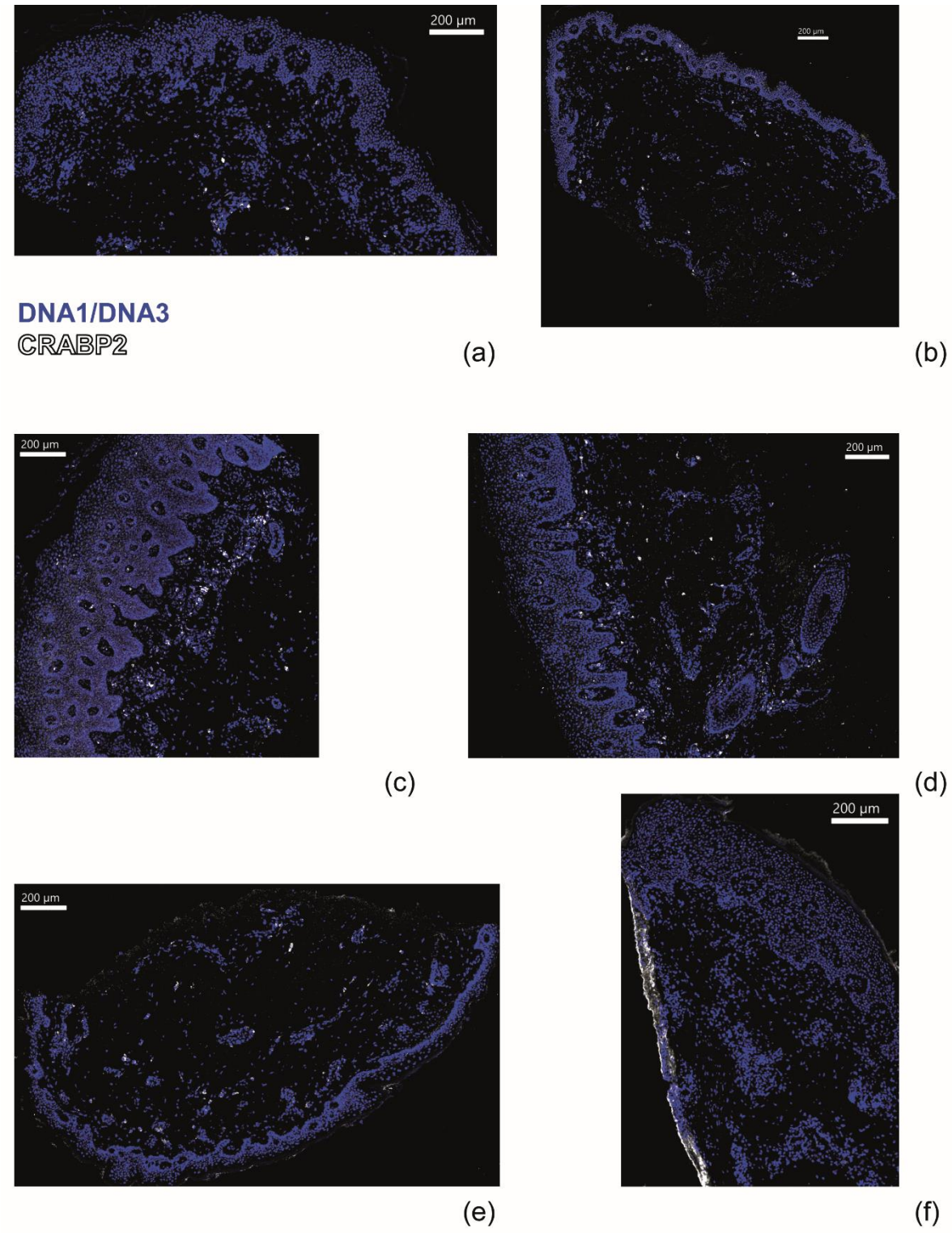


Figure 7.17 Hyperion: CRABP2 staining. (a) PS L (untreated) (b) PS NL (untreated) (c) PS L (NB-UVB) (d) PS L (Secukinumab) (e) HC (f) AD L. L; lesional, NL; non-lesional.

Cells staining positive for CRABP2 were found to co-express several other immunological markers. The receptor tyrosine kinase KIT, which is expressed on multiple haematopoietic progenitors, as well as melanocytes and cutaneous mast cells, was also diffusely stained (**Figure 7.18**). KIT, also known as CD117 and mast cell/stem cell growth factor receptor (SCFR), is encoded by the proto-oncogene *c-kit*.

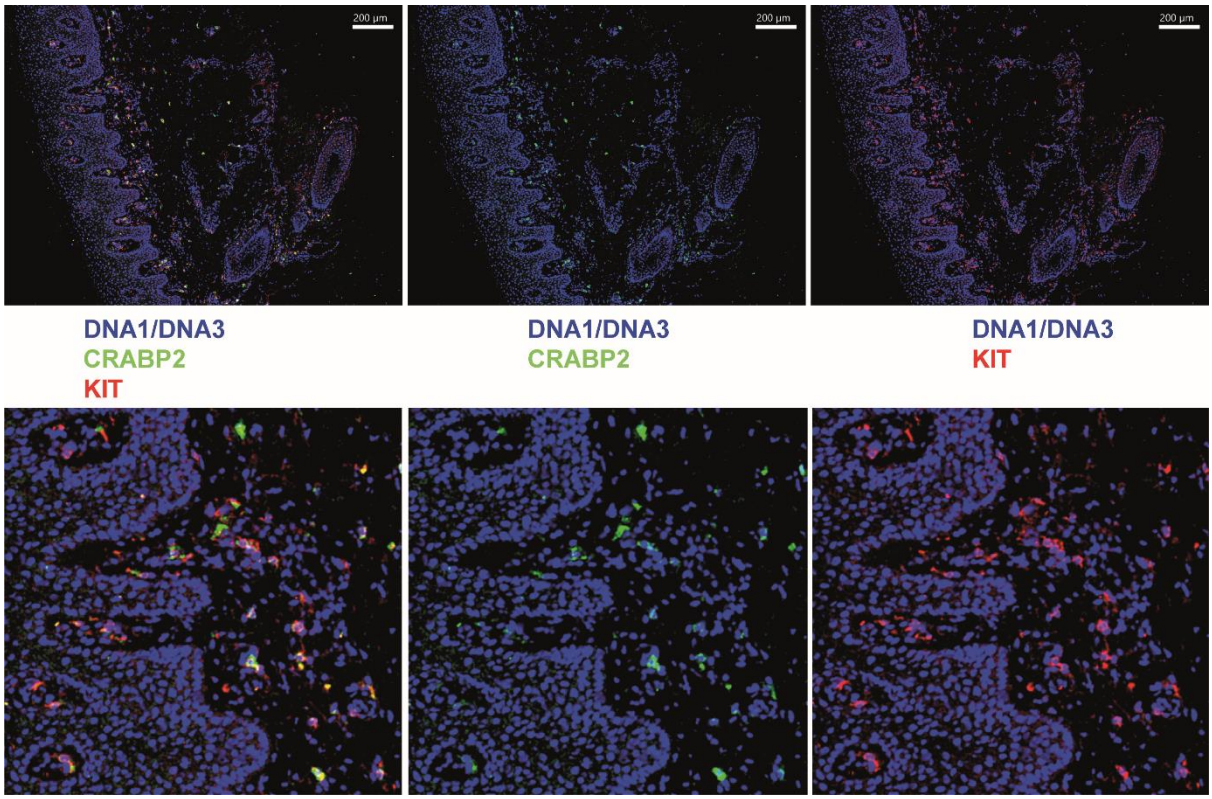


Figure 7.18 Hyperion: CRABP2 co-localisation with KIT.

CD45 (**Figure 7.18**) and CRTH2 also demonstrated co-expression with CRABP2, but staining for CD14, CD56 and the myeloid dump was negative (data not shown). CD1a was negative for CRABP2-expressing cells in the dermis.

Overall, staining was suggestive, but not definitively characteristic, of innate lymphoid cells (ILC).

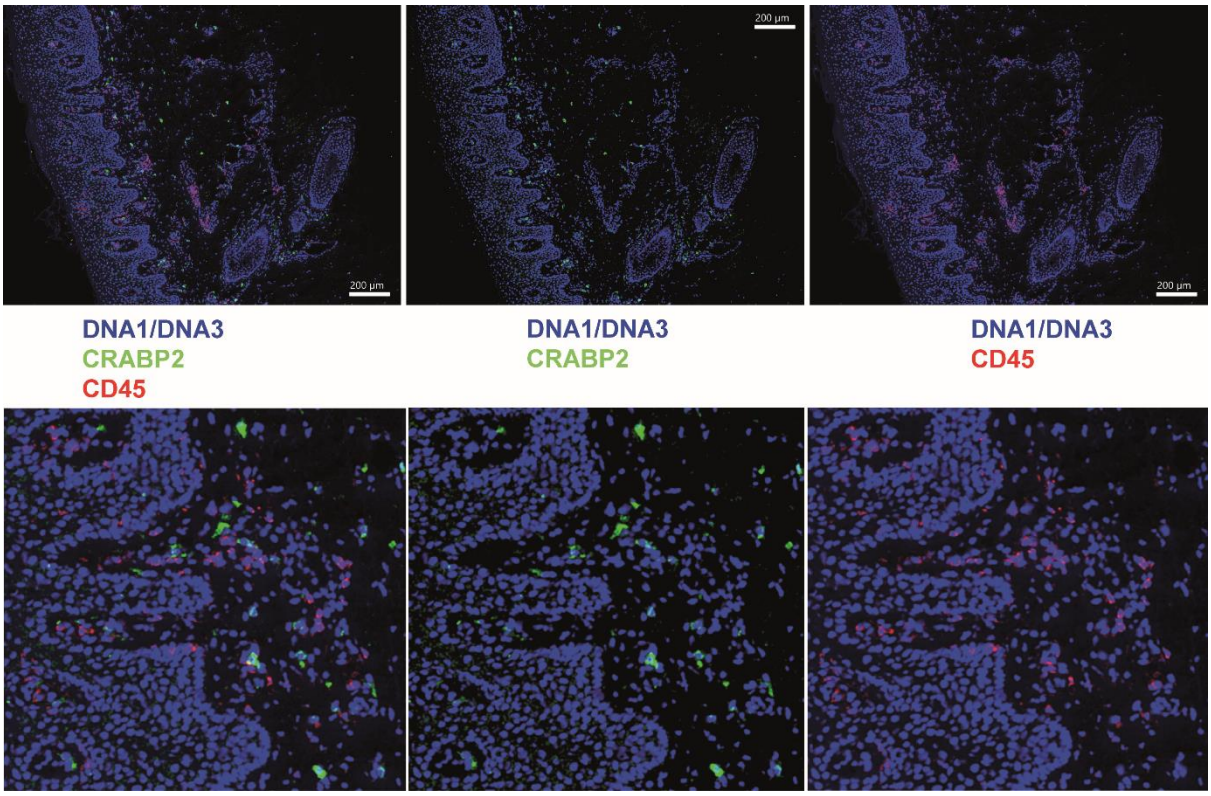


Figure 7.19 Hyperion: CRABP2 co-localisation with CD45.

LCN2

Hyperion™ staining with LCN2 identified dense staining, mostly in keratinocytes, that was most prominent in psoriatic skin (**Figure 7.19**).

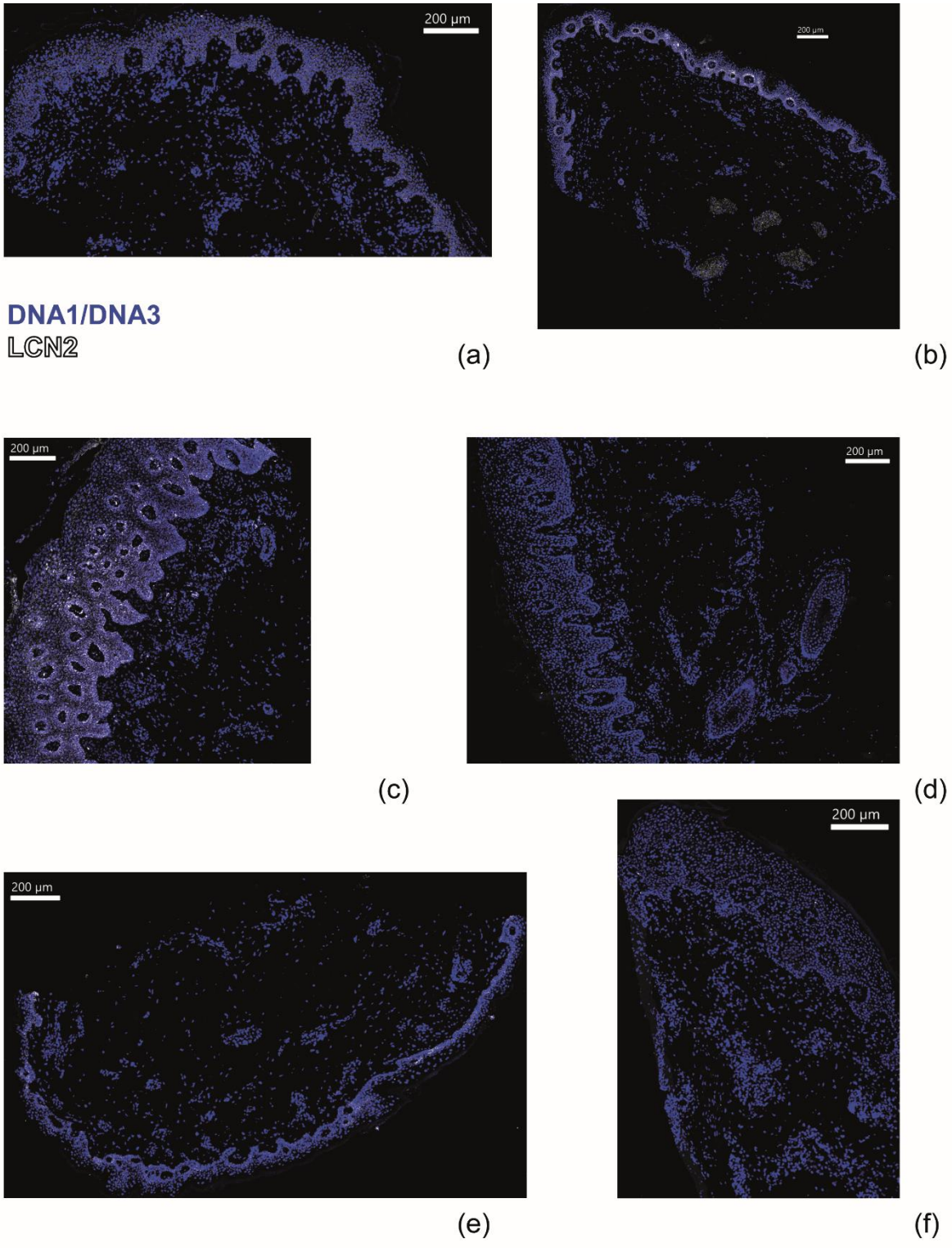


Figure 7.20 Hyperion: LCN2 staining. (a) PS L (untreated) (b) PS NL (untreated) (c) PS L (NB-UVB) (d) PS L (Secukinumab) (e) HC (f) AD L. L; lesional, NL; non-lesional.

ApoE

ApoE staining was less prominent than for CRABP2 and LCN2 (**Figure 7.20**). Some staining was noted in the epidermis and peri-follicular region of PS L (Secukinumab). Overall the strongest staining was in healthy skin (**Figure 7.20 (e)**).

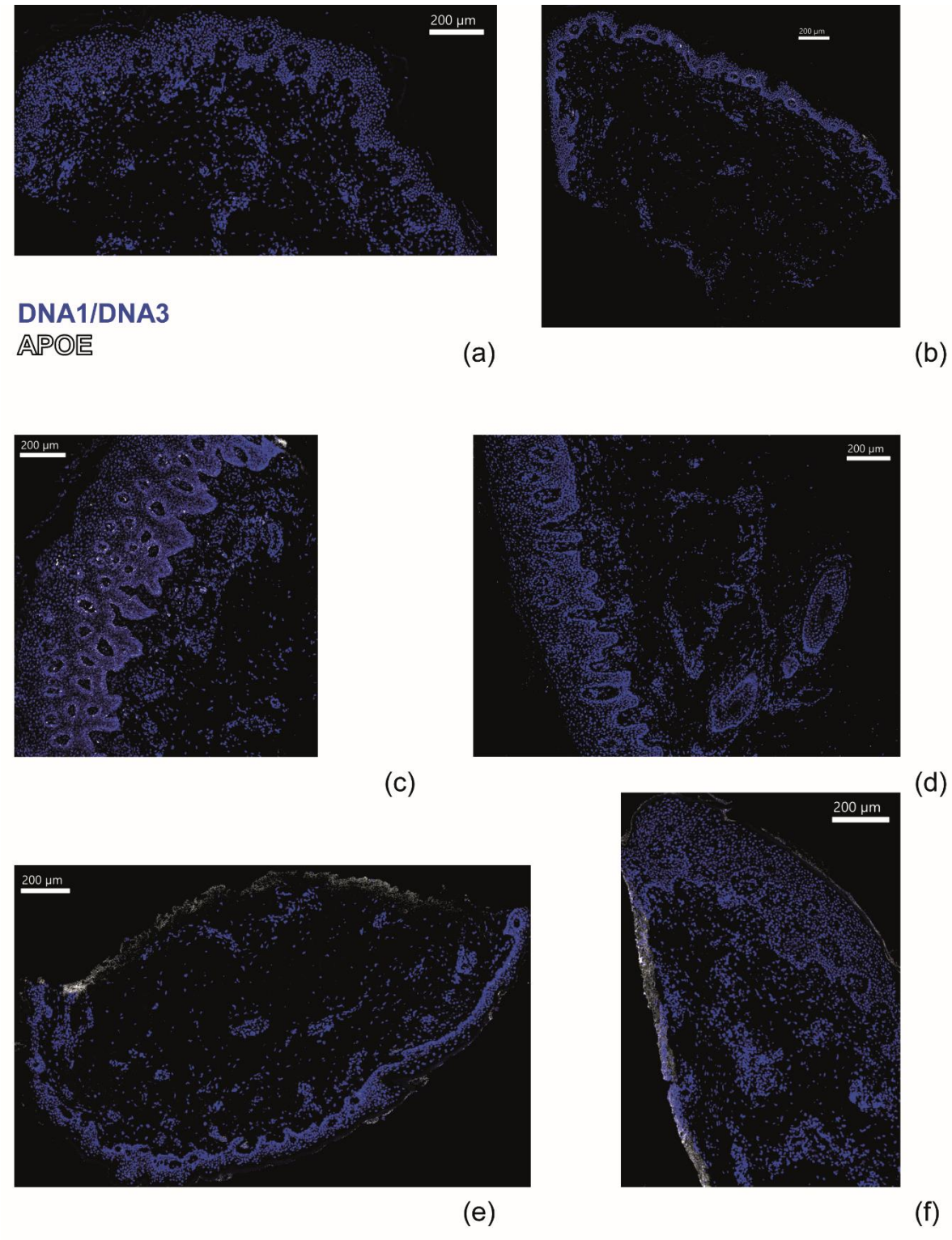


Figure 7.21 Hyperion: ApoE staining. (a) PS L (untreated) (b) PS NL (untreated) (c) PS L (NB-UVB) (d) PS L (Secukinumab) (e) HC (f) AD L. L; lesional, NL; non-lesional.

Expression of candidate genes of interest in sebaceous glands

Staining of CRABP2, LCN2 and ApoE was apparent in sebaceous glands in healthy surplus skin (**Figure 7.21**).

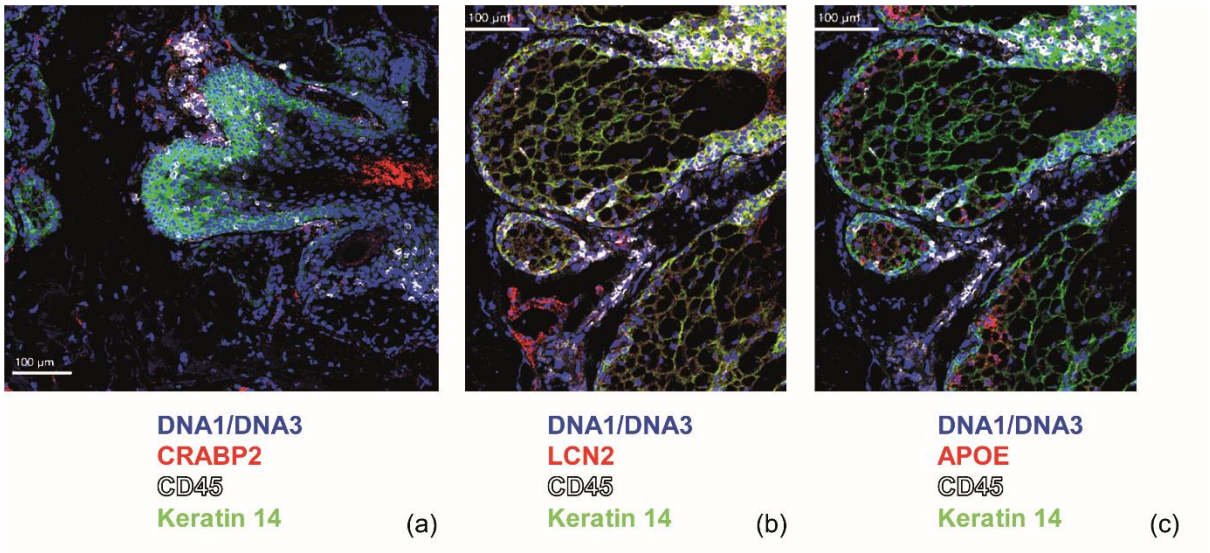


Figure 7.22 Hyperion: Expression in sebaceous glands of (a) CRABP2 (b) LCN2 (c) ApoE.

7.4.3 Validation of candidate genes results summary

Four genes related to retinoid and lipid binding were selected for protein validation. IF IHC interpretation was limited by artefact but Hyperion™ provided illuminating insight into the distribution of these proteins and their co-localisation with other markers in the skin. Protein expression correlated with mRNA expression, validating RNA-Seq results.

7.5 Discussion

Assessment of our RNA-Seq data, detailed analysis of resources including published literature, public gene datasets (GEO Profiles/GEO DataSets) and tools such as the Human Cell Atlas(Reynolds et al., 2021) facilitated the identification of four genes for protein validation. All four encode proteins relevant to lipid pathways of interest for this project, in particular, retinoid metabolism. Published studies supported a potentially

important role for these genes and their proteins in psoriasis. Meta-analysis of DEG in PS L vs PS NL skin (MAD-3, MAD-5 transcriptomes) has demonstrated FC>2 for all four genes (in a positive direction for *CRABP2*, *FABP5* and *LCN2* and in a negative direction for *APOE*) (Tian et al., 2012). In our data, mRNA for *CRABP2*, *FABP5* and *LCN2*, all of which can bind RA, was upregulated in PS L vs HC skin for all treatment groups. These genes then appeared downregulated following NB-UVB or secukinumab therapy, suggesting that these treatments may affect gene expression, either directly or indirectly. However, the results were not significant, which may be attributable to the small sample size.

Quantitative proteomics comparing keratome biopsies (epidermis and papillary dermis) of PS L and PS NL skin in four patients demonstrated 128 proteins with altered abundance including CRABP2, FABP5 and LCN2 (Williamson et al., 2013). Protein validation with IF IHC as outlined above was limited by the size of the biopsies and the lack of follicles in most of the samples. However, the results suggest that key binding proteins in the retinoid metabolic pathway, particularly CRABP2, are present in both healthy and chronically inflamed skin. Quantitative proteomic analysis of our samples would be helpful, which may contribute to the understanding of the therapeutic benefit of retinoids in this disease. Non-specific staining of the stratum corneum was accentuated in the acanthotic, hyperproliferative stratum corneum characteristic of lesional psoriasis. Cutaneous autofluorescence was also a potential issue and ultimately the DyLight® 594 kit was used for all staining as the DyLight® 488 kit proved too autofluorescent when trialled for LCN2 staining.

CRABP2 staining has been shown to be increased in PS L vs PS NL skin (Bianchi et al., 2018). This is unsurprising given the epidermal predilection for this stain and keratinocyte hyperproliferation in PS L skin. This is also in keeping with our results on Hyperion™.

Hyperion™ staining also revealed co-expression of several other proteins (KIT, CD45 and CRTH2) with CRABP2. This staining pattern suggests the possibility that these cells may be part of the ILC family. ILC have been shown to express CD1a and have already been implicated in inflammatory skin disease, specifically eczema, in other work from our lab (C. Hardman et al., 2017). Further evaluation is required, but this initial staining tentatively suggests that ILC may also be implicated in psoriatic inflammation.

Our findings for LCN2 echoed those of Shao et al, who found increased mRNA and protein expression in the epidermis and dermis of PS L vs HC skin (Shao et al., 2016). LCN2 protein has been identified in both lesional and non-lesional skin of psoriasis (Abdel Hay et al., 2020) and is significantly higher in psoriatic compared to healthy control skin (Abdel Hay et al., 2020; El-Hadidi et al., 2014). Based on our Hyperion™ results, as for CRABP2, this also appears to be attributable to the substantially thickened epidermis in lesional psoriasis.

APOE was the only gene of the four selected that was significantly downregulated vs HC across all PS/AD samples in our data. This is in keeping with the general widespread downregulation of genes relevant to lipid pathways in PS skin vs HC skin. Interestingly, downregulation was less marked in PS R (NB-UVB). Hyperion™ demonstrated the most ApoE staining in the healthy skin sample, supporting the downregulation of this gene in diseased skin on mRNA-Seq.

For all four genes, expression was downregulated in AD skin, more so in AD NL skin for *CRABP2*, *FABP5* and *LCN2* and to a similar level in AD L and AD NL skin (vs HC) for *APOE*. For the three genes encoding proteins capable of binding RA, this raises the possibility of opposing changes to retinoid metabolism in AD vs PS. However, it is

notable that the first-generation retinoid alitretinoin is a recommended systemic treatment for chronic hand eczema (www.nice.org.uk).

All three proteins assessed on Hyperion™ (CRABP2, LCN2, ApoE) stained sebaceous gland to varying degrees. LCN2 and ApoE were found more peripherally while CRABP2 appeared localised to the centre of the gland. Sebaceous glands produce sebum, a source of FA, squalene, cholesterol, cholesteryl esters and wax esters among other lipids. Some of these molecules have been identified as CD1a ligands(De Jong et al., 2014) and this thesis has investigated the role of others in CD1a signalling (**Chapter 6**). The cholesterol and retinoid metabolic pathways are linked via the enzyme LAL and it is germane that proteins known to bind RA such as CRABP2 and LCN2 would localise to the gland. Although the role of ApoE in the skin has yet to be fully elucidated, as a known cholesterol binding protein, its location in the sebaceous gland is apposite.

Of note, CRABP2 and FABP5 both bind atRA, but transport it to different receptors [RAR (α, β, γ) and PPARβ/δ, respectively] with subsequent activation of opposing signalling pathways (Schug et al., 2007). Which pathway is activated is dependent on the ratio of CRABP2 to FABP5 in the cell; the CRABP2/RAR pathway has a higher binding affinity for RA than FABP5/PPARβ/δ (Schug et al., 2007). Most of the scientific investigation of these proteins to date has been done in the context of cancer, with minimal data on the role of these opposing pathways in inflammatory skin disease. RNA-Seq data showed upregulation of both genes encoding these proteins in untreated PS L vs HC skin: *CRABP2* Log2FC=1.004 (not statistically significant), *FABP5* Log2FC=1.569 (statistically significant). Validating these proteins by IF IHC did not provide any statistical information on differences in expression (CRABP2 staining appeared more prominent than FABP5 in untreated PS L skin but this may have been due to artefact/non-specific staining). Unfortunately, FABP5 was not used in the Hyperion™ panel due to a lack of

detectable signal. If the protein expression levels were in a similar ratio to that of the mRNA, this would indicate that in untreated PS L skin, retinoid signalling may possibly be diverted down the PPARβ/δ pathway, which in HaCaT cells has been shown to inhibit TNF-α-induced apoptosis, as opposed to CRABP2 enhancement of TNF-α-induced apoptosis (Schug et al., 2007). This may be a contributing factor to the epidermal acanthosis seen in psoriasis, as more RA in the skin is diverted down a pro-survival pathway.

Hyperion™ staining also demonstrated the stark differences in cutaneous architecture between PS L and PS NL skin. Keratin 10 is expressed in the supra-basal epidermis and is a marker of epidermal differentiation. In our RNA-Seq data, *KRT10* is upregulated (log2FC>2) in all psoriasis groups (L and NL/R) except for PS L (Secukinumab) (**Chapter 3**). However, Hyperion™ demonstrated the strongest staining in PS NL and HC skin. A study of spreading psoriatic plaques found that there were significant increases in the proportion of keratinocytes expressing KRT10 in healthy skin compared to PS NL (distant to lesional) skin and in PS NL (both distant and adjacent to lesional) skin vs PS L (inner margin) skin (Mommers et al., 2000).

Keratin 14 stained strongly in the basal and supra-basal layers of both epidermal samples. This protein maintains the structural integrity of the epidermis and is usually found in the basal layer in healthy skin. However, it has been identified in the supra-basal layers and even stratum corneum of autoimmune skin disorders, including psoriasis (Wei et al., 2016).

In the visible dermis of the untreated PS L specimen, there is widespread CD45 staining. CD45 is a marker of differentiated haematopoietic cells, and in this context may identify the mixed inflammatory infiltrates seen in psoriasis. CD45 staining is less prominent in

PS NL skin, although residual staining suggests the presence of inflammatory infiltrates in plaque-adjacent, clinically normal skin. This suggests that even clinically normal skin in psoriasis patients, at least that adjacent to active inflammation, is poised for the development of clinical disease, which may be triggered by some as yet unconfirmed factor.

CD1a was mainly co-expressed with langerin in both healthy and psoriatic skin, implying the presence of LC, but there was an additional population of $CD1a^+$ cells in AD skin. $CD3^+$ cells were noted in the epidermis in untreated PS L skin. An apparent reduction in CD1a staining in the PS L (NB-UVB) sample suggests modulation of LC by this treatment. There is conflicting data in the literature regarding the effect of NB-UVB on LC, as summarised by Johnson-Huang et al (Johnson-Huang et al., 2010).

A limitation of the study was that only a few sections were processed, however the concurrence with RNA-Seq data and confirmation with public datasets adds weight to the relevance of the observations.

7.6 Chapter Summary

In this chapter, validation of protein expression for four genes identified as relevant to psoriasis and retinoid/lipid pathways in the skin was undertaken. IF IHC and Hyperion™ results corroborated RNA-Seq data and support the alteration of these pathways as potential contributors to inflammatory skin disease.

8 Chapter 8 Final overall discussion and future directions

8.1 Summary of results

The aim of this project was to identify novel lipid ligands for CD1a, including in the context of inflammatory disease, namely psoriasis and its treatment. There was some evidence implicating the CD1a pathway in psoriasis based on work already done in our lab (Cheung et al., 2016). Anti-CD1a antibody in an IMQ mouse model of psoriasis demonstrated clinical improvement and abrogated type 17 signalling(C. S. Hardman et al., 2022; J. H. Kim et al., 2016) while also significantly blocking the IL-17/IL-22 cytokine response in moDC-stimulated $CD45RO^{+}$ cells from the blood of patients with psoriasis (J. H. Kim et al., 2016).

Most of the ligands tested in this thesis are not well studied in the context of disease and are formed through dynamic pathways that may be heavily influenced by a complex range of environmental factors. However, the data presented suggests that RE and NFA may be candidate CD1a ligands. The retinyl and cholesteryl esters are storage forms of lipids that mainly reside within the cell or sebum, compartmentalised from CD1a. The binding of ligands to CD1a may be due to exposure to them in the event of inflammation causing a cutaneous breach or increased production of potential ligands such as the NFA. It is also feasible that CD1a ligands may be present in small amounts in the epidermal environment, for example due to cellular apoptosis as a regulatory mechanism, where they may be sampled by LC and occupy the CD1a cleft in homeostasis. CD1a itself is located predominantly at the cell surface- permitting capture of exogenous lipids- as well as in the Birbeck granules (Sugita et al., 2004) and undergoes a shallow endocytic recycling pathway similar to MHC I (Barral et al., 2008).

In testing candidate lipids, the question is not only whether they bind to the CD1a cleft but whether they can replace the endogenous (likely inhibitory) ligands already *in situ*. The ratio of activating to inhibitory lipids in the cellular environment is thought to influence CD1a binding and T cell activation (De Jong, 2015). This was the rationale for 3-day loaded gels using known CD1a lipid ligands. It is worth noting that any topically applied treatment in psoriasis is usually delivered in a vehicle consisting of varying amounts of oil and water, which itself may theoretically influence CD1a signalling. In this thesis, Psoriderm™, an over-the-counter bath additive already formulated directly for patient use, was examined as well as distilled coal tar, to try and control for this.

The cause of psoriasis is unknown and Genome Wide Association Studies have sought to identify genetic predisposition and disease associations, as summarised by Antonatos et al (Antonatos et al., 2023). A recent Mendelian randomisation study suggested causality for MUFA and ω-6 PUFA in psoriasis (Li et al., 2024). Our RNA-Seq data supported published results regarding abnormal lipid pathways in psoriasis, with the downregulation of multiple genes involved in lipid pathways in both lesional and non-lesional skin suggesting that the skin of patients with psoriasis is abnormal at a gene expression level, whether clinically affected or not. Changes in expression of genes encoding phospholipases may influence the availability of ligands for CD1a binding. Expression of genes of retinoid pathways were also altered, which is unsurprising when it is considered that retinoids are an established therapy in this disease. However, the complexity of these pathways and the number of enzymes makes it difficult to fully delineate the implications of these alterations. The results of our RNA-Seq analysis also echoed published literature and GEO DataSets results regarding differential gene expression in psoriasis, although our dataset was unique in the variety of biopsies from patients with psoriasis under different therapeutic modalities. There is only one other dataset from patients treated with an anti-IL-17A biologic (ixekizumab), however,

samples were all of lesional skin, taken at baseline, weeks 1, 2 and 4 of treatment, without a healthy control group (GSE 178228), while our samples were taken after a minimum of three months of treatment. Imaging mass cytometry with Hyperion™ was used for validation of several proteins important to lipid and retinoid pathways (**Chapter 7**) and confirmed the differential expression of these genes in psoriatic vs healthy skin identified in the RNA-Seq data (**Chapter 3**).

8.2 Limitations of methods used

The identification of candidate CD1a ligands posed a number of challenges.

A number of ligands had been identified in the literature, but the field was rapidly evolving. Initial published studies suggested potentially stringent criteria for CD1a-binding but further work revealed diversity in chain length and polarity of ligands and the revelation that direct recognition of bound ligand by the TCR of reactive T cells may not be necessary. The starting point for this project was therefore based on clinical knowledge of psoriasis therapeutics, with a focus on longstanding psoriasis treatments where the mode of action had not been fully elucidated, such as coal tar derivatives and acitretin. Particular challenges related to the complex composition of the coal tar derivatives, the toxicity of acitretin and difficulties related to solubility.

Possible endogenous lipid antigens related to pathways that were known to be disrupted in inflammatory skin disease were also examined. For RE and CE, these storage forms of active metabolites were putatively CD1a ligands in homeostasis, while NFA are dynamic molecules possibly acting as CD1a ligands in the context of inflammation, when they have the potential to be formed locally in large amounts. A nitrogen stream was installed to facilitate drying of these chemicals to remove solvent excipients while

avoiding dissipation of the small volume of lipid. There were also issues with purchased materials; for example, the contents of one large (1mg) vial of 9-NO were subsequently found not to produce a shift on IEF gels. Cholesterol and its esters were the most challenging as they were fine powders/flakes with associated challenges in accurate generation of solutions. The main assay challenges related to solubility of these lipids and sonication in a warm water bath was used in an attempt to overcome this but was not always successful and cell-based assays and flow cytometry may have been affected.

There were many technical issues with ELISpot assays with low spot numbers and attempts to elicit the underlying cause were unsuccessful. Therefore, these results cannot be reliably interpreted. ELISA did suggest some changes in T cell IFN-γ secretion with lipid-pulsed K562 cells. Unfortunately, GM-CSF and IL-22 clones mostly did not reach the limit of assay detection for IL-17A, TNF-α and IL-22.

Cholesterol and its esters were generally made up fresh for use in experiments, while RE and NFA were aliquoted and dissolved on receipt of the original package, then frozen at -20C. Any vials kept at 4˚C and used for numerous experiments were discarded within 4-6 weeks of initial use. However, although precautions were taken to avoid contamination, it is not known whether repeated sonication may have had any long-term effect on lipid composition/structure that may have influenced CD1a loading.

Assessment of potential CD1a ligands *in vitro* may differ from that *in vivo*, not least because cells used as surrogate APC (K562 cells and moDC in this project) are not identical. The K562 model has been validated as a surrogate for APC (De Jong et al., 2010), however their use adds complexity as cellular factors are relevant; e.g. retinoids and their receptors have been shown to have effects in chronic myelogenous leukaemia (CML) and K562 cells are a leukaemia cell line derived from a patient with CML. CD1a

on the surface of K562 cells differs from recombinant protein (from 293T cells), which was employed in the IEF gel assays. It has been suggested that CD1a expression levels in moDC are lower compared to those in LC-like DC and langerin, which may have a role in antigen uptake and processing, is minimally expressed in moDC and not at all in K562 (Hunger et al., 2004). The concentration of the lipids used was based on toxicity testing in order to minimise impact on the cells, however, this also means that use of a higher concentration to saturate the cells and possibly improve ligand loading and potentially cytokine signal detection was not possible.

As for most scientific work, the experiments presented here are an approximation of a biological system which is not yet fully understood, with the caveats that entails.

Finally, all of this work took place during the Covid-19 pandemic, when there were restrictions in place with regards to laboratory access and access to clinical samples and delays in obtaining consumables, particularly some of the candidate lipid antigens used which were shipped from Canada.

8.3 Future Directions

Investigation of potential CD1a ligands as reported in this thesis, although without definitive proof, strongly suggests that retinyl esters and NFA may bind CD1a and exert effects on human T cells. Next steps would be to overcome technical issues and repeat further polyclonal assays on a larger scale. If it was feasible to identify any CD1a-reactive T cell clones from these assays, isolation and expansion of such clones with further assessment of characteristics such as additional surface markers and TCR sequencing would be useful, e.g. in the case of 10-NO, which exhibited a reduction in IFN-γ signalling, to ascertain whether these cells were inflammatory or regulatory T cells.

Solving the crystal structure of the TCR of CD1a-reactive T cell clones for these ligands would also further inform our understanding of the potential role of these lipids in the immune response. Subsequently, further investigation of these ligands with murine models could be attempted. Topical application of these ligands in IMQ models of psoriasis in transgenic CD1a mice may help to elucidate their clinical impact on inflammation. As CD1a is located in the epidermis, it is potentially accessible as a topical therapeutic target and so pharmacological development and human trials may be possible future options if such studies yielded significant results.

Further analysis of RNA-Seq data, in particular genes that remain differentially regulated compared to healthy skin at sites of clinical resolution of disease may inform greater understanding of the effects of NB-UVB and secukinumab and the reason for disease relapse on cessation of treatment.

Hyperion™ imaging mass cytometry offers novel imaging with exquisite levels of detail of the expression of proteins in diseased and healthy skin. As discussed in **Chapter 7**, the final choice of proteins for validation by IF IHC and Hyperion™ was determined from a shortlist of genes of interest based on our RNA-Seq data, the literature, GEO Profiles and GEO DataSets and the Human Developmental Cell Atlas (Reynolds et al., 2021). It would be informative to examine other genes from this shortlist in more detail, particularly those that exhibited changes in differential expression (vs healthy controls) in untreated and clinically resolved psoriasis (e.g. **Table 4.2**).

8.4 Final thoughts

The field of CD1a biology is rapidly evolving and the implication of this pathway in cutaneous inflammatory disease offers exciting opportunities for accessible therapeutic

targets. Many endogenous CD1a ligands that have been identified are found in healthy skin, suggesting that an imbalance in the lipid environment may play a role in disease and restoration of lipid homeostasis may be relevant to disease resolution. Replacement of displaced lipids or addressing environmental factors such as changes in the cutaneous microbiome that alter the lipid milieu are potential new avenues in approaching the management of skin disease. Greater understanding of the psoriatic transcriptome and how it differs from that of healthy skin may inform identification of relevant biological pathways for investigation as possible therapeutic targets.

References

Abdel Hay, R., Samir, N., Safwat, M., Rashed, L., & Soliman, M. (2020). Tissue lipocalin-2 in psoriasis: is it a marker of metabolic disturbance or a possible marker of therapeutic efficacy after narrow band ultraviolet B? *Journal of Dermatological Treatment*, *31*(5), 519–523. https://doi.org/10.1080/09546634.2019.1605141

Acosta-Rodriguez, E. V., Rivino, L., Geginat, J., Jarrossay, D., Gattorno, M., Lanzavecchia, A., Sallusto, F., & Napolitani, G. (2007). Surface phenotype and antigenic specificity of human interleukin 17-producing T helper memory cells. *Nature Immunology*, *8*(6), 639–646. https://doi.org/10.1038/ni1467

Addison, R., Weatherhead, S. C., Pawitri, A., Smith, G. R., Rider, A., Grantham, H. J., Cockell, S. J., & Reynolds, N. J. (2021). Therapeutic wavelengths of ultraviolet B radiation activate apoptotic, circadian rhythm, redox signalling and key canonical pathways in psoriatic epidermis. *Redox Biology*, *41*. https://doi.org/10.1016/j.redox.2021.101924

Alekseyenko, A. V, Perez-Perez, G. I., De Souza, A., Strober, B., Gao, Z., Bihan, M., Li, K., Methé, B. A., & Blaser, M. J. (2013). Community differentiation of the cutaneous microbiota in psoriasis. *Microbiome*, *1*(1), 1–17. https://doi.org/10.1186/2049-2618-1-31

Algermissen, B., Sitzmann, J., LeMotte, P., & Czarnetzki, B. (1996). Differential expression of CRABP II, psoriasin and cytokeratin 1 mRNA in human skin diseases. *Archives of Dermatological Research*, *288*(8), 426–430.

Almutawa, F., Alnomair, N., Wang, Y., Hamzavi, I., & Lim, H. W. (2013). Systematic review of UV-based therapy for psoriasis. *American Journal of Clinical Dermatology*, *14*(2), 87–109. https://doi.org/10.1007/s40257-013-0015-y

Amatya, N., Garg, A. V., & Gaffen, S. L. (2017). IL-17 Signaling: The Yin and the Yang. *Trends in Immunology*, *38*(5), 310–322. https://doi.org/10.1016/j.it.2017.01.006

Antille, C., Tran, C., Sorg, O., Carraux, P., Didierjean, L., & Saurat, J. H. (2003). Vitamin A Exerts a Photoprotective Action in Skin by Absorbing Ultraviolet B Radiation. *Journal of Investigative Dermatology*, *121*(5), 1163–1167. https://doi.org/10.1046/j.1523-1747.2003.12519.x

Antonatos, C., Grafanaki, K., Georgiou, S., Evangelou, E., & Vasilopoulos, Y. (2023). Disentangling the complexity of psoriasis in the post-genome-wide association era. In *Genes and Immunity* (Vol. 24, Issue 5, pp. 236–247). Springer Nature. https://doi.org/10.1038/s41435-023-00222-x

Arican, O., Aral, M., Sasmaz, S., & Ciragil, P. (2005). Serum levels of TNF-α, IFN-γ, IL-6, IL-8, IL-12, IL-17, and IL-18 in patients with active psoriasis and correlation with disease severity. *Mediators of Inflammation*, *2005*(5), 273–279. https://doi.org/10.1155/MI.2005.273

Assarsson, M., Duvetorp, A., Dienus, O., Söderman, J., & Seifert, O. (2018). Significant changes in the skin microbiome in patients with chronic plaque psoriasis after treatment with narrowband ultraviolet B. *Acta Dermato-Venereologica*, *98*(4), 428–436. https://doi.org/10.2340/00015555-2859

Ataseven, A., Kesli, R., Kurtipek, G. S., & Ozturk, P. (2014). Assessment of lipocalin 2, clusterin, soluble tumor necrosis factor receptor-1, interleukin-

6, homocysteine, and uric acid levels in patients with psoriasis. *Disease Markers*, *2014*. https://doi.org/10.1155/2014/541709

Auboeck, J., Romani, N., Grubauer, G., & Fritsch, P. (1986). HLA-DR expression on keratinocytes is a common feature of diseased skin. *British Journal of Dermatology*, *114*(4), 465–472. https://doi.org/10.1111/j.1365-2133.1986.tb02851.x

Austin, L. M., Ozawa, M., Kikuchi, T., Walters, I. B., & Krueger, J. G. (1999). The majority of epidermal T cells in psoriasis vulgaris lesions can produce type 1 cytokines, interferon-γ, interleukin-2, and tumor necrosis factor-α, defining TC1 (cytotoxic T lymphocyte) and TH1 effector populations: A type 1 differentiation bias is al. *Journal of Investigative Dermatology*, *113*(5), 752–759. https://doi.org/10.1046/j.1523-1747.1999.00749.x

Bagchi, S., He, Y., Zhang, H., Cao, L., Van Rhijn, I., Moody, D. B., Gudjonsson, J. E., & Wang, C. R. (2017). CD1b-autoreactive T cells contribute to hyperlipidemia-induced skin inflammation in mice. *Journal of Clinical Investigation*, *127*(6), 2339–2352. https://doi.org/10.1172/JCI92217

Baker, P. R. S., Lin, Y., Schopfer, F. J., Woodcock, S. R., Groeger, A. L., Batthyany, C., Sweeney, S., Long, M. H., Iles, K. E., Baker, L. M. S., Branchaud, B. P., Chen, Y. E., & Freeman, B. A. (2005). Fatty acid transduction of nitric oxide signaling: Multiple nitrated unsaturated fatty acid derivatives exist in human blood and urine and serve as endogenous peroxisome proliferator-activated receptor ligands. *Journal of Biological Chemistry*, *280*(51), 42464–42475. https://doi.org/10.1074/jbc.M504212200

Baker, P. R. S., Schopfer, F. J., Sweeney, S., & Freeman, B. A. (2004). Red cell membrane and plasma linoleic acid nitration products: Synthesis, clinical identification, and quantitation. *Proceedings of the National Academy of Sciences*, *101*(32), 11577–11582. www.pnas.orgcgidoi10.1073pnas.0402587101

Baran, A., Świderska, M., Myśliwiec, H., & Flisiak, I. (2017). Effect of psoriasis activity and topical treatment on serum lipocalin-2 levels. *Journal of Dermatological Treatment*, *28*(2), 136–140. https://doi.org/10.1080/09546634.2016.1180340

Barral, D. C., Cavallari, M., McCormick, P. J., Garg, S., Magee, A. I., Bonifacino, J. S., De Libero, G., & Brenner, M. B. (2008). CD1a and MHC class I follow a similar endocytic recycling pathway. *Traffic*, *9*(9), 1446–1457. https://doi.org/10.1111/j.1600-0854.2008.00781.x

Barrett, T., Wilhite, S. E., Ledoux, P., Evangelista, C., Kim, I. F., Tomashevsky, M., Marshall, K. A., Phillippy, K. H., Sherman, P. M., Holko, M., Yefanov, A., Lee, H., Zhang, N., Robertson, C. L., Serova, N., Davis, S., & Soboleva, A. (2013). NCBI GEO: Archive for functional genomics data sets - Update. *Nucleic Acids Research*, *41*(Database Issue), 991–995. https://doi.org/10.1093/nar/gks1193

Bécherel, P. A., Le Goff, L., Ktorza, S., Chosidow, O., Francès, C., Issaly, F., Mencia-Huerta, J. M., Debré, P., Mossalayi, M. D., & Arock, M. (1996). CD23-mediated nitric oxide synthase pathway induction in human keratinocytes is inhibited by retinoic acid derivatives. *Journal of Investigative Dermatology*, *106*(6), 1182–1186. https://doi.org/10.1111/1523-1747.ep12347939

Bécherel, P. A., Mossalayi, M. D., LeGoff, L., Francès, C., Chosidow, O., Debré, P., & Arock, M. (1994). Mechanism of anti-inflammatory action of retinoids on keratinocytes. *Lancet*, *344*(8936), 1570–1571.

Berod, L., Friedrich, C., Nandan, A., Freitag, J., Hagemann, S., Harmrolfs, K., Sandouk, A., Hesse, C., Castro, C. N., BäHre, H., Tschirner, S. K., Gorinski, N., Gohmert, M., Mayer, C. T., Huehn, J., Ponimaskin, E., Abraham, W. R., MüLler, R., Lochner, M., & Sparwasser, T. (2014). De novo fatty acid synthesis controls the fate between regulatory T and T helper 17 cells. *Nature Medicine*, *20*(11), 1327–1333. https://doi.org/10.1038/nm.3704

Bhattacharya, D., Basta, B., Mato, J. M., Craig, A., Fernández-Ramos, D., Lopitz-Otsoa, F., Tsvirkun, D., Hayardeny, L., Chandar, V., Schwartz, R. E., Villanueva, A., & Friedman, S. L. (2021). Aramchol downregulates stearoyl CoA-desaturase 1 in hepatic stellate cells to attenuate cellular fibrogenesis. *JHEP Reports*, *3*(3). https://doi.org/10.1016/j.jhepr.2021.100237

Bianchi, L., Costanza, G., Campione, E., Ruzzetti, M., Di Stefani, A., Diluvio, L., Giardina, E., Cascella, R., Cordiali-Fei, P., Bonifati, C., Chiricozzi, A., Novelli, G., Ensoli, F., & Orlandi, A. (2018). Biomolecular index of therapeutic efficacy in psoriasis treated with anti-TNF-α agents. *Giornale Italiano Di Dermatologia e Venereologia*, *153*(3), 316–325. https://doi.org/10.23736/S0392-0488.16.05427-4

Bickers, D. R., & Lowy, D. R. (1989). Carcinogenesis: A fifty-year historical perspective. *Journal of Investigative Dermatology*, *92*(4 SUPPL.), 121–131. https://doi.org/10.1038/jid.1989.39

Birkinshaw, R. W., Pellicci, D. G., Cheng, T.-Y., Keller, A. N., Sandoval-Romero, M., Gras, S., De Jong, A., Uldrich, A. P., Moody, D. B., Godfrey, D. I., & Rossjohn, J. (2015). αβ T cell antigen receptor recognition of CD1a presenting self lipid ligands. *Nature Immunology*, *16*(3), 258–266. https://doi.org/10.1038/ni.3098

Bissonnette, R., Papp, K., Maari, C., Yao, Y., Robbie, G., White, W. I., Le, C., & White, B. (2010). A randomized, double-blind, placebo-controlled, phase I study of MEDI-545, an anti-interferon-alfa monoclonal antibody, in subjects with chronic psoriasis. *Journal of the American Academy of Dermatology*, *62*(3), 427–436. https://doi.org/10.1016/j.jaad.2009.05.042

Black, A. P. B., Ardern-Jones, M. R., Kasprowicz, V., Bowness, P., Jones, L., Bailey, A. S., & Ogg, G. S. (2007). Human keratinocyte induction of rapid effector function in antigen-specific memory CD4+ and CD8+ T cells. *European Journal of Immunology*, *37*(6), 1485–1493. https://doi.org/10.1002/eji.200636915

Blauvelt, A., Prinz, J. C., Gottlieb, A. B., Kingo, K., Sofen, H., Ruer-Mulard, M., Singh, V., Pathan, R., Papavassilis, C., & Cooper, S. (2015). Secukinumab administration by pre-filled syringe: Efficacy, safety and usability results from a randomized controlled trial in psoriasis (FEATURE). *British Journal of Dermatology*, *172*(2), 484–493. https://doi.org/10.1111/bjd.13348

Blomhoff, R. (2001). Vitamin A and carotenoid toxicity. *Food and Nutrition Bulletin*, *22*(3), 320–334. https://doi.org/10.1177/156482650102200309

Blomhoff, R., Beckman-Sundh, U., Brot, C., Solvoll, K., Steingrimsdóttir, L., & Carlsen, M. H. (2003). Health risks related to high intake of preformed

retinol (vitamin A) in the Nordic countries. *Nordic Council of Ministers*, 113. http://folk.uio.no/runeb/pdf filer/Vitamin A toxicity.PDF

Blomhoff, R., & Blomhoff, H. K. (2006). Overview of retinoid metabolism and function. In *Journal of Neurobiology* (Vol. 66, Issue 7, pp. 606–630). https://doi.org/10.1002/neu.20242

Bonacci, G., Baker, P. R. S., Salvatore, S. R., Shores, D., Khoo, N. K. H., Koenitzer, J. R., Vitturi, D. A., Woodcock, S. R., Golin-Bisello, F., Cole, M. P., Watkins, S., St. Croix, C., Batthyany, C. I., Freeman, B. A., & Schopfer, F. J. (2012). Conjugated linoleic acid is a preferential substrate for fatty acid nitration. *Journal of Biological Chemistry*, *287*(53), 44071–44082. https://doi.org/10.1074/jbc.M112.401356

Boniface, K., Bernard, F.-X., Garcia, M., Gurney, A. L., Lecron, J.-C., & Morel, F. (2005). IL-22 Inhibits Epidermal Differentiation and Induces Proinflammatory Gene Expression and Migration of Human Keratinocytes. *Journal of Immunology*, *174*(6), 3695–3702. https://doi.org/10.4049/jimmunol.174.6.3695

Boniface, K., Guignouard, E., Pedretti, N., Garcia, M., Delwail, A., Bernard, F. X., Nau, F., Guillet, G., Dagregorio, G., Yssel, H., Lecron, J. C., & Morel, F. (2007). A role for T cell-derived interleukin 22 in psoriatic skin inflammation. *Clinical and Experimental Immunology*, *150*(3), 407–415. https://doi.org/10.1111/j.1365-2249.2007.03511.x

Bos, J. D., Zonneveld, I., Das, P. K., Krieg, S. R., van der Loos, C. M., & Kapsenberg, M. L. (1987). The skin immune system (SIS): Distribution and immunophenotype of lymphocyte subpopulations in normal human skin. *Journal of Investigative Dermatology*, *88*(5), 569–573. https://doi.org/10.1111/1523-1747.ep12470172

Bourgeois, E. A., Subramaniam, S., Cheng, T.-Y., De Jong, A., Layre, E., Ly, D., Salimi, M., Legaspi, A., Modlin, R. L., Salio, M., Cerundolo, V., Moody, D. B., & Ogg, G. (2015). Bee venom processes human skin lipids for presentation by CD1a. *Journal of Experimental Medicine*, *212*(2), 149–163. https://doi.org/10.1084/jem.20141505

Bovenschen, H. J., Van De Kerkhof, P. C., Van Erp, P. E., Woestenenk, R., Joosten, I., & Koenen, H. J. P. M. (2011). Foxp3 regulatory T cells of psoriasis patients easily differentiate into IL-17A-producing cells and are found in lesional skin. *Journal of Investigative Dermatology*, *131*(9), 1853–1860. https://doi.org/10.1038/jid.2011.139

Bowcock, A. M., Shannon, W., Du, F., Duncan, J., Cao, K., Aftergut, K., Catier, J., Fernandez-Vina, M. A., & Menter, A. (2001). Insights into psoriasis and other inflammatory diseases from large-scale gene expression studies. In *Human Molecular Genetics* (Vol. 10). http://hg.wustl.edu

Boyman, O., Hefti, H. P., Conrad, C., Nickoloff, B. J., Suter, M., & Nestle, F. O. (2004). Spontaneous Development of Psoriasis in a New Animal Model Shows an Essential Role for Resident T Cells and Tumor Necrosis Factor-α. *Journal of Experimental Medicine*, *199*(5), 731–736. https://doi.org/10.1084/jem.20031482

Brembilla, N. C., Senra, L., & Boehncke, W. H. (2018). The IL-17 family of cytokines in psoriasis: IL-17A and beyond. *Frontiers in Immunology*, *9*(AUG). https://doi.org/10.3389/fimmu.2018.01682

Bryan, E., Teague, J. E., Eligul, S., Arkins, W. C., Moody, D. B., Clark, R. A., & Van Rhijn, I. (2024). Human Skin T Cells Express Conserved T-Cell Receptors that Cross-React with Staphylococcal Superantigens and

CD1a. *Journal of Investigative Dermatology*, *144*(4), 833-843.e3. https://doi.org/10.1016/j.jid.2023.09.284

Buchan, G. J., Bonacci, G., Fazzari, M., Salvatore, S. R., & Gelhaus Wendell, S. (2018). Nitro-fatty acid formation and metabolism. In *Nitric Oxide - Biology and Chemistry* (Vol. 79, pp. 38–44). Academic Press Inc. https://doi.org/10.1016/j.niox.2018.07.003

Caporarello, N., Salmeri, M., Scalia, M., Motta, C., Parrino, C., Frittitta, L., Olivieri, M., Toscano, M. A., Anfuso, C. D., & Lupo, G. (2015). Role of cytosolic and calcium independent phospholipases A2 in insulin secretion impairment of INS-1E cells infected by S. aureus. *FEBS Letters*, *589*(24), 3969–3976. https://doi.org/10.1016/j.febslet.2015.11.035

Chamcheu, J. C., Chaves-Rodriquez, M. I., Adhami, V. M., Siddiqui, I. A., Wood, G. S., Jack Longley, B., & Mukhtar, H. (2016). Upregulation of PI3K/AKT/mTOR, FABP5 and PPARβ/δ in human psoriasis and imiquimod-induced murine psoriasiform dermatitis model. *Acta Dermato-Venereologica*, *96*(6), 854–856. https://doi.org/10.2340/00015555-2359

Chan, J. R., Blumenschein, W., Murphy, E., Diveu, C., Wiekowski, M., Abbondanzo, S., Lucian, L., Geissler, R., Brodie, S., Kimball, A. B., Gorman, D. M., Smith, K., Malefyt, R. D. W., Kastelein, R. A., McClanahan, T. K., & Bowman, E. P. (2006). IL-23 stimulates epidermal hyperplasia via TNF and IL-20R2-dependent mechanisms with implications for psoriasis pathogenesis. *Journal of Experimental Medicine*, *203*(12), 2577–2587. https://doi.org/10.1084/jem.20060244

Chang, H. W., Yan, D., Singh, R., Liu, J., Lu, X., Ucmak, D., Lee, K., Afifi, L., Fadrosh, D., Leech, J., Vasquez, K. S., Lowe, M. M., Rosenblum, M. D., Scharschmidt, T. C., Lynch, S. V., & Liao, W. (2018). Alteration of the

cutaneous microbiome in psoriasis and potential role in Th17 polarization. *Microbiome*, *6*(1), 1–27. https://doi.org/10.1186/s40168-018-0533-1

Chaudhuri, R. K., & Bojanowski, K. (2014). Bakuchiol: A retinol-like functional compound revealed by gene expression profiling and clinically proven to have anti-aging effects. *International Journal of Cosmetic Science*, *36*(3), 221–230. https://doi.org/10.1111/ics.12117

Cheuk, S., Wikén, M., Blomqvist, L., Nylén, S., Talme, T., Ståhle, M., & Eidsmo, L. (2014). Epidermal Th22 and Tc17 Cells Form a Localized Disease Memory in Clinically Healed Psoriasis. *Journal of Immunology*, *192*(7), 3111–3120. https://doi.org/10.4049/jimmunol.1302313

Cheung, K. L., Jarrett, R., Subramaniam, S., Salimi, M., Gutowska-Owsiak, D., Chen, Y.-L., Hardman, C., Xue, L., Cerundolo, V., & Ogg, G. (2016). Psoriatic T cells recognize neolipid antigens generated by mast cell phospholipase delivered by exosomes and presented by CD1a. *Journal of Experimental Medicine*, *213*(11), 2399–2412. https://doi.org/10.1084/jem.20160258

Chiba, H., Michibata, H., Wakimoto, K., Seishima, M., Kawasaki, S., Okubo, K., Mitsui, H., Torii, H., & Imai, Y. (2004). Cloning of a Gene for a Novel Epithelium-specific Cytosolic Phospholipase A2, cPLA2δ, Induced in Psoriatic Skin. *Journal of Biological Chemistry*, *279*(13), 12890–12897. https://doi.org/10.1074/jbc.M305801200

Chiricozzi, A., Suárez-Fariñas, M., Fuentes-Duculan, J., Cueto, I., Li, K., Tian, S., Brodmerkel, C., & Krueger, J. G. (2016). Increased expression of interleukin-17 pathway genes in nonlesional skin of moderate-to-severe

psoriasis vulgaris. *British Journal of Dermatology*, *174*(1), 136–145. https://doi.org/10.1111/bjd.14034

Chodorowska, G. (1998). Plasma concentrations of IFN-γ and TNF-α in psoriatic patients before and after local treatment with dithranol ointment. *Journal of the European Academy of Dermatology and Venereology*, *10*(2), 147–151. https://doi.org/10.1016/S0926-9959(97)00182-7

Clark, R. A., Chong, B., Mirchandani, N., Brinster, N. K., Yamanaka, K., Dowgiert, R. K., & Kupper, T. S. (2006). The Vast Majority of CLA + T Cells Are Resident in Normal Skin. *Journal of Immunology*, *176*(7), 4431–4439. https://doi.org/10.4049/jimmunol.176.7.4431

Clark, R. A., Huang, S. J., Murphy, G. F., Mollet, I. G., Hijnen, D., Muthukuru, M., Schanbacher, C. F., Edwards, V., Miller, D. M., Kim, J. E., Lambert, J., & Kupper, T. S. (2008). Human squamous cell carcinomas evade the immune response by down-regulation of vascular E-selectin and recruitment of regulatory T cells. *Journal of Experimental Medicine*, *205*(10), 2221–2234. https://doi.org/10.1084/jem.20071190

Clark, R. A., & Kupper, T. S. (2007). IL-15 and dermal fibroblasts induce proliferation of natural regulatory T cells isolated from human skin. *Blood*, *109*(1), 194–202. https://doi.org/10.1182/blood-2006-02-002873

Collins, C. A., & Watt, F. M. (2008). Dynamic regulation of retinoic acid-binding proteins in developing, adult and neoplastic skin reveals roles for β-catenin and Notch signalling. *Developmental Biology*, *324*(1), 55–67. https://doi.org/10.1016/j.ydbio.2008.08.034

Cooper, M. F., McGrath, H., & Shuster, S. (1976). Epidermal lipid metabolism in psoriasis and lichen simplex. *British Journal of Dermatology*, *94*(4), 369–378. https://doi.org/10.1111/j.1365-2133.1976.tb06114.x

Cotton, R. N., Wegrecki, M., Cheng, T.-Y., Chen, Y.-L., Veerapen, N., Le Nours, J., Orgill, D. P., Pomahac, B., Talbot, S. G., Willis, R., Altman, J. D., De Jong, A., Van Rhijn, I., Clark, R. A., Besra, G. S., Ogg, G., Rossjohn, J., & Moody, D. B. (2021). CD1a selectively captures endogenous cellular lipids that broadly block T cell response. *Journal of Experimental Medicine*, *218*(7). https://doi.org/10.1084/jem.20202699

Dallaglio, K., Marconi, A., Truzzi, F., Lotti, R., Palazzo, E., Petrachi, T., Saltari, A., Coppini, M., & Pincelli, C. (2013). E-FABP induces differentiation in normal human keratinocytes and modulates the differentiation process in psoriatic keratinocytes in vitro. *Experimental Dermatology*, *22*(4), 255–261. https://doi.org/10.1111/exd.12111

Dawson, T. L. (2007). Malassezia globosa and restricta: Breakthrough understanding of the etiology and treatment of dandruff and seborrheic dermatitis through whole-genome analysis. *Journal of Investigative Dermatology. Symposium Proceedings*, *12*(2), 15–19. https://doi.org/10.1038/sj.jidsymp.5650049

De Jong, A. (2015). Activation of human T cells by CD1 and self-lipids. *Immunological Reviews*, *267*, 16–29.

De Jong, A., Cheng, T.-Y., Huang, S., Gras, S., Birkinshaw, R. W., Kasmar, A. G., Van Rhijn, I., Peña-Cruz, V., Ruan, D. T., Altman, J. D., Rossjohn, J., & Moody, D. B. (2014). CD1a-autoreactive T cells recognize natural skin oils that function as headless antigens. *Nature Immunology*, *15*(2), 177–185. https://doi.org/10.1038/ni.2790

De Jong, A., Peña-Cruz, V., Cheng, T.-Y., Clark, R. A., Van Rhijn, I., & Moody, D. B. (2010). CD1a-autoreactive T cells are a normal component of the

human αβ T cell repertoire. *Nature Immunology*, *11*(12), 1102–1109. https://doi.org/10.1038/ni.1956

De Jongh, G. J., Zeeuwen, P. L. J. M., Kucharekova, M., Pfundt, R., Van Der Valk, P. G., Blokx, W., Dogan, A., Hiemstra, P. S., Van De Kerkhof, P. C., & Schalkwijk, J. (2005). High expression levels of keratinocyte antimicrobial proteins in psoriasis compared with atopic dermatitis. *Journal of Investigative Dermatology*, *125*(6), 1163–1173. https://doi.org/10.1111/j.0022-202X.2005.23935.x

De Lalla, C., Lepore, M., Piccolo, F. M., Rinaldi, A., Scelfo, A., Garavaglia, C., Mori, L., De Libero, G., Dellabona, P., & Casorati, G. (2011). High-frequency and adaptive-like dynamics of human CD1 self-reactive T cells. *European Journal of Immunology*, *41*(3), 602–610. https://doi.org/10.1002/eji.201041211

Debes, G. F., & McGettigan, S. E. (2019). Skin-Associated B Cells in Health and Inflammation. *Journal of Immunology*, *202*(6), 1659–1666. https://doi.org/10.4049/jimmunol.1801211

Deng, J., Leijten, E., Nordkamp, M. O., Zheng, G., Pouw, J., Tao, W., Hartgring, S., Balak, D., Rijken, R., Huang, R., Radstake, T., Lu, C., & Pandit, A. (2022). Multi-omics integration reveals a core network involved in host defence and hyperkeratinization in psoriasis. *Clinical and Translational Medicine*, *12*(12). https://doi.org/10.1002/ctm2.976

Dou, J., Zhang, L., Xie, X., Ye, L., Yang, C., Wen, L., Shen, C., Zhu, C., Zhao, S., Zhu, Z., Liang, B., Wang, Z., Li, H., Fan, X., Liu, S., Yin, X., Zheng, X., Sun, L., Yang, S., … Zhang, X. (2017). Integrative analyses reveal biological pathways and key genes in psoriasis. *British Journal of Dermatology*, *177*(5), 1349–1357. https://doi.org/10.1111/bjd.15682

Duhen, T., Geiger, R., Jarrossay, D., Lanzavecchia, A., & Sallusto, F. (2009). Production of interleukin 22 but not interleukin 17 by a subset of human skin-homing memory T cells. *Nature Immunology*, *10*(8), 857–863. https://doi.org/10.1038/ni.1767

Duthie, M. S., Kimber, I., & Norval, M. (1999). The effects of ultraviolet radiation on the human immune system. In *British Journal of Dermatology* (Vol. 140, Issue 6, pp. 995–1009). https://doi.org/10.1046/j.1365-2133.1999.02898.x

Edgar, R., Domrachev, M., & Lash, A. E. (2002). Gene Expression Omnibus: NCBI gene expression and hybridization array data repository. *Nucleic Acids Research*, *30*(1), 207–210. http://www.ninds.nih.gov/

Eidsmo, L., & Martini, E. (2018). Human Langerhans cells with pro-inflammatory features relocate within psoriasis lesions. *Frontiers in Immunology*, *9*, 1–8. https://doi.org/10.3389/fimmu.2018.00300

El-Hadidi, H., Samir, N., Shaker, O. G., & Otb, S. (2014). Estimation of tissue and serum lipocalin-2 in psoriasis vulgaris and its relation to metabolic syndrome. *Archives of Dermatological Research*, *306*(3), 239–245. https://doi.org/10.1007/s00403-013-1414-x

Fahlén, A., Engstrand, L., Baker, B. S., Powles, A., & Fry, L. (2012). Comparison of bacterial microbiota in skin biopsies from normal and psoriatic skin. *Archives of Dermatological Research*, *304*(1), 15–22. https://doi.org/10.1007/s00403-011-1189-x

Feingold, K. R., & Jiang, Y. J. (2011). The mechanisms by which lipids coordinately regulate the formation of the protein and lipid domains of the stratum corneum Role of fatty acids, oxysterols, cholesterol sulfate and

ceramides as signaling molecules. *Dermato-Endocrinology*, *3*(2), 113–118. https://doi.org/10.4161/derm.3.2.14496

Finlay, A. Y., & Khan, G. K. (1994). Dermatology Life Quality Index (DLQI)—a simple practical measure for routine clinical use. *Clinical and Experimental Dermatology*, *19*(3), 210–216. https://doi.org/10.1111/j.1365-2230.1994.tb01167.x

Flowers, M. T., Paton, C. M., O'Byrne, S. M., Schiesser, K., Dawson, J. A., Blaner, W. S., Kendziorski, C., & Ntambi, J. M. (2011). Metabolic changes in skin caused by scd1 deficiency: A focus on retinol metabolism. *PLoS ONE*, *6*(5). https://doi.org/10.1371/journal.pone.0019734

Foster, B. Y. C. A., Yokozeki, H., Rappersberger, K., Koning, F., Volc-platzer, I. B., Rieger, A., Coligan, J. E., Wolff, K., & Stingl, G. (1990). Human epidermal T cell predominantly belong to the lineage expressing αβ T cell receptor. *Journal of Experimental Medicine*, *171*(April), 997–1013.

Fredriksson, T., & Pettersson, U. (1978). Severe psoriasis — Oral therapy with a new retinoid. *Dermatologica*, *157*(4), 238–244. https://doi.org/10.1159/000250839

Freeman, B. A., Baker, P. R. S., Schopfer, F. J., Woodcock, S. R., Napolitano, A., & D'Ischia, M. (2008). Nitro-fatty acid formation and signaling. *Journal of Biological Chemistry*, *283*(23), 15515–15519. https://doi.org/10.1074/jbc.R800004200

Gao, Z., Tseng, C. H., Strober, B. E., Pei, Z., & Blaser, M. J. (2008). Substantial alterations of the cutaneous bacterial biota in psoriatic lesions. *PLoS ONE*, *3*(7). https://doi.org/10.1371/journal.pone.0002719

Gara, A., Estrada, E., Rothman, S., & Lorincz, A. L. (1964). Deficient cholesterol esterifying ability of lesion-free skin surfaces in psoriatic individuals. *Journal of Investigative Dermatology*, *43*(6), 559–564. https://doi.org/10.1038/jid.1964.198

Garner, R. M., Mould, D. R., Chieffo, C., & Jorkasky, D. K. (2019). Pharmacokinetic and Pharmacodynamic Effects of Oral CXA-10, a Nitro Fatty Acid, After Single and Multiple Ascending Doses in Healthy and Obese Subjects. *Clinical and Translational Science*, *12*(6), 667–676. https://doi.org/10.1111/cts.12672

Gericke, J., Ittensohn, J., Mihály, J., Álvarez, S., Álvarez, R., Töröcsik, D., de Lera, Á. R., & Rühl, R. (2013). Regulation of Retinoid-Mediated Signaling Involved in Skin Homeostasis by RAR and RXR Agonists/Antagonists in Mouse Skin. *PLoS ONE*, *8*(4). https://doi.org/10.1371/journal.pone.0062643

Gilat, T., Somjen, G. J., Mazur, Y., Leikin-Frenkel, A., Rosenberg, R., Halpern, Z., & Konikoff, F. M. (2001). Fatty acid bile acid conjugates (FABACs)-New molecules for the prevention of cholesterol crystallisation in bile. *Gut*, *48*(1), 75–79. www.gutjnl.com

Gollnick, H. P. M. (1996). Oral retinoids-efficacy and toxicity in psoriasis. *British Journal of Dermatology, Supplement*, *135*(49), 6–17. https://doi.org/10.1111/j.1365-2133.1996.tb15661.x

Gordon, D. A., Fenjves, E. S., Williams, D. L., & Taichman, L. B. (1989). Synthesis and secretion of apolipoprotein e by cultured human keratinocytes. *Journal of Investigative Dermatology*, *92*(1), 96–99. https://doi.org/10.1111/1523-1747.ep13071302

Gottlieb, S. L., Gilleaudeau, P., Johnson, R., Estes, L., Woodworth, T. G., Gottlieb, A. B., & Krueger, J. G. (1995). Response of psoriasis to a lymphocyte-selective toxin (DAB389IL-2) suggests a primary immune, but not keratinocyte, pathogenic basis. *Nature Medicine*, *1*(5), 442–447. https://doi.org/10.1038/nm0595-442

Griffiths, C. E. M., Armstrong, A. W., Gudjonsson, J. E., & Barker, J. N. W. N. (2021). Psoriasis. In *Lancet* (Vol. 397, Issue 10281, pp. 1301–1315). Elsevier B.V. https://doi.org/10.1016/S0140-6736(20)32549-6

Griffiths, C. E. M., Voorhees, John. J., & Nickoloff, B. J. (1989). Gamma interferon induces different keratinocyte cellular patterns of expression of HLA-DR and DQ and intercellular adhesion molecule-I (ICAM-I) antigens. *British Journal of Dermatology*, *120*(1), 1–7. https://doi.org/10.1111/j.1365-2133.1989.tb07759.x

Grubauer, G., Feingold, K. R., & Elias, P. M. (1987). Relationship of epidermal lipogenesis to cutaneous barrier function. *Journal of Lipid Research*, *28*(6), 746–752.

Gruber, F., Kremslehner, C., & Narzt, M. S. (2019). The impact of recent advances in lipidomics and redox lipidomics on dermatological research. *Free Radical Biology and Medicine*, *144*(January), 256–265. https://doi.org/10.1016/j.freeradbiomed.2019.04.019

Gudjonsson, J. E., Ding, J., Johnston, A., Tejasvi, T., Guzman, A. M., Nair, R. P., Voorhees, J. J., Abecasis, G. R., & Elder, J. T. (2010). Assessment of the psoriatic transcriptome in a large sample: Additional regulated genes and comparisons with in vitro models. *Journal of Investigative Dermatology*, *130*(7), 1829–1840. https://doi.org/10.1038/jid.2010.36

Gudjonsson, J. E., Ding, J., Li, X., Nair, R. P., Tejasvi, T., Qin, Z. S., Ghosh, D., Aphale, A., Gumucio, D. L., Voorhees, J. J., Abecasis, G. R., & Elder, J. T. (2009). Global gene expression analysis reveals evidence for decreased lipid biosynthesis and increased innate immunity in uninvolved psoriatic skin. *Journal of Investigative Dermatology*, *129*(12), 2795–2804. https://doi.org/10.1038/jid.2009.173

Gudjonsson, J. E., Johnston, A., Stoll, S. W., Riblett, M. B., Xing, X., Kochkodan, J. J., Ding, J., Nair, R. P., Aphale, A., Voorhees, J. J., & Elder, J. T. (2010). Evidence for altered wnt signaling in psoriatic skin. *Journal of Investigative Dermatology*, *130*(7), 1849–1859. https://doi.org/10.1038/jid.2010.67

Guo, X. (2000). Esterification of all-trans-retinol in normal human epithelial cell strains and carcinoma lines from oral cavity, skin and breast: reduced expression of lecithin:retinol acyltransferase in carcinoma lines. *Carcinogenesis*, *21*(11), 1925–1933. https://doi.org/10.1093/carcin/21.11.1925

Gupta, D. S., Kaul, D., Kanwar, A. J., & Parsad, D. (2010). Psoriasis: Crucial role of LXR-α RNomics. *Genes and Immunity*, *11*(1), 37–44. https://doi.org/10.1038/gene.2009.63

Guttman-Yassky, E., Brunner, P. M., Neumann, A. U., Khattri, S., Pavel, A. B., Malik, K., Singer, G. K., Baum, D., Gilleaudeau, P., Sullivan-Whalen, M., Rose, S., Jim On, S., Li, X., Fuentes-Duculan, J., Estrada, Y., Garcet, S., Traidl-Hoffmann, C., Krueger, J. G., & Lebwohl, M. G. (2018). Efficacy and safety of fezakinumab (an IL-22 monoclonal antibody) in adults with moderate-to-severe atopic dermatitis inadequately controlled by conventional treatments: A randomized, double-blind, phase 2a trial.

Journal of the American Academy of Dermatology, *78*(5), 872-881.e6. https://doi.org/10.1016/j.jaad.2018.01.016

Guttman-Yassky, E., Lowes, M. A., Fuentes-Duculan, J., Zaba, L. C., Cardinale, I., Nograles, K. E., Khatcherian, A., Novitskaya, I., Carucci, J. A., Bergman, R., & Krueger, J. G. (2008). Low Expression of the IL-23/Th17 Pathway in Atopic Dermatitis Compared to Psoriasis 1. *Journal of Immunology*, *181*, 7420–7427. http://www.ncbi.nlm.nih.gov/LocusLink

Gyöngyösi, A., Szatmari, I., Pap, A., Dezso, B., Pos, Z., Széles, L., Varga, T., & Nagy, L. (2013). RDH10, RALDH2, and CRABP2 are required components of PPAR γ-directed ATRA synthesis and signaling in human dendritic cells. *Journal of Lipid Research*, *54*(9), 2458–2474. https://doi.org/10.1194/jlr.M038984

Hagens, G., Roulin, K., Hotz, R., Saurat, J.-H., Hellman, U., & Siegenthaler, G. (1999). Probable interaction between S100A7 and E-FABP in the cytosol of human keratinocytes from psoriatic scales. *Molecular and Cellular Biochemistry*, *192*, 123–128.

Haider, A. S., Cohen, J., Fei, J., Zaba, L. C., Cardinale, I., Toyoko, K., Ott, J., & Krueger, J. G. (2008). Insights into gene modulation by therapeutic TNF and IFNγ antibodies: TNF regulates IFNγ production by T cells and TNF-regulated genes linked to psoriasis transcriptome. *Journal of Investigative Dermatology*, *128*(3), 655–666. https://doi.org/10.1038/sj.jid.5701064

Haider, A. S., Lowes, M. A., Suárez-Fariñ, M., Zaba, L. C., Cardinale, I., Khatcherian, A., Novitskaya, I., Wittkowski, K. M., & Krueger, J. G. (2008). Identification of Cellular Pathways of ‘Type 1,’ Th17 T Cells, and TNF-and Inducible Nitric Oxide Synthase-Producing Dendritic Cells in

Autoimmune Inflammation through Pharmacogenomic Study of Cyclosporine A in Psoriasis 1. *Journal of Immunology*, *180*(3), 1913–1920. www.bioconductor.

Han, Y., Liu, T., & Lu, L. (2013). Apolipoprotein E Gene Polymorphism in Psoriasis: A Meta-analysis. *Archives of Medical Research*, *44*(1), 46–53. https://doi.org/10.1016/j.arcmed.2012.10.009

Hao, J., Yu, J., Yorek, M. S., Yu, C. L., Pope, R. M., Chimenti, M. S., Xiong, Y., Klingelhutz, A., Jabbari, A., & Li, B. (2023). Keratinocyte FABP5-VCP complex mediates recruitment of neutrophils in psoriasis. *Cell Reports*, *42*(11). https://doi.org/10.1016/j.celrep.2023.113449

Harden, J. L., Hamm, D., Gulati, N., Lowes, M. A., & Krueger, J. G. (2015). Deep Sequencing of the T-cell Receptor Repertoire Demonstrates Polyclonal T-cell Infiltrates in Psoriasis. *F1000Research*, *4*(460). https://doi.org/10.12688/f1000research.6756.1

Harden, J. L., Johnson-Huang, L. M., Chamian, M. F., Lee, E., Pearce, T., Leonardi, C. L., Haider, A., Lowes, M. A., & Krueger, J. G. (2015). Humanized anti-IFN-γ (HuZAF) in the treatment of psoriasis. *Journal of Allergy and Clinical Immunology*, *135*(2), 553-556.e3. https://doi.org/10.1016/j.jaci.2014.05.046

Hardman, C., Chen, Y.-L., Salimi, M., Jarrett, R., Johnson, D., Järvinen, V. J., Owens, R. J., Repapi, E., Cousins, D. J., Barlow, J. L., McKenzie, A. N. J., & Ogg, G. (2017). CD1a presentation of endogenous antigens by group 2 innate lymphoid cells. *Science Immunology*, *2*(18). https://doi.org/10.1126/sciimmunol.aan5918

Hardman, C. S., Chen, Y. L., Wegrecki, M., Ng, S. W., Murren, R., Mangat, D., Silva, J. P., Munro, R., Chan, W. Y., O'Dowd, V., Doyle, C., Mori, P.,

Popplewell, A., Rossjohn, J., Lightwood, D., & Ogg, G. S. (2022). CD1a promotes systemic manifestations of skin inflammation. *Nature Communications*, *13*(1). https://doi.org/10.1038/s41467-022-35071-1

Harrington, L. E., Hatton, R. D., Mangan, P. R., Turner, H., Murphy, T. L., Murphy, K. M., & Weaver, C. T. (2005). Interleukin 17-producing CD4+ effector T cells develop via a lineage distinct from the T helper type 1 and 2 lineages. *Nature Immunology*, *6*(11), 1123–1132. https://doi.org/10.1038/ni1254

Headington, J. T., Gupta, A. K., Goldfarb, M. T., Nickoloff, B. J., Hamilton, T. A., Ellis, C. N., & Voorhees, J. J. (1989). A Morphometric and Histologic Study of the Scalp in Psoriasis: Paradoxical Sebaceous Gland Atrophy and Decreased Hair Shaft Diameters Without Alopecia. *Archives of Dermatology*, *125*(5), 639–642. https://doi.org/10.1001/archderm.1989.01670170053007

Hijnen, D., Knol, E. F., Gent, Y. Y., Giovannone, B., Beijn, S. J. P., Kupper, T. S., Bruijnzeel-Koomen, C. A. F. M., & Clark, R. A. (2013). CD8+ T cells in the lesional skin of atopic dermatitis and psoriasis patients are an important source of IFN-γ, IL-13, IL-17, and IL-22. *Journal of Investigative Dermatology*, *133*(4), 973–979. https://doi.org/10.1038/jid.2012.456

Hirahara, K., Liu, L., Clark, R. A., Yamanaka, K., Fuhlbrigge, R. C., & Kupper, T. S. (2006). The Majority of Human Peripheral Blood CD4 + CD25 high Foxp3 + Regulatory T Cells Bear Functional Skin-Homing Receptors . *Journal of Immunology*, *177*(7), 4488–4494. https://doi.org/10.4049/jimmunol.177.7.4488

Ho, A. W., & Kupper, T. S. (2019). T cells and the skin: from protective immunity to inflammatory skin disorders. *Nature Reviews Immunology*, *19*(8), 490–502. https://doi.org/10.1038/s41577-019-0162-3

Holleran, W. M., Uchida, Y., Halkier-Sorensen, L., Haratake, A., Hara, M., Epstein, J. H., & Elias, P. M. (1997). Structural and biochemical basis for the UVB-induced alterations in epidermal barrier function. *Photodermatology Photoimmunology and Photomedicine*, *13*(4), 117–128. https://doi.org/10.1111/j.1600-0781.1997.tb00214.x

Hori, S., Nomura, T., & Sakaguchi, S. (2003). Control of regulatory T cell development by the transcription factor Foxp3. *Science*, *299*(3), 1057–1061. https://doi.org/10.1126/science.1079490

Huang, S., Shahine, A., Cheng, T.-Y., Chen, Y.-L., Ng, S. W., Balaji, G., Farquhar, R., Gras, S., Hardman, C., Altman, J., Tahiri, N., Minnaard, A., Ogg, G., Mayfield, J., Rossjohn, J., & Moody, B. (2023). CD1 lipidomes reveal lipid-binding motifs and size-based antigen-display mechanisms. *Cell*, *186*(21), 4583-4596.e13. https://doi.org/10.1016/j.cell.2023.08.022

Hunger, R. E., Sieling, P. A., Ochoa, M. T., Sugaya, M., Burdick, A. E., Rea, T. H., Brennan, P. J., Belisle, J. T., Blauvelt, A., Porcelli, S. A., & Modlin, R. L. (2004). Langerhans cells utilize CD1a and langerin to efficiently present nonpeptide antigens to T cells. *Journal of Clinical Investigation*, *113*(5), 701–708. https://doi.org/10.1172/JCI200419655

Ilic, D., Bollinger, J. M., Gelb, M., & Mauro, T. M. (2014). SPLA2 and the epidermal barrier. *Biochimica et Biophysica Acta - Molecular and Cell Biology of Lipids*, *1841*(3), 416–421. https://doi.org/10.1016/j.bbalip.2013.11.002

Ivanov, I. I., McKenzie, B. S., Zhou, L., Tadokoro, C. E., Lepelley, A., Lafaille, J. J., Cua, D. J., & Littman, D. R. (2006). The Orphan Nuclear Receptor RORγt Directs the Differentiation Program of Proinflammatory IL-17+ T Helper Cells. *Cell*, *126*(6), 1121–1133. https://doi.org/10.1016/j.cell.2006.07.035

Iversen, O. J., Lysvand, H., & Slupphaug, G. (2017). Pso p27, a SERPINB3/B4-derived protein, is most likely a common autoantigen in chronic inflammatory diseases. *Clinical Immunology*, *174*, 10–17. https://doi.org/10.1016/j.clim.2016.11.006

Jabbari, A., Suárez-Fariñas, M., Dewell, S., & Krueger, J. G. (2012). Transcriptional profiling of psoriasis using RNA-seq reveals previously unidentified differentially expressed genes. In *Journal of Investigative Dermatology* (Vol. 132, Issue 1, pp. 246–249). Nature Publishing Group. https://doi.org/10.1038/jid.2011.267

Jacobson, N. G., Szabo, S. J., Weber-Nordt, R. M., Zhong, Z., Schreiber, R. D., Darnell, J. E., & Murphy, K. M. (1995). Interleukin 12 signaling in T helper type 1 (Th1) cells involves tyrosine phosphorylation of signal transducer and activator of transcription (Stat)3 and Stat4. *Journal of Experimental Medicine*, *181*(5), 1755–1762. https://doi.org/10.1084/jem.181.5.1755

Jakobsson, A., Westerberg, R., & Jacobsson, A. (2006). Fatty acid elongases in mammals: Their regulation and roles in metabolism. In *Progress in Lipid Research* (Vol. 45, Issue 3, pp. 237–249). https://doi.org/10.1016/j.plipres.2006.01.004

Janowski, B. A., Willy, P. J., Devi, T. R., Falck, J. R., & Mangelsdorf, D. J. (1996). An oxysterol signalling pathway mediated by the nuclear receptor LXRα. *Nature*, *383*(6602), 728–731.

Jarrett, R., Salio, M., Lloyd-Lavery, A., Subramaniam, S., Bourgeois, E., Archer, C., Cheung, K. L., Hardman, C., Chandler, D., Salimi, M., Gutowska-Owsiak, D., De La Serna, J. B., Fallon, P. G., Jolin, H., McKenzie, A., Dziembowski, A., Podobas, E. I., Bal, W., Johnson, D., … Ogg, G. (2016). Filaggrin inhibits generation of CD1a neolipid antigens by house dust mite-derived phospholipase. *Science Translational Medicine*, *8*(325). https://doi.org/10.1126/scitranslmed.aad6833

Johnson-Huang, L. M., Suárez-Farĩas, M., Sullivan-Whalen, M., Gilleaudeau, P., Krueger, J. G., & Lowes, M. A. (2010). Effective narrow-band UVB radiation therapy suppresses the IL-23/IL-17 Axis in normalized psoriasis plaques. *Journal of Investigative Dermatology*, *130*(11), 2654–2663. https://doi.org/10.1038/jid.2010.166

Kamata, M., Tada, Y., Tatsuta, A., Kawashima, T., Shibata, S., Mitsui, H., Asano, Y., Sugaya, M., Kadono, T., Kanda, N., Watanabe, S., & Sato, S. (2012). Serum lipocalin-2 levels are increased in patients with psoriasis. *Clinical and Experimental Dermatology*, *37*(3), 296–299. https://doi.org/10.1111/j.1365-2230.2011.04265.x

Kansanen, E., Jyrkkänen, H. K., Volger, O. L., Leinonen, H., Kivelä, A. M., Häkkinen, S. K., Woodcock, S. R., Schopfer, F. J., Horrevoets, A. J., Ylä-Herttuala, S., Freeman, B. A., & Levonen, A. L. (2009). Nrf2-dependent and -independent responses to nitro-fatty acids in human endothelial cells: Identification of heat shock response as the major pathway

activated by nitro-oleic acid. *Journal of Biological Chemistry*, *284*(48), 33233–33241. https://doi.org/10.1074/jbc.M109.064873

Kashem, S. W., Haniffa, M., & Kaplan, D. H. (2017). Antigen-Presenting Cells in the Skin. *Annual Review of Immunology*, *35*(1), 469–499. https://doi.org/10.1146/annurev-immunol-051116-052215

Kasmar, A. G., Van Rhijn, I., Magalhaes, K. G., Young, D. C., Cheng, T.-Y., Turner, M. T., Schiefner, A., Kalathur, R. C., Wilson, I. A., Bhati, M., Gras, S., Birkinshaw, R. W., Tan, L. L., Rossjohn, J., Shires, J., Jakobsen, S., Altman, J. D., & Moody, D. B. (2013). Cutting Edge: CD1a Tetramers and Dextramers Identify Human Lipopeptide–Specific T Cells Ex Vivo. *Journal of Immunology*, *191*(9), 4499–4503. https://doi.org/10.4049/jimmunol.1301660

Kellum, R. E. (1967). Human Sebaceous Gland Lipids. *Archives of Dermatology*, *95*(2), 218–220. https://doi.org/10.1001/archderm.1967.01600320074015

Kim, J., Bissonnette, R., Lee, J., Correa da Rosa, J., Suárez-Fariñas, M., Lowes, M. A., & Krueger, J. G. (2016). The Spectrum of Mild to Severe Psoriasis Vulgaris Is Defined by a Common Activation of IL-17 Pathway Genes, but with Key Differences in Immune Regulatory Genes. *Journal of Investigative Dermatology*, *136*(11), 2173–2182. https://doi.org/10.1016/j.jid.2016.04.032

Kim, J. E., Lee, J., Huh, Y. J., Kim, K., Chaparala, V., Krueger, J. G., & Kim, J. (2024). Genomic Profiling of the Overlap Phenotype between Psoriasis and Atopic Dermatitis. *Journal of Investigative Dermatology*, *144*(1), 43-52.e6. https://doi.org/10.1016/j.jid.2023.06.194

Kim, J. H., Hu, Y., Yongqing, T., Kim, J., Hughes, V. A., Le Nours, J., Marquez, E. A., Purcell, A. W., Wan, Q., Sugita, M., Rossjohn, J., & Winau, F. (2016). CD1a on Langerhans cells controls inflammatory skin disease. *Nature Immunology*, *17*(10), 1159–1166. https://doi.org/10.1038/ni.3523

Kooyman, D. J. (1932). LIX.-Lipids of the skin: Some changes in the lipids of the epidermis during the process of keratinization. *AMA Archives of Dermatology and Syphilology*, *25*(2), 245–255. https://jamanetwork.com/

Koutoulogenis, G. S., & Kokotos, G. (2021). Nitro fatty acids (No2-fas): An emerging class of bioactive fatty acids. In *Molecules* (Vol. 26, Issue 24). MDPI. https://doi.org/10.3390/molecules26247536

Kozłowska, D., Myśliwiec, H., Harasim-Symbor, E., Milewska, A. J., Chabowski, A., & Flisiak, I. (2021). Serum fatty acid binding protein 5 (FABP5) as a potential biomarker of inflammation in psoriasis. *Molecular Biology Reports*, *48*(5), 4421–4429. https://doi.org/10.1007/s11033-021-06461-3

Kryczek, I., Bruce, A. T., Gudjonsson, J. E., Johnston, A., Aphale, A., Vatan, L., Szeliga, W., Wang, Y., Liu, Y., Welling, T. H., Elder, J. T., & Zou, W. (2008). Induction of IL-17 + T Cell Trafficking and Development by IFN-γ: Mechanism and Pathological Relevance in Psoriasis . *Journal of Immunology*, *181*(7), 4733–4741. https://doi.org/10.4049/jimmunol.181.7.4733

Kuljpers, A. L. A., Bergers, M., Siegenthaler, G., Zeeuwen, P. L. J. M., Van De Kerkhof, P. C. M., & Schalkwijk, J. (1997). Skin-derived Antileukoproteinase (SKALP) and Epidermal Fatty Acid-binding Protein (E-FABP): Two Novel Markers of the Psoriatic Phenotype that Respond

Differentially to Topical Steroid. *Acta Dermato-Venereologica (Stockh)*, *77*, 14–19.

Kulski, J. K., Kenworthy, W., Bellgard, M., Taplin, R., Okamoto, K., Oka, A., Mabuchi, T., Ozawa, A., Tamiya, G., & Inoko, H. (2005). Gene expression profiling of Japanese psoriatic skin reveals and increased activity in molecular stress and immune response signals. *Journal of Molecular Medicine*, *83*, 964–975.

Kundu, J., Kim, D. H., Kundu, J. K., & Chun, K. S. (2014). Thymoquinone induces heme oxygenase-1 expression in HaCaT cells via Nrf2/ARE activation: Akt and AMPKα as upstream targets. *Food and Chemical Toxicology*, *65*, 18–26. https://doi.org/10.1016/j.fct.2013.12.015

Kurlandsky, S. B., Duell, E. A., Kang, S., Voorhees, J. J., & Fisher, G. J. (1996). Auto-regulation of retinoic acid biosynthesis through regulation of retinol esterification in human keratinocytes. *Journal of Biological Chemistry*, *271*(26), 15346–15352. https://doi.org/10.1074/jbc.271.26.15346

Lammintausta, K., Zimerson, E., Hasan, T., Susitaival, P., Winhoven, S., Gruvberger, B., Beck, M., Williams, J. D., & Bruze, M. (2010). An epidemic of furniture-related dermatitis: Searching for a cause. *British Journal of Dermatology*, *162*(1), 108–116. https://doi.org/10.1111/j.1365-2133.2009.09419.x

Lampe, M. A., Burlingame, A. L., Whitney, J., Williams, M. L., Brown, B. E., Roitman, E., & Elias, P. M. (1983). Human stratum corneum lipids: characterization and regional variations. *Journal of Lipid Research*, *24*(2), 120–130. http://www.ncbi.nlm.nih.gov/pubmed/6833889

Langley, R. G., Elewski, B. E., Lebwohl, M., Reich, K., Griffiths, C. E. M., Papp, K., Puig, L., Nakagawa, H., Spelman, L., Sigurgeirsson, B., Rivas, E., Tsai, T. F., Wasel, N., Tyring, S., Salko, T., Hampele, I., Notter, M., Karpov, A., Helou, S., & Papavassilis, C. (2014). Secukinumab in plaque psoriasis - Results of two phase 3 trials. *New England Journal of Medicine*, *371*(4), 326–338. https://doi.org/10.1056/NEJMoa1314258

Langrish, C. L., Chen, Y., Blumenschein, W. M., Mattson, J., Basham, B., Sedgwick, J. D., McClanahan, T., Kastelein, R. A., & Cua, D. J. (2005). IL-23 drives a pathogenic T cell population that induces autoimmune inflammation. *Journal of Experimental Medicine*, *201*(2), 233–240. https://doi.org/10.1084/jem.20041257

Lavker, R. M., Grove, G. L., & Kligman, A. M. (1981). The atrophogenic effect of crude coal tar on human epidermis. *British Journal of Dermatology*, *105*(1), 77–82. https://doi.org/10.1111/j.1365-2133.1981.tb00885.x

Le Nours, J., Shahine, A., & Gras, S. (2018). Molecular features of lipid-based antigen presentation by group 1 CD1 molecules. *Seminars in Cell and Developmental Biology*, *84*, 48–57. https://doi.org/10.1016/j.semcdb.2017.11.002

Lee, D. D., Stojadinovic, O., Krzyzanowska, A., Vouthounis, C., Blumenberg, M., & Tomic-Canic, M. (2009). Retinoid-responsive transcriptional changes in epidermal keratinocytes. *Journal of Cellular Physiology*, *220*(2), 427–439. https://doi.org/10.1002/jcp.21784

Li, J., Li, X., Hou, R., Liu, R., Zhao, X., Dong, F., Wang, C., Yin, G., & Zhang, K. (2015). Psoriatic T cells reduce epidermal turnover time and affect cell proliferation contributed from differential gene expression. *Journal of Dermatology*, *42*(9), 874–880. https://doi.org/10.1111/1346-8138.12961

Li, J., Olshansky, M., Carbone, F. R., & Ma, J. Z. (2016). Transcriptional analysis of T cells resident in human skin. *PLoS ONE*, *11*(1), 1–16. https://doi.org/10.1371/journal.pone.0148351

Li, J., Shen, Q., Guo, C., Wang, Y., Ma, Y., & Zhang, Y. (2024). Causality of unsaturated fatty acids and psoriasis a Mendelian randomization study. *Frontiers in Nutrition*, *11*. https://doi.org/10.3389/fnut.2024.1280962

Liang, S. C., Tan, X. Y., Luxenberg, D. P., Karim, R., Dunussi-Joannopoulos, K., Collins, M., & Fouser, L. A. (2006). Interleukin (IL)-22 and IL-17 are coexpressed by Th17 cells and cooperatively enhance expression of antimicrobial peptides. *Journal of Experimental Medicine*, *203*(10), 2271–2279. https://doi.org/10.1084/jem.20061308

Lin, A. M., Rubin, C. J., Khandpur, R., Wang, J. Y., Riblett, M., Yalavarthi, S., Villanueva, E. C., Shah, P., Kaplan, M. J., & Bruce, A. T. (2011). Mast Cells and Neutrophils Release IL-17 through Extracellular Trap Formation in Psoriasis. *Journal of Immunology*, *187*(1), 490–500. https://doi.org/10.4049/jimmunol.1100123

Liu, S. Y., Aliyari, R., Chikere, K., Li, G., Marsden, M. D., Smith, J. K., Pernet, O., Guo, H., Nusbaum, R., Zack, J. A., Freiberg, A. N., Su, L., Lee, B., & Cheng, G. (2013). Interferon-Inducible Cholesterol-25-Hydroxylase Broadly Inhibits Viral Entry by Production of 25-Hydroxycholesterol. *Immunity*, *38*(1), 92–105. https://doi.org/10.1016/j.immuni.2012.11.005

Lundberg, J. O., Weitzberg, E., Cole, J. A., & Benjamin, N. (2004). Nitrate, bacteria and human health. *Nature Reviews Microbiology*, *2*(7), 593–602. www.nature.com/reviews/micro

Ma, J., Chen, J., Xue, K., Yu, C., Dang, E., Qiao, H., Fang, H., Pang, B., Li, Q., Sun, Z., Qiao, P., Wang, L., Wang, G., & Shao, S. (2022). LCN2

Mediates Skin Inflammation in Psoriasis through the SREBP2–NLRC4 Axis. *Journal of Investigative Dermatology*, *142*(8), 2194-2204.e11. https://doi.org/10.1016/j.jid.2022.01.012

Ma, S., Gobis, K., Swindell, W. R., Chaudhuri, R., Bojanowski, R., & Bojanowski, K. (2017). Synthesis and activity of the salicylic acid ester of bakuchiol in psoriasis-surrogate keratinocytes and skin substitutes. *Clinical and Experimental Dermatology*, *42*(3), 251–260. https://doi.org/10.1111/ced.13024

Madsen, P., Rasmussen, H. H., Leffers, H., Honoré, B., & Celis, J. E. (1992). Molecular cloning and expression of a novel keratinocyte protein (psoriasis-associated fatty acid-binding protein [PA-FABP]) that is highly upregulated in psoriatic skin and that shares similarity to fatty acid-binding proteins. *Journal of Investigative Dermatology*, *99*(3), 299–305. https://doi.org/10.1111/1523-1747.ep12616641

Mallbris, L., O, K. P., Hulthén, A., skin Bengt Sandstedt, human, Cowland, J. B., & Borregaard, N. (2002). Neutrophil gelatinase-associated lipocalin is a marker for dysregulated keratinocyte differentiation in human skin. *Experimental Dermatology*, *11*, 584–591.

Mason, A., Mason, J., Cork, M., Hancock, H., & Dooley, G. (2013). Topical treatments for chronic plaque psoriasis. *Cochrane Database of Systematic Reviews*, *28*(3), 1–805. https://doi.org/10.1016/j.jaad.2013.06.027

Mathers, A. R., Carey, C. D., Killeen, M. E., Diaz-Perez, J. A., Salvatore, S. R., Schopfer, F. J., Freeman, B. A., & Falo, L. D. (2017). Electrophilic nitro-fatty acids suppress allergic contact dermatitis in mice. *Allergy*, *72*(4), 656–664. https://doi.org/10.1111/all.13067

Mathers, A. R., Carey, C. D., Killeen, M. E., Salvatore, S. R., Ferris, L. K., Freeman, B. A., Schopfer, F. J., & Falo, L. D. (2018). Topical electrophilic nitro-fatty acids potentiate cutaneous inflammation. *Free Radical Biology and Medicine*, *115*, 31–42. https://doi.org/10.1016/j.freeradbiomed.2017.11.009

Matos, T. R., O'Malley, J. T., Lowry, E. L., Hamm, D., Kirsch, I. R., Robins, H. S., Kupper, T. S., Krueger, J. G., & Clark, R. A. (2017). Clinically resolved psoriatic lesions contain psoriasis-specific IL-17-producing αβ T cell clones. *Journal of Clinical Investigation*, *127*(11), 4031–4041. https://doi.org/10.1172/JCI93396

McCusker, M. M., & Grant-Kels, J. M. (2010). Healing fats of the skin: The structural and immunologic roles of the Ω-6 and Ω-3 fatty acids. *Clinics in Dermatology*, *28*(4), 440–451. https://doi.org/10.1016/j.clindermatol.2010.03.020

Mehta, N. N., Teague, H. L., Swindell, W. R., Baumer, Y., Ward, N. L., Xing, X., Baugous, B., Johnston, A., Joshi, A. A., Silverman, J., Barnes, D. H., Wolterink, L., Nair, R. P., Stuart, P. E., Playford, M., Voorhees, J. J., Sarkar, M. K., Elder, J. T., Gallagher, K., … Gudjonsson, J. E. (2017). IFN-γ and TNF-α synergism may provide a link between psoriasis and inflammatory atherogenesis. *Scientific Reports*, *7*(1). https://doi.org/10.1038/s41598-017-14365-1

Meunier, L., Vian, L., Lagoueyte, C., Lavabre-Bertrand, T., Duperray, C., Meynadier, J., & Cano, J. P. (1996). Quantification of CD1a, HLA-DR, and HLA class I expression on viable human Langerhans cells and keratinocytes. *Communications in Clinical Cytometry*, *26*(4), 260–264.

https://doi.org/10.1002/(SICI)1097-0320(19961215)26:4<260::AID-CYTO4>3.0.CO;2-G

Miao, C., Li, J., Li, Y., & Zhang, X. (2019). Obesity and dyslipidemia in patients with psoriasis: A case-control study. *Medicine (Baltimore)*, *98*(31), 1–5.

Michalek, R. D., Gerriets, V. A., Jacobs, S. R., Macintyre, A. N., MacIver, N. J., Mason, E. F., Sullivan, S. A., Nichols, A. G., & Rathmell, J. C. (2011). Cutting Edge: Distinct Glycolytic and Lipid Oxidative Metabolic Programs Are Essential for Effector and Regulatory CD4+ T Cell Subsets. *Journal of Immunology*, *186*(6), 3299–3303. https://doi.org/10.4049/jimmunol.1003613

Miyake, T., Ogawa, E., Mikoshiba, A., Kobayashi, A., Hosoe, H., Kashiwabara, S., Uhara, H., Owada, Y., & Okuyama, R. (2012). Epidermal-type FABP is a predictive marker of clinical response to systemic treatment and ultraviolet therapy in psoriatic skin lesions. In *Journal of Dermatological Science* (Vol. 68, Issue 3, pp. 199–202). https://doi.org/10.1016/j.jdermsci.2012.09.007

Mommers, J. M., Van Rossum, M. M., Van Erp, P. E. J., & Van De Kerkhof, P. C. M. (2000). Clinical and Laboratory Investigations Changes in Keratin 6 and Keratin 10 (Co-)Expression in Lesional and Symptomless Skin of Spreading Psoriasis. *Dermatology*, *201*(1), 15–20.

Monnot, G. C., Wegrecki, M., Cheng, T.-Y., Chen, Y.-L., Sallee, B. N., Chakravarthy, R., Karantza, I. M., Tin, S. Y., Khaleel, A. E., Monga, I., Uwakwe, L. N., Tillman, A., Cheng, B., Youssef, S., Ng, S. W., Shahine, A., Garcia-Vilas, J. A., Uhlemann, A. C., Bordone, L. A., … De Jong, A. (2023). Staphylococcal phosphatidylglycerol antigens activate human T

cells via CD1a. *Nature Immunology*, *24*(1), 110–122. https://doi.org/10.1038/s41590-022-01375-z

Moody, D. B., & Cotton, R. N. (2017). Four pathways of CD1 antigen presentation to T cells. *Current Opinion in Immunology*, *46*(Dc), 127–133. https://doi.org/10.1016/j.coi.2017.07.013

Moody, D. B., Young, D. C., Cheng, T.-Y., & Rosat, J.-P. (2004). T Cell Activation by Lipopeptide Antigens. *Science*, *303*(5657), 527–531. https://doi.org/10.1126/science.1089353

Morita, H., Hori, M., & Kitano, Y. (1996). Modulation of picryl chloride-induced contact hypersensitivity reaction in mice by nitric oxide. *Journal of Investigative Dermatology*, *107*(4), 549–552. https://doi.org/10.1111/1523-1747.ep12582805

Motta, S., Monti, M., Sesana, S., Mellesi, L., Ghidoni, R., & Caputo, R. (1994). Abnormality of Water Barrier Function in Psoriasis: Role of Ceramide Fractions. *Archives of Dermatology*, *130*(4), 452–456. https://doi.org/10.1001/archderm.1994.01690040056007

Myśliwiec, H., Baran, A., Harasim-Symbor, E., Myśliwiec, P., Milewska, A. J., Chabowski, A., & Flisiak, I. (2017). Serum fatty acid profile in psoriasis and its comorbidity. *Archives of Dermatological Research*, *309*(5), 371–380. https://doi.org/10.1007/s00403-017-1748-x

Nair, R. P., Duffin, K. C., Helms, C., Ding, J., Stuart, P. E., Goldgar, D., Gudjonsson, J. E., Li, Y., Tejasvi, T., Feng, B. J., Ruether, A., Schreiber, S., Weichenthal, M., Gladman, D., Rahman, P., Schrodi, S. J., Prahalad, S., Guthery, S. L., Fischer, J., … Abecasis, G. R. (2009). Genome-wide scan reveals association of psoriasis with IL-23 and NF-κB pathways. *Nature Genetics*, *41*(2), 199–204. https://doi.org/10.1038/ng.311

Nair, R. P., Stuart, P. E., Nistor, I., Hiremagalore, R., Chia, N. V. C., Jenisch, S., Weichenthal, M., Abecasis, G. R., Lim, H. W., Christophers, E., Voorhees, J. J., & Elder, J. T. (2006). Sequence and haplotype analysis supports HLA-C as the psoriasis susceptibility 1 gene. *American Journal of Human Genetics*, *78*(5), 827–851. https://doi.org/10.1086/503821

Nencioni, A., Grü, F., Zobywlaski, A., Denzlinger, C., Brugger, W., & Brossart, P. (2002). Dendritic Cell Immunogenicity Is Regulated by Peroxisome Proliferator-Activated Receptor 1. *Journal of Immunology*, *169*, 1228–1235. http://journals.aai.org/jimmunol/article-pdf/169/3/1228/1155314/1228.pdf

Nestle, F. O., Conrad, C., Tun-Kyi, A., Homey, B., Gombert, M., Boyman, O., Burg, G., Liu, Y. J., & Gilliet, M. (2005). Plasmacytoid predendritic cells initiate psoriasis through interferon-α production. *Journal of Experimental Medicine*, *202*(1), 135–143. https://doi.org/10.1084/jem.20050500

Nestle, F. O., Di Meglio, P., Qin, J. Z., & Nickoloff, B. J. (2009). Skin immune sentinels in health and disease. *Nature Reviews Immunology*, *9*(10), 679–691. https://doi.org/10.1038/nri2622

Nicolai, S., Wegrecki, M., Cheng, T.-Y., Bourgeois, E. A., Cotton, R. N., Mayfield, J. A., Monnot, G. C., Le Nours, J., Van Rhijn, I., Rossjohn, J., Moody, D. B., & De Jong, A. (2020). Human T cell response to CD1a and contact dermatitis allergens in botanical extracts and commercial skin care products. *Science Immunology*, *5*(43), 5430. http://immunology.sciencemag.org/

Nicolaides, N. (1974). Skin Lipids - Their Biochemical Uniqueness. *Science*, *186*(4158), 19–26. https://doi.org/10.1126/science.186.4158.19

Nomura, I., Gao, B., Boguniewicz, M., Darst, M. A., Travers, J. B., & Leung, D. Y. M. (2003). Distinct patterns of gene expression in the skin lesions of atopic dermatitis and psoriasis: A gene microarray analysis. *Journal of Allergy and Clinical Immunology*, *112*(6), 1195–1202. https://doi.org/10.1016/j.jaci.2003.08.049

Nowowiejska, J., Baran, A., & Flisiak, I. (2021). Aberrations in lipid expression and metabolism in psoriasis. In *International Journal of Molecular Sciences* (Vol. 22, Issue 12). MDPI. https://doi.org/10.3390/ijms22126561

Ntambi, J. M., Miyazaki, M., Stoehr, J. P., Lan, H., Kendziorski, C. M., Yandell, B. S., Song, Y., Cohen, P., Friedman, J. M., & Attie, A. D. (2002). Loss of stearoyl-CoA desaturase-1 function protects mice against adiposity. *Proceedings of the National Academy of Sciences*, *99*(17), 11482–11486. www.pnas.orgcgidoi10.1073pnas.132384699

O'Byrne, S. M., & Blaner, W. S. (2013). Retinol and retinyl esters: Biochemistry and physiology. *Journal of Lipid Research*, *54*(7), 1731–1743. https://doi.org/10.1194/jlr.R037648

Oestreicher, J. L., Walters, I. B., Kikuchi, T., Gilleaudeau, P., Surette, J., Schwertschlag, U., Dorner, A. J., Krueger, J. G., & Trepicchio, W. L. (2001). Molecular classification of psoriasis disease-associated genes through pharmacogenomic expression profiling. In *The Pharmacogenomics Journal* (Vol. 1). www.nature.com/tpj

Okasha, E. F., Bayomy, N. A., & Abdelaziz, E. Z. (2018). Effect of Topical Application of Black Seed Oil on Imiquimod-Induced Psoriasis-like Lesions in the Thin Skin of Adult Male Albino Rats. *Anatomical Record*, *301*(1), 166–174. https://doi.org/10.1002/ar.23690

Oppmann, B., Lesley, R., Blom, B., Timans, J. C., Xu, Y., Hunte, B., Vega, F., Yu, N., Wang, J., Singh, K., Zonin, F., Vaisberg, E., Churakova, T., Liu, M. ru, Gorman, D., Wagner, J., Zurawski, S., Liu, Y. J., Abrams, J. S., … Kastelein, R. A. (2000). Novel p19 protein engages IL-12p40 to form a cytokine, IL-23, with biological activities similar as well as distinct from IL-12. *Immunity*, *13*(5), 715–725. https://doi.org/10.1016/S1074-7613(00)00070-4

Ormerod, A. D., Dwyer, C. M., Reid, A., Copeland, P., & Thompson, W. D. (1997). Inducible nitric oxide synthase demonstrated in allergic and irritant contact dermatitis. *Acta Dermato-Venereologica*, *77*(6), 436–440.

Ormerod, A. D., Dwyer, C. M., Weller, R., C R Dominic H Cox, M. R., & Price, R. (1997). A comparison of subjective and objective measures of reduction of psoriasis with the use of ultrasound, reflectance colorimetry, computerized video image analysis, and nitric oxide production. *Journal of the American Academy of Dermatology*, *37*(1), 51–57.

Ormerod, A. D., Weller, R., Copeland, P., Benjamin, N., Ralston, S. H., Grabowksi, P., & Herriot R. (1998). Detection of nitric oxide and nitric oxide synthases in psoriasis. *Archives of Dermatological Research*, *290*(1–2), 3–8.

Ortiz-Salvador, J. M., Saneleuterio-Temporal, M., Magdaleno-Tapial, J., Velasco-Pastor, M., Pujol-Marco, C., Sahuquillo-Torralba, A., Mateu-Puchades, A., Pitarch-Bort, G., Marí-Ruiz, J. I., Mataix-Díaz, J., Montesinos-Villaescusa, E., Miralles-Botella, J., García-Fernández, L., Martorell-Calatayud, A., Belinchón-Romero, I., Sánchez-Carazo, J. L., & Pérez-Ferriols, A. (2019). A prospective multicenter study assessing effectiveness and safety of secukinumab in a real-life setting in 158

patients. *Journal of the American Academy of Dermatology*, *81*(2), 427–432. https://doi.org/10.1016/j.jaad.2019.02.062

Otsuka, Y., Watanabe, E., Shinya, E., Okura, S., Saeki, H., Geijtenbeek, T. B. H., & Takahashi, H. (2018). Differentiation of Langerhans Cells from Monocytes and Their Specific Function in Inducing IL-22–Specific Th Cells. *The Journal of Immunology*, *201*(10), 3006–3016. https://doi.org/10.4049/jimmunol.1701402

Paiva-Lopes, M. J., Batuca, J. R., Gouveia, S., Alves, M., Papoila, A. L., & Alves, J. D. (2020). Antibodies towards high-density lipoprotein components in patients with psoriasis. *Archives of Dermatological Research*, *312*(2), 93–102. https://doi.org/10.1007/s00403-019-01986-x

Pan, Y., Tian, T., Park, C. O., Lofftus, S. Y., Mei, S., Liu, X., Luo, C., O'Malley, J. T., Gehad, A., Teague, J. E., Divito, S. J., Fuhlbrigge, R., Puigserver, P., Krueger, J. G., Hotamisligil, G. S., Clark, R. A., & Kupper, T. S. (2017). Survival of tissue-resident memory T cells requires exogenous lipid uptake and metabolism. *Nature*, *543*(7644), 252–256. https://doi.org/10.1038/nature21379

Park, H., Li, Z., Yang, X. O., Chang, S. H., Nurieva, R., Wang, Y. H., Wang, Y., Hood, L., Zhu, Z., Tian, Q., & Dong, C. (2005). A distinct lineage of CD4 T cells regulates tissue inflammation by producing interleukin 17. *Nature Immunology*, *6*(11), 1133–1141. https://doi.org/10.1038/ni1261

Park, K., & Scott, A. L. (2010). Cholesterol 25-hydroxylase production by dendritic cells and macrophages is regulated by type I interferons. *Journal of Leukocyte Biology*, *88*(6), 1081–1087. https://doi.org/10.1189/jlb.0610318

Patel, P., Wang, J. Y., Mineroff, J., & Jagdeo, J. (2024). Evaluation of curcumin for dermatologic conditions: a systematic review. In *Archives of Dermatological Research* (Vol. 316, Issue 1). Institute for Ionics. https://doi.org/10.1007/s00403-023-02754-8

Paul, C., Lacour, J. P., Tedremets, L., Kreutzer, K., Jazayeri, S., Adams, S., Guindon, C., You, R., & Papavassilis, C. (2015). Efficacy, safety and usability of secukinumab administration by autoinjector/pen in psoriasis: A randomized, controlled trial (JUNCTURE). *Journal of the European Academy of Dermatology and Venereology*, *29*(6), 1082–1090. https://doi.org/10.1111/jdv.12751

Piesche, M., Roos, J., Kühn, B., Fettel, J., Hellmuth, N., Brat, C., Maucher, I. V., Awad, O., Matrone, C., Comerma Steffensen, S. G., Manolikakes, G., Heinicke, U., Zacharowski, K. D., Steinhilber, D., & Maier, T. J. (2020). The Emerging Therapeutic Potential of Nitro Fatty Acids and Other Michael Acceptor-Containing Drugs for the Treatment of Inflammation and Cancer. In *Frontiers in Pharmacology* (Vol. 11). Frontiers Media S.A. https://doi.org/10.3389/fphar.2020.01297

Pion, I. A., Koenig, K. L., & Lim, H. W. (1995). Is dermatologic usage of coal tar carcinogenic?. A review of the literature. *Dermatologic Surgery*, *21*(3), 227–231. https://doi.org/10.1016/1076-0512(94)00037-Q

Porcelli, S., Brenner, M. B., Greenstein, J. L., Balk, S. P., Terhorst, C., & Bleicher, P. A. (1989). Recognition of cluster of differentiation 1 antigens by human CD4-CD8- cytolytic T lymphocyte. *Nature*, *341*(6241), 447–450. https://doi.org/10.1038/341447a0

Rácz, E., Prens, E. P., Kurek, D., Kant, M., De Ridder, D., Mourits, S., Baerveldt, E. M., Ozgur, Z., Van Ijcken, W. F. J., Laman, J. D., Staal, F. J.,

& Van Der Fits, L. (2011). Effective treatment of psoriasis with narrow-band UVB phototherapy is linked to suppression of the IFN and Th17 pathways. *Journal of Investigative Dermatology*, *131*(7), 1547–1558. https://doi.org/10.1038/jid.2011.53

Randolph, R. K., & Simon, M. (1993). Characterization of retinol metabolism in cultured human epidermal keratinocytes. *Journal of Biological Chemistry*, *268*(13), 9198–9205. https://doi.org/10.1016/s0021-9258(18)98336-5

Randolph, R. K., & Simon, M. (1995). Metabolic Regulation of Active Retinoid Concentrations in Cultured Human Epidermal Keratinocytes by Exogenous Fatty Acids. *Archives of Biochemistry and Biophysics*, *318*(1), 6–14.

Randolph, R. K., & Simon, M. (1996). All-trans-retinoic acid regulates retinol and 3,4-didehydroretinol metabolism in cultured human epidermal keratinocytes. *Journal of Investigative Dermatology*, *106*(1), 168–175. https://doi.org/10.1111/1523-1747.ep12329900

Randolph, R. K., & Simon, M. (1997). Metabolism of all-trans-retinoic acid by cultured human epidermal keratinocytes. *Journal of Lipid Research*, *38*(7), 1374–1383. https://doi.org/10.1016/s0022-2275(20)37420-4

Reischl, J., Schwenke, S., Beekman, J. M., Mrowietz, U., Stürzebecher, S., & Heubach, J. F. (2007). Increased expression of Wnt5a in psoriatic plaques. *Journal of Investigative Dermatology*, *127*(1), 163–169. https://doi.org/10.1038/sj.jid.5700488

Res, P. C. M., Piskin, G., de Boer, O. J., van der Loos, C. M., Teeling, P., Bos, J. D., & Teunissen, M. B. M. (2010). Overrepresentation of IL-17A and IL-22 Producing CD8 T Cells in Lesional Skin Suggests Their Involvement in

the pathogenesis of psoriasis. *PLoS ONE*, *5*(11). https://doi.org/10.1371/journal.pone.0014108

Reynolds, G., Vegh, P., Fletcher, J., Poyner, E. F. M., Stephenson, E., Goh, I., Botting, R. A., Huang, N., Olabi, B., Dubois, A., Dixon, D., Green, K., Maunder, D., Engelbert, J., Efremova, M., Polański, K., Jardine, L., Jones, C., Ness, T., … Haniffa, M. (2021). Developmental cell programs are co-opted in inflammatory skin disease. *Science*, *371*(6527). https://doi.org/10.1126/science.aba6500

Rittié, L., Tejasvi, T., Harms, P. W., Xing, X., Nair, R. P., Gudjonsson, J. E., Swindell, W. R., & Elder, J. T. (2016). Sebaceous Gland Atrophy in Psoriasis: An Explanation for Psoriatic Alopecia? *Journal of Investigative Dermatology*, *136*(9), 1792–1800. https://doi.org/10.1016/j.jid.2016.05.113

Ro, B. I., & Dawson, T. L. (2005). The role of sebaceous gland activity and scalp microfloral metabolism in the etiology of seborrheic dermatitis and dandruff. *Journal of Investigative Dermatology Symposium Proceedings*, *10*(3), 194–197. https://doi.org/10.1111/j.1087-0024.2005.10104.x

Rodríguez-Zúñiga, M. J. M., & García-Perdomo, H. A. (2017). Systematic review and meta-analysis of the association between psoriasis and metabolic syndrome. *Journal of the American Academy of Dermatology*, *77*(4), 657-666.e8. https://doi.org/10.1016/j.jaad.2017.04.1133

Roelofzen, J. H. J., Aben, K. K. H., Oldenhof, U. T. H., Coenraads, P. J., Alkemade, H. A., Van De Kerkhof, P. C. M., Van Der Valk, P. G. M., & Kiemeney, L. A. L. M. (2010). No increased risk of cancer after coal tar treatment in patients with psoriasis or eczema. *Journal of Investigative Dermatology*, *130*(4), 953–961. https://doi.org/10.1038/jid.2009.389

Roelofzen, J. H. J., Aben, K. K. H., Van Der Valk, P. G. M., Van Houtum, J. L. M., Van De Kerkhof, P. C. M., & Kiemeney, L. A. L. M. (2007). Coal tar in dermatology. *Journal of Dermatological Treatment*, *18*(6), 329–334. https://doi.org/10.1080/09546630701496347

Romaní, J., Caixàs, A., Ceperuelo-Mallafré, V., Carrascosa, J. M., Ribera, M., Rigla, M., Vendrell, J., & Luelmo, J. (2013). Circulating levels of lipocalin-2 and retinol-binding protein-4 are increased in psoriatic patients and correlated with baseline PASI. *Archives of Dermatological Research*, *305*(2), 105–112. https://doi.org/10.1007/s00403-012-1306-5

Romanowska, M., Reilly, L., Palmer, C. N. A., Gustafsson, M. C. U., & Foerster, J. (2010). Activation of PPARβ/δ causes a psoriasis-like skin disease in vivo. *PLoS ONE*, *5*(3). https://doi.org/10.1371/journal.pone.0009701

Rothman, S. (1950). Abnormalities in the chemical composition of the skin surface film in psoriasis. *AMA Archives of Dermatology and Syphilology*, *62*(6), 814–819. https://jamanetwork.com/

Sakaguchi, S., Sakaguchi, N., Asano, M., Itoh, M., & Toda, M. (1995). Immunologic self-tolerance maintained by activated T cells expressing IL-2 receptor alpha-chains (CD25). Breakdown of a single mechanism of self-tolerance causes various autoimmune diseases. *Journal of Immunology*, *155*(3), 1151–1164. http://www.ncbi.nlm.nih.gov/pubmed/7636184

Samarasekera, E. J., Sawyer, L., Wonderling, D., Tucker, R., & Smith, C. H. (2013). Topical therapies for the treatment of plaque psoriasis: Systematic review and network meta-analyses. In *British Journal of*

Dermatology (Vol. 168, Issue 5, pp. 954–967). https://doi.org/10.1111/bjd.12276

Sampath, H., Flowers, M. T., Liu, X., Paton, C. M., Sullivan, R., Chu, K., Zhao, M., & Ntambi, J. M. (2009). Skin-specific deletion of stearoyl-CoA desaturase-1 alters skin lipid composition and protects mice from high fat diet-induced obesity. *Journal of Biological Chemistry*, *284*(30), 19961–19973. https://doi.org/10.1074/jbc.M109.014225

Saurat, J. H., Didierjean, L., Masgrau, E., Piletta, P. A., Jaconi, S., Chatellard-Gruaz, D., Gumowski, D., Masouyé, I., Salomon, D., & Siegenthaler, G. (1994). Topical retinaldehyde on human skin: Biologic effects and tolerance. *Journal of Investigative Dermatology*, *103*(6), 770–774. https://doi.org/10.1111/1523-1747.ep12412861

Sbidian, E., Chaimani, A., Garcia-Doval, I., Do, G., Hua, C., Mazaud, C., Droitcourt, C., Hughes, C., Ingram, J. R., Naldi, L., Chosidow, O., & Le Cleach, L. (2017). Systemic pharmacological treatments for chronic plaque psoriasis: A network meta-analysis. In *Cochrane Database of Systematic Reviews*. https://doi.org/doi:10.1002/14651858.CD011535.pub2.

Sbidian, E., Maza, A., Montaudié, H., Gallini, A., Aractingi, S., Aubin, F., Cribier, B., Joly, P., Jullien, D., Le Maître, M., Misery, L., Richard, M. A., Paul, C., Ortonne, J. P., & Bachelez, H. (2011). Efficacy and safety of oral retinoids in different psoriasis subtypes: A systematic literature review. *Journal of the European Academy of Dermatology and Venereology*, *25*(SUPPL. 2), 28–33. https://doi.org/10.1111/j.1468-3083.2011.03993.x

Schmidt, C., Penneys, N. S., & Ziboh, V. A. (1977). Cholesterol and cholesteryl ester content in normal and pathologic scale. *Journal of*

Investigative Dermatology, *68*(4), 206–209. https://doi.org/10.1111/1523-1747.ep12493028

Scholz, C. F. P., & Kilian, M. (2016). The natural history of cutaneous propionibacteria, and reclassification of selected species within the genus propionibacterium to the proposed novel genera acidipropionibacterium gen. Nov., cutibacterium gen. nov. and pseudopropionibacterium gen. nov. *International Journal of Systematic and Evolutionary Microbiology*, *66*(11), 4422–4432. https://doi.org/10.1099/ijsem.0.001367

Schopfer, F. J., Baker, P. R. S., Giles, G., Chumley, P., Batthyany, C., Crawford, J., Patel, R. P., Hogg, N., Branchaud, B. P., Lancaster, J. R., & Freeman, B. A. (2005). Fatty acid transduction of nitric oxide signaling: Nitrolinoleic acid is a hydrophobically stabilized nitric oxide donor. *Journal of Biological Chemistry*, *280*(19), 19289–19297. https://doi.org/10.1074/jbc.M414689200

Schopfer, F. J., & Khoo, N. K. H. (2019). Nitro-Fatty Acid Logistics: Formation, Biodistribution, Signaling, and Pharmacology. In *Trends in Endocrinology and Metabolism* (Vol. 30, Issue 8, pp. 505–519). Elsevier Inc. https://doi.org/10.1016/j.tem.2019.04.009

Schräder, M., Bendik, I., Becker-André, M., & Carlberg, C. (1993). Interaction between retinoic acid and vitamin D signaling pathways. *Journal of Biological Chemistry*, *268*(24), 17830–17836. https://doi.org/10.1016/s0021-9258(17)46779-2

Schug, T. T., Berry, D. C., Shaw, N. S., Travis, S. N., & Noy, N. (2007). Opposing Effects of Retinoic Acid on Cell Growth Result from Alternate Activation of Two Different Nuclear Receptors. *Cell*, *129*(4), 723–733. https://doi.org/10.1016/j.cell.2007.02.050

Shamshiev, A., Gober, H. J., Donda, A., Mazorra, Z., Mori, L., & De Libero, G. (2002). Presentation of the same glycolipid by different CD1 molecules. *Journal of Experimental Medicine*, *195*(8), 1013–1021. https://doi.org/10.1084/jem.20011963

Shamsi, S. (2019). Psoralea corylifolia Babchi: A popular herb of Unani, Ayurvedic and Chinese system of medicine for Vitiligo. *International Journal of Herbal Medicine*, *7*(4), 51–55.

Shao, S., Cao, T., Jin, L., Li, B., Fang, H., Zhang, J., Zhang, Y., Hu, J., & Wang, G. (2016). Increased Lipocalin-2 Contributes to the Pathogenesis of Psoriasis by Modulating Neutrophil Chemotaxis and Cytokine Secretion. *Journal of Investigative Dermatology*, *136*(7), 1418–1428. https://doi.org/10.1016/j.jid.2016.03.002

Siegenthaler, G., Gumowski-Sunek, D., & Saurat, J. H. (1990). Metabolism of natural retinoids in psoriatic epidermis. *Journal of Investigative Dermatology*, *95*(5 Suppl), 47S-48S.

Siegenthaler, G., Hotz, R., Chatellard-Gruaz, D., Didierjean, L., Hellmant, U., & Saurat, J.-H. (1994). Purification and characterization of the human epidermal fatty acid-binding protein: localization during epidermal cell differentiation in viva and in vitro. *Biochemical Journal*, *302*, 363–371. http://portlandpress.com/biochemj/article-pdf/302/2/363/614470/bj3020363.pdf

Siegenthaler, G., Hotz, R., Chatellard-Gruaz, D., Jaconi, S., & Saurat, J.-H. (1993). Characterization and expression of a novel human fatty acid-binding protein: the epidermal type (E-FABP). *Biochemical and Biophysical Research Communications*, *190*(2), 482–487.

Siegenthaler, G., Saurat, J.-H., & Ponect, M. (1990). Retinol and retinal metabolism Relationship to the state of differentiation of cultured human keratinocytes. *Biochemical Journal*, *268*, 371–378. http://portlandpress.com/biochemj/article-pdf/268/2/371/599615/bj2680371.pdf

Siegenthaler, G., Tomatis, I., Chatellard-Gruaz, D., Jaconi, S., Eriksson, U., & Saurat, J. H. (1992). Expression of CRABP-I and-II in human epidermal cells Alteration of relative protein amounts is linked to the state of differentiation. *Biochemical Journal*, *287*, 383–389. http://portlandpress.com/biochemj/article-pdf/287/2/383/608411/bj2870383.pdf

Siegenthaler, G., Tomatis, I., Didierjean, L., Jaconi, S., & Saurat, J.-H. (1992). Overexpression of cellular retinoic acid-binding protein type II (CRABP-II) and down-regulation of CRABP-I in psoriatic skin. *Dermatology*, *185*(4), 251–256.

Skyvalidas, D., Mavropoulos, A., Tsiogkas, S., Dardiotis, E., Liaskos, C., Mamuris, Z., Roussaki-Schulze, A., Sakkas, L. I., Zafiriou, E., & Bogdanos, D. P. (2020). Curcumin mediates attenuation of pro-inflammatory interferon γ and interleukin 17 cytokine responses in psoriatic disease, strengthening its role as a dietary immunosuppressant. *Nutrition Research*, *75*, 95–108. https://doi.org/10.1016/j.nutres.2020.01.005

Sørensen, O. E., Cowland, J. B., Theilgaard-Mönch, K., Liu, L., Ganz, T., & Borregaard, N. (2003). Wound Healing and Expression of Antimicrobial Peptides/Polypeptides in Human Keratinocytes, a Consequence of

Common Growth Factors. *Journal of Immunology*, *170*(11), 5583–5589. https://doi.org/10.4049/jimmunol.170.11.5583

Sorg, O., Tran, C., Carraux, P., Didierjean, L., & Saurat, J.-H. (1999). Retinol and Retinyl Ester Epidermal Pools Are Not Identically Sensitive to UVB Irradiation and Anti-Oxidant Protective Effect. *Dermatology*, *199*(4), 302–307. www.karger.comwww.karger.com/journals/drm

Sorokin, A. V., Domenichiello, A. F., Dey, A. K., Yuan, Z. X., Goyal, A., Rose, S. M., Playford, M. P., Ramsden, C. E., & Mehta, N. N. (2018). Bioactive Lipid Mediator Profiles in Human Psoriasis Skin and Blood. *Journal of Investigative Dermatology*, *138*(7), 1518–1528. https://doi.org/10.1016/j.jid.2018.02.003

Suárez-Fariñas, M., Li, K., Fuentes-Duculan, J., Hayden, K., Brodmerkel, C., & Krueger, J. G. (2012). Expanding the psoriasis disease profile: Interrogation of the skin and serum of patients with moderate-to-severe psoriasis. *Journal of Investigative Dermatology*, *132*(11), 2552–2564. https://doi.org/10.1038/jid.2012.184

Suárez-Fariñas, M., Lowes, M. A., Zaba, L. C., & Krueger, J. G. (2010). Evaluation of the Psoriasis Transcriptome across Different Studies by Gene Set Enrichment Analysis (GSEA). *PLoS ONE*, *5*(4). https://doi.org/10.1371/journal.pone.0010247

Sugita, M., Cernadas, M., & Brenner, M. B. (2004). New insights into pathways for CD1-mediated antigen presentation. *Current Opinion in Immunology*, *16*(1), 90–95. https://doi.org/10.1016/j.coi.2003.11.014

Sugiyama, H., Gyulai, R., Toichi, E., Garaczi, E., Shimada, S., Stevens, S. R., McCormick, T. S., & Cooper, K. D. (2005). Dysfunctional Blood and Target Tissue CD4 + CD25 high Regulatory T Cells in Psoriasis:

Mechanism Underlying Unrestrained Pathogenic Effector T Cell Proliferation . *Journal of Immunology*, *174*(1), 164–173. https://doi.org/10.4049/jimmunol.174.1.164

Swindell, W. R., Xing, X., Stuart, P. E., Chen, C. S., Aphale, A., Nair, R. P., Voorhees, J. J., Elder, J. T., Johnston, A., & Gudjonsson, J. E. (2012). Heterogeneity of inflammatory and cytokine networks in chronic plaque psoriasis. *PLoS ONE*, *7*(3). https://doi.org/10.1371/journal.pone.0034594

Szabo, S. J., Kim, S. T., Costa, G. L., Zhang, X., Fathman, C. G., & Glimcher, L. H. (2000). A novel transcription factor, T-bet, directs Th1 lineage commitment. *Cell*, *100*(6), 655–669. https://doi.org/10.1016/S0092-8674(00)80702-3

Szatmari, I., Gogolak, P., Im, J. S., Dezso, B., Rajnavolgyi, E., & Nagy, L. (2004). Activation of PPARγ specifies a dendritic cell subtype capable of enhanced induction of iNKT cell expansion. *Immunity*, *21*(1), 95–106. https://doi.org/10.1016/j.immuni.2004.06.003

Tachi, M., & Iwamori, M. (2008). Mass spectrometric characterization of cholesterol esters and wax esters in epidermis of fetal, adult and keloidal human skin. *Experimental Dermatology*, *17*(4), 318–323. https://doi.org/10.1111/j.1600-0625.2007.00647.x

Tee, C. B., Sei, Y., & Kajiwara, S. (2019). Secreted Hydrolytic and Haemolytic Activities of Malassezia Clinical Strains. *Mycopathologia*, *184*(2), 227–238. https://doi.org/10.1007/s11046-019-00330-1

Teng, Y., Xie, W., Tao, X., Liu, N., Yu, Y., Huang, Y., Xu, D., & Fan, Y. (2021). Infection-provoked psoriasis: Induced or aggravated (Review). *Experimental and Therapeutic Medicine*, *21*(6). https://doi.org/10.3892/etm.2021.9999

Thaçi, D., Blauvelt, A., Reich, K., Tsai, T. F., Vanaclocha, F., Kingo, K., Ziv, M., Pinter, A., Hugot, S., You, R., & Milutinovic, M. (2015). Secukinumab is superior to ustekinumab in clearing skin of subjects with moderate to severe plaque psoriasis: CLEAR, a randomized controlled trial. *Journal of the American Academy of Dermatology*, *73*(3), 400–409. https://doi.org/10.1016/j.jaad.2015.05.013

Thierfelder, W. E., Van Deursen, J. M., Yamamoto, K., Tripp, R. A., Sarawar, S. R., Carson, R. T., Sangster, M. Y., Vignali, D. A. A., Doherty, P. C., Grosveld, G. C., & Ihle, J. N. (1996). Requirement for Stat4 in interleukin-12-mediated responses of natural killer and T cells. *Nature*, *382*(6587), 171–174. https://doi.org/10.1038/382171a0

Tian, S., Krueger, J. G., Li, K., Jabbari, A., Brodmerkel, C., Lowes, M. A., & Suárez-Fariñas, M. (2012). Meta-Analysis Derived (MAD) Transcriptome of Psoriasis Defines the 'Core' Pathogenesis of Disease. *PLoS ONE*, *7*(9). https://doi.org/10.1371/journal.pone.0044274

Törmä, H., Löntz, W., Liu, W., Rollman, O., & Vahlquist, A. (1994). Expression of cytosolic retinoid-binding protein genes in human skin biopsies and cultured keratinocytes and fibroblasts. *British Journal of Dermatology {199'i)*, *131*(2), 243–249.

Trifari, S., Kaplan, C. D., Tran, E. H., Crellin, N. K., & Spits, H. (2009). Identification of a human helper T cell population that has abundant production of interleukin 22 and is distinct from TH-17, TH1 and TH2 cells. *Nature Immunology*, *10*(8), 864–871. https://doi.org/10.1038/ni.1770

Trinchieri, G., Wysocka, M., D'Andrea, A., Rengaraju, M., Aste-Amezaga, M., Kubin, M., Valiante, N. M., & Chehimi, J. (1992). Natural killer cell

stimulatory factor (NKSF) or interleukin-12 is a key regulator of immune response and inflammation. *Progress in Growth Factor Research*, *4*(4), 355–368. https://doi.org/10.1016/0955-2235(92)90016-B

Tsikas, D., Zoerner, A. A., Mitschke, A., & Gutzki, F. M. (2009). Nitro-fatty acids occur in human plasma in the picomolar range: A targeted nitro-lipidomics GC-MS/MS study. *Lipids*, *44*(9), 855–865. https://doi.org/10.1007/s11745-009-3332-4

Tsikas, D., Zoerner, A., Mitschke, A., Homsi, Y., Gutzki, F. M., & Jordan, J. (2009). Specific GC-MS/MS stable-isotope dilution methodology for free 9- and 10-nitro-oleic acid in human plasma challenges previous LC-MS/MS reports. *Journal of Chromatography B: Analytical Technologies in the Biomedical and Life Sciences*, *877*(26), 2895–2908. https://doi.org/10.1016/j.jchromb.2008.12.062

Turina, M. C., Landewé, R., & Baeten, D. (2017). Lessons to be learned from serum biomarkers in psoriasis and IBD–the potential role in SpA. In *Expert Review of Clinical Immunology* (Vol. 13, Issue 4, pp. 333–344). Taylor and Francis Ltd. https://doi.org/10.1080/1744666X.2017.1244004

Vacharanukrauh, P., Meephansan, J., Tangtanatakul, P., Soonthornchai, W., Wongpiyabovorn, J., Serirat, O., & Komine, M. (2021). High-Throughput RNA Sequencing Reveals the Effect of NB-UVB Phototherapy on Major Inflammatory Molecules of Lesional Psoriasis. *Psoriasis: Targets and Therapy*, *Volume 11*, 133–149. https://doi.org/10.2147/ptt.s335913

Vahlquist, A. (1982). Vitamin A in human skin: I. Detection and identification of retinoids in normal epidermis. *Journal of Investigative Dermatology*, *79*(2), 89–93. https://doi.org/10.1111/1523-1747.ep12500032

Van Rhijn, I., Godfrey, D. I., Rossjohn, J., & Moody, D. B. (2015). Lipid and small-molecule display by CD1 and MR1. *Nature Reviews Immunology*, *15*(10), 643–654. https://doi.org/10.1038/nri3889

Villanova, F., Flutter, B., Tosi, I., Grys, K., Sreeneebus, H., Perera, G. K., Chapman, A., Smith, C. H., Di Meglio, P., & Nestle, F. O. (2014). Characterization of innate lymphoid cells in human skin and blood demonstrates increase of NKp44+ ILC3 in psoriasis. *Journal of Investigative Dermatology*, *134*(4), 984–991. https://doi.org/10.1038/jid.2013.477

Vincent, M. S., Leslie, D. S., Gumperz, J. E., Xiong, X., Grant, E. P., & Brenner, M. B. (2002). CD1-dependent dendritic cell instruction. *Nature Immunology*, *3*(12), 1163–1168. https://doi.org/10.1038/ni851

Wagner, C., Hois, V., Pajed, L., Pusch, L. M., Wolinski, H., Trauner, M., Zimmermann, R., Taschler, U., & Lass, A. (2020). Lysosomal acid lipase is the major acid retinyl ester hydrolase in cultured human hepatic stellate cells but not essential for retinyl ester degradation. *Biochimica et Biophysica Acta - Molecular and Cell Biology of Lipids*, *1865*(8). https://doi.org/10.1016/j.bbalip.2020.158730

Wang, J., Liu, Y., Zhang, Y., Wang, S., Kang, S., Mi, N., Li, R., & Zou, Y. (2023). Identification immune response genes in psoriasis after treatment with secukinumab. *BMC Medical Genomics*, *16*(1). https://doi.org/10.1186/s12920-023-01507-w

Wang, P., Killeen, M. E., Sumpter, T. L., Ferris, L. K., Falo, L. D., Freeman, B. A., Schopfer, F. J., & Mathers, A. R. (2021). Electrophilic nitro-fatty acids suppress psoriasiform dermatitis: STAT3 inhibition as a contributory

mechanism. *Redox Biology*, *43*. https://doi.org/10.1016/j.redox.2021.101987

Wang, Y., Lam, K. S. L., Kraegen, E. W., Sweeney, G., Zhang, J., Tso, A. W. K., Chow, W. S., Wat, N. M. S., Xu, J. Y., Hoo, R. L. C., & Xu, A. (2007). Lipocalin-2 is an inflammatory marker closely associated with obesity, insulin resistance, and hyperglycemia in humans. *Clinical Chemistry*, *53*(1), 34–41. https://doi.org/10.1373/clinchem.2006.075614

Wefers, H., Melnik, B. C., Fluer, M., Bluhm, C., Lehmann, P., & Plewig, G. (1991). Influence of UV irradiation on the composition of human stratum corneum lipids. *Journal of Investigative Dermatology*, *96*(6), 959–962.

Wegrecki, M., Ocampo, T. A., Gunasinghe, S. D., von Borstel, A., Tin, S. Y., Reijneveld, J. F., Cao, T. P., Gully, B. S., Le Nours, J., Moody, D. B., Van Rhijn, I., & Rossjohn, J. (2022). Atypical sideways recognition of CD1a by autoreactive γδ T cell receptors. *Nature Communications*, *13*(1). https://doi.org/10.1038/s41467-022-31443-9

Wei, X., Fricker, K., Enk, A. H., & Hadaschik, E. N. (2016). Altered expression of keratin 14 in lesional epidermis of autoimmune skin diseases. *International Journal of Dermatology*, *55*(6), 620–628.

Weinstein, G. D., Koo, J. Y. M., Krueger, G. G., Lebwohl, M. G., Lowe, N. J., Menter, M. A., Lew-Kaya, D. A., Sefton, J., Gibson, J. R., Walker, P. S., Ast, E., Bagel, J., Breneman, D. L., Bright, R. D., Davis, S. A., Duvic, M., Eisen, D., Feldman, S. R., Fiedler, V. C., … Wolf, D. I. (2003). Tazarotene cream in the treatment of psoriasis: Two multicenter, double-blind, randomized, vehicle-controlled studies of the safety and efficacy of tazarotene creams 0.05% and 0.1% applied once daily for 12 weeks.

Journal of the American Academy of Dermatology, *48*(5), 760–767. https://doi.org/10.1067/mjd.2003.103

Weinstein, G. D., Krueger, G. G., Lowe, N. J., Duvic, M., Friedman, D. J., Jegasothy, B. V., Jorizzo, J. L., Shmunes, E., Tschen, E. H., Lew-Kaya, D. A., Lue, J. C., Sefton, J., Gibson, J. R., & Chandraratna, R. A. S. (1997). Tazarotene gel, a new retinoid, for topical therapy of psoriasis: Vehicle-controlled study of safety, efficacy, and duration of therapeutic effect. *Journal of the American Academy of Dermatology*, *37*(1), 85–92. https://doi.org/10.1016/S0190-9622(97)70216-0

Weller, R., Pattullo, S., Smith, L., Golden, M., Ormerod, A., & Benjamin, N. (1996). Nitric oxide is generated on the skin surface by reduction of sweat nitrate. *Journal of Investigative Dermatology*, *107*(3), 327–331. https://doi.org/10.1111/1523-1747.ep12363167

Werner, B., Brenner, F. M., & Böer, A. (2008). Histopathologic study of scalp psoriasis: Peculiar features including sebaceous gland atrophy. *American Journal of Dermatopathology*, *30*(2), 93–100. https://doi.org/10.1097/DAD.0b013e31816421fd

Wertz, P. W., Madison, K. C., & Downing, D. T. (1989). Covalently bound lipids of human stratum corneum. *Journal of Investigative Dermatology*, *92*(1), 109–111. https://doi.org/10.1111/1523-1747.ep13071317

Williamson, J. C., Scheipers, P., Schwämmle, V., Zibert, J. R., Beck, H. C., & Jensen, O. N. (2013). A proteomics approach to the identification of biomarkers for psoriasis utilising keratome biopsy. *Journal of Proteomics*, *94*, 176–185. https://doi.org/10.1016/j.jprot.2013.09.010

Willinger, T. (2019). Oxysterols in intestinal immunity and inflammation. *Journal of Internal Medicine*, *285*(4), 367–380. https://doi.org/10.1111/joim.12855.

Wolk, K., Kunz, S., Witte, E., Friedrich, M., Asadullah, K., & Sabat, R. (2004). IL-22 increases the innate immunity of tissues. *Immunity*, *21*(2), 241–254. https://doi.org/10.1016/j.immuni.2004.07.007

Wolk, K., Witte, E., Wallace, E., Döcke, W. D., Kunz, S., Asadullah, K., Volk, H. D., Sterry, W., & Sabat, R. (2006). IL-22 regulates the expression of genes responsible for antimicrobial defense, cellular differentiation, and mobility in keratinocytes: A potential role in psoriasis. *European Journal of Immunology*, *36*(5), 1309–1323. https://doi.org/10.1002/eji.200535503

Yamamoto, K., Miki, Y., Sato, M., Taketomi, Y., Nishito, Y., Taya, C., Muramatsu, K., Ikeda, K., Nakanishi, H., Taguchi, R., Kambe, N., Kabashima, K., Lambeau, G., Gelb, M. H., & Murakami, M. (2015). The role of group IIF-secreted phospholipase A 2 in epidermal homeostasis and hyperplasia. *Journal of Experimental Medicine*, *212*(11), 1901–1919. https://doi.org/10.1084/jem.20141904

Yang, L., Fan, X., Cui, T., Dang, E., & Wang, G. (2017). Nrf2 Promotes Keratinocyte Proliferation in Psoriasis through Up-Regulation of Keratin 6, Keratin 16, and Keratin 17. *Journal of Investigative Dermatology*, *137*(10), 2168–2176. https://doi.org/10.1016/j.jid.2017.05.015

Yang, R., Zhou, Q., Wen, C., Hu, J., Li, H., Zhao, M., & Zhao, H. (2013). Mustard seed (Sinapis Alba Linn) attenuates imiquimod-induced psoriasiform inflammation of BALB/c mice. *Journal of Dermatology*, *40*(7), 543–552. https://doi.org/10.1111/1346-8138.12119

Yao, Y., Richman, L., Morehouse, C., de los Reyes, M., Higgs, B. W., Boutrin, A., White, B., Coyle, A., Krueger, J., Kiener, P. A., & Jallal, B. (2008). Type I interferon: Potential therapeutic target for psoriasis? *PLoS ONE*, *3*(7). https://doi.org/10.1371/journal.pone.0002737

Young, E. (1970). The external treatment of psoriasis: A controlled investigation of the effects of coal tar. *British Journal of Dermatology*, *82*(5), 510–515. https://doi.org/10.1111/j.1365-2133.1970.tb02215.x

Yu, G., Wang, L. G., Han, Y., & He, Q. Y. (2012). ClusterProfiler: An R package for comparing biological themes among gene clusters. *OMICS A Journal of Integrative Biology*, *16*(5), 284–287. https://doi.org/10.1089/omi.2011.0118

Yu, Z., Gong, Y., Cui, L., Hu, Y., Zhou, Q., Chen, Z., Yu, Y., Chen, Y., Xu, P., Zhang, X., Guo, C., & Shi, Y. (2020). High-throughput transcriptome and pathogenesis analysis of clinical psoriasis. *Journal of Dermatological Science*, *98*(2), 109–118. https://doi.org/10.1016/j.jdermsci.2020.03.006

Zaba, L. C., Cardinale, I., Gilleaudeau, P., Sullivan-Whalen, M., Fariñas, M. S., Fuentes-Duculan, J., Novitskaya, I., Khatcherian, A., Bluth, M. J., Lowes, M. A., & Krueger, J. G. (2007). Amelioration of epidermal hyperplasia by TNF inhibition is associated with reduced Th17 responses. *Journal of Experimental Medicine*, *204*(13), 3183–3194. https://doi.org/10.1084/jem.20071094

Zajonc, D. M., Crispin, M. D. M., Bowden, T. A., Young, D. C., Cheng, T.-Y., Hu, J., Costello, C. E., Rudd, P. M., Dwek, R. A., Miller, M. J., Brenner, M. B., Moody, D. B., & Wilson, I. A. (2005). Molecular mechanism of lipopeptide presentation by CD1a. *Immunity*, *22*(2), 209–219. https://doi.org/10.1016/j.immuni.2004.12.009

Zajonc, D. M., Elsliger, M. A., Teyton, L., & Wilson, I. A. (2003). Crystal structure of CD1a in complex with a sulfatide self antigen at a resolution of 2.15 Å. *Nature Immunology*, *4*(8), 808–815. https://doi.org/10.1038/ni948

Zhang, H., Wu, L. M., & Wu, J. (2011). Cross-talk between apolipoprotein e and cytokines. *Mediators of Inflammation*, *2011*, 1–10. https://doi.org/10.1155/2011/949072

Zhou, X., Krueger, J. G., Kao, M.-C. J., Lee, E., Du, F., Menter, A., Hung Wong, W., & Bowcock, A. M. (2003). Novel mechanisms of T-cell and dendritic cell activation revealed by profiling of psoriasis on the 63,100-element oligonucleotide array. *Physiological Genomics*, *13*, 69–78. https://doi.org/doi:10.1152/physiolgenomics.00157.2002

Zhu, K., & Mrowietz, U. (2001). Inhibition of dendritic cell differentiation by fumaric acid esters. *Journal of Investigative Dermatology*, *116*(2), 203–208.

List of Figures

Figure 1.1 Algorithm for psoriasis treatment according to NICE (National Institute for Health and Care Excellence) guidelines, www.nice.org.uk. 19

Figure 3.1 Schematic of elliptical skin biopsy 86

Figure 3.2 Principal Component Analysis (PCA) plots comparing (a) PS, AD and HC (b) PS by treatment group 91

Figure 3.3 Differential gene expression untreated psoriasis (a) PS L vs HC (b) PS NL vs HC. . 93

Figure 3.4 Scatter plot PS untreated 94

Figure 3.5 Differential gene expression NB-UVB-treated PS (a) PS L (NB-UVB) vs HC (b) PS R (NB-UVB) vs HC 94

Figure 3.6 Scatter plot NB-UVB-treated psoriasis 95

Figure 3.7 Differential gene expression secukinumab-treated PS (a) PS L (Secukinumab) vs HC (b) PS R (Secukinumab) vs HC 96

Figure 3.8 Scatter plot secukinumab-treated psoriasis 97

Figure 3.9 Differential gene expression, psoriasis cohort I 98

Figure 3.10 Differential gene expression, psoriasis cohort II 99

Figure 3.11 Dot plots comparing gene expression of key cytokines across disease groups 109

Figure 3.12 Dot plots comparing gene expression of key cytokines between psoriasis treatment groups 111

Figure 3.13 Module-Trait Relationships using Weighted Gene Co-expression Network Analysis (WGCNA). 113

Figure 3.14 Module-Trait relationships: Turquoise module I 114

Figure 3.15 Module-Trait relationships: Turquoise module II 115

Figure 3.16 Module-Trait relationships: Midnight Blue Module I 116

Figure 3.17 Module-Trait Relationships: Midnight Blue Module II 116

Figure 3.18 Module-Trait relationships: Cyan Module I 117

Figure 3.19 Module-Trait relationships: Cyan Module II 118

Figure 3.20 Turquoise module WGCNA (a) Co-expression network (b) STRING. 120

Figure 3.21 Midnight Blue Module WGCNA (a) Co-expression network (b) STRING. 121

Figure 3.22 Cyan Module WGCNA (a) Co-expression network (b) STRING. 123

Figure 3.23 Black Module WGCNA (a) Co-expression network (b) STRING. 124

Figure 4.1 Interaction of Sterol and Retinoid pathways 134

Figure 4.2 Chemical structure of Retinyl Esters 137

Figure 4.3 IEF gels: Retinyl esters 144

Figure 4.4 Pre-loaded IEF gels: GD3 and Retinyl Esters 144

Figure 4.5 Pre-loaded IEF gels: LPC and Retinyl Esters 145

Figure 4.6 K562 Toxicity Testing: Retinyl Esters 148

Figure 4.7 Dextramer staining (Healthy control C2933): Retinyl Esters 149

Figure 4.8 Dextramer staining (Psoriasis PS2650): Retinyl Esters 150

Figure 4.9 CD1a expression on moDC: Retinyl Esters 152

Figure 4.10 IFN-γ ELISpot (Healthy controls): Retinyl Esters I 154

Figure 4.11 IFN-γ ELISpot (Psoriasis): Retinyl Esters I 155

Figure 4.12 IFN-γ ELISpot: Retinyl Esters II 156

Figure 4.13 IFN-γ ELISA: Retinyl Esters 157

Figure 4.14 BK6 functional assay (3 experiments): Retinyl Esters 158

Figure 5.1 Chemical structures of Nitro-Fatty Acids 166

Figure 5.2 IEF gels: Nitro-Fatty Acids *176*

Figure 5.3 Pre-loaded IEF gels: Nitro-Fatty Acids *179*

Figure 5.4 K562 Toxicity Testing: Nitro-Fatty Acids *181*

Figure 5.5 Dextramer staining: 9-NO *183*

Figure 5.6 Dextramer staining: 10-NO *185*

Figure 5.7 Dextramer staining NO2-CLA *187*

Figure 5.8 CD1a expression on moDC: Nitro-Fatty Acids *188*

Figure 5.9 IFN-γ ELISA: Nitro-Fatty Acids *190*

Figure 6.1 Interaction of Sterol and Retinoid pathways *197*

Figure 6.2 Chemical structures of cholesterol and cholesteryl esters *200*

Figure 6.3 Chemical structure of acitretin *203*

Figure 6.4 IEF gels: Cholesterol and Cholesteryl Esters *211*

Figure 6.5 Pre-loaded IEF gels: GD3 and Cholesterol and Cholesteryl Esters *212*

Figure 6.6 K562 Toxicity Testing: Cholesterol and Cholesteryl Esters *215*

Figure 6.7 Dextramer staining: Cholesterol *217*

Figure 6.8 IFN-γ ELISA: Cholesterol and Cholesteryl Esters *218*

Figure 6.9 IEF gels: Coal tar derivatives and acitretin *223*

Figure 6.10 K562 Toxicity Testing: Coal tar derivatives and acitretin *225*

Figure 6.11 CD1a expression on moDC: Coal tar derivatives and acitretin *226*

Figure 6.12 IFN-γ ELISpot: Coal tar derivatives and acitretin I *228*

Figure 6.13 IFN-γ ELISpot: Coal tar derivatives and acitretin II *231*

Figure 6.14 IEF gels: Other lipids *232*

Figure 7.1 Unsupervised Uniform Manifold Approximation and Projection (UMAP) plot of single cell mRNA expression clustered by cell type..... 239

Figure 7.2 Pathway for choosing candidate genes for validation..... 245

Figure 7.3 Single Cell Atlas: UMAP plots of mRNA expression of CRABP2 in psoriasis and healthy skin..... 257

Figure 7.4 Single Cell Atlas: UMAP plots of mRNA expression of FABP5 in psoriasis and healthy skin..... 261

Figure 7.5 Single Cell Atlas: UMAP plots of mRNA expression of LCN2 in psoriasis and healthy skin..... 266

Figure 7.6 Single Cell Atlas: UMAP plots of APOE mRNA expression in psoriasis and healthy skin..... 269

Figure 7.7 Immunofluorescence immunohistochemistry: Healthy Control DER008B..... *270*

Figure 7.8 Immunofluorescence immunohistochemistry: AD2634..... 271

Figure 7.9 Immunofluorescence immunohistochemistry: PS2784 L (untreated)..... 271

Figure 7.10 Immunofluorescence immunohistochemistry: PS2684 NL (untreated) 272

Figure 7.11 Immunofluorescence immunohistochemistry: PS2501 L (NB-UVB) 273

Figure 7.12 Immunofluorescence immunohistochemistry: PS2501 NL (NB-UVB)..... 273

Figure 7.13 Immunofluorescence immunohistochemistry: PS2510 L (Secukinumab) 274

Figure 7.14 Immunofluorescence immunohistochemistry: PS2510 NL (Secukinumab)..... 274

Figure 7.15 Hyperion: Tissue architecture 276

Figure 7.16 Hyperion: CD1a expression 278

Figure 7.17 Hyperion: CRABP2 staining 279

Figure 7.18 Hyperion: CRABP2 co-localisation with KIT. 280

Figure 7.19 Hyperion: CRABP2 co-localisation with CD45..... 281

Figure 7.20 Hyperion: LCN2 staining 282

Figure 7.21 Hyperion: ApoE staining 284

Figure 7.22 Hyperion: Expression in sebaceous glands of (a) CRABP2 (b) LCN2 (c) ApoE. .. 285

List of Tables

Table 1.1 Biologic therapies currently approved for use in psoriasis (NICE UK) 20

Table 1.2 Known CD1a antigens 33

Table 2.1 Media 38

Table 2.2 Buffers 40

Table 2.3 Final concentrations of cells for co-culture step of experiments 41

Table 2.4 Flow Cytometry antibodies. 46

Table 2.5 Compensation beads for flow cytometry. 47

Table 2.6 Candidate CD1a lipid antigens 49

Table 2.7 CD1a used for IEF gels 59

Table 2.8 IEF gel (3-day) example: retinyl oleate with LPC 62

Table 2.9 Loading of biotinylated CD1a monomers 64

Table 2.10 Tetramer assembly. 64

Table 2.11 Tetramer staining 65

Table 2.12 Loading of biotinylated CD1a dextramers 67

Table 2.13 BK6 Functional Assay: Cell plating for control wells 71

Table 3.1 Published mRNA expression studies 75

Table 3.2 Patient cohort 84

Table 3.3 Differentially Expressed Genes (vs healthy control): Untreated psoriasis 101

Table 3.4 Differentially Expressed Genes (vs healthy control): Psoriasis (all subgroups) 104

Table 4.1 Selection of DEG relevant to retinoid pathways 138

Table 4.2 Comparison of DEG in PS L and PS R groups 140

Table 4.3 Enriched Gene Ontology (GO) terms relevant to retinoid pathways 142

Table 5.1 Selection of DEG relevant to NFA pathways 169

Table 5.2 Enriched Gene Ontology (GO) terms relevant to NFA pathways 171

Table 6.1 Selection of DEG relevant to sterol pathways 205

Table 6.2 Enriched Gene Ontology (GO) terms relevant to sterol pathways 207

Table 6.3 Solubility of cholesterol and cholesteryl esters in a variety of solvents post sonication 209

Table 7.1 GEO Profiles Datasets for psoriatic and healthy human skin 238

Table 7.2 Antibodies for RNA-Seq validation. 240

Table 7.3 Hyperion™ Panel 242

Table 7.4 Antibody conjugation for Hyperion™ 244

Table 7.5 RNA-Seq: Differential expression of candidate genes of interest in untreated psoriasis group: PS L vs PS NL 245

Table 7.6 GEO Profiles Top 250 DEG vs candidate genes of interest: PS L vs PS NL skin 247

Table 7.7 GEO Profiles: Geo DataSet Top 250 DEG vs candidate genes of interest: PS L vs HC skin. 252

Table 7.8 CRABP2: Differential gene expression in the skin of psoriasis and atopic dermatitis compared to healthy control 255

Table 7.9 FABP5: Differential gene expression in the skin of psoriasis and atopic dermatitis compared to healthy control 259

Table 7.10 LCN2: Differential gene expression in the skin of psoriasis and atopic dermatitis compared to healthy control 264

Table 7.11 APOE: Differential gene expression in the skin of psoriasis and atopic dermatitis compared to healthy control 267